Circular RNAs: New players in Ageing and Age-related Chronic Disease

Shahnaz Haque

Submitted by Shahnaz Haque of the University of Exeter Medical School as a thesis for the degree of Doctor of Philosophy in Medical Studies, 1 July 2020

I certify that all the material in this thesis is my own work and that no unchanged or unacknowledged material has previously been submitted and approved for the award of degree by this or any other University.

Signature 

……

Declarations

I declare that this thesis has been written by myself and that the piece of research work has not be submitted for any other degree or professional qualification. I confirm that the work submitted to the Univeristy of Exeter is my own, except where the research was presented in the form of co-authored publications. My contribution and those of the other authors to this work have been explicitly indicated below. The contributions of the co-authors have been explcicitly mentioned in the publications.

The experimental work is almost entirely my own work except the generataion of circRNA profiles. The preparation of RNA samples for CircleSeq was undertaken by Dr Karen Moore and initial bioinformatics analysis was done by Dr Ryan Ames. Senescent cells were provided by Dr Eva Latorre. Treated pancreatic EndoC-βH1 beta cells were provided by Dr Nicola Jeffrey. RNA extraction from mice smples and RNA quantification was done by Dr Ben Lee and Dr Jonathan Locke. I confirm that appropriate credit has been given within this thesis and published papers where reference has been made to the work of others.

Abstract

Circular RNAs (circRNAs) are an emerging class of non-coding RNA that may regulate expression during normal and disease states. Although circRNAs accumulate in *in vivo* models of ageing, their role in this process and its physiological consequences remains largely unanswered. In the course of this thesis, I assessed dysregulation of circRNA expression in RNA samples from ageing human peripheral blood and examined associations of their expression with various ageing outcomes in human, mammalian longevity and senescence in human cell types of various lineages, and in blood and islet samples from patients with type 2 diabetes; an exemplar disease of ageing.

Of the 15 circRNAs validated in this study, I identified 4 (*circDEF6*, c*ircEP300, circFOXO3* and *circFNDC3B*) that were associated with ageing outcomes (parental longevity or hand grip strength) in the InCHIANTI population study of ageing. *CircFOXO3* and *circEP300* also demonstrated differential expression in one or more human senescent cell types. 4 ageing outcomes associated circRNAs appeared to be conserved in mouse of which *circPlekhm1* nominally correlated with median strain lifespan.

As type 2 diabetes is an exemplar chronic disease of ageing, I also aimed to examine the role of circRNA in this disorder. I first defined the circRNA repertoire in human pancreatic islets and assessed their differential expression in conjunction with type 2 diabetes status and genotype at T2D risk loci. Following this, I determined their responsiveness to diabetomimetic stimuli in the human EndoC-βH1 beta cell line, and the potential for use as biomarkers of T2D in human peripheral blood. 4 of the five

most abundant circRNAs expressed in human pancreatic islets *circCIRBP*, *circZKSCAN*, *circRPH3AL* and *circCAMSAP1,* were associated with diabetes status in islets. C*ircCIRBP* and *circRPH3AL* were also differentially expressed in β-cells in response to elevated fatty acid. Despite this, no associations with T2D diabetes risk loci was identified. Cumulatively, the data generated from my work suggest that circRNAs have potential as regulators of gene expression during ageing and age-related disease, raising the possibility that they may have future utility as biomarkers or therapeutic targets for the management of age-related chronic disease outcomes.

Table of contents

List of figures

List of Tables

List of Abbreviations

ATP	Adenosine triphosphate
AS	Alternative splicing
AMPK	AMP-activated protein kinase
ANOVA	Analysis of variance
ANG	Angiogenin
AD	Alzheimer's disease
AUC	Area under the curve
BMI	Body mass index
CDK2	Cyclin dependent kinase 2
CIRBP	Cold Inducible RNA Binding Protein
circRNAs	Circular RNAs
circSNX27	circRNA_100338
cDNA	Complementary DNA
CDKN2A	Cyclin Dependent Kinase Inhibitor 2A
dNTPs	Deoxyribonucleotide triphosphates
DMSO	Dimethylsulfoxide
DR	Dietary restriction
DDR	DNA damage response
ETC	Electron transport chain
EIciRNAs	Exon-intron circRNAs
ESE	Exon splicing enhancer
ESS	Exon splicing silencer
ECM	Extracellular matrix
FSK/DEX	Forskolin/ dexamethasone
PHA-4	Defective PHArynx development protein
f-circRNA	Fusion-circRNAs
TTP	Tristetraprolin
GO	Gene ontology
GECs	Glomerular endothelial cells
G6Pase	Glucose 6-phosphatase
IGT	Impaired Glucose tolerance
G3BP1	GTPase Activating Protein (SH3 domain) Binding Protein 1
HSC	Haematopoietic stem cells
HCC	Hepatocellular carcinoma
hnRNP	Heterogeneous nuclear ribonucleoproteins
circDYRK1A	Hsa_circ_0000190
circRPPH1	Hsa_circ_0000520
circSRPRH	Hsa_circ_0001649
circPRRC2B	Hsa_circ_0001895
circEIF4G3	Hsa_circ_0005075
circABCC	Hsa_circ_001569
circKIAA0907	Hsa_circ_002059
circADAMTS9	Hsa_circ_0066444
hg19	Human genome reference 19
HUVECs	Human umbilical vein endothelial cells

ciRNAs	Intronic circRNAs
FU3	Follow up 3
FU4	Follow up 4
GWAS	Genome wide association studies
GH	Growth hormone
GM	Gut microbiome
IGF-1	Insulin-like growth factor-1
IIS	Insulin/insulin-like growth factor-1 signalling
daf2	Insulin-like receptor subunit beta
SI	Insulin secretory index
ISE	Intron splicing enhancer
ISS	Intron splicing silencer
lncRNAs	Long non-coding RNAs
mTOR	Mechanistic target of rapamycin kinase
miRNA	microRNA
MDA	Multiple misplacement amplification
MBL/MBNL1	Muscleblind
NSC	Neural stem cells
NGS	Next generation sequencing
NAD	Nicotinamide adenine dinucleotide
ncRNAs	Non-coding RNAs
NFQ	Nonfluorescent quencher
NOVA1	NOVA alternative splicing regulator 1
nt	Nucleotides
SKN-1	Skinhead-1
NuRD	Nucleosome remodelling and deacetylase
PES1	Pescadillo ribosomal biogenesis factor 1
OA	Osteoarthritis
PEPCK	Phosphoenolpyruvate carboxykinase 2
PLS	Parental longevity score
PD	Parkinson’s disease
PBS	Phosphate-buffered saline
PTEN	Phosphatase and tensin homolog
PI3K	Phosphatidylinositol-4,5-bisphosphate 3-kinase
PAI-1	Plasminogen activator inhibitor-1
PCR	Polymerase chain reaction
PTBP2	Polypyrimidine Tract Binding Protein 2
PD	Population doubling
pre-mRNA	Pre-messenger RNA
AKT	Protein kinase B
QKI	Quaking
qPCR	Quantitative PCR
ROS	Reactive oxygen species
ROD1	Regulator Of Differentiation 1
RB 1	Retinoblastoma transcriptional corepressor 1
RT	Reverse transcription

RAVER1	Ribonucleoprotein, PTB Binding 1
RISC	RNA-induced silencing complex
RBPs	RNA-binding proteins
RIN	RNA Integrity Number
SRSF	Serine/arginine-rich splicing factors
snRNPs	Small nuclear ribonucleoproteins
SFs	Splicing factors
SSs	Splice sites
SIRT1	Sirtuin-1
SAHF	Senescence-associated heterochromatin foci
SASP	Senescence-associated secretory phenotype
SNEV	pre-mRNA processing factor 19
sncRNAs	Short non coding RNAs
snRNA	Small nuclear RNA
SOD1	Superoxide dismutase 1
SA β-Gal	Senescence-associated beta-galactosidase
SCID	Severe combined immune-deficient
SV40LT	Simian Vacuolating Virus 40 TAg
SNPs	Single nucleotide polymorphisms
TIA1	T-cell-restricted intracellular antigen-1
TDP-43	TAR-DNA binding protein
TGF-β	Transforming growth factor beta
TLR	Toll-like receptors
TE	Tris-EDTA
T2D	Type 2 diabetes
UPR	Unfolded Protein Response
UTRs	Untranslated regions
UNGs	Uracil-DNA glycosylases
VEGF	Vascular endothelial growth factor

Acknowledgements

I am grateful to Almighty Creator for every single thing that HE has given me, is and will be leading me through. I am extremely thankful to HIM for giving me a supportive environment during the course of this research. I am thankful to the Devon Northcott Medical Trust for the research funding they provided. I am thankful to each of the TeamRNA members including Dr Cece Tonneau, Emad Manni, Dr Eva Latorre, Jed Lye, Laura Bramwell and Ryan Frankum. I am extremely grateful for all the professional support from Dr Ben Lee as well each one of my co-supervisors Professor Mike Weedon and Dr Ryan Ames. I do not have enough words to thank Dr Nicola Jeffery especially for driving me all day through Exeter on April 23, 2018. I am equally grateful to many others most of whom I met for the first time during that time and everyone else who reached out to me during April 2018. I am thankful to Amelia Coughlman and her family. I am glad to have Dr Sadia Moriam Asmi by my side since my school days.

I have always felt extremely blessed to have Professor Lorna Harries as my supervisor in many more ways than I will be able to express. Last but not the least I am extremely grateful to my LORD for granting me my mother Rahima Begum (Rehana Sharif), my father Professsor S M Fazlul Haque and my mother's Smoni Zafeera. I am ever so grateful to those who respected, loved and brought smiles to the faces of these people in my life. I am more than fortunate to be given the mother who sacrificed to extreme lengths to have ends meet for everyone around her. The struggles she went through from her very childhood and the way she carried forward surmounting all the hurdles no matter how emotionally hurtful, her sacrifices for everyone around her instead of prioritizing herself, her immense strength despite her vulnerability and softness is

something I always cherish. I am equally lucky to have a father who only provided for everyone around him without thinking about himself and have Smoni who has surprisingly displayed much motherly affection and immense strength many a times. I will forever be grateful to every single person who have loved, respected and only wished all the very best from the core of their heart for these special people in my life. I am thankful for the unconditional and unquestionable sacrifice that each one of these three people continue to make for me. Their sacrifices and my supervisor's support is much more than I can ever put into words. It would be an underestimation if I say I thank these four for everything. I sincerely hope, with the mercy of ALLAH, I can make Smoni Zafeera, each one of my parents Rahima Begum and Fazlul Haque, my maternal grandmother Halima Begum, my maternal aunt Jannat, my paternal grandfather and my supervisor Lorna Harries proud with utmost positivity throughout the coming days of my life. I hope all my shortcomings, just like any ordinary human beings', are pardoned by all and forgiven as well as erased by my LORD in this world and the hereafter. I sincerely hope I can make a positive impact on those around me personally and through my career in science. I hope, all throughout, my LORD makes me a better and a wiser version of myself every moment in time so that I can be the best version that HE loves to see of myself and those who matter to me the most in this world and the next.

Chapter 1

Introduction

1.1 Ageing

Ageing is a multifactorial process that leads to gradual deterioration of physical and physiological functionality at the cellular, tissue and organ levels. It is the primary risk factor for chronic ageing pathologies such as cancer, sarcopenia, diabetes, and cardiovascular and neurodegenerative illnesses, which account for the bulk of morbidity and mortality in both the developed and the developing world (Goldman et al., 2013; Kirkland, 2016). Physiological parameters, such as loss of muscle and bone mass, frailty, immobility, cognitive impairment, impaired immune function and a reduced ability to respond to stress increase with the risk of developing geriatric syndromes (MacIntosh, Morley, and Chapman, 2000). Although time-dependent accumulation of cellular damage is widely accepted as one of the key causes of ageing, this accumulated damage may provide compensatory advantages to cells that would otherwise become hyperplastic and/or transformed (Gems and Partridge, 2013; Kirkwood, 2005; Vijg and Campisi, 2008).

While advances in medical technologies and services have contributed to an extension of average lifespans of populations, extension of lifespan does not necessarily equate to an improvement in healthspan. In fact, ~20-55% of the total healthcare costs is needed for the management of ageing-associated chronic comorbidities (Fullfact, 2018). While some individuals experience relatively disease-free ageing, others may encounter ageing outcomes in early midlife. Children of long-lived parents seem to have lower rates of ageing disorders or attributed mortalities, and greater life expectancies (Dutta et al.,2014; 2013). Many long-lived individuals suffer from multiple comorbidities that profoundly affect their disability-adjusted life years (Kehler, 2019).

Offsprings of non-agenarians and centenarians delay or escape age-related diseases, have a life-long survival advantage and have lower prevalence of and mortality from age-related diseases such as coronary heart disease, type 2 diabetes and cancer when they reach middle age. In fact, 21 “ageing-signature” genes were identified in middle-age offsprings which were likely engaged in metabolism, epigenetic control and immune function including *ASF1A* and *IL7R*. Reduced expression of *ASF1A* and *IL7R* at middle age might assist in maintenance of chromatin structure and the immune system (Passtoors et al., 2012).

Analysis of differential expression of genes involved in lipid metabolism and favourable lipid profile between centenarians and their partners show changes in expression of several genes (*MSR1*, *TPI1*, *DBI*, *AGPAT2* and *PLTP*) were upregulated while several others were (*NR1D1*, *PLCG1*, *HMGCR* and *FABP6*) were downregulated in centenarian compared to their partners. The expression of *ADRBK1*, *F2R*, *GSR*, *LRRC16A* and *ARG1* in centenarians also associated with that in their offsprings. This might contribute to the lower incidence cardiovascular diseases and kidney dysfunction in centenarians and their offsprings (He et al., 2016).

Analysis of DNA methylation levels of peripheral blood mononuclear cells of offsprings of semi-supercentenarians reveal they have a lower epigenetic age than age-matched controls. In addition, centenarians are younger than expected based on their chronological age (Horvath et al., 2015). A study on peripheral blood mononuclear cells of healthy octo/nonagenarians and their offsprings showed several transcripts dysregulated between the two groups which included changes in gene expression associated with increased apoptosis (*BAK1*), cell cycle regulation (*CDKN1B*),

metabolic process (*LRPAP1*), insulin action (*IGF2R*) and increased immune and inflammatory response (*IL27RA*), whereas response to stress (*HSPA8*), damage stimulus (*XRCC6*), and chromatin remodelling (*TINF2*). These results suggested that systemic telomere maintenance, metabolism, cell signalling, and redox regulation may be important for individuals to maintain their healthy state with advancing age and that these processes play an important role in the determination of the healthy life-span (Rahman et al., 2013). It is known that the efficiency of autophagic/lysosomal degradation declines with ageing and leads to increased intracellular accumulation of waste products that can lead to age-related neurodegenerative disease and cardiovascular disease in the elderly and descendants of these ceneterians may partially inherit the trait. The waste-cleaning activity via autophagy may serve as a conserved mechanism to prolong the life span across various species, including humans (Xiao et al., 2018).

Several comparative studies of offspring of long-lived individuals with age-matched controls, such as the Longevity Gene Study, the Leiden Longevity Study, the New England Centenarian Study, and the Long Life Family Study show offsprings of long lived indviduals display favourable blood lipid profiles, lower prevalence of hypertension and metabolic and cardiovascular disease and all-cause mortality compared to their peer age-matched controls. The glucose levels correlate with the number of T2D SNPs in the Leiden Longevity Study which might contribute to the improved metabolic profile and glucose tolerance in spite of the presence of T2D GWAS SNPs. Other studies have identified association of longevity with variants of APOE and *FOXO3A*. Centenarians and their offsprings may have the potential to delay age-related methylation or other epigenetic changes (Ar, 2013). The forkhead

box O3A (*FOXO3A*) transcription factor contains alleles associated which may contribute towards extended lifespan by increasing expression or activity of *FOXO3A*. ApoE is a multifunctional protein that is important for the metabolism of cholesterol and TG in an isoform-dependent manner. *APOE* allele carriers exhibit abnormal levels of TC and LDL-C levels. *APOE* ε4 allele is a frailty gene and has been shown to associate with survival to beyond 90 years. Studies with rodents show the *ε*4 form of APOE exhibits an impaired ability to promote amyloid β proteolysis. In fact, nonagenarians and centenarians are less likely to carry an *APOEε4* allele which decreases the risk of Alzheimer's Disease while the *ε*2 allele is enriched in long-lived individuals (Tindale et al., 2017). An allele in apolipoprotein C3 involved in fat metabolism is also enriched in centenarians and may confer them a favourable lipid profile over their matched peers (Atzmon et al., 2006).

Other genes with variants enriched in centenarians include those in human telomerase reverse transcriptase that is associated with longer telomere length which might lead to centenarians and their offspring maintaining longer telomeres that eventually confer protection from age-related diseases (Wheeler and Kim, 2011). Other studies have shown that 3′-phosphoadenosine 5′-phosphosulfate synthase 2 is significantly higher in offspring of long-lived parents. Mutations in host genes of this protein is seen skeletal dysplasias patients and might cause premature joint degeneration due to impaired proteoglycan sulfation (Yerges-Armstrong et al., 2016).

Irisin which is a type III domain-containing protein 5 of skeletal muscle, acts in the white adipose tissue by promoting the acquisition of a brown adipocyte phenotype prone to energy expenditure and therefore might help in reducing the risk of obesity

and insulin resistance. Recently two single-nucleotide polymorphisms in the gene were shown to be associated with *in vivo* insulin sensitivity which in centenarians maybe associated with insulin sensitivity/signalling. In addition, it can help preserve vascular function and skeletal muscle mass as well as its levels in circulation can predict telomere length in healthy adults (Sanchis-Gomar et al., 2014.).

Sequence analysis of the *IGF1* and *IGF1* receptor genes of female centenarians, their offspring and offspring-matched controls showed overrepresentation of heterozygous mutations in the *IGF1R* gene amongst centenarians and their offsprings. This overrepresentation was associated with high serum IGFI levels as well as reduced activity of the IGFIR/IGF1 with an inverse relation to insulin sensitivity, all of which might have a crucial factor in modulation lifespan and human longevity (Suh et al., 2008; Vitale et al., 2012).

Results from a study on the response of lymphocytes to the induced oxidative stress in semi-supercentenarians, their offspring, elderly controls and young individuals show that the ratio of the ROS levels is comparatively similar in centenarian and young individuals in almost all subsets of T or B lymphocytes, and NK-cells. The change in response to oxidative stress might be due to the observed differences in epigenetics and DNA methylation in genes like *GGT1, GGT6, GPX5, GPX6, GSTM,* and *LDHD* that minimize the oxidative damages and therefore preserve a better cellular response especially in the immune system during longevity in humans (Sizzano et al., 2018) .

Association of RNA editing genes *ADARB1* and *ADARB2* with extreme ageing and lifespan has also been reported in four centenarian studies and invertebrate models.

These two genes in the adenosine- to -inosine RNA editing pathway assists in post-transcriptionally converting adenosine residues to inosine which leads to change in gene expression profile and protein function. Invertebrate mutants of *adr-1* and *adr-2* display shorter lifespans possibly due to the declines in ADAR function as a result of knockdown of RNA editing genes which result in increased RNAi activity. This increased RNAi might target genes downstream of *daf-16*, thereby reducing the increases in lifespan otherwise evident in wild type strains (Sebastiani et al., 2009).

Ageing or senescence increase vulnerability to chronic age-associated diseases. Often, the same underlying changes that cause grey hair also inversely affect the functionalities of other organ systems. For instance, chronic diseases of ageing, like type 2 diabetes (T2D), which affects millions of patients, share molecular mechanisms with ageing including inflammation and oxidative stress. Additionally, T2D also leads to impairments and comorbidities that are themselves chronic diseases of ageing, like kidney impairment and cardiovascular disease (Schernthaner and Schernthaner-Reiter, 2018). Insulin sensitivity appears to decline with age (Chandler-Laney et al., 2011). Factors contributing to age-associated insulin resistance include visceral adiposity and associated lipotoxicity, inflammation, oxidative stress, mitochondrial dysfunction and possibly an intrinsic decline in insulin sensitivity in skeletal muscle (Hurrle and Hsu, 2017; Kitada et al., 2019). Ageing is also a strong predictor of acute hypoglycaemia. Older patients with diabetic kidney disease, who are under an intensive glucose-lowering regimen, are at high risk of severe hypoglycaemia (Schernthaner and Schernthaner-Reiter, 2018). Ageing arteries also seem to exhibit chronic inflammation similar to that seen in diabetes and related complications like

hypertension. In fact, acute hyperglycaemia effects vessel function in T2D (Gordin and Groop, 2016).

Although centenarians have some insulin resistance compared with their offspring or short-lived individuals, it is possible it may confer protective repair or adaptive responses. Offspring of centenarians or those who had one parent who lived into the eighth decade of life also tend to have longer healthspans, are healthier and have a lower risk of developing diabetes. This may be due to variant genotypes of the Forkhead box O3 (*FOXO3A)* and insulin growth factor receptor (*IGF1*) genes amongst others inherited from their parents (Halter et al., 2014).

The evidence outlined above shows that ageing outcomes, like T2D and others, may not be distinct disorders, but instead a cumulative effect of the dysfunction of key hallmarks culminating in a decline in health and normal physiology that drives ageing. While lifestyle and environmental factors may affect lifespan, inherited genetic backgrounds may be attributed to ~25% of the factors affecting lifespan and patterns of progression to ageing outcomes as determined by comparing the age of death of monozygotic and dizygotic twins in family studies where it is seen that the inluecne of genetic factor is more pronounced at older ages and in males more than in females (vB Hjelmborg et al., 2006; Herskind et al., 1996). In fact, genetic backgrounds have even been shown to influence the effects of lifespan extension in response to dietary restriction (DR) in mice (Liao et al., 2010; Rikke et al., 2010). Therefore, it is important to unlock the factors that modulate this heterogeneous pattern of ageing in order to not only extend lifespan, but also extend healthy disability-

adjusted life years. The following sections briefly outline some of the causal factors and consequences of ageing.

1.2 Ageing and common disease

The increase in life-expectancy in the recent decades is associated with significant prevalence of chronic co-morbidities. It is estimated that 86% of the elderly population have one or more of the chronic ageing disorders. Of these, 56% of the elderly require healthcare related to cardiovascular diseases, 46% musculoskeletal, 14% respiratory conditions and as much as 30% neurological diseases (Naughton, Bennett, and Feely, 2006). In England alone, the prevalence of co-morbidities in the ageing population is between 40% to 75% (Melzer et al., 2015). There appears to be significant increases in these morbidities with advancing age. For instance, the estimated prevalence of coronary heart disease increases from 15% in the 65+yrs to 35% in the 85+yrs old (Melzer et al., 2015). A similar pattern is seen with heart failure which shows a three –fold increase from 65+ to 85+ yrs. There is an estimated increase from 45% to 70% for hypertension between the aforementioned age groups. Similarly, the prevalence of cancer increases from 5% to 8-16%, the prevalence of osteoarthritis increases from 20 to 35% while that of diabetes increases from 15% to 20% from the 65+ to 85+ year old age groups (Melzer et al., 2015).

Cardiovascular and metabolic diseases are amongst the common chronic disease of ageing. These include chronic ischemic heart disease, heart failure, and arrhythmia, as well as type 2 diabetes and the metabolic syndrome. (Ungvari et al., 2010; Zieman, Melenovsky, and Kass, 2005). Amongst other chronic diseases of the ageing is

osteoarthritis which results in high rates of severe hip and knee arthritis in the elderly (Greene and Loeser, 2015). Mild short-term memory loss and slower processing speed also accompany normal ageing and adversely affect cognitive performance in personal life such as safe driving. Amongst the disorder associated with cognitive impairment is dementia (Ljubenkov and Geschwind, 2016). Alzheimer's disease (AD) is the most common form of dementia accounting for an up to 80% of dementia in the 65+ years of the elderly population (Alzheimer's Association 2015). Elderly with dementia often require caregiver support and possibly assistive technologies to improve safety on a daily basis (Ljubenkov and Geschwind, 2016) .

Diabetes is an exemplar disease of ageing, as well as being a risk factor for other co-morbidities of the ageing such as cardiovascular disease (Odden et al., 2014) amongst others. Various genome wide association studies have detected 403 type 2 diabetes (T2D) genetic variants influencing multiple processes in tissues and cells such as β-cells, islet development, islet senescence, islet function, adipocytes, skeletal muscle, liver and other tissues (Mahajan et al., 2018). Although each of them has a minute effect on the risk of T2D, they explain around 20% of the risk of T2D (Mahajan et al., 2018). Because T2D is such a heterogeneous disorder, it demands an individualized approach to treatment; therefore, it is necssary to unravel the mechanism or biomarker vehicle which we can use to implement the individualized therapeuctic approach.

In non-diabetic individuals, glucose homeostasis in the body is maintained by the normal insulin secretory response from the pancreatic β-cells. When blood glucose levels are high, hepatic glucose production is suppressed (Cersosimo et al., 2000). Instead, glucose uptake is increased by hepatic, gastrointestinal and peripheral

tissues especially the muscle which is regulated by glycogen synthesis and mainly glycolysis (Cersosimo et al., 2000).

In non-diabetic fat cells, insulin inhibits lipolysis and suppresses the release of free fatty acids (Bays, Mandarino, and DeFronzo, 2004). However, insulin resistance during T2D prevents insulin from acting on fat cells; this leads to increased lipolysis and higher levels of free fatty acid which cause lipotoxicity and further aggravates insulin resistance (Kashyap et al., 2003). High levels of free fatty acid levels lead to further increase in glucose production which accompanies decline in use of peripheral glucose and aggravates impaired pancreatic β-cell function (Kashyap et al., 2003). In T2D, decreased peripheral glucose uptake in muscle as well as higher blood glucose is evident during insulin resistance (Hunter and Garvey, 1998). Although initially, pancreatic β-cells may try to compensate by producing insulin to maintain normal blood glucose levels, but eventually β-cell function may progressively deteriorate beyond compensatory capacity. In addition to the impaired insulin secretion, there appears an aberrant production of the α-cell hormone glucagon due to the inefficient release of gastrointestinal incretins after meal intake (Knop et al., 2007). This effect may be compounded by the impaired insulin response which would otherwise suppress glucose production. This means there is higher than normal levels of glucagon levels, which would otherwise in a healthy individual be suppressed during hyperglycemia as well as hyperinsulinemia and oppose the effects of insulin, thus increasing hepatic glucose production and ensure that glucose supply especially to the brain is well-maintained. α-cell dysfunction is also an essential contributor to fasting hyperglycemia as a result of the elevated hepatic glucose and elevated glucagon (Dunning and Gerich, 2007).

The high levels of glucose levels in T2D induce hypoxia and hypoxia-induced pathways in β-cells and isolated islets (Wilding, 2014) can lead to decline in the function of both β and α-cells although the rate of β-cell apoptosis is higher compared to the other cells (Bloch et al., 2012). T2D individuals with insulin resistance also have high FFA concentrations (McGarry, 2002) and fat content in insulin-responsive tissues like the skeletal muscle or liver (Pan et al., 1997; Krssak et al., 1999; Jacob et al., 1999). The high FFA induces reactive oxygen species (ROS) production in the β-cells (Carlsson, Borg, and Welsh, 1999; Li, Frigerio, and Maechler, 2008) which inversely effects survival of the β-cells through changes in enzyme activity, ion channel transport, receptor signal transduction, dysregulated gene expression and apoptosis (Keane et al., 2015; Newsholme et al., 2012).

While the pancreas can adapt to conditions of increased insulin demand in normal circumstances like pregnancy by increasing its functional mass, these adaptations are provoked by limited hyperglycemic events that lead to very low concentrations of IL-1β by the β-cells (Maedler et al., 2002). The low concentrations of IL-1β in fact enhances β-cell proliferation (Schumann et al., 2007). However, in the face of prolonged exposure to nutrients, IL-1β stimulates release of chemokines, which in turn leads to the increase in intra-islet macrophages in T2D recruitment of macrophages which elevates the levels of IL-1β expression and impair the function of the β-cells (Böni-Schnetzler et al., 2008). Oleate, palmitate and stearate are the most common source of FFAs from the diet and also stimulate IL-1β expression not only in islet cells but also in muscle (Senn, 2006), macrophage, and adipocyte cell lines (Nguyen et al., 2007) and in coronary artery endothelial cells (Staiger et al., 2004). However, β-cells appear to be more sensitive to changes in local IL-1β levels than other islet cells due

to their high number of IL-1 receptors (Scarim et al., 1997; Böni-Schnetzler et al., 2009). Other interleukin like IL-6 increases glucagon secretion from α-cells under fasting conditions or hypoglycemic conditions in islets (Barnes et al., 2014). It promotes α-cell proliferation and prevents α-cell apoptosis during stress while accelerating β-cell apoptosis (Ellingsgaard et al., 2008). It might be a compensatory mechanism in the face of impaired β-cell function, which however, leads to hyperglucagonemia in the diabetic scenario.

One mechanism linking ageing and T2D is pancreatic β-cell impairment. Even healthy individuals with normal glucose tolerance demonstrate impaired insulin secretion with age, although β-cell impairment is worse in those with pre-diabetes and T2D (Szoke et al., 2008). Differential expression of cell cycle proteins controlling cellular senescence, such as $p16^{Ink4A}$, has also been shown to impair β-cell function (Helman et al., 2016). DNA methylation at the promoters of cell cycle genes is seen in ageing mouse pancreatic β-cells and may explain the impaired proliferative capacity of these cells of the pancreas (Avrahami et al., 2015). Like elderly individuals, patients with T2D tend to be overweight and insulin-resistant, which promotes dyslipidaemia and atherogenesis (Halter et al., 2014). In turn, insulin resistance and lipotoxicity aggravate inflammation and macrophage proliferation, promoting amyloid formation and increased ROS, which further contribute to β-cell failure (Halter et al., 2014).

1.3 The hallmarks of Ageing

Most of the common, chronic diseases of ageing are caused by the failure of a few basic health maintenance mechanisms collectively titled the ‘Hallmarks’ of ageing

(López-Otín et al., 2013).The Hallmarks of ageing (Fig 1) include genomic instability (Moskalev et al., 2013b; Mostoslavsky et al., 2006), telomere attrition (Blackburn, Greider, and Szostak, 2006), epigenetic alterations (Talens et al., 2012), loss of proteostasis (van Ham, Holmberg, et al., 2010), dysregulated nutrient sensing (Fontana, Partridge, and Longo, 2010; Harrison et al., 2009), mitochondrial dysfunction (Green, Galluzzi, and Kroemer, 2011), cellular senescence (Baker et al., 2011), stem cell exhaustion (Molofsky et al., 2006; Gruber et al., 2006; Conboy and Rando, 2012) and altered intercellular communication (Laplante and Sabatini, 2012; Rando and Chang, 2012; Russell and Kahn, 2007; Zhang et al., 2013).

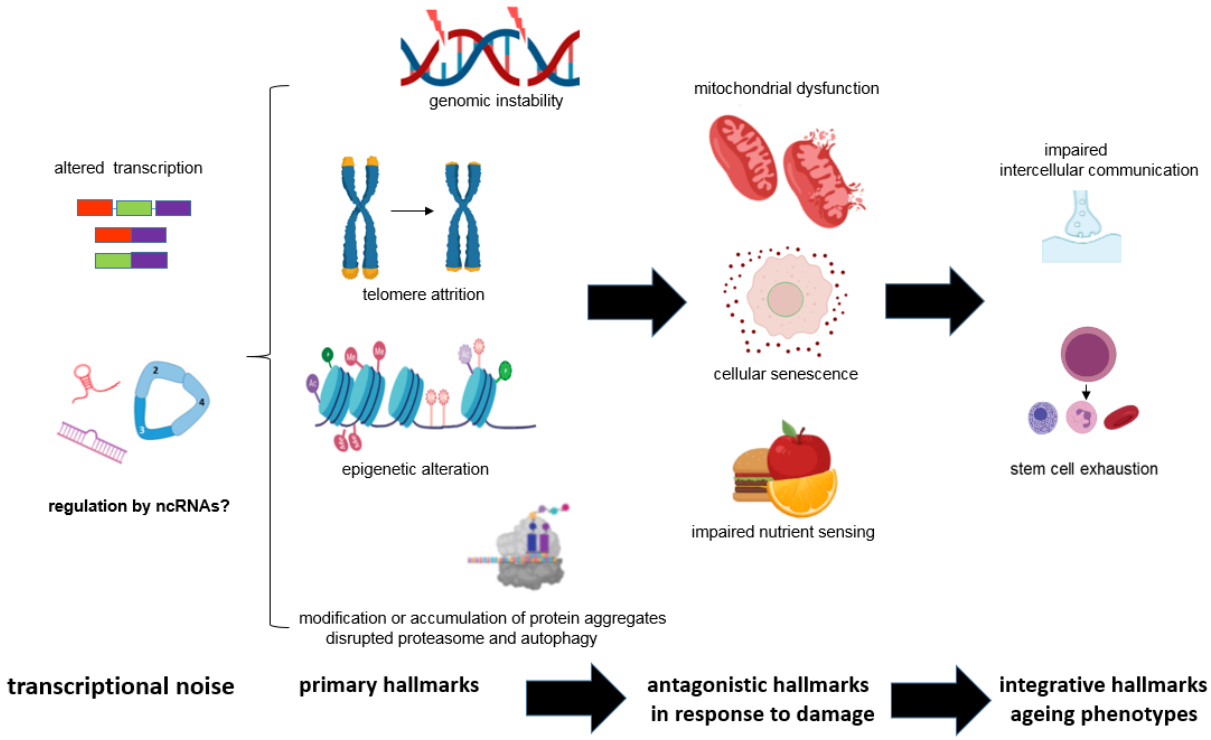

Figure 1 Hallmarks of ageing. *The current hallmarks are grouped into nine major groups. Transcriptional noise is evident in ageing and ageing-related disorders. This may lead to the primary hallmarks of ageing that can cause cellular damage. In response to initial cellular damage, the cells attempt to compensate through antagonistic responses. These compensatory can impose deleterious effect if the damage is chronic which eventually can lead to the integrative hallmarks of ageing that is cumulatively responsible for the functional decline evident in ageing.*

1.3.1 Dysregulated nutrient signalling

Nutrient signalling pathways are cellular pathways that are activated or regulated based on nutrient availability some of which affect ageing and are briefly described below; for instance, declines in endocrine signalling and function correlate with ageing. This disrupts homeostasis and the balance of the stress response due to aberrant hormone production. For instance, age-related changes in reproductive hormones in both male and females correlate with increasing risk of developing chronic ageing phenotypes like heart diseases and impaired cognitive performance, and a decline in adrenal steroids is associated with T2D (Jones and Boelaert, 2015).

The conserved insulin and insulin-like growth factor-1 (IGF-1) signalling (IIS) pathway, responsible for the regulation of growth, metabolism and resistance to stress in response to nutrient availability, has been linked to ageing in worms. The IIS pathway is one of the most conserved pathways controlling ageing, and targets many conserved factors including the FOXO family of transcription factors and mammalian target of rapamycin mTOR complexes (Barzilai et al., 2012; Fontana, Partridge, and Longo, 2010; Kenyon, 2010b). Insulin like receptor (daf2) mutant worms and mouse models have extended lifespans (Tatar et al., 2001; Blüher, Kahn, and Kahn, 2003; Holzenberger et al., 2003). IIS affects lifespan by virtue of its effects on sirtuin deactylases, which confer histone modification (López-Otín et al., 2013).

Mice with mutant growth hormone (GH), which regulates IGF signalling, also display extension of lifespan (van Heemst 2010). Plasma IGF-1 also correlates with lifespan in rodent models (Yuan et al., 2009). IGF-1 and insulin signalling are both glucose sensors in cells, and are cumulatively known as the IIS pathway. Functional

modification due to genetic polymorphisms of the growth hormone (*GH*), the Insulin-like growth receptor 1 (*IGF1*) and the insulin receptor (*INSR*) genes, along with genes encoding downstream effectors like AKT Serine/threonine kinase 1(*AKT*), mammalian target of rapamycin (*MTOR*) and Forkhead box (*FOXO*) family genes. Variants in the phosphatase and tensin homolog (*PTEN*) or phosphoinositide 3-kinase (*PI3K*) genes, have also been linked to longevity in both human and rodent models (Barzilai et al., 2012; Fontana, Partridge, and Longo, 2010; Foukas et al., 2013; Kenyon 2010b; Ortega-Molina et al., 2012). Downregulation of GH and IGF-1 levels, and thus the IIS pathway, is common to ageing (Schumacher et al., 2008). Downregulation of the type 5-adenylyl cyclase hormone in rodents has also been shown to correlate with decreased levels of GH and increased longevity, and is coupled with increased resistance to oxidative stress and increased Ras signalling (Yan et al., 2007). Another hormone, Klotho, has been shown to supress the IIS pathway and promote longevity in rodent models (Imura et al., 2007; Urakawa et al., 2006).

Other signalling pathways such as the transforming growth factor beta (TGFβ) pathway are mediated by activation of the SMAD transcription factors DAF-8 and DAF-14, and the inhibition of DAF-3, which both arrests cell cycle progression and causes apoptosis. It is targeted by the FOXO transcription factor DAF-16 in IIS pathway, suggesting that both these pathways might act through a common subset of downstream adaptors in the ageing physiology (Shaw et al., 2007). Findings from invertebrate models investigating the role of the gut microbiome (GM) in longevity have shown that depletion of FOXO/DAF-16 prolongs life, indicating that the GM nitric oxide also modulates transcription of these pathways to extend lifespan (Gusarov et al., 2013; Kenyon 2010b; Zhang and Hou, 2013).

1.3.2 Dietary restriction and nutrient sensing signalling

The most efficient environmental intervention to slow ageing is dietary restriction (DR) without causing malnutrition. Studies have shown the association of short- or long-term DR with lifespan extension and the association of splicing factor profiles in mouse models, often irrespective of background strain (Lee et al., 2019). DR may enforce its influence on lifespan in several ways, including the modulation of inflammation, proteostasis, autophagy, mitochondrial dysfunction, oxidative damage and genomic instability through IIS, IGF-1, sirtuin- and AMP-activated protein kinase (AMPK) mTOR-dependent signalling pathways (Picca, Pesce, and Lezza, 2017; Kenyon 2010a). Thus, it is not surprising that DR enhances healthspan. Evident pathways in DR include those mediated by AMPK and target of rapamycin (mTOR).

In addition, mTOR itself is associated with different aspects of ageing. It is a serine/threonine kinase that operates through the mammalian target of rapamycin complex 1 and 2 (mTORC1 and mTORC2) complexes (Saxton and Sabatini, 2017). The first component is involved in cell growth through its role in protein synthesis, as well as turnover in response to growth factors, nutrients, oxygen or DNA damage, and lipid/glucose as well as nucleotide metabolism. The second component binds with kinases from other signalling pathways to modulate cell proliferation and survival in response to IIS (Saxton and Sabatini, 2017). Like IIS mutants, knockdowns of mTOR in worms and the use of rapamycin to target mTOR in mice extend lifespan (Vellai et al., 2003). In fact, mTOR signalling has been shown to increase lifespan under DR in model organisms (Heintz et al., 2017).

AMPK is also induced by DR and enhances lifespan in rodents (Anisimov et al., 2005; Baur et al., 2006; Dasgupta and Milbrandt, 2007; Zhang and Hou, 2013). It phosphorylates FOXO and inhibits translation by blocking TOR, suggesting further crosstalk between AMPK, IIS and TOR pathways (Greer et al., 2007; Inoki, Zhu, and Guan, 2003).

The hallmarks of ageing include loss of transcriptional and protein homeostasis. Pre-mRNA splicing is a key link between regulation of gene expression and diversification of the proteome as mentioned in earlier sections. Studies with *in vitro* model show that modulation of spliceosome components may prolong healthy ageing. Specifically, splicing factor 1 is required for lifespan extension through dietary restriction via the AMPK -TORC1 pathway (Heintz et al., 2017). Dietary restriction also uses alternative splicing by coupling to nonsense-mediated decay and induces posttranscriptional regulation of longevity genes to diversify the proteome to allow the remodelling required for enhanced longevity in worms and rodent models (Rollins et al., 2019; Tabrez et al., 2017).

The commensal GM has been shown to sense nutrients in invertebrate models. Treatment with metformin causes an AMPK-dependent increase in lifespan in invertebrate models as a consequence of the effect of the drug on microbes as opposed to the host (Storelli et al., 2011). An extension in lifespan is observed by the effect of the endogenously expressed non-coding RNA (ncRNAs) DsrA of the bacteria which suppresses diacylglycerol lipase which leads to decreased longevity in invertebrates (Nicholson et al., 2012; Liu et al., 2012). In fact, in humans, the GM seems to be stable from the third to the eighth decades of life (Biagi et al., 2010). After

100 years of life, the GM seems to show profound adaptive remodelling and be composed of highly diverse species (Santoro et al., 2018). While there appears to be shrinkage of the dominant symbiotic bacterial species, this shrinkage is counterbalanced by an increase in potentially longevity-subdominant species (Biagi et al., 2016).

1.3.3 Mitochondrial dysfunction

Mitochondria are thought to be key organelles regulating organismal ageing. They operate by controlling the cellular metabolic rate, the production and removal of ROS, and apoptosis (Wallace, 2005). A decline in mitochondrial quality and activity has been associated both with normal ageing and the development of age-related diseases. As we age, our mitochondria show a gradual decline in their ability to generate energy and an increase in the levels of ROS. ROS can lead to DNA mutation and a deterioration in proteostasis (Lesnefsky and Hoppel, 2006; Korovila et al., 2017). ROS can also damage the very proteins that control the replication of mitochondria or introduce additional errors into the copies of daughter mitochondria (Korovila et al., 2017). Mitochondria from the elderly look different compared with those from young individuals. They have a swollen morphology. Their numbers also decline as they lose their ability to efficiently replicate in their dysfunctional state (Gerencser et al., 2008; Seo et al., 2010; Figge et al., 2012). In aged flies, mitochondria are round or have concentric cristae devoid of sharp ridges, and have disorganized inner membranes. Their respiratory activity is also compromised and is accompanied by an increase in ROS production (Brandt et al., 2019). Oxygen uptake decreases while peroxide yield increases, suggesting that old flies may retain a lot of inactive mitochondria (Cochemé

et al., 2011). Mitochondrial respiration is also compromised in hearts of old mice. They have wider cristae and less swirls. They are not filled with closely stacked, parallel cristae, unlike in young hearts where there is a high level of respiratory activity and hence the potential for adenosine triphosphate (ATP) production facilitated by a larger membrane area. The larger membrane area in the latter harbours the ATP synthase for oxidative phosphorylation (Brandt et al., 2019). However, heart mitochondria appear to be protected from oxidative damage, as is suggested by their low and unchanging peroxide yield. It might be that, in vital organs like the heart that are slow to regenerate, mitochondria are more effectively protected from damage compared with those in other organs, like the liver and kidneys, that have high rates of turnover of cells. Kidney mitochondria in old mice have morphology that is similar to those of apoptotic cells. This might be due to the high rate of continuous turnover and short lifespan of kidney cells. The granular appearance of mitochondria in old mice suggests that they may contain granules that retain lipids, glycoproteins and denatured respiratory chain complexes (Brandt et al., 2019). Like mitochondria from the kidney, mitochondria from old livers in mice also have granules and an apoptosis-like phenotype. They are also void of a central matrix (Brandt et al., 2019). The lack of sharp cristae ridges and junctions in the void membranes suggest that these membranes may harbour ATP synthase for efficient oxidative phosphorylation.

As many as thousands of copies of mitochondrial DNA can exist per cell, it is believed that errors in mitochondrial DNA might need to exceed a threshold of 60% of all mitochondria within a given tissue for any significant aberrant phenotypic change to appear (Rossignol et al., 2003). Different ways in which mitochondiral dygsfunction may affect ageing are illustrated in Fig 2. A process called mitophagy eliminates

damaged mitochondria, but this process becomes less efficient with age due to the decline in activity of mitochondrial enzymes (e.g. citrate synthase), the decrease in the respiratory capacity per mitochondrion (i.e. substrate-dependent oxygen consumption), and increases in ROS production and errors passed on to daughter mitochondria. This allows dysfunctional mitochondria to survive longer and accumulate over time (Luo et al., 2013). Findings from a recent study confirmed that stem-like cells, within immortalized human mammary epithelial cell cultures, harbour uneven distributions of young and old mitochondria after cell division (Katajisto et al., 2015). Thus, mitochondria-induced changes in a cell's metabolic profile maybe sufficient to trigger cellular senescence and longevity.

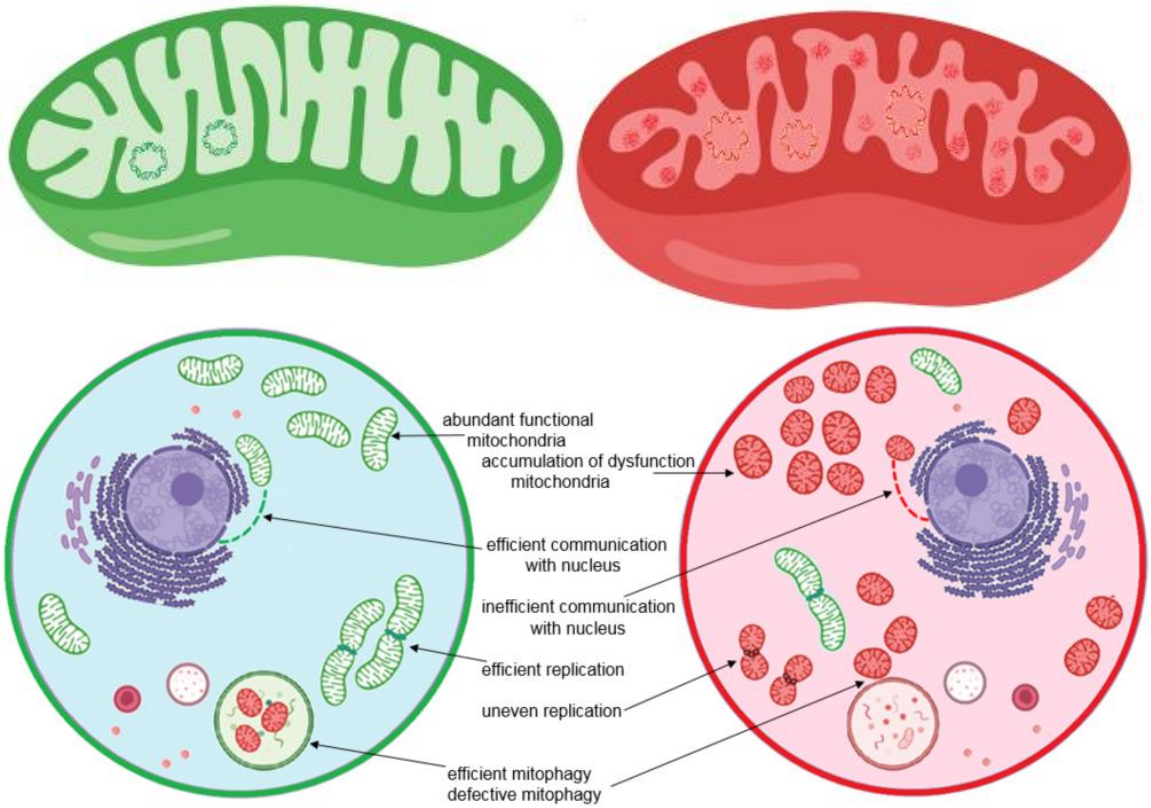

Figure 2 Mitochondrial dysfunction in ageing. *Ageing is associated with decline in mitochondrial function which includes in decline in mitochondrial numbers and inefficient mitophagy. A decline in mitochondrial function leads to malfunction of the electron transport chain, decline in ATP generation, accumulation of mtDNA mutation, generation of ROS that eventually affect various aspect of physiology of cells during ageing (Green=young cell; Red=senescent cell).*

1.4 Cellular senescence and the senescence-associated secretory phenotype (SASP)

Cellular senescence is a stable arrest of the cell cycle, as well as the cellular growth of previously replicative cells. Senescent cells are characterized by flattened and granular morphological features, an altered transcriptome, splicing pattern or epigenome and the senescence-associated secretory phenotype (SASP) (de Magalhães and Passos, 2018; Latorre et al., 2018). Senescence is often induced by a persistent DNA damage response (DDR) and accompanies the expression of antiproliferatives, like $p16^{INK4a}$, which lead to the activation of downstream damage mediated by pathways involving mTOR and amongst others. The activation of these pathways is followed by the downregulation of nuclear lamins, which triggers extensive chromatin remodelling as well as secretion of the SASP (Campisi and di Fagagna, 2007; Childs et al., 2015; Herranz et al., 2015; Kuilman et al., 2010; Laberge et al., 2015).

Potential ways in which senescence might affect ageing at the cellular level is shown in Fig 3. During ageing, chronic SASP secretion induces senescence in neighbouring cells, and leads to chronic inflammation and impaired tissue homeostasis (Acosta et al., 2013; van Deursen, 2014). Despite being non-profliferative, senescent cells are metabolically active (Dörr et al., 2013). Senescence can promote impaired tissue or organ homeostasis through the cumulative action of disruption of the extracellular matrix, aberrant cell differentiation, stimulation of inflammation and ROS-dependent gap junction-mediated cell–cell contact induction of contagious paracrine senescence signals in neighbouring cells (Nelson et al., 2012). It can also affect ageing in non-proliferative cells like neurons and cardiomyocytes by inducing SASP (Sikora, Bielak-Zmijewska, and Mosieniak, 2014).

Temporary senescence confers protection in early life through tumour suppression, wound healing, tissue repair or embryonic development, when it is cleared by the immune system. It is possible that senescence is a cell-intrinsic compensatory mechanism for the removal of potentially damaged cells that would otherwise acquire oncogenic potential. However, in the absence of renewal of progenitor and stem cells to re-establish cell numbers, accumulation of senescent cells and alterations in their secretome, i.e. the SASP, may aggravate the damage seen in ageing. The SASP is enriched with pro-inflammatory cytokines and chemokines that attract immune cells, factors that cause stem cell dysfunction (Beroukhim et al., 2010; Brady et al., 2011; Coppé et al., 2006; Kandoth et al., 2013; Liu et al., 2004; Sluss et al., 2004; Xu et al., 2015).

Age-related decline in immune function leads to a decline in wound healing, reduced response to infections and persistent low chronic inflammation known as inflammageing, which may be be partially induced by senescent cells producing the SASP (de Magalhães and Passos, 2018; Latorre et al., 2018). To test the role of cellular senescence, Baker and Deursen (2016) engineered $p16^{Ink4a}$ positive senescent cells in mice to die when treated with a drug. The study showed that clearance of the $p16^{Ink4a}$-positive cells reduced age-related dysfunction of the kidneys, heart and fat by preserving the performance of glomeruli, cardioprotective K_{ATP} channels and adipocytes, respectively. The kidneys functioned more efficiently and hearts were more resilient to stress, and there appeared to be an extension of lifespan after eliminating senescent cells in these mice (Baker et al., 2016; 2011). In other studies, the senolytic cocktail which selectively kill sensnencent cells, composed of dasatinib and quercetin has been shown to cause selective elimination of senescent

cells, and decrease the number of naturally occurring senescent cells and their secretion of frailty-related pro-inflammatory cytokines in explants of human adipose tissue. Intermittent oral administration of senolytics to both senescent cell-transplanted younger and naturally aged mice alleviated physical dysfunction, increased post-treatment survival by 36% and reduced mortality hazard by 65%. This provides evidence that while senolytics can enhance the remaining health- and lifespans in old mice, senescent cells can also cause physical dysfunction and decreased survival, even in young mice (Xu et al., 2018). Reversal of senescence in cellular models using small molecules based on the polyphenol resveratrol leads to the rescue of morphology and splicing patterns resembling those of young-passage cells (Latorre et al., 2018). One study has suggested that these reversed cells resume the cell cycle independently of SIRT1, SASP modulation or senolysis, as there appears to be an increase in the number of proliferating cells, which is additionally accompanied by an increase in telomere lengths, resetting the telomere clock (Latorre et al., 2017b).

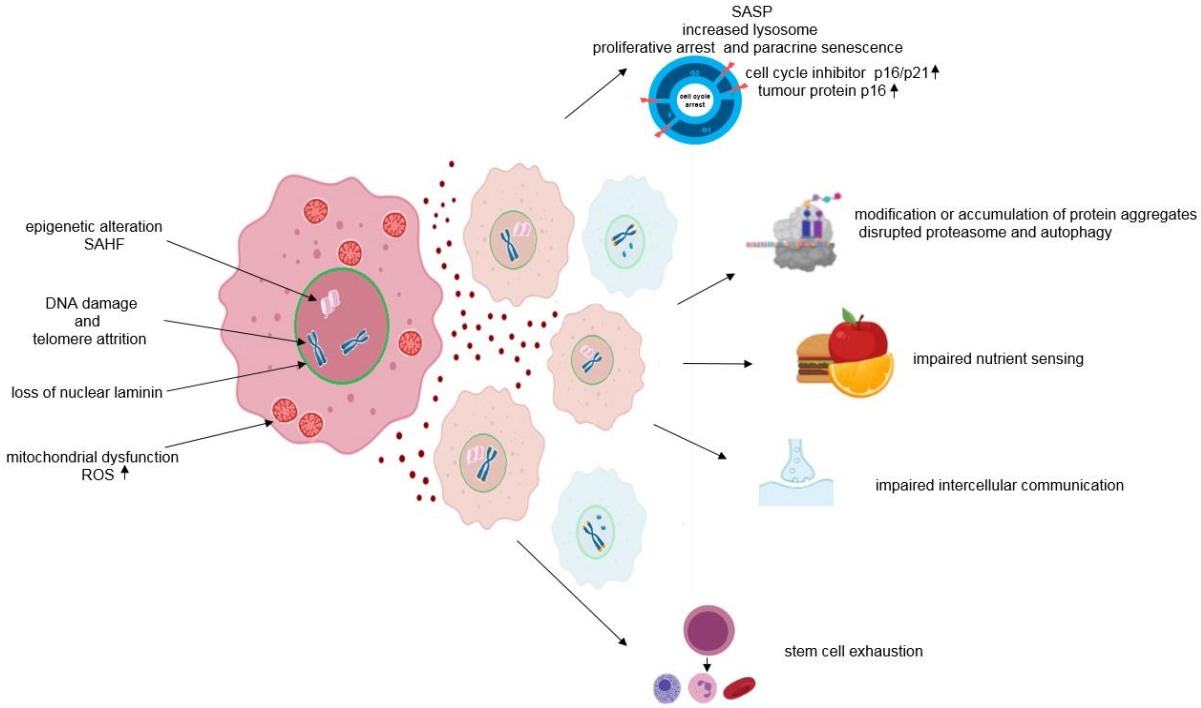

Figure 3 Senescent cells are one of the key features of ageing. *During ageing cellar exposed to various stresses such as DNA damage, mitotic stress, epigenetic stress, ROS /oxidative stress, oncogenic mutation, loss of tumour suppression and telomere attrition. All of these may lead the cells to senescece and induce senescence through the secretion of SASP in the neighbouring cells.*

1.5 Stem cell exhaustion

Stem cells are essential for the maintenance of tissue homeostasis or regeneration. A quantitative or qualitative decline in stem cell is one of the many drivers of ageing. Study in worms show germline stem cells are regulators of longevity as genetic manipulation to eliminate the germline stem cells leads to doubling of lifespan of the worms (Arantes-Oliveira et al., 2002; Hsin and Kenyon, 1999). A decline in the regenerative potential of tissues as the result of ageing-related damage stimuli is evident in ageing (López-Otín et al., 2013). Decreased cell cycle activity of haemopoetic stem cells correlate with the accumulation of DNA damage, overexpression of cell cycle-inhibitory proteins and telomere shortening in experimental models (Janzen et al., 2006; Rossi et al., 2007). Recent research findings indicate that the transplantation of muscle-derived stem cells from young to progeroid rodents improves their degenerative potential through the systemic secretion of certain entities, even in tissues where donor cells are absent (Lavasani et al., 2012), and is evidenced by the fact that deteriorating haematopoiesis leads to reduced production of adaptive immune cells during immunosenescence (Beerman et al., 2010).

1.6 Genomic instability and nuclear architecture

Exposure to extrinsic factors like chemicals, ionizing radiation, ultraviolet light and intrinsic factors like ROS generated within the cell can lead to nuclear and mitochondrial DNA damage. DNA damage may accumulate as a result of mutation through a variety of nucleotide changes induced by deletions, substitutions, insertions, frameshift mutations, the oxidation of nucleotides, deaminations, or through changes in DNA configuration as a result of crosslinks and strand breaks (Fig 4). During ageing,

the ability to repair DNA damage is increasingly impaired, leading to the replication of damaged nuclear DNA in humans as well as mitochondrial DNA in mouse models. This is evident not only in normal ageing, but also in outcomes of accelerated ageing (Moskalev et al., 2013a; Moro, 2019). This loss of genomic integrity may lead to changes in gene expression and protein function at the cellular level that can lead to a reduced cell number though cell cycle arrest, either leading to apoptosis or senescence (Hoeijmakers, 2009; Freitas and de Magalhães, 2011).

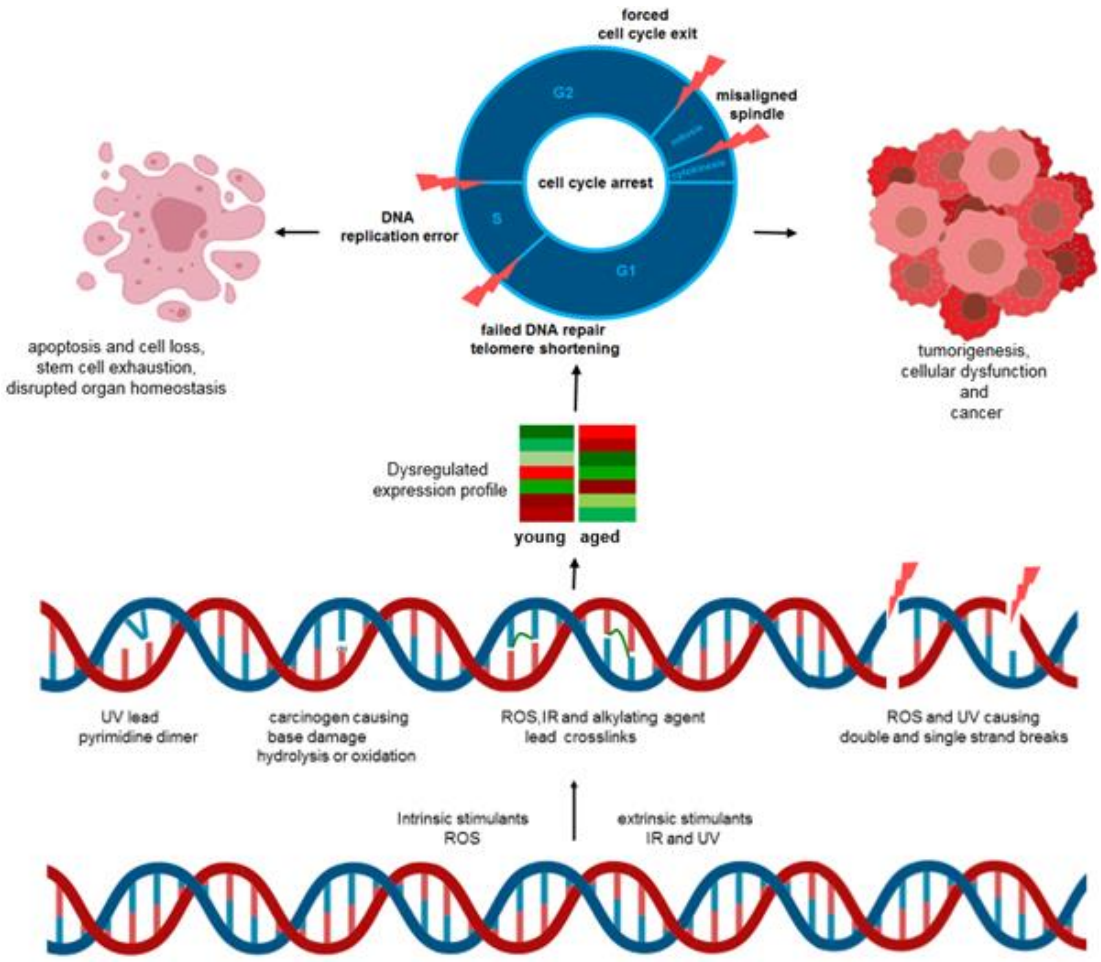

Figure 4 DNA damage and mutation during ageing. *Throughout the course of an organism's life, cells are exposes to extrinsic and extrinsic mutagens that lead to various types of mutation in the nuclear and mitochondrial DNA that may lead to dysregulation of gene expression and translation. These can often lead to dysregulation of cell cycle which can lead to loss of cells through apoptosis o confer them oncogenic potential.*

Through the course of an organism's lifetime, it faces endogenous challenges like DNA replication errors as well as ROS. The microenvironment of the cells in the body also faces continuous exposure to exogenous physical, chemical and biological agents. All of these cumulatively lead to the accumulation of DNA disintegrity and instability, which cause point mutations, translocations, chromosomal gains and losses, telomere shortening and gene disruption due to the integration of mobile elements, i.e. viruses or transposons (Dechat et al., 2008; Gonzalez-Suarez et al., 2009; Liu et al., 2004). Increased chromosomal aneuploidies and copy number variations can also lead to ageing phenotypes (Faggioli et al., 2012; Forsberg et al., 2012; Jacobs et al., 2012; Laurie et al., 2012). The various forms of DNA damage or alteration can, eventually, lead to aberrant transcription of many genes during normal human ageing. This can result in the dysfunction of cells, which necessitates their removal by apoptosis or senescence (Freund et al., 2012; Gregg et al., 2012; Ragnauth et al., 2010; Scaffidi and Misteli, 2006; Shimi et al., 2011)

1.7 Epigenetic alterations and chromatin remodelling

Eukaryotic genomic DNA is compressed into chromatin as nucleosomes consisting of histone octamers, made up of two copies each of the core histones H2A, H2B, H3 and H4, each wrapped by 146 bp of DNA (Luger et al., 1997). In this compressed form, gene transcription is blocked due to the inability of transcription factors to access the DNA (Lawrence, Daujat, and Schneider, 2016; C. Jiang and Pugh, 2009). Epigenetic changes involve alterations in DNA methylation, histone methylation, acetylation states, histone post-translational modification and chromatin remodelling that occur during the course of a cell's life (Talens et al., 2012), which together regulate

the condensed heterochromatin or relaxed euchromatin states to make DNA less or more accessible, respectively, to affect the transcription levels of genes and their biological functions.

It is well known that changes in DNA methylation at CpG islands correlate with ageing and, as such, are markers of stem cell division and cell ageing in general (Yang et al., 2016). There appears to be a decrease in global DNA methylation across the genome that facilitates deheterochromatization of the genome with advancing ageing. However, some promoter regions and CpG islands, like in tumour suppressor genes (e.g. *CDKN2A*, *LOX*, *RUNX3* and *TIG1*), become aberrantly hypermethylated (Issa et al., 2001; 1996; Singhal, Mays-Hoopes, and Eichhorn, 1987; So et al., 2006; Sommer et al., 2006; Waki et al., 2003). Thus, it is not surprising that histone demethylases have been shown to associate with the IIS signalling pathway, which is key to lifespan (Jin et al., 2011; Maegawa et al., 2010). Increased histone H4K16 acetylation, and H4K20 and H3K4 trimethylation, as well as decreased H3K9 and H3K27 trimethylation, have also been linked to age-associated epigenetic changes (Fraga and Esteller, 2007; Han and Brunet, 2012). In addition, global loss of heterochromatin and redistribution has been linked to the ageing process (Pegoraro et al., 2009). Chromatin-remodelling complexes and chromatin regulators such as, alter histone–DNA interactions and contribute to the global condensation of senescence-associated heterochromatin foci (SAHF) (Zhang et al., 2005). The formation of SAHF is thought to silence the expression of proliferation-promoting genes, which may contribute to senescence-associated growth arrest in ageing (Narita et al., 2003).

1.8 DNA double strand breaks and mutations

Different types of DNA damage can lead to genomic instability. Accumulation of DNA double-strand breaks (DSBs) and inefficient DSB repair-causing mutations have been reported in both *in vitro* and *in vivo* models of ageing. Transposition of transposable elements can also lead to mutations (Sedelnikova et al., 2008; 2004; Singh et al., 2001). The mTOR inhibitor rapamycin has been shown to reduce DNA damage in rodents (Dao et al., 2015). Besides mTOR, calorie restriction, which is also linked to prolonged lifespan, has also been positively associated with enhanced efficiency of nucleotide excision repair and non-homologous end joining (Lee et al., 2011; Stuart et al., 2004).

1.9 Telomere Attrition

Telomeres are protective caps, composed of long repetitive sequences of TTAGGG, at both ends of chromosomes. They protect the strands from getting shorter during cell division. They allow anchorage to telomere-binding proteins as well as confer protection against events that could otherwise lead to cell death. Telomere lengths are highly heterogeneous and can vary from 5000–15,000 bp at birth. The telotypes of individuals depend on the telomere lengths of their parents (Andrew et al., 2006; Codd et al., 2010; Hunt et al., 2008; Jeanclos et al., 2000; Levy et al., 2010; Mangino et al., 2008; Moyzis et al., 1988; Slagboom, Droog, and Boomsma, 1994; Vasa-Nicotera et al., 2005).

Normal ageing, age-related pathologies and premature ageing syndromes have all been associated with the shortening of telomeres (Aubert and Lansdorp, 2008; Johnson, Sinclair, and Guarente, 1999). A demonstrataion of possible role of telomere

shortening in ageing in Fig 5. Shortening of telomeres has been linked to decreased cellular metabolism in rodent models, where it accompanies mitochondrial dysfunction and aberrant Ca^{2+} signalling, and leads to the disruption of organ homeostasis, e.g. affecting the insulin secretory potential of pancreatic β-cells (Guo et al., 2011; Sahin et al., 2011). Short telomeres can induce cellular senescence, upregulate the secretion of inflammatory factors and alter expression profiles by disrupting the heterochromatin states of genes. As they become progressively shorter, telomeres become dysfunctional and induce the DDR, resulting in apoptosis and permanent cell cycle arrest (Njajou et al., 2007).

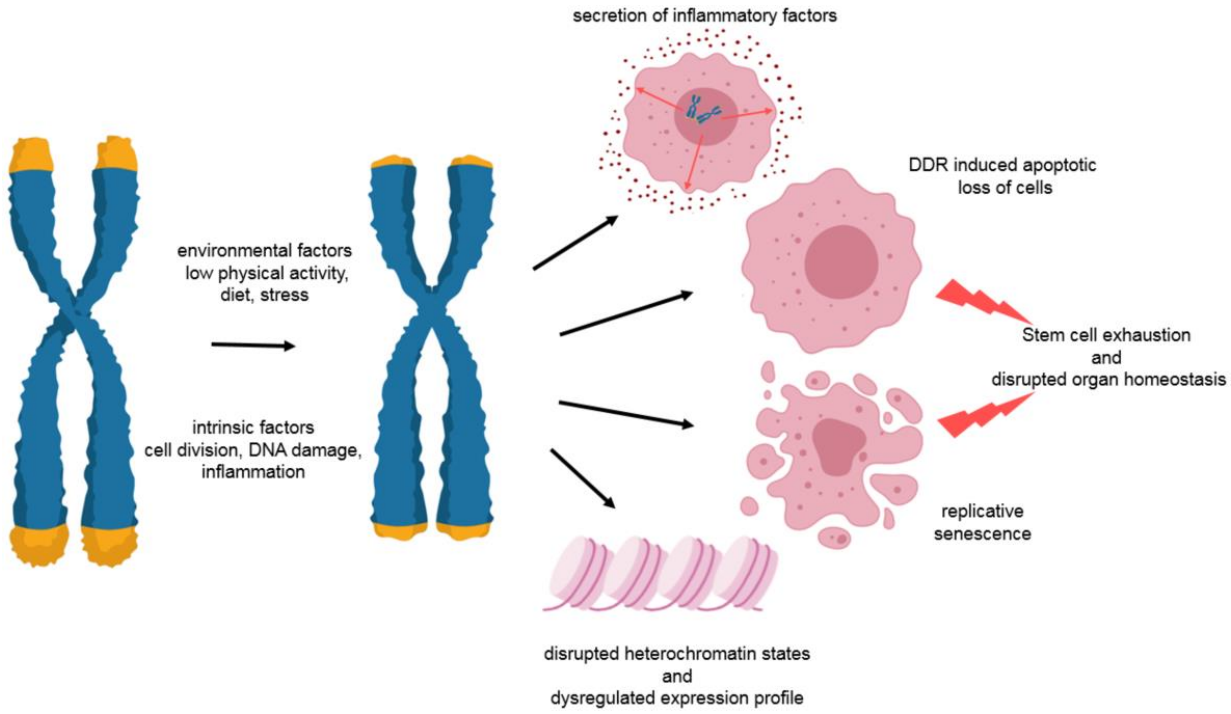

Figure 5 Telomere attrition. *Telomere shortening can lead to loss of genetic material with each successive cell division during the course of an organism's life. This can lead to changes in chromatin states of genetic material that affect the expression of inflammatory cytokines, induce DNA damage responses as well as replicative senescence which can cumulatively lead to loss of stem cell and disrupt organ homeostasis ultimately leading to organ failure in ageing.*

1.10 Altered Transcription

RNA metabolism involves an array of events coordinated by the interaction of coding as well as ncRNAs with RNA-binding proteins (RBPs) for the transcription, maturation, post-transcriptional modification, subcellular transport and degradation operated by RNP complexes (Glisovic et al., 2008). Ageing has been associated with an increase in transcriptional noise, and the aberrant production and maturation of mRNA transcripts (Harries et al., 2011). Other studies have reported age-related transcriptional changes in genes involved in inflammatory, mitochondrial and lysosomal degradation in ageing tissues (de Magalhães, Curado, and Church, 2009). Age-related differential expression of ncRNAs is also known to be associated with lifespan (Dimmeler and Nicotera, 2013).

1.10.1 Regulation of gene expression

Age-linked differential expression analyses have categorized the regulation of gene expression into six hallmarks of cellular ageing. These are: downregulation of genes encoding mitochondrial proteins, downregulation of genes of the protein synthesis machinery, dysregulation of immune system genes, downregulation of growth factor signalling, constitutive responses to stress including DNA damage and the dysregulation of gene expression as well as mRNA processing.

The downregulation of genes encoding mitochondrial proteins, such as nuclear-encoded components of the ETC and mitochondrial ribosomal proteins, is evident in diverse types of organisms ranging from humans, rodents and flies to worms (Frenk and Houseley, 2018). Although reductions in mRNA levels of mitochondrial proteins

are small, they lead to reductions in the ETC, ATP synthase, the tricarboxylic acid cycle and mitochondrial ribosomal proteins in humans (Frenk and Houseley, 2018).

The downregulation of protein synthesis machinery, such as ribosomal proteins and ribosomes, in ageing might be a protective programme aimed at mitigating age-related outcomes. Downregulation of ribosome biogenesis and ribosomal protein genes is not causal for ageing, because both caloric restriction and rapamycin treatment extend health- and lifespan, but conversely they lead to the downregulation of mRNA levels of ribosomal proteins through reduced mTOR activity (Iadevaia, Liu, and Proud, 2014). In fact, low expression of ribosomal protein mRNA correlates with longevity in long- and short-lived cell types in humans (Baumgart et al., 2016; Seim, Ma, and Gladyshev, 2016).

Downregulation of genes associated with cell growth is evident in old human and worm muscle tissues (Ma et al., 2016; Zahn et al., 2006). Similar patterns of change in the expression profiles of GH/IGF-1 signalling pathway genes are seen in aged mouse livers (Schumacher et al., 2008) and vascular endothelial growth factor (VEGF), which is required for skeletal muscle capillarization, evident in old mice and humans (Ryan et al., 2006; Wagatsuma, 2006). In fact, perturbations of the IIS pathway extend lifespan and delay ageing pathologies across worms, flies, mice and humans (Fontana, Partridge and Longo, 2010). It is also possible that, during ageing, reduced mitochondrial activity and protein synthesis lead to the inhibition of cell growth and proliferation, due to reductions in the generation of energy and raw materials. It could also simply signify an increasing prevalence of senescent cells during ageing as a result of transcriptional profile changes that lead to cell cycle arrest, and hence the

accumulation of senescent cells (Shelton et al., 1999). Repairing of otherwise somatic damage is expensive and, perhaps, takes place only when reproduction is negatively impacted (Kirkwood, 1977).

Changes in the expression of stress response-associated genes are observed during ageing in flies (Frenk and Houseley, 2018). In fact, exposure of flies to heat stress extends lifespan (Sarup, Sørensen, and Loeschcke, 2014). Heat shock proteins are also upregulated in ageing worms and mice (Walther et al., 2015; Hamatani et al., 2004). The Unfolded Protein Response (UPR^{mt}) stress response regulates genes that are involved in protein folding and changes in ROS defence, metabolism and modulation of the innate immune response (Nargund et al., 2015; Schulz and Haynes, 2015). It is suggested that activation of the UPR^{mt} extends lifespan in worms carrying *Clk1* mutations, lowering ROS levels and suppressing the UPR^{mt} (Nargund et al., 2012).

Dysregulation of gene expression and mRNA processing may be associated with highly conserved age-dependent changes in chromatin structure. Transcriptomic noise and transcriptional drift result in opposing changes in transcripts of the same functional group and increase in organisms during ageing (Rangaraju et al., 2015). Manipulation of transcriptional drift, by inhibiting serotonergic signalling, alleviates physiological deterioration and enhances lifespan in ageing mice (Southworth, Owen, and Kim, 2009). Senescent cells tend to harbour clusters of heterochromatinized DNA, i.e. SAHF. This is seen with widespread foci of hypomethylation in senescent human myofibroblasts (Narita et al., 2003; Cruickshanks et al., 2013). Increased transcriptional variability can also be due to changes in post-transcriptional processing

of mRNA. Microarray data from human peripheral blood suggest that pathways most likely to be disrupted with ageing are those involving genes associated with mRNA splicing, polyadenylation and other post-transcriptional events (Harries et al., 2011), and age-linked changes in the transcript levels of splicing factors (Holly et al., 2013). Additionally, a correlation is seen between the expression of splicing factors *HNRNPA1* and *HNRNPA2B1*, and both lifespan in mice and longevity in humans (Lee et al., 2016). In fact, a recent study has demonstrated the effects of global defects in pre-mRNA splicing in ageing worms, showing that a homologue of splicing factor-1 (SFA-1) in worms is required for lifespan extension under DR conditions in a TORC1- and alternatively spliced transcript-dependent fashion (Heintz et al., 2017).

Age-related changes in expression are evident in normal ageing, and are also associated with lifespan and predictive markers of ageing phenotypes such as cognitive function (Harries et al., 2011; 2012; Holly et al., 2013; Lee et al., 2019). Altered expression of splicing factors has been reported in peripheral blood in human and mouse models, as well as in senescent cell cultures. In fact, in mouse models, altered expression of slicing factors is evident in young long-lived mice, indicating that the pattern of splicing factor expression in early life may be driver of lifespan in some cases, while in other cases it may be a causal outcome of ageing (Lee et al., 2016). Likewise, young litters of long-lived mice show enhanced isoforms of trp53 that promote cellular growth, while older mice have downregulated Cdknt2a, which promotes senescence (Huang et al., 2002; Almog, Goldfinger, and Rotter, 2000; Wu et al., 1997; Tominaga, 2015). As stated earlier, the reversal of senescent phenotypes *in vitro* has been achieved through the modulation of expression patterns of splicing factors (Latorre et al., 2017a; Latorre et al., 2018).

1.11 Splicing and splicing factors

Constitutive splicing occurs when splicing events do not contribute to isoform diversification because constitutive splicing always pertains the way in which mRNA is spliced in exactly the same way every time (Ding and Elowitz, 2019). This is unlike alternative splicing which allows generation of isoforms using different exons in different orders. Splicing can be executed by the major spliceosome U2 or by the minor spliceosome U12 (Fig 6). The spliceosome involved in U2-dependent splicing consists of U1, U2, U4, U5 and U6 small nuclear ribonucleoprotein particles (snRNPs), and non-snRNPs. The minor spliceosome, like the major spliceosome, contains the U5 snRNP; however, instead of U1, U2, U4 and U6, it has functionally analogous U11, U12, U4atac and U6atac (Patel and Steitz, 2003). Both operate in a similar manner, and 99% of human introns are spliced out by the major U2 spliceosome. Most U2-dependent introns harbour a 5' SS with a GTNAG sequence, and 3' SS end with CAG or TAG. However, a common atypical U2-dependent splicing event can occur around a 5' SS that starts with a GC. The introns spliced by the minor U12-dependent spliceosome account for small percentage of all nuclear introns, and have a longer consensus sequence at the 5' SS and branch points. The minor U12-dependent spliceosome carries out non-canonical splicing to remove rare introns with different SSs. These introns containing non-consensus AT–AC and a high degree of conservation at the 5′ SS instead of the typical GT–AG or relatively variable sequences at the 5′SS (Jackson, 1991).

The assembly of the spliceosome through two transesterification reactions leads to the generation of an mRNA from pre-mRNA. The first step of this assembly process is the generation of the E-complex, which involves the recognition of the 5' SS by U1, branch point recognition by non-snRNPs, and recognition of the polypyrimidine tract

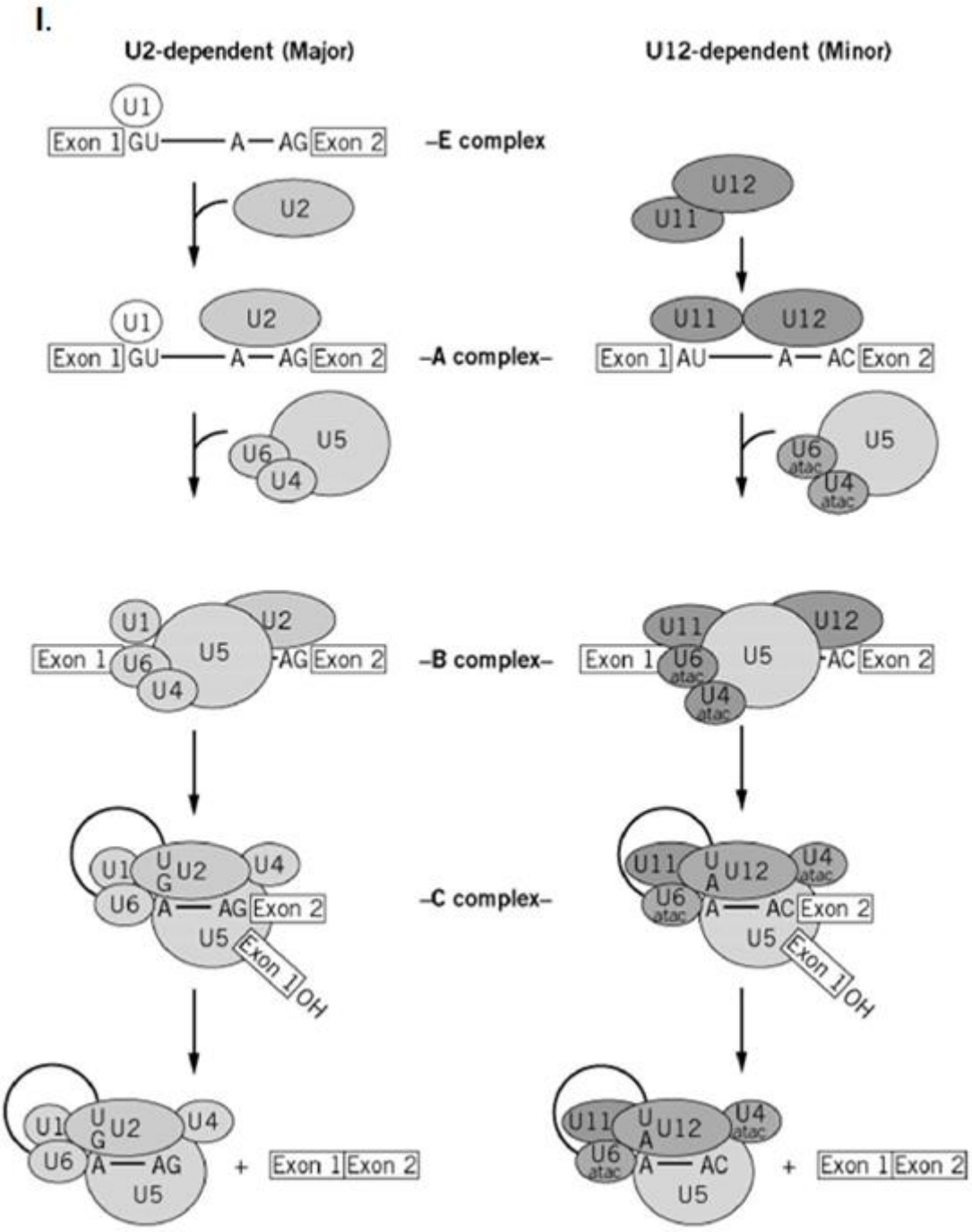

Figure 6 Mechanism of splicing (I) and different types of alternative splicing (AS) events and (II). *Splicing events can be executed by the major U2 or by the minor U12 spliceosome. While the U2-dependent splicing consists of U1, U2, U4, U5 and U6 small snRNPs, the minor spliceosome consist of U11, U12, U4atac and U6atac instead of U1, U2, U4 and U6 besides the U5 snRNP. Both operate in a similar manner to generate alternative isoforms ("Advanced Genome Bioinformatics").*

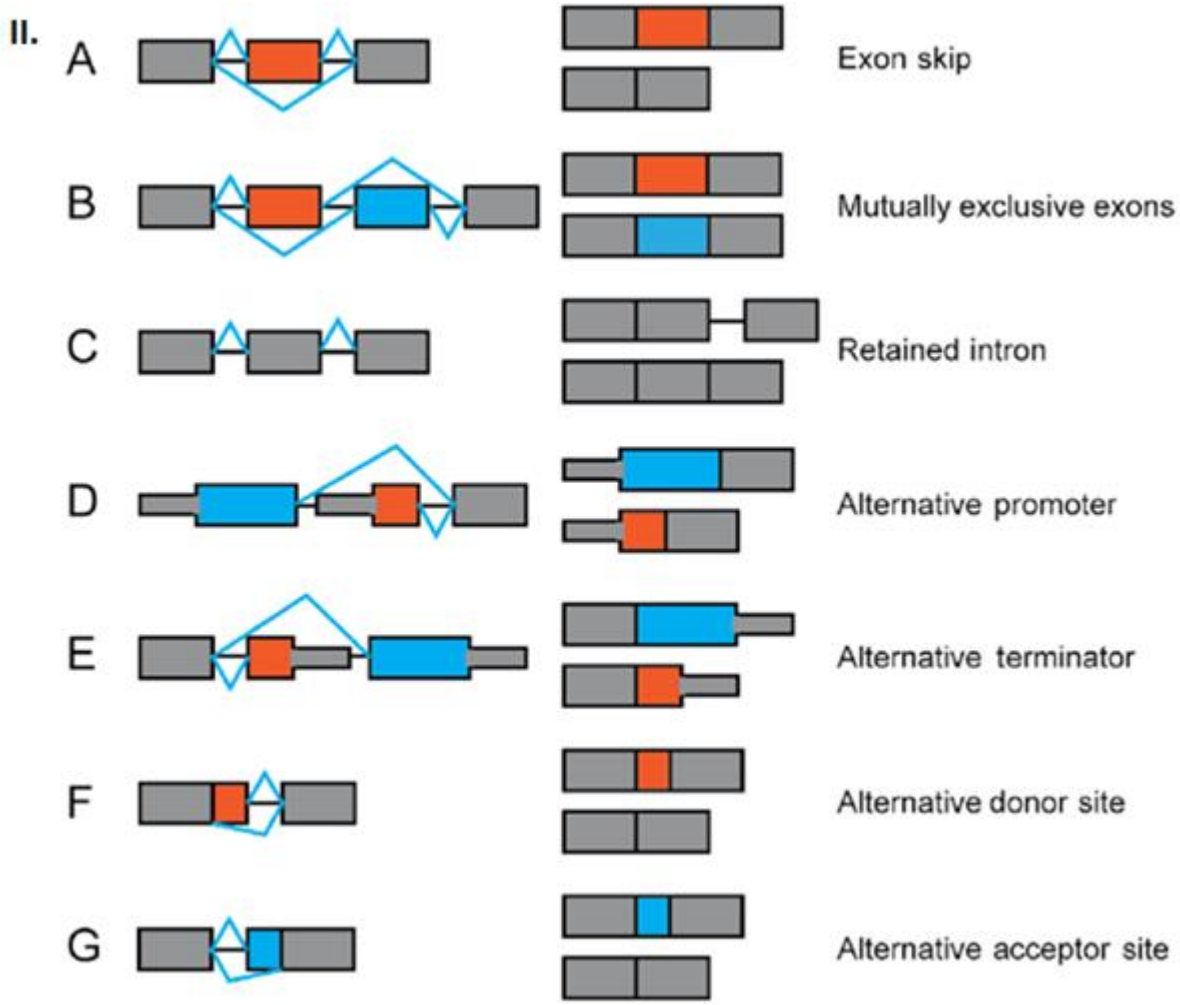

Figure 6 Mechanism of splcing (I) and different types of alternative splicing (AS) events and (II). (*A) Exon skipping occurs when an exon is removed alongside the introns flanking either side of it; (B) Mutually exclusive exons are generated when one exon in exclucded at the expense of other being retained in the transcript; (C) Retained intron splicing is formed when an intron is retained in the final transcript; (D and E) Alternative promoters and alternative terminators are in transcripts which exons with more than one initiator or terminator; (F and G) Alternative 5' splice site and alternative 3' splice site selections are generated from exons with more than one splice site at the donor or acceptor end of an exon (Shi et al., 2018).*

and the 3’ SS by U2. This is followed by the generation of the pre-spliceosome A-complex, where U2 binds to the branch point. This event is followed by the generation of the pre-catalytic B-complex when U4–6 assemble together. Thereafter, conformational rearrangement occurs leading to the assembly of the catalytically active C-complex. In this complex, the first reaction allows the binding of U2, U5 and U6 to lariat introns and exons. A second catalytic reaction caused by this C-complex cleaves off the lariat from the 3’ SS and completes the ligation of exons spanning either side of the lariat (Jackson, 1991).

Alternative mRNA splicing (AS) occurs in >95% of multi-exon human genes and increases the diversity and function of the proteome. Alternative splicing (AS) is a co-transcriptional process whereby one gene can generate many mRNAs and proteins. It allows the generation of a diverse proteome from 95% of genes (Pan et al., 2008). There are seven types of alternative splicing (Fig 6) which are exon skipping, mutually exclusive exons, retained intron, alternative promoter, alternative terminator, alternative donor site and alternative acceptor site. Exon Skipping is the most common mode of splicing mechanism whereby exons are included or excluded from the final transcript. Mutually exclusive splicing event occurs when two exons are retained while another is spliced out in a non-independent manner. Intron Retention which is thought to permit retaining of the non-coding portions of the gene and may lead to demornity in the protein structure and function. Alternative promoters and alternative terminators are used to generate isoforms with more than one initiator or terminator exon. Other types of splicing involve the use of alternative 5′ splice site and alternative 3′ splice site at the start or end of an exon (Shi et al., 2018).

During transcription, DNA is transcribed to pre-messenger RNA (pre-mRNA) by RNA polymerase II. This pre-mRNA is processed to exclude introns, ligate exons, and allow the addition of a poly(A) tail at the 3’ end and cap at the 5’ end to protect the mRNA from initial degradation (Hocine, Singer, and Grünwald, 2010). Splicing, as described earlier, is executed by the spliceosome, which is comprised of a ribonucleoprotein (RNP) complex. This complex recognizes highly conserved short sequences at 5’ donor splice sites (SSs) of the introns, 3’ acceptor SSs of the introns, branch points and polypyrimidine tracts. The polypyrimidine promotes the assembly of the spliceosome while the branch point, which always retains A, is located 18–40 nucleotides (nt) upstream of the 3’ SS and initiates a nucleophilic attack on the 5′ donor SS. The branch point is characterized by a partially conserved YNYYRAY sequence (Y = pyrimidine, N = any nucleotide, R = purine and A = adenine) (Matera and Wang, 2014; Will and Lührmann, 2011). The choice of SS is determined by the balance of *cis*-acting enhancer or silencer elements (exonic splicing silencer ESS, intronic splicing silencer ISS, exonic splicing enhancer ESE and intronic splicing enhancer ISE), and *trans*-acting splicing repressors or activating factors (SR: serine/arginine-rich family of nuclear phosphoproteins and hnRNPS). Generally, the SRs interact with ESE and ISE to promote splicing, while hnRNPs interact with ESS and ISS to inhibit AS (Smith and Valcárcel, 2000).

AS is regulated by ratios of *trans*-acting proteins (activators and repressors) binding to *cis*-acting sites or ‘elements’ (enhancers and silencers) on pre-mRNAs. ESE and ISE drive constitutive splicing, while ESS and ISS are crucial in driving AS (Wang and Wang, 2014). Splicing activators in the SR protein family bind to splicing enhancers (ESE and ISE), while splicing inhibitors (hnRNPs) bind to splicing silencers (ESS and

ISS). Their ratio determines donor and acceptor splicing site usage (Ramanouskaya and Grinev, 2017). Additionally, splicing factors (SFs) that serve as activators on intronic enhancer elements may also serve as repressors on splicing elements of exons and vice versa (Lim et al., 2011). Of the seven types of AS (Fig 6), the most common form is cassette exon splicing caused by canonical splicing, whereby an exon can be excluded or retained in alternate isoforms. The other six types of AS are mutually exclusive exons, retained introns, the use of alternative promoters or terminators, and the use of alternative donor or acceptor sites (Sibley, Blazquez and Ule, 2016).

Splicing factors have been associated with cellular senescence and linked to organ degeneration (Deschênes and Chabot, 2017; Fujita et al., 2009; Latorre et al., 2017a). In fact, age-related splicing has been shown to alter metabolism, DNA repair and ion channels in neurodegenerative diseases (Tollervey et al., 2011). Dysfunction of the splicing proteins hnRNP A1 and PTB1 has also been shown to alter the metabolism of cholesterol, and contribute to vascular stiffness and endothelial senescence in cardiovascular diseases (Rizzacasa et al., 2017). The pre-mRNA splicing factor senescence evasion factor (SNEV), which aids spliceosome assembly and mRNA processing, is also known to suppress senescence as well as apoptosis (Dellago et al., 2012).

Expression of splicing factors, splicing enhancers, and silencers is dysregulated in the blood of ageing humans. This dysregulation can lead to alterations in the SS usage of genes, as well as modulate ratios of alternatively expressed transcripts in a tissue-specific manner (Harries et al., 2011; Holly et al., 2013). In mouse models, lifespan-

associated copy number variations are also preferentially localized in or within the proximities of genes encoding proteins for splicing events (Glessner et al., 2013). The expression of hnRNP splicing factors is also associated with normal ageing and parental longevity in humans, lifespan in mice and *in vitro* models of senescence (Harries et al., 2011; Holly et al., 2013). Recent findings have shown that two splicing factors, *HNRNPA2B1* and *HNRNPA1*, are associated with parental longevity and might be key to determining lifespan in humans (Lee et al., 2016). While some hnRNPs are upregulated, others are downregulated in the blood of offspring of long-lived humans. Long-lived animals also have downregulated splicing factors, which may confer an ability to sustain a splicing pattern that promotes healthy ageing as a result of cellular plasticity (Lee et al., 2016). It is possible that the balance of splicing enhancers and silencers is disrupted during ageing, which may change according to the choice of SSs. This may eventually lead to the generation of the dysregulated ageing transcriptome that is a feature of ageing outcomes such as tumours, and AD and Parkinson's disease (PD) (Scuderi et al., 2014; Danan-Gotthold et al., 2015; Lisowiec et al., 2015).

1.12 Proteostasis and mRNA turnover

Protein homeostasis or 'proteostasis' is the process that regulates optimum environment for functional proteins within the cell in order to maintain the cellular proteome, disruption of which can lead to severe challenged cellular environment in pathologies like AD. Gene expression and therefore proteome content can be controlled by the amount of mRNA clearance as well as by the stability and accessibility of mRNA to other molecules, differential rates of mRNA translation and

degradation. mRNA turnover determines the lifetime of cytoplasmic mRNAs and thereby controls gene expression. mRNA granules that harbour the mRNA decay machinery involved in translational repression or transient storage, are therefore also contributing factors to expression (Borbolis and Syntichaki, 2015). The removal of aberrant protein aggregates occurs through the ubiquitin-proteasome or the autophagosome-lysosome pathway. Targeting of RNA granules to vacuoles can lead to efficient PBs/SGs clearance, regulating the abundance of proteins as well as simultaneously degrading the mRNAs inside these vacuoles (Buchan et al., 2013).

Mature mRNAs consist of coding regions, with 3' and 5' untranslated regions (UTRs) that are important for stability and translation. They also have a 5' cap and a 3' poly(A) tail, both of which protect the mRNA from degradation and facilitate translation initiation in the cytoplasm (Cheng et al., 2016; Temperley et al., 2003). The rate of transcribed mRNA translation and the fate of an mRNA in the cytoplasm are determined by post-transcriptional modifications and packaging of mRNAs with proteins into RNPs, which regulate mRNA turnover and degradation. Post-transcriptional mechanisms can regulate the concentrations and localization of mRNAs of translated proteins (Chan et al., 2018).

Proteostasis is the mechanism whereby proteins are stabilized by the correct folding and refolding of misfolded peptides. Loss of proteostasis is a key feature in ageing and ageing-related outcomes. While a global reduction in mRNA translation might prevent the production of aberrant proteins, high levels of non-functional proteins can cause proteotoxicity in cells (Ciryam et al., 2013; Walther et al., 2015). Studies using invertebrate models of ageing have indicated that a progressive loss of proteome

balance occurs during ageing. This loss of proteome balance is a result of decreased numbers of ribosomal subunit proteins and regulation of miRNA-mediated translational repression (Walther et al., 2015).

It is possible that, with ageing, there is a decline in the cell's ability to prevent or repair ROS-induced oxidative damage, which leads to the accumulation of immobile dysfunctional proteins (Beckman and Ames, 1998). This is evident in experimental model organisms where the conserved protein degradation system, i.e. autophagy, declines with age, preventing the degradation of damaged cellular proteins (Bareja, Lee, and White, 2019). Progressive declines in the preservation of a functional proteome and the accumulation of defects in protein quality control are evident in age-related neurodegenerative disorders (Koga, Kaushik, and Cuervo 2011; Vilchez, Saez, and Dillin, 2014). In line with this, DR linked to lifespan extension is known to induce autophagy-related defective protein clearance (Hansen et al., 2007). Age-related proteotoxicity can also operate without chaperones and proteases to restore or remove misfolded polypeptides, and degrade them in an attempt to renew intracellular proteins. It is an attempt to prevent the accumulation as well as chronic expression of damaged proteins, which could otherwise lead to the development of pathologies such as AD and PD (Powers et al., 2009; van Ham et al., 2010). In fact, the two principal proteolytic quality control systems, the autophagy-lysosomal system and the ubiquitin-proteasome system deteriorate with age (Rubinsztein, Mariño, and Kroemer 2011; Tomaru et al., 2012). Defects in mRNA silencing or decay factors in cytoplasmic mRNP granules, i.e. processing defects, have been inversely linked to lifespan and stress resistance in invertebrate models (Cornes et al., 2015; Kato et al., 2011; Rousakis et al., 2014).

1.13 Regulation of gene expression by ncRNAs

Non-coding RNAs (ncRNAs) are RNAs that do not code proteins, such as ribosomal RNA, transfer RNA small nuclear RNA and small nucleolar RNAs. Eukaryotic regulatory ncRNAs can be broadly divided into long ncRNAs (lncRNAs) (> ~200 nt) and short ncRNAs (sncRNAs) (~20–30 nt, e.g. miRNAs). LncRNAs bind with RNA-binding proteins (RBPs) without processing activity in the RNP complex. They control gene expression as well as translation by regulating chromatin modification, transcription, splicing, mRNA decay, translation, protein transport and assembly. In contrast, sncRNAs bind with RNA-processing proteins that cleave primary transcripts into smaller sncRNA pieces, which are assembled into RNP machineries known as RNA-induced silencing complexes and mediate RNA interference by complementarity to regulate gene expression. Dysregulation of lncRNAs and sncRNAs like miRNAs is associated with ageing (Huan et al., 2018; Marttila et al., 2020).

1.14 Emerging class of ncRNA: circRNA

Circular RNAs (circRNAs) are a class of ncRNA that are present in wide variety of cells, in various tissue types across species and are thought to modulate gene expression. CircRNAs in higher organisms are reported to be produced by back-splicing events and can be synthesized from all regions of the genome, deriving mostly from exons but less commonly, from antisense, intergenic, intragenic or intronic regions (Lan et al., 2016). CircRNAs are both spatially and temporally regulated and evidence is emerging that they may have importance in normal development of tissues or organs but also in disease pathogenesis. Most circRNAs have been reported in the brain (Jeck et al., 2013; Veno et al., 2015; Barrett and Salzman, 2016; Legnini et al., 2017b). They can be found in most cell sub-compartments but the majority localize

predominantly to the cytoplasm (Du et al., 2016b). However, they can also be found in the nucleus and may have the potential to regulate RNA-Pol-II-mediated transcription (Bose and Ain 2018). They can vary in size from 200-4000 nt and usually harbour 1 to 5 exons, ~25% of circRNAs can retain introns. CircRNAs are non-polyadenylated, single-stranded, covalently closed RNAs, which are generated by backsplicing from as much as 20% of genes in mammals. CircRNAs are inherently stable by virtue of their closed covalent structure as well as exonuclease resistance and are thought to be stable in exosomes (Cocquerelle et al., 1993; Schwanhausser et al., 2011; Jeck et al., 2013; Lan et al., 2016; Lasda and Parker, 2016b). This observation opens up the interesting possibility that circRNAs, like miRNAs, may have roles in paracrine signalling or have roles in cell-to-cell cross talk.

1.14.1 Biogenesis of circRNAs

In conventional linear splicing, the spliceosome joins exons in a 5' to 3' configuration. In contrast, circRNAs arise when the 3' 'tail' of a downstream exon of a gene is back-spliced to the 5' 'head' of an earlier exon (which may include itself) leading to the circularization of exons in between (Fig. 7) (Cocquerelle et al., 1993). These splicing decisions are, as in linear splicing, regulated by *trans*-acting splicing factors and *cis* sequence elements (Kramer et al., 2015). Several sequence features influencing circRNA formation have been described. Firstly, intron length has been reported to play a part; introns flanking back-spliced sites tend to be comparatively longer than those flanking non-circularised exons (Salzman et al., 2013). This may be because larger introns may form more RNA-RNA interactions, facilitating circularization of embedded exons; the double-strand RNA-editing enzyme *ADAR1*, which is capable

of melting stem structures within these RNA-RNA interactions, is associated with suppression of circRNA expression in *C. elegans* (Ivanov et al., 2015). Intronic sequences flanking *circRNAs* are *enriched* for A-to-I substitutions and *hyper-editing* events. Unsurprisingly thus ADAR knockdown leads to accumulation of circRNAs (Ivanov et al., 2015). ADAR is an RNA-editing enzyme that binds double-stranded RNA and deaminates adenosine to inosine base. ADAR1 and ADAR2 interact with double-stranded ALU repeat. ADAR antagonizes competing RNA-RNA interactions of introns during circRNA biogenesis by melting stems within these interactions (Ivanov et al., 2015). Secondly, exon length may also be a factor; exons of single-exon circRNAs are on average 3-fold longer compared with non-circularised exons; longer exons may be sterically preferentially favoured for 3'- 5' splicing at canonical splice sites (Salzman et al., 2012; Jeck et al., 2013; Starke et al., 2015). Thirdly, RNAs that are hyper-edited are enriched for circRNA sequences (Ivanov et al., 2015). Finally, sequence content may also be important. Repetitive sequences are known to promote back splicing; back-spliced exons that form circRNAs are frequently enriched in paired ALU tandem repeats that have been shown to promote circularization (Jeck et al., 2013). Miniature introns with as few as 30 to 40-nt inverted repeats are also sufficient to promote circularization (Liang and Wilusz, 2014).

CircRNA formation may also be dependent on the specific binding of regulatory proteins. RNA binding proteins such as Quaking (QKI) and Muscleblind (MBL/MBNL1) have been described to bind to introns flanking back-spliced sites and may drive circularization (Ashwal-Fluss et al., 2014; Conn et al., 2015). The *MBL* gene itself encodes a circular form which regulates the expression of its linear transcript and modulation of MBL levels strongly affects circMbl expression (Ashwal-Fluss et al.,

2014). Circular RNA formation has also been shown to depend on the rate of transcription of their parent genes. CircRNA producing genes are generally longer and exhibit faster transcription than genes that do not produce circRNAs, and artificially slowing the rate of transcription with mutant RNA polymerases results in lower levels of circRNA biogenesis (Zhang et al., 2016a).

Intronic circRNAs (ciRNAs) can also be generated form lariat introns. CiRNAs are devoid of linear fragments spanning the 3′ end of the intron to the branch point but are produced by a 2′,5′-phosphodiester bond arising from canonical linear splicing (Zhang et al., 2013). A 7-nt GU-rich element occurring close to a 5’ splice site and with an 11-nt C-rich motif around the branch point within intronic sequences has been reported to be important for formation of ciRNAs (Zhang et al., 2013) **.**

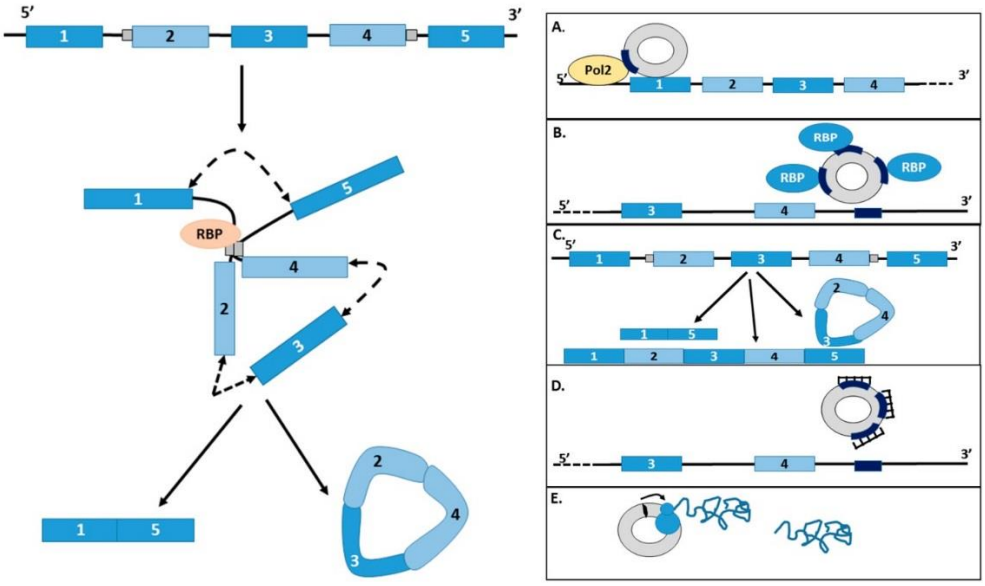

Figure 7 Diagram of circRNA generation and possible modes of action. *Biogenesis of circular RNA (circRNA). The linear primary transcript contains exons (blue boxes), introns (black lines), and possibly repetitive elements or sequence motifs (grey boxes). Circular exons are generated from back-splicing events between the splice donor site of a downstream exon and the splice acceptor site of an upstream*

*exon. This can be mediated by specific sequence elements (grey boxes) or by interaction with RNA binding proteins (RBPs). Splicing events are indicated by dashed lines with double arrowheads. This may result in the production of a circular RNA and a linear RNA which lacks the circularised exons. Proposed roles of circRNA in the regulation of transcription and translation. circRNAs may regulate genes at several levels. (**A**) Firstly, nuclear circRNAs can interact with promoter regions of target genes and interact with RNA polymerase II (Pol2) to repress or enhance transcription; (**B**) Secondly, circRNAs can sequester RBPs that regulate mRNA processing and, thus, alter the splicing patterns of the genes in question, or moderate mRNA stability. RBP binding sites are given by dark blue boxes; (**C**) Thirdly, the biogenesis of circular RNAs may results in the production of a linear RNA lacking the circularised exons. The formation of circRNAs can thus reduce the amount of linear transcript produced; (**D**) circRNAs can act as micro RNA (miRNA) sponges, sequestering them away from their binding sites in target genes, which are given by dark blue boxes; (**E**) Circular RNAs can also be translated. The initiation codon is given by black oval, and the translating ribosome and nascent polypeptide are indicated.*

1.14.2 CircRNA mediated regulation of expression

Splicing events do not always produce a linear transcript. circRNAs are a class of RNA that are emerging as key new members of the gene regulatory milieu, which are produced by back-splicing events within genes. In circRNA formation, rather than being spliced in a linear fashion, exons can be circularised by use of the 3′ acceptor splice site of an upstream exon, leading to the formation of a circular RNA species. CircRNAs have been demonstrated across species and have the potential to present genetic information in new orientations distinct from their parent transcript. The importance of these RNA players in gene regulation and normal cellular homeostasis is now beginning to be recognised. They have several potential modes of action, from serving as sponges for micro RNAs and RNA binding proteins, to acting as transcriptional regulators (Haque and Harries 2017).

1.14.2.1 CircRNAs as miRNA Sponges

CircRNA can bind specific miRNAs or groups of miRNAs, sequestering them and suppressing their function (van Rossum et al., 2016), in a phenomenon termed the competitive endogenous RNA hypothesis (Tay et al., 2014). CircRNA *CDR1as* has been documented to contain up to 74 binding sites for the miRNA miR-7, and also binds Argonaute (AGO) proteins of the RNA-induced silencing complex (RISC) that regulate miRNA action (Memczak et al., 2013). There is also some suggestion that the relationships between circRNAs and miRNAs may be partly autoregulatory; *CDR1as* also binds miR-671, which induces AGO-mediated cleavage of *CDR1as* itself, which could act to release miR-7 (Hansen et al., 2013). However, circRNAs containing multiple binding sites for single miRNAs may be the exception rather than the rule since most circRNAs identified to date do not contain enrichment of binding sites for specific miRNAs (Guo et al., 2014). Emerging evidence suggests that circRNAs may act by sequestration of modules of coordinately regulated miRNAs; the circRNA *circHIPK3* contains binding sites for 9 miRNAs with growth-suppressive properties (Zheng et al., 2016b). The presence of multiple binding sites may not be a prerequisite for efficient miRNA regulation however, since *circHIPK3* contains only 2 binding sites for miR-124, yet retains the ability to regulate this miRNA (Zheng et al., 2016b). Most of the research investigating the role of circRNA-miRNA interaction has been performed through correlation of the levels of miRNA and circRNA expression in vitro. Evidence for circRNAs acting as miRNA sponges can also be seen in data arising from the *CDR1as* knockout mouse. Levels of both miR-7 and miR-671 were seen to be lower in knockout animals, and these changes were also correlated with defects in synaptic transmission (Piwecka et al., 2017). It is likely that a circRNA with multiple binding sites will affect the expression of larger number of miRNA targets. However,

experimental validation of the minimal number of miRNA binding sites for a candidate circRNA to be functional is still required for many circRNAs. An arena to explore is whether a single miRNA binding site would be sufficient for efficient circRNA:miRNA sponging interactions. It would be also interesting to know what levels of circRNA expression is required for the optimal miRNA sequestration ability of these entities. The interaction between circRNAs and miRNAs may also go beyond their role in miRNA sequestration; they may also be important for the storage, sorting, and localization of miRNAs adding an additional level of regulation to miRNA-controlled regulation of target genes (Hansen et al., 2011; van Rossum et al., 2016).

1.14.2.2 CircRNAs as Transcriptional and Translational Regulators

A specific category of circRNAs, nuclear exon-intron circRNAs (EIciRNAs) can also interact with the transcription machinery. These variant circRNAs, which retains some intronic sequence from their linear gene can interact with the U1 component of the spliceosomal machinery, recruiting RNA polymerase II to the promoter region of genes and enhancing expression of its target genes (Li et al., 2015c). CircRNAs can also modulate the expression of the cognate transcript if the circularisation event includes the translation initiation codon of its native gene. This may cause their cognate linear mRNAs arising from the same gene to escape translation, thus regulating protein expression as in the case of *circHIPK3, circDMD* and *circFMN* (Chao et al., 1998; Gualandi et al., 2003; Grigull et al., 2004a; Jeck et al., 2013). Recently, *circPABPN1* has been reported to supress binding of *PABPN1* mRNA to HuR. *PABPN1* translation is positively associated with HuR and the interaction of *circPABPN1* interaction with HuR reduces the translational efficiency of *PABPN1* transcripts. Thus, circRNAs like

circPABPN1 can act as competitors with their cognate mRNA for RBPs and can also modulate the rate of translation of target mRNAs (Abdelmohsen et al., 2017).

1.14.2.3 CircRNAs as Competitors of Linear Splicing

All isoforms produced from a given gene arise from a common pre-mRNA. It follows therefore that the production of a circRNA may have consequences for the abundance of the remaining transcripts encoded by that gene. An example of this lies in the Muscleblind (*MBL*) gene. *MBL* contains sequences that form a circRNA transcript that contains binding sites for MBL itself. Production of the circMBL therefore forms an autoregulatory loop that regulates the production of the linear transcript in favour of the circular form (Ashwal-Fluss et al., 2014). In Arabidopsis, a circRNA derived from the *SEPALLATA3* gene has been shown to interact with its cognate DNA forming a R-loop, causing a pause in transcription and also affecting recruitment of splicing factors to the nascent transcript and affecting alternative splicing through exon-skipping (Conn et al., 2017).

1.14.2.4 CircRNAs as sponges for RNA binding proteins

In addition to their role as miRNA sponges, circRNAs can also act as sponges for other entities such as RNA binding proteins (RBPs) that can regulate gene expression. RBPs, like miRNAs, bind specific sequences within their target genes and control all stages within the lifecycle of an mRNA from splicing and nuclear export to stability and subcellular localisation (Grigull et al., 2004b). CircRNAs interacting with RNA binding protein components of the gene regulatory machinery such as HuR have been reported (Abdelmohsen et al., 2017).

1.15 CircRNA in diseases of ageing

In accordance with a pivotal role in gene regulation, perturbation of circRNA expression is beginning to be reported in association with disease. Altered circRNA expression has been reported in several diseases like cancer, heart disease, neurological disorders, diabetes and atherosclerosis, although the precise mechanisms by which they operate are yet to be disclosed. In post-mitotic cells, circRNA turnover is not as fast as linear transcripts which degrade easily. As such proliferative cells or cells that become apoptotic are likely to have less circRNA than post-mitotic cells (Bachmayr-Heyda et al., 2015; Song et al., 2016).

Ageing as has been discussed earlier is associated with global changes in splicing patterns. Since, circRNAs are also thought to be generated as isoforms from splicing. It is therefore possible that advancing age also affects progressive accumulation of circRNAs. In fact, splicing factors hnRNP and SR proteins has been shown to regulate Laccase2 circRNA expression in flies (Kramer et al., 2015). In addition, expression of 34 circRNAs changes in photoreceptor neurons of ageing flies (Hall et al., 2017). Similarly ~300 circRNA were dysregulated in mouse (Gruner et al., 2016). Like splicing factor FUS was also seen to regulate circRNAs expression *in vitro* mouse motor neurons (Errichelli et al., 2017).

CircRNAs are known to accumulate in ageing brain (Gruner et al., 2016). This may be partly due to the endonuclease-resistant nature of circRNA molecules, but at least two circRNAs have been previously described to have role in ageing or cellular senescence. CircRNA *circPVT1* has been demonstrated to suppress cellular senescence by sequestration of miRNA let-7, which lifts its inhibitory action on its target genes *IGF2BP1, KRAS* and *HMGA2* which act to promote cell proliferation (Panda et al., 2017). Conversely, the *circFOXO3* circRNA was found to promote

senescence in the heart muscle of aged mice and humans through its action on the *ID1, E2F1, FAK* and *HIF1A* target genes (Du et al., 2016b). This circRNA is also known to silence cell proliferation through its regulation of the Cell Division Kinase 2 (*CDK2*) gene and the cyclin dependent kinase inhibitor p21 (Du et al., 2016b).

1.15.1 CircRNAs in Cancer

In accordance with their known role in modulating cell cycle, proliferation and cellular senescence as demonstrated *in vitro* studies, circRNAs have been implicated in cancer. CircRNA *hsa_circ_001569 (circABCC)* may play a role in the modulating gene expression in colorectal cancer, by virtue of its action on miR-145. MiR-145 is a negative regulator of target genes such as *E2F5, BAG4* and *FMNL2* which are known to be involved in the suppression of proliferation (Xie et al., 2016). Similarly, *CDR1as* has also been implicated in several cancer subtypes including hepatocellular carcinoma (HCC). *CDR1as* expression is known to be correlated with hepatic microvascular invasion in HCC tissue (Xu et al., 2017b) and *Hsa_circ_0000520 (circRPPH1), hsa_circ_0005075 (circEIF4G3), hsa_circ_0066444 (circADAMTS9)* and *hsa_circ_0001649 (circSRPRH)* have all been shown to be expressed at different levels in HCC compared to adjacent normal liver tissues (Qin et al., 2016; Shang et al., 2016). *Hsa_circ_0005075 (circEIF4G3)* correlated with tumour size while *hsa_circ_0001649 (circSRPRH)* was downregulated and also correlated with tumour size in addition to the prevalence of tumour embolus and could be involved in tumorigenesis and metastasis of HCC (Qin et al., 2016; Shang et al., 2016). CircRNA *circZKSCAN1* has also been shown to be lower in tumour and correlated with tumour size in HCC (Yao et al., 2017).

Large-scale dysregulation of circRNA expression has been noted in bladder carcinoma, where microarray analysis revealed that 469 circRNA were differentially expressed, 285 showing increased expression in bladder cancer compared with 184 showing downregulation. Of these, *circTCF25* regulates miRNAs miR-103a-3p/miR-107, with *circTCF25* upregulation being associated with increased levels of 13 targets associated with cell proliferation, migration and invasion in bladder cancer (Zhong et al., 2016). Similarly, increased expression of circRNA *circMYLK* in bladder cancer leads to overexpression of *DNMT3B*, *VEGFA* and *ITGB1* genes, involved in promotion of proliferation, and are molecular targets of miRNA-29a-3p (Huang et al., 2016). CircRNA *circHIAT1* has also been reported to respond to signalling through the androgen receptor to promote tumour migration and invasion in clear cell renal cell carcinoma, by enhancement of *CDC42* expression through regulation of miR-195-5p/29a-3p and miR-29c-3p target genes (Wang et al., 2017b). Recently, fusion-circRNAs *(f-circRNA)* have been shown to accelerate proliferation rate and instigate cellular transformation. Furthermore, f-circRNAs f-circM9 and f-circPR have been shown to confer resistance to therapeutics due to protective effects of drug-induced apoptosis in cancer cells *in vitro* via a MAPK/AKT dependent signaling pathway (Guarnerio et al., 2016)**.**

1.15.2 CircRNAs in Neurological Disease

CDR1as has been associated with neurodegenerative conditions such as Alzheimer's disease (AD). In patients with moderate to advanced stages of sporadic AD, *CDR1as* expression has been reported to be reduced, which may lead to elevated miR-7 expression and consequent downregulation of miR-7 dependent mRNAs. One target,

ubiquitin protein ligase A, is responsible for the clearance of amyloid peptides in AD and other degenerative disorders (Lukiw, 2013). Although most of studies with circRNAs have been conducted *in vitro*, recently Piwecka *et. al*. generated a knockout murine model for Cdr1as. The brains of these transgenic mice had upregulated expression of miR-7 genes, such as *c-Fos*. Cdr1as knockout mice demonstrate impaired synaptic transmission and information processing defects (Piwecka et al., 2017). CircRNAs also have potential roles in memory; *circPAIP2* has been suggested to upregulate memory-related gene *PAIP2* through the PABP-associated pathway (Khoutorsky et al., 2013). A role for circRNAs in major depressive disorder is also suggested by the observation that a significant change of *hsa_circRNA_103636* expression was noted in patients after 8 weeks on antidepressant therapies (Cui et al., 2016).

1.15.3 CircRNAs in Osteoarthritis

Osteoarthritis (OA) occurs because of degenerative changes in the joint cartilage. 71 circRNAs were seen to be differentially expressed in the cartilage of patients with OA compared with non-OA controls. The circRNA *Circ-CER* appears to be of particular importance. *Circ-CER* expression was shown to increase with increased expression of pro-inflammatory signalling molecules. Suppression of *circ-CER* resulted in reduced MMP13 expression and remodelling of the extracellular matrix (ECM). The authors suggest that this observation arises from a sponging effect of *Circ-CER* on miR-136, which is known to target the *MMP13* gene (Liu et al., 2016).

1.15.4 CircRNAs in Cardiovascular Disease

The *CDKN2A/CDKN2B* locus expresses an alternatively spliced non-coding transcript, *ANRIL*, which encodes a circular form in addition to its linear. *CircANRIL* has been reported to regulate the pescadillo homologue 1 (*PES1*) gene transcript, which is involved in pre-rRNA processing and ribosome biogenesis. Sequestration of this essential factor and suppression of these key processes in vascular smooth muscle cells and macrophages was shown to cause nucleolar stress and p53 activation, resulting in apoptosis and features of atherosclerosis (Holdt et al., 2016). Some circRNAs have been shown to be protective in heart function; the circRNA Heart-related circRNA *HRCR* has been implicated in protection from cardiac hypertrophy and heart failure, by virtue of its binding of the inflammatory onco-miR miR-223 (Taibi et al., 2014; Wang et al., 2016). Some RBM20-dependent circRNAs have also been reported to be differentially regulated in dilated cardiomyopathy (Khan et al., 2016). Similarly, circRNA *MFACR* has been shown to sponge miR-652-3p in the cytoplasm, promoting mitochondrial fission and cardiomyocyte cell death by enhancing translation of *MTP18* in animal models (Wang et al., 2017a). Similarly, high levels of *circRNA_000203* and *circRNA_010567* have been reported in cardiomyocytes from diabetic mice treated with angiotensin II. These circRNAs are thought to downregulate miR-26b-5p, miR-141 and miR-141 thereby upregulating the transforming growth factor beta *(TGFB1)* gene. This leads to suppression of fibrosis-associated protein resection in Col I, Col III and α-SMA, promoting fibrosis in the myocardium (Tang et al., 2017; Zhou and Yu, 2017).

1.15.5 CircRNAs and Infection

Microbial lipopolysaccharide induces the activation of Toll-like receptors (TLR) pathways leading to activation of NF-κB and modulation of genes which are key to antimicrobial defences and adaptive immunity. c*ircRasGEF1B* has been suggested to modulate the expression of ICAM-1 as part of the lipopolysaccharide response. Knock down of this circRNA in vitro leads to 27-39% reduction in ICAM-1epression *in vitro* (Ng et al., 2016). In mouse macrophage cells, activation of TLR4, TLR9, TLR3, TLR2 and TLR1 receotors all regulate the expression of *circRasGEF1B* (Ng et al., 2016). Genetically modifying *circRasGEF1B* expression was shown to reduce *ICAM1* expression levels, which under normal conditions, would promote binding of leukocytes to endothelium cells and their transmigration into target tissues (Ng et al., 2016). Thus deficiency of *circRasGEF1B* may prevent migration of leukocyte cells to inflammatory sites and interfere with the healing process and in cancer cells may additionally affect the activation of cytotoxic T-lymphocytes, which is needed for driving release of cytolytic granules into tumour cells (Ng et al., 2016).

A potential role for circRNA in response to viral infection has been reported. HeLa cells transfected with circRNA demonstrated induced expression of 84 innate immunity-related genes, such as *RIGI* and *OASl*, which were upregulated by as much as 500-fold and 200-fold respectively (Chen et al., 2017b)**.** Concurrent with these changes was a 10-fold decrease in infection rate against Venezulan equine encephalitis virus, which was shared by nearby non-transfected cells indicating some paracrine action respectively (Chen et al., 2017b)**.** CircRNAs can act as competitors with viral mRNA for binding to RNA-binding domain containing immune factor NF90 and its isoform NF110. These factors can promote circularization by stabilizing the

binding of intronic RNA pairs in the nucleus. However, viral infection results in transportation of these immune factors from the nucleus to the cytoplasm. This, in turn, acts to render the circRNA available for binding to viral mRNA and prevention of viral infection of the host cell (Li et al., 2017b).

1.15.6 CircRNAs in Type 2 Diabetes

In addition to the role of *CDR1as* in regulation of insulin secretion through modulation of PAX6, recent studies have suggested that circRNAs may have utility as biomarkers of diabetes. 489 circRNAs were found to be differentially expressed in the peripheral blood of patients with type 2 diabetes, and furthermore, circRNA *hsa_circ_0054633* was found to be capable of predicting pre-diabetes with an area under the curve (AUC) of 0.84 ($p = <0.001$) (Zhao et al., 2017c). In other studies, several circRNAs have been shown to be differentially expressed in serum of patients with diabetic retinopathy compared to both controls, and diabetes patients without retinopathy. Of these, *hsa_circRNA_100750* is derived from stromal interaction molecule 1 which is upregulated in diabetic patients. *Hsa_circRNA_104387* is known to sequester miR-29a which is prevent the loss of renal function in diabetic patients. Hsa_circRNA_103410 is known as a regulator of miR-126 known to inhibit *VEGF* and *MMP9* expression. Thus *hsa_circRNA_103410* could promote endothelial injury in the retina, while *hsa_circRNA_100192*, could, by sequestering miR-146, promote NF-κB activation, adenosine deaminase-2 expression and inflammatory responses as is observed in vitro (Gu et al., 2017). These observations raise the exciting possibility that circRNAs expressed in accessible tissues may be useful markers of disease in inaccessible organs such as pancreas. *CircHIPK3* has been found to be dysregulated

in diabetic retinas which may contribute to elevated levels of *VEGFC*, *FZD4*, and *WNT2* expression by virtue of its effects on miR-30a-3p (Shan et al., 2017).

1.16 CircRNAs as Diagnostic and Prognostic Markers

Because circRNAs are highly nuclease-resistant, they are more stable than linear transcripts, and may be released into the extracellular space via the exosomes (Suzuki et al., 2006; Lasda and Parker, 2016a). Half-lives of circRNAs can vary significantly, but can be as much as 50 hrs. On average, their half-lives are around 2.5 fold longer than the median half-lives of their linear counterparts (Enuka et al., 2016). A substantial number of circRNAs are expressed in blood at comparatively higher levels than their linear mRNAs, thus making circRNAs attractive tools for diagnostics to trace the mechanism of coded genes otherwise inaccessible by the canonical RNA pathways-dependent assays (Memczak et al., 2015). A selection of circRNAs reported as potential biomarkers for different diseases are summarized in Table 1. Over 400 circRNAs have been detected to be present in cell-free saliva and could potentially be used for non-invasive diagnostics approach (Bahn et al., 2015). CircRNAs have been suggested as potential biomarkers for several types of cancer. In murine models, tumour-derived exosomal circRNAs in the serum correlate with tumour mass (Li et al., 2015b) and thus may be promising biomarkers for cancer detection. CircRNA *hsa_circ_0001649 (circSHPRH)* has shown some utility as a biomarker for hepatocellular carcinoma, is downregulated with tumour status and is associated with the occurrence of the tumour embolus as well as the size of the tumour (Qin et al., 2016). *Hsa_circ_002059 (circKIAA0907)* is downregulated in gastric cancer and is associated with grade and distal metastasis and could therefore be used as a

prognostic marker (Li et al., 2015a). Another circRNA, *hsa_circ_0000190 (circDYRK1A)*, is downregulated in plasma samples of patient with gastric cancer, where its expression levels correlated with tumour diameter, lymphatic metastasis, distal metastasis (Chen et al., 2017a). Similarly, *Hsa_circ_0001895 (circPRRC2B)* is was also shown to be downregulated in gastric cancer tissues and correlated with cell differentiation and Borrmann type (Shao et al., 2017). In hepatitis B infected hepatocellular carcinoma (HCC) patients, *circRNA_100338 (circSNX27)* has been shown to regulate levels of miR-141-3p, and its expression correlated with low cumulative survival rate and metastatic progression (Huang et al., 2017).

1.17 Tools to detect circRNA

Over the past few years, at least eleven circRNA detection software systems have been developed. These tools can recognize circRNA sequence from RNA-Seq data based on two different strategies. One approach is the candidate-based, also known as the pseudo-reference based approach. KNIFE, NCLScan and PTESFinder all abide by this approach where putative circRNA sequences need to be provided with information for gene annotation. Although KNIFE can directly retrieve back-spliced junctions prior to gene annotations, the other two softwares generate putative circRNA sequences post-alignment with the genome or transcriptome (Jeck and Sharpless, 2014; Chen et al., 2015; Meng et al., 2017).

CircRNA_finder, CIRCexplorer, DCC, MapSplice, Segemehl, find-circ and UROBORUS detect circRNA sequences based on the second approach for identification of circRNA sequences which is the fragmented-base or segmented read

approach. In this approach, the software detects back-spliced sites based on reads mapped to alignment of multiple split reads against the genome. While find-circ and UROBORUS detect back-spliced sequences using the first and last 20 bp after mapping the sequences against the genomes, the rest of the detection tools generate splice alignment algorithms to identify back-spliced junctions (Jeck and Sharpless, 2014; Chen et al., 2015; Meng et al., 2017). Comparisons of the different circRNA detection algorithms have now been made, which add information on the relative strengths and caveats of these different approaches (Hansen et al., 2016). Searchable repositories for circRNA sequences such as circBase are also now emerging (Glazar et al., 2014), which should prove useful to researchers interested in these RNA species in the future.

CircRNA can also be detected indivually using primers designed against the backsplice junctions. However, it might be sometimes difficult to amplify using regular amplification methods due to the fact that circRNAs may harbour secondary hair-loop structures. Moreover, it can make the process cumbersome since each potential exon retained withing a circRNA would need to be verified using primers design aginst every possible combination of junctions with the succeeding exons. In other cases, the low expression of circRNA in samples means samples would have to be treated for RNAase R to enrich the circRNA and it is possible that while most will be retained in samples, some may not escape this digestion process.

Table 1 Examples of circRNA and their potential role in ageing-related disease.

CircRNA	Pathologic condition	Possible mode of function	Potential Application
Cdr1as	hepatocellular carcinoma	May be a sponge for miR-7	Biomarker with the ability to predict hepatic microvascular invasion; expressed in hepatocellular carcinoma tissues (Xu et al., 2017a).
circ-ITCH	hepatocellular carcinoma	May inhibit Wnt/beta-Catenin pathway	Potential prognostic marker with the ability to predict survival; expressed in hepatocellular carcinoma tissues (Guo et al., 2017).
circZKSCAN1	hepatocellular carcinoma	May modulate expression of apoptotic genes *RAC2*, *EFNA3*, and caspase 3 and cell proliferation related genes *TGFB1*, *ITGB4, CXCR4*, *BIRC5* and *CCND1*; may modulate promoted cell proliferation, migration, and invasion in vitro	Expressed in tumour tissues (Li et al., 2017b).
hsa_circ_0058246	gastric cancer		Potential prognostic marker with the ability to predict clinical outcome; expressed in tumour tissues (Fang et al., 2017).
hsa_circ_0001017, hsa_circ_0061276	gastric cancer		Prognostic with the ability to predict disease-free survival; expressed in plasma (Li et al., 2017a).
hsa_circRNA_101308, hsa_circRNA_104423, hsa_circRNA_104916, hsa_circRNA_100269	gastric cancer		May predict the early recurrence of stage III gastric cancer after radical surgery; expressed in tumour tissues (Zhang et al., 2017).
circPVT1	gastric cancer	May act as sponge for miR-125 family; may promote cell proliferation	Potential prognostic marker with the ability to predict overall survival and disease-free survival; expressed in gastric cancer tissues (Yang et al., 2017).
hsa_circRNA_105055, hsa_circRNA_086376, hsa_circRNA_102761	colorectal cancer	May act as sponge for miR-7 regulating target genes *PRKCB*, *EPHA3*, *BRCA1* and *ABCC1*;potential role in lung metastasis	Potential biomarker (Zeng et al., 2017).

hsa_circ_0092285, hsa_circ_0058794, hsa_circ_0088088, hsa_circ_0038644	rheumatoid arthritis	May be involved in response to oxidative stress; endocytic traffic in actin cytoskeleton; could promote lipid breakdown and increase free fatty acid levels; could alter LPS immune response	Potential biomarker expressed in peripheral blood mononuclear cells (Zheng et al., 2017).
circRNA_104871, circRNA_003524, circRNA_101873, circRNA_103047	rheumatoid arthritis		Potential biomarker expressed in peripheral blood mononuclear cells (Ouyang et al., 2017).
hsa-circ-0005870	hypertension	May at as sponge miRNAs, hsa-miR-6807-3p, hsa-miR-5095, hsa-miR-1273g-3p, hsa-miR-5096 and hsa-miR-619-5p possibly affecting TGF-beta pathway important in hypertension	Potential biomarker expressed in plasma (Wu et al., 2017).
hsa_circ_0124644,	coronary artery disease		Potential diagnostic biomarker; expressed in blood (Zhao et al., 2017b).
Hsa_circ_0089378, hsa_circ_0083357, hsa_circ_0082824, hsa_circ_0068942, hsa_circ_0057576, hsa_circ_0054537, hsa_circ_0051172, hsa_circ_0032970, hsa_circ_0006323	coronary artery disease	May promote expression of transient receptor potential cation channel subfamily M member 3 by inhibiting hsa-miR-130a-3p	Potential biomarker expressed in plasma (Pan et al., 2017).
circR-284	carotid disease, ischemic stroke	May act as an inhibitor of miR-221/miR-222	Potential diagnostic biomarker and expression demonstrated in serum (Bazan et al., 2017).
hsa_circ_0054633	diabetes		Potential biomarker with the ability to predict pre-diabetes and type 2 diabetic status. Expressed in blood (Zhao et al., 2017c).

1.18 Research Hypothesis

Given the importance of correct gene regulation in maintaining homeostasis during the ageing process, I hypothesised that circRNAs may have roles to play in ageing, longevity and in age related diseases such as type 2 diabetes.

1.19 Aim and Objectives of thesis

CircRNAs have increasingly been implicated in age-related diseases including cancer and degenerative disease. They have also been reported as potential prognosis biomarkers for various disorders (Table 1). The objective of this thesis is to characterise the circRNA portfolio in the peripheral blood of ageing people, and also in the pancreatic islets of donors with T2D, as an exemplar disease of ageing. Finally, I aimed to determine whether circRNAs associated with T2D in diabetic islets had potential as biomarkers of this disorder in human patients.

My objectives were to:

1) Produce the first circRNA profile in a large cohort of ageing people, and then follow up specific circRNA in relation to ageing phenotypes in a human population, to cellular senescence in aged human cells of different cell types and to median strain lifespan in mouse strains with differing longevity.
2) Explore circRNA expression in relation to diabetes status and co-localisation to the GWAS association signals in the pancreatic islets of donors with T2D, an exemplary disease of ageing and in beta cell models subjected to diabetomimetic stresses.
3) To assess the utility of differentially-expressed islet circRNA as biomarkers of impaired glucose tolerance or overt T2D in human peripheral blood samples.

1.19.1 Chapter 3: CircRNAs expression in human peripheral blood could change with age and predict age-related disease outcomes

The aim of this chapter was to investigate if circRNA expression is deregulated in ageing. To address this, we generated the first circRNA profile from samples of pooled 'old' of median age 87 years and 'young' of median age 33 years for age-related expression differences in peripheral blood RNA samples from the InCHIANTI study of ageing, which is a population cohort from the Chianti region of Tuscany, Italy. This population has been followed from 1988 until 2014. I selected the top 15 circRNAs showing the most discrepant expression with age for further study in this human cohort.

Following this, I investigated if the expression of the circRNAs associated with ageing, frailty (measured by grip strength) and longevity as measured by attained parental age. I also assessed the differential expression of these circRNAs *in vitro* model of senescence in cells of different origins (fibroblasts, endothelial cells, astrocytes and cardiomyocytes), and where bioinformatics evidence of sequence conservation existed, in two tissues from 6 mouse strains of different median strain lifespan (A/J, NOD.B10Sn-H2b/J, PWD/PhJ, 129S1/SvImJ, C57BL/6J and WSB/EiJ) obtained in collaboration with the Jackson Laboratory Nathan Shock Center of Excellence).

1.19.2 Chapter 4: CircRNA expressions islets may be associated with common genetic variation at the GWAS loci associated with T2D

The aim of this chapter was to determine if circRNA expression was also dysregulated in chronic disorders of the ageing. I selected T2D as an exemplary disease of the ageing and investigated if circRNA expression in islets correlates with T2D status or

is driven by the genotype of the lead SNP of previously established T2D-GWAS signal. We have generated one of the first comprehensive circRNA profile from human pancreatic islets. I identified 13 circRNAs corresponding to 6 genes which co-localise to the genomic regions containing T2D-GWAS signals. This led to the hypothesis that the expression of these circRNAs may correlate with T2D status and may be driven by the variant of the lead SNP of the concerned GWAS recombination window.

I established a tissue expression profile of each circRNA indicating that circRNAs could be regulated independently from the corresponding linear mRNAs derived from the parental gene. I examined if the expression of these circRNAs correlated with T2D status, the genotype of the lead SNP at the T2D risk loci with which they overlapped and stress responses mirroring the diabetic environment *in vitro* models of diabetes.

1.19.3 Chapter 5: circRNAs expressed in human primary islets may have potential as diagnostic markers for T2D

I have identified 4 circRNAs which are abundantly expressed in human islets and display associations with diabetes status. Should these also be expressed in peripheral blood, they may serve as novel dagnostics or therapeutic biomarker for T2D, since they are stable and have longer half-lives than linear mRNAs. I assessed the expression of circRNAs that differed in expression by T2D status in peripheral blood to test if they could serve as potential biomarkers for T2D and pre-diabetic individuals.

Chapter 2

Methods

2.1 Human Samples

2.1.1. Peripheral blood samples

Samples of RNA and clinical data were available from the InCHIANTI study of ageing and the EXETER 10K/DARE study. Details of participant recruitment and follow-up procedures have been described in previous studies (Holly et al., 2014; Ferrucci et al., 2000). The InCHIANTI study is a longitudinal population study from the Tuscany region of Italy. Participants were assessed at three follow-up visits (FU2: 2004–2006, FU3: 2007–2010 and FU4: 2012–2014) after the baseline visit (Ferrucci et al., 2000). Data for ageing cohort were generated using the RNA samples from FU3 and the clinical/phenotypic data from the assessments at both FU3 and FU4. Clinical and demographic data used from the follow-up visits included measurement of potential confounding factors such as body mass index (BMI), sex, level of education (none, elementary, secondary, high school or university), study site, smoking and white blood counts (neutrophil, lymphocyte, monocyte and eosinophil percentages). Informed consent for the InCHIANTI study was obtained from all participants and ethical approval was obtained from the Instituto Nazionale Riposo e Cura Anziani institutional review board, Italy. Characteristics of the participants used for each study are provided in the relevant chapter.

The EXETER 10K study was used for chapters 4 and 5. The study consisted of samples collected from volunteer individuals recruited since 2010 ans used in previous study. They had been living in the South West of England and were predominantly of Caucasian British origin. The participants were either non-diabetic, had impaired glucose tolerance or were diabetic. Whole-blood samples were collected in 2011/2012 using the PAXgene system (Debey-Pascher et al., 2009) and extracted using a

PAXgene Blood RNA kit (QIAGEN, Paisley, UK). Written informed consent was obtained from all participants. Ethical permission was granted through the National Institute for Health Research Clinical Facility (REC 09/H0106/75). Patient demographics are provided in the relevant chapter.

2.1.2 Human islet samples

RNA samples from islets RNA extractions done by RNAlater®-ICE and ProCell Biotech for snap-frozen islets purchased from (Newport Beach, CA) or from the Integrated Islet Distribution Program islet repository (https://iidp.coh.org). RNA extraction was done using the miRVana isolation kit (ThermoFisher Scientific, USA). The protocol is discussed later in this section.

2.2 Primary cultures of *in vitro* models of senescence

Primary cultures with four different origins have been used to study the role of circRNAs in senescence as a substitute *in vitro* model to understand the ageing process. The primary cultures were generated from cells that were directly obtained from tissue or organs via dissection("Primary Culture - an Overview | ScienceDirect Topics" n.d.). Thus, they provided a physiologically relevant tool reflecting the *in vivo* microenvironment with minimal culture variability. The cells I worked with in chapter 3 had undergone senescence and RNA extraction before the onset of my work by Dr Eva Latorre and Dr Alice Holly.

2.3 Culture protocols for cellular senescence

Human senescent cell culture had been previously carried out by Dr Alice Holly and Dr Eva Latorre, as described in the following publications (Lye et. al. 2019; Latorre et al., 2017a; Latorre and Harries, 2017; Latorre et al., 2018). β-Gal staining on senescent cells was performed by Dr Eva Latorre. Each culture requires a different time period to reach senescence. For instance, endothelial cells attain confluency within 3 days in early passages but 10 days in late passages, while fibroblasts slow from 4–27 days. To obtain senescence, cells were counted and equal numbers of cells seeded at each passage. Each passage was then grown continuously at the respective optimal conditions until growth slowed to <0.5 population doubling/week. Briefly, the cells were fixed, washed in phosphate-buffered saline (PBS) and stained with freshly prepared staining solution, which resulted in blue precipitation in cells. Cells were then washed again with PBS and evaluated by light microscopy. SA β-Gal-stained cells were stored in mounting medium such as glycerol instead of PBS if they were to be visualized by microscopy at a later date.

2.4 Cultivation of EndoC βH1 cells as an *in vitro* model to study T2D

Human EndoC-βH1 cultured cells (EndoCells, Institut national de la santé et de la recherche médicale, France) were used as an *in vitro* model to dissect the potential role of circRNAs in T2D. The treated RNA was available from cultured EndoC-βH1 human beta cells subjected to different diabetomimetic stresses was provided by Dr Nicola Jeffery. The cell line, which was derived from human foetal pancreas, was transduced with a lentiviral vector expressing an oncogene that is under the control of the insulin promoter. The cells were then transduced with human telomerase reverse transcriptase and grafted into severe combined immune-deficient (SCID) mice to

generate pancreatic tissues. The grafted and differentiated human β-cells expressed a Simian Vacuolating Virus 40 Tag (SV40LT) alongside insulin and formed insulinomas. These insulinomas were transduced with a lentiviral vector expressing human telomerase reverse transcriptase and once again transplanted into other SCID mice to amplify proliferating β-cells. The tissues were then removed from the mice and expanded via *in vitro* culture to generate immortalized EndoC βH1 cultures. The cultures are stable for at least 80 passages, express many β-cell specific markers and secrete insulin, especially in response to glucose stimulation (Ravassard et al., 2011).

EndoC-βH1 cells (Endo Cells, INSERM, France) were generated in extracellular matrix (ECM)-coated (2 µg/mL, Sigma-Aldrich, Steinheim, Germany) yellow-capped T25 flasks (Sarstedt, Nümbrecht, Germany) containing culture media consisting of Dulbecco's Modified Eagle's medium (DMEM) (4.5 g/L, ThermoFisher Scientific, Waltham, MA, USA) and matrigel fibronectin (100 µg/m from bovine plasma, Sigma-Aldrich, Steinheim, Germany). The EndoC-βH1 cells were then cultivated in culture media containing DMEM (1 g/L glucose, ThermoFisher Scientific, Waltham, MA, USA), Bovine Serum Albumin (BSA) fraction V (2% Merck Chemicals, Darmstadt, Germany), nicotinamide (10 mM, Sigma-Aldrich, Steinheim, Germany), β-2-mercaptoethanol (50 µM), transferrin (5.5 µg/mL), sodium selenite (6.7 ng/mL), penicillin (100 U/mL) and streptomycin (100 µg/mL, Sigma-Aldrich, Steinheim, Germany) at 37°C with CO_2. After 3 days, 50% of the culture medium was replaced with fresh medium and cells were split when they reached ~90% confluency. Cells were treated to glycaemic, lipotoxic, cytotoxic and hypoxic stress as described in a recent study from our group (Jeffery et al., 2019). The treated EndoC βH1 cells were used for the generation of partial data for chapter 4 of the current project.

2.5 Peripheral blood RNA extraction

Whole-blood samples for RNA analysis were collected using the PAXgene system (Debey-Pascher, Eggle and Schultze 2009). The PAXgene Blood RNA Tube (BD Biosciences), which contains stabilization reagents to maintain transcript levels at the level they were at the time of bleed. This minimizes handling variability without impacting intracellular RNA profiles and the integrities of the RNAs for downstream workflows. Since the PAXgene system stabilizes intracellular RNA in blood for 3 days at room temperature and for 5 days at 2–8°C, it allows for fluctuations in room temperature to up to 25°C during transportation. Additionally, variability is minimized because all of the steps prior to RNA extraction, i.e. collection, stabilization, transport and storage, are executed in a single tube that is used to draw blood samples from subjects.

For this study, PAXgene tubes were shipped on dry ice. Samples were then stored at ultra-low temperatures for later use. For RNA extraction, samples were thawed for at least a few hours. Supernatants were removed following centrifugation and ribonuclease (RNase)-free water was added to pellets. Successive centrifugation ensured the removal of more supernatant. Addition of lysis buffer lysed the cells and an automated QIAcube system was used to manage the subsequent stages of proteinase K incubation to digest proteins, further fragmentation of cell debris using a PAXgene shredder column and the addition of ethanol to facilitate the precipitation of nucleic acids. A PAXgene RNA spin column (Qiagen) was then used to sieve the RNA. The column was washed followed by DNase I treatment to eliminate DNA, and RNA was eluted in an elution buffer heated at 65°C.

2.6 RNA extraction from mouse tissues

Stocks of spleen and skeletal muscle RNA from young and old mice from six different strains was available. These strains (A/J, NOD.B10Sn-H2b/J, PWD/PhJ, 129S1/SvImJ, C57BL/6J and WSB/EiJ) had varying median strain lifespans (623–1005 days), and RNA was originally extracted by Dr Ben Lee. These samples have been verified by the. These tissue samples were kindly provided by the Jackson Laboratory Nathan Shock Center of Excellence and were shipped using the snap-frozen RNAlater®-ICE Collection protocol (Life Technologies, Carlsbad, CA). The basic principle of the SNAP-frozen procedure involves freezing RNA samples at -196°C in liquid nitrogen. The RNAlater® RNA stabilization solution contains ethylenediaminetetraacetic acid (EDTA), sodium citrate and ammonium sulphate, all of which can penetrate cells rapidly and inactivate RNases to prevent the degradation of RNA. The samples can stay stable for 1 week at room temperature and pressure. The dissected tissues samples were immersed in this solution and then snap-frozen. The snap-frozen samples were stored at -80°C and later shipped in dry ice. The samples were then stored at -80°C until they were defrosted for RNA extraction.

TRI Reagent® was used to extract RNA from mouse tissues using the phenol:chloroform principle. TRI Reagent®, i.e. TRIzol, is composed of phenol and guanidium isothiocyanate (RNA work and RNA qauntification was done by Dr Ben Lee). It lyses cells, denatures proteins and eliminates RNases, thus preventing the degradation of many RNA entities. Chloroform added to the supernatant facilitates phase separation, which means that RNA is confined to the aqueous phase, protein to the organic phase and DNA to the interface between the two. This facilitates the isolation of RNAs, DNAs and proteins from each same sample simultaneously. In this

protocol, $MgCl_2$ in the protocol stabilizes long RNA to interact with smaller RNA, and this enables enriched extraction of smaller RNA entities and enhances the recovery of small RNAs by stabilizing the phosphate backbones of the RNA entities (Hummon et al., 2007). The reagent also inhibits RNases and allows the segregation of RNA into the aqueous layer. Beads added with the magnesium buffer are used to homogenize tissue samples. The centrifugation step helps to separate the phases containing RNA from that containing DNA. Overnight incubation with isopropanol at -20°C aids precipitation of the RNA. The final ethanol washes remove any residue reagents. The washed pellets are then suspended in Tris-EDTA (1x TE) buffer or RNase-free water and stored at -80°C for future use.

Briefly, RNAlater® tissues were placed in TRI Reagent® solution containing $MgCl_2$. Samples were homogenized using a bead mill (Retsch Technology GmbH, Haan, Germany) followed by phase separation using chloroform. Total RNA was precipitated from the aqueous phase through overnight incubation with isopropanol at −20°C. RNA pellets were then ethanol-washed, re-suspended in RNase-free dH_2O and stored at -80°C for later use.

2.7 RNA extraction from donor islets

Islet RNA extractions were originally carried out by Dr Jonathan Locke. RNAlater®-ICE was used to ship some samples of islet cells, while other donor islet samples were shipped in the form of snap-frozen islets purchased from ProCell Biotech (Newport Beach, CA) or from the Integrated Islet Distribution Program islet repository (https://iidp.coh.org). Snap freezing involves the rapid freezing of tissues using either

dry ice, a dry ice/ethanol slurry or liquid nitrogen. The process maintains the integrity of samples by reducing the chances of water being present in cells and tissues, thus preventing the formation of ice crystals during the freezing process, and by reducing the activities of proteases and nucleases in samples, which would otherwise lead to extensive degradation of RNA or proteins.

Islet samples harvested as above can later be used for total RNA extraction using the miRVana isolation kit. The protocol involves the use of organic acid-phenol:chloroform extraction and a glass fibre filter under specialized binding to efficiently isolate RNA entities as small as 10-mers (ThermoFisher Scientific, USA). Samples are first denatured with lysis buffer. Ethanol is then added and the samples filtered through a cartridge containing a glass filter that immobilizes the RNAs. The filter is then washed a few times and the RNA eluted with a low-ionic-strength solution.

2.8 RNA extraction from cultured cells

Confluent cell cultures were seeded in 6-well plates and grown in their optimal culture conditions unless otherwise mentioned. RNA was extracted using TRI Reagent®. Briefly, cells were washed twice with 500 mL Dulbecco's PBS. TRI Reagent® (Sigma-Aldrich, Steinheim, Germany), $MgCl_2$ (10 µL, ThermoFisher Scientific, Waltham, MA, USA) and chloroform (200 µL, ThermoFisher Scientific, Waltham, MA, USA) were then used to harvest RNA. Samples were centrifuged at 14,800 rpm at 4°C for 20 min. The clear aqueous layer was removed from the centrifuged samples and isopropanol (500 µL, ThermoFisher Scientific, Waltham, MA, USA) was added for overnight precipitation. Precipitated samples were centrifuged at 14,800 rpm at 4°C for 45 min to allow RNA pellet formation. The pellets were then repeatedly washed using ethanol

(75% molecular grade, ThermoFisher Scientific, Waltham, MA, USA). The washed pellets were air dried, resuspended in RNase-free dH_2O (20 µL, Fisher Scientific, New Hampshire, USA) and stored at -80°C for later use. Diluted samples were used to determine the RNA concentration using a Bionalyzer. RNA used in this work was extracted by Dr Nicola Jeffery.

2.9 cDNA synthesis from cell cultures, tissues and islets

RNA is a single-stranded unstable molecule that is used to quantify the expression of transcripts by quantitative PCR (qPCR). RT-PCR allows the amplification of RNA to complementary DNA (cDNA) from an original RNA template using genetically engineered reverse transcriptase. The SuperScript® VILO™ cDNA synthesis kit contains a reaction mix containing random primers, $MgCl_2$ and deoxyribonucleotide triphosphates (dNTPs) in its buffer. It also includes an RNAseOUT™ recombinant RNase inhibitor, and a genetically modified Moloney Murine Leukaemia Virus enzyme (reverse transcriptase) that has reduced RNAse H activity and high thermostability for highly efficient cDNA synthesis at a wide range of temperatures (42–60°C). The enzyme is not inhibited by rRNA or tRNA. Thus, it allows the use of total RNA to make cDNA. The reduced RNase H activity means that the RNA from the RNA–DNA hybrid is not rapidly degraded. The RNase inhibitor is a non-competitive inhibitor protein that protects against RNase A-, RNase B- or RNase C-mediated degradation of RNA. The protocol facilities cDNA synthesis with as little as 2.5 µg of total RNA in a 20-µL standard reaction. The RNAseOUT™ recombinant ribonuclease inhibitor prevents degradation of the template RNA, which might occur in the presence of ribonuclease contamination in the total RNA.

In the first step, an RNA–DNA hybrid is generated. The reverse transcriptase RNase H degrades the RNA from the RNA–DNA hybrid. The single-stranded DNA strand is then extended to a cDNA by the DNA-dependent DNA polymerase activity of the reverse transcriptase. This cDNA is then used as a template in subsequent steps for amplification like a normal PCR.

RNA was normalized during all the reverse transcription as the concentrations of RNA were adjusted to 100 ng/µL before using them as template for reverse transcription. cDNA synthesis was carried out with random primers and dNTPs, as recommended by the SuperScript® VILO™ cDNA synthesis kit protocol, for the study of the islet samples and the generation of data for tissue panels (ThermoFisher Scientific, Waltham, MA USA). The reaction mix contained SuperScript® (2.0 µL), VILO™ buffer (4.0 µL), dH_2O (Fisher Scientific New Hampshire, USA) and 100 ng/µL RNA in a final reaction volume of 20 µL. Reaction conditions were 25°C for 10 min, 42°C for 60 min and 85°C for 5 min.

Like the VILO™ kit, the enzyme mix in the EvoScript kit contains a Protector RNase inhibitor alongside the reverse transcriptase enzyme. The reverse transcriptase can execute cDNA synthesis at high temperatures and over a broad range of temperatures. However, the EvoScript reverse transcriptase has RNase activity, which facilitates degradation of the RNA from the RNA–DNA hybrid and allows PCR primers to bind easily to the cDNA. This is why the enzyme has to be added as the last reagent when using this kit for RT. Additional reagents include a reaction buffer containing

random primers, oligo(dT)$_{18}$, dNTPs and Mg(OAc)$_2$. The oligo(dT)$_{18}$ allows the efficient synthesis of cDNAs from RNA templates with difficult secondary structures.

cDNA synthesis was performed with the EvoScript kit using Universal cDNA master mix (Roche Life Science, Burgess Hill, UK). Samples were normalized to 100 ng/µL RNA prior to RT. Similar to the VILO™ kit, the enzyme in this kit is also thermostable during the high-temperature denaturing step. However, as mentioned earlier, the enzyme mix does have RNase activity. Therefore, the enzyme was added last to avoid digestion of the sample. Cycling conditions were 42°C for 30 min and 85°C for 5 min and 65°C for 15 min.

2.10 High-capacity cDNA synthesis

RT is the process by which single-stranded cDNA is synthesized and amplified in a qPCR from template RNA with the help of a reverse transcriptase enzyme. The High-Capacity cDNA Reverse Transcription Kit facilities the quantitative conversion of as little as 0.2–2 µg of total RNA to high-quality, single-stranded cDNA in a single 20-µL reaction.

cDNA synthesis was carried out using the High-Capacity cDNA Reverse Transcription Kit containing RT buffer (1.0 µL of 10x RT buffer), dNTPs (0.4 µL of 25x dNTPs), RT random primers (1.0 µL of 10x RT random primers), nuclease-free dH$_2$O (2.4 µL, Fisher Scientific, New Hampshire, USA) and RNA (5.0 µL) in a final reaction volume of 10.0 µL per sample. Reaction-containing samples in 96-well plates were run at 25°C

for 10 min, 37°C for 120 min and 85°C for 5 min, followed by an inactivation period at 95°C for 10 min.

2.11 CircRNA probe design

Custom-designed RT-qPCR assays for the quantification of relative expression were designed for unique backspliced circRNA junctions (ThermoFisher Scientific, Foster City, USA). Each target sequence was checked for the presence of single nucleotide polymorphisms (SNPs) in potential primer- or probe-binding regions prior to ordering. Assays were shipped in custom single tubes from ThermoFisher Scientific (Foster City, USA). For the mouse studies, sequences were first assessed for species conservation by alignment of human backspliced junctions to the mouse genome using the University of Santa Cruz genome browser (https://genome.ucsc.edu). Those predicted to have conserved backspliced junctions in humans and rodents were taken forward for analysis in mouse models of ageing.

2.12 Pre-amplification of template cDNA

Since circRNAs are often expressed at low levels, it can be difficult to detect the differential expression of these entities from the minute amounts of RNA or cDNA that are used for downstream high-throughput expression protocols like open arrays. Pre-amplification allows the enrichment of limited amounts of RNA samples, while keeping gene expression profiles unaltered by retaining the relative copy numbers of the starting target cDNA sequences. Up to 100 targets can be pre-amplified simultaneously using pooled assays of target TaqMan® gene expression assays with as little as 1–250 ng of cDNA samples. A standard real-time PCR reaction starts with

RT of total RNA using random primers, and is followed by real-time PCR using gene-specific primers and probes. In contrast, the TaqMan® PreAmp amplification protocol incorporates an intermediate step between RT and real-time PCR, through which the cDNA is enriched 1000–16,000-fold through a pre-amplification reaction for 10–14 cycles. The resulting pre-amplified cDNA samples can be diluted and used as starting templates for subsequent high-throughput singleplex real-time PCRs with pools from each TaqMan® assay.

Intially pre-amplification was done on few random samples using 1, 2.5 and 5 ng/µL of RNA in a 10 µL reaction, each of which was diluted to 1:10, 1:15 and 1:20 dilutions. qPCR was using housekeeper genes to detect the optimum cDNA quantity and concentration to achieve comparable Ct. This indicated 2.5 ng/µL at the dltuion of 1:10 to be optimum template for pre-amplification. Pre-amplification was carried out in 96-well plates using the TaqMan® PreAmp Master Mix (5 µL of 2x mix, ThermoFisher Scientific, Waltham, MA, USA), pooled assay mix (2.5 µL, Thermo Fisher) and cDNA (2.5 µL) in a final reaction volume of 10 µL per sample. cDNA input was already normalized since 2.5 µL was used in this step from a 20 µL revrese transction reachtion mix each containing 100ng of RNA as described earlier. Reactions were run at 95°C for 10 min with 14 cycles consisting of 95°C for 15 sec and 60°C for 4 min, followed by 95°C for 10 min. Deactivation was performed for 10 min at 85°C to minimize variability in Ct values, as the pre-amplified products were used for downstream analysis of high-throughput expression on the open array platform

2.13 Quantitative expression assays using RT-qPCR

RT-qPCR is a process by which gene expression can be assessed based on the relative input of cDNA reverse transcribed from RNA samples. RT-qPCR allows the quantitative detection of amplified products at the end of each PCR cycle. The assays used to conduct RT-qPCR contain PCR primers and oligonucleotide probes, which are short oligonucleotides that are complementary to a target sequence on the template amplicon. TaqMan® probes are dual-labelled hydrolysis probes that contain a reporter dye like fluoresceins FAM™ or VIC™ at the 5' end, and a minor-groove binder (MGB) moiety containing a non-fluorescent quencher at the 3' end. The MGB stabilizes the binding of the probe to the complementary target amplicon and increases the melting temperature without requiring a longer probe. This results in low background fluorescence and a higher specificity of amplification can be attained using shorter oligonucleotide probes.

Initially, a high temperature of 95°C denatures the double-stranded cDNA. When the temperature is lowered in the next step to 60°C, primers and probes anneal to the target sequence. When the probe is intact, there is no emission from the reporter dye. As primers at both ends of the target execute extension, the 5' Taq DNA polymerase cleaves the reporter from the probe at the 5'–3' exonuclease cavity causing the separation of the 5' fluorophore and the 3' quencher moieties linked to the probe. This results in the emission of a fluorescent signal from the reporter dye when the enzyme reaches the TaqMan probe. The fluorescent signal thus emitted is proportional to the number of probes cleaved and hence the number of amplicons amplified in a given cycle. This in turn reflects the amount of input RNA that was reverse transcribed to cDNA. Removal of the probe from the target strand also allows the completion of

primer extension. With subsequent PCR cycles, additional reporter dye molecules are cleaved resulting in an increase in fluorescence intensity that is proportional to the number of amplicons produced. High expression indicates that a greater amount of the starting copy number cDNA template is present in the sample. A greater amount of template cDNA causes an increase in fluorescence to be detected over a shorter period of time. As a result, more and more dye molecules are proportionately released in the exponential phase.

Quantification of the expression of target genes is done by real-time RT-qPCR, using template cDNA that has been reverse transcribed from RNA extracted from sample tissues and cells. TaqMan® assays, i.e. oligonucleotide probes designed against target sequences or the backspliced junctions of circRNAs, hybridize to template cDNAs and stimulate the DNA polymerase enzyme to add dNTPs. $MgCl_2$ in the reaction mix acts as a cofactor for the Taq polymerase to allow the annealing of primers, and the removal of phosphates from the dNTPs for the formation of phosphodiester bonds between 3' OHs of adjacent nucleotides and 5' phosphates of subsequent nucleotides.

The TaqMan® assays, as described earlier for RT-qPCR, comprise a fluorescent fluorophore reporter at the 5' end and a quencher fluorophore at the 3' end, probes and primers. The reporter most commonly used is FAM™, which emits a green fluorescence signal, and the quencher is Black Hole Quencher Dye 1. An ideal target sequence for amplification should be 75–200 bp to prevent primer dimer formation, have 50–60% GC content and have no secondary structure. Primer design should take these factors into consideration and ensure that the melting temperature is between 50 and 66°C. In addition, primers should not be designed against secondary

structures or long repeats of G/C, the 3’ ends of the primer pairs should not be complementary to avoid primer dimer formation and, where possible, G/C should be at the ends of the primers. The probe should ideally be <30 bp in length and have a melting temperature 5–10°C above that of the primers. The probe should ideally have 30–80% GC content, and more Cs than Gs so that the target sequence has more Gs than Cs. Additionally, it should not have G at the 5’ end as this quenches the florescence signal even after hydrolysis has taken place.

Uracil-DNA glycosylases (UNGs) are a superfamily of six enzymes that are named after the *uracil-N-glycosylase* gene. They are well-preserved DNA repair enzymes that eliminate uracil incorporated in DNA/cDNA. They remove uracil from single- or double-stranded dU-containing DNA by catalysing hydrolysis of the N-glycosylic bonds between uracil residues and sugars. UNG activation allows the degradation of misprimed or non-specific products, resulting in the existence of only nucleic acid templates intended for PCR amplification in samples. However, UNGs cannot be fully heat deactivated and can degrade amplified products. They can also be inactivated during 50–55°C RT steps during RT-PCR. Thus, they are not able to eliminate or degrade dU bases from the first cDNA strands synthesized during RT-PCR. Therefore, UNG-containing reaction mixes were not used in the course of this research project.

RT-qPCR was performed to assess the expression of target genes and circRNAs. The reaction mixes used for RT-qPCR included TaqMan® Universal PCR mastermix II (2.5 µL, no AmpErase® UNG) (ThermoFisher Scientific, Waltham, MA, USA), dH_2O (1.75 µL, Fisher Scientific, USA), cDNA (0.5 µL) and TaqMan® gene assay (0.25 µL, ThermoFisher Scientific, Waltham, MA, USA) in 5 µL final reaction volumes. The

reaction mixes were centrifuged at 3000 rpm, vortexed and centrifuged again at 3000 rpm, and then transferred to 384-well qPCR plates. qPCR was run at 50°C for 2 min, 95°C for 10 min and 50 cycles each consisting of 15 s at 95°C, 30s and 1 min at 60°C. Samples assays were conducted in triplicate. To ensure quality control for RT-qPCR, 'no template control' was used for each assay in every qRT-PCR run. In addition, three endogenous control genes were used to normalize candidate transcript Ct value relaive to the the three housekeeping genes for each experiment.

2.14 High-throughput expression assays using OpenArray®

The TaqMan® OpenArray® allows high-throughput expression profiling of as many as 3072 reactions on each plate. Four such plates can be run simultaneously. Each of these plates harbours 48 subarrays containing 64 300-µM wells, which each have hydrophilic and hydrophobic coatings to ensure that the small amounts of reaction mix are confined to their respective wells. The reaction mixes are loaded onto the plates by a robot, which is immediately followed by each plate being sealed with oil to prevent evaporation of samples from the arrays (ThermoFisher Scientific, Waltham, USA).

High-throughput expression of circRNAs was assayed using 2x OpenArray® Real-Time Master mix (2.5 µL, ThermoFisher Scientific, Waltham, MA, USA), diluted pre-amplified cDNA (1.2 µL) and RNase-free dH_2O (1.3 µL, Fisher Scientific, USA) on custom OpenArray® plates (ThermoFisher Scientific, Waltham, USA). The resulting data were uploaded using ThermoFisher Scientific cloud software and analysed with STATA16.0.

2.15 Relative quantification using RT-qPCR

During RT-qPCR, an algorithm allows threshold cycle C_t, which reaches beyond the baseline of the reference dye for each sample, to be measured during the exponential phase of the PCR cycle. In this phase, the PCR product doubles efficiently and is directly proportional to the amount of template cDNA. Therefore, in this phase, the increase in the reporter's fluorescence signal is directly proportional to the number of amplicons generated. As the qPCR reagents continue to be consumed, the reaction tends to slow and transitions to a linear phase. At this stage, amplification ceases to double at each successive cycle, until it reaches the endpoint or plateau stage when the reaction halts. When a PCR reaction starts, Taq polymerase digests the oligonucleotide probe at the 5' end, and cleaves the quencher from the 3' end once the template cDNA has been duplicated or elongation is complete (ThermoFisher Scientific, Waltham, USA). This allows the FAM™ reporter to fluoresce. The fluorescence signal can be detected by the optical media of QuantStudio12.0 at each cycle. This allows quantification of expression at each subsequent cycle. The Ct value relating to the fluorescence signal is then used to relatively quantify gene or circRNA expression. The C_t value is the number of the PCR cycle when fluorescence has increased beyond the background signal and, inversely, relates to the exponentially amplified cDNA. It represents the comparative levels of RNA in the original non-reverse-transcribed RNA samples. A low C_t value signifies a high amount of initial template cDNA and therefore higher expression, and vice versa. Relative quantification of gene expression in any given sample is assessed by the comparative C_t method, in which expression is compared relative to a set of reference housekeeping genes as well as normalized to the C_t levels of control samples.

The $\Delta\Delta C_t$ method was used to determine relative expression throughout this thesis (Livak and Schmittgen 2001; Rutledge 2004; Schmittgen and Livak 2008). Although relative expression can be assessed relative to the means of endogenous housekeeping genes, expression was assessed relative to the global geometric mean of the entire set of transcripts. Throughout this project, the geometric mean across all transcripts for each sample was used for the initial normalization of ΔC_t. The expression of each individual circRNA was normalized to the global mean of expression of each circRNA across the samples throughout this thesis, since expression of the housekeeping genes was not stable.

As mentioned earlier, the threshold C_t, at which florescence is above the background fluorescence for each transcript but within the exponential phase of the amplification curve in qPCR, can be used to determine the relative fold-change or relative quantification of one sample compared to another. The C_t values of endogenous control or housekeeping genes were used as the first filter for the normalization of gene expression for each sample because these genes are thought to display stable expression under varying conditions, since they are needed for key fundamental processes such a survival. RefFinder online software was used to determine if housekeeping genes were the most stable (https://www.heartcure.com.au/reffinder/). Throughout the course of this project, geometric means across all transcripts for each sample were used for initial normalization. ΔC_t was calculated by subtracting the geometric mean from the C_t value of each transcript for a sample. The $\Delta\Delta C_t$ was next calculated by subtracting the ΔC_t of a sample compared to the median ΔC_t of a control group. Since the C_t was collected in the exponential phase, a transformation of $\Delta\Delta C_t$ to $2^{-\Delta\Delta Ct}$ transforms this relative change in cycle number, i.e. CT, into a fold-change

representing the doubling during the PCR phase of the qPCR. Data were transformed to ensure a normal distribution where samples numbers were high and outliers were removed based on the z-scores beyond ±3 standard deviations (SPSS, IMP, USA).

2.16 Statistical Analysis

Multivariate linear regression analysis was carried out to assess the association of expression of circRNA in the peripheral blood with age and ageing-related outcomes using StataSE15 (StataCorp, Texas, USA). In the multivariate regression model, adjustments were made for potential confounders like BMI, sex, level of education (none, elementary, secondary, high school or university), study site, smoking and white blood counts (neutrophil, lymphocyte, monocyte and eosinophil percentages). Age was additionally adjusted for all other measures of association, i.e. hand grip strength and parental longevity score. Statistical analysis was completed using StataSE15 (StataCorp, Texas, USA).

Differential expression of circRNA, *in vitro* cultures of senescent cells and treated EndoC βH1 cells were assessed by one-way analysis of variance ANOVA using StataSE15 (StataCorp, Texas, USA). Any potential correlation of expression level was then correlated with diabetic status (no diabetes or impaired glucose intolerance i.e. IGT, T2D or overt diabetes) and islet genotypes were assessed by one-way ANOVA using StataSE15 (StataCorp, Texas, USA). Adjustment was made for potential confounders including age, sex, BMI and ethnicity.

2.17 Generation of a circRNA profile using RNA-Sequencing

The first step in RNA-Sequencing (RNA-Seq) is to construct a strand-specific library from total RNA that can be treated to remove rRNAs, poly(A) mRNAs or small RNAs, depending on the target research question. While poly(A) pull-down RNA-Seq libraries are used for mRNA transcriptome profiling in most cases, ribosomal-depleted or total RNA libraries are mostly used for circRNA profiling (Barrett and Salzman, 2016). To retain the transcriptional direction include direct ligation of RNA adaptors before RT, direct ligation of DNA adaptors to single-stranded cDNA, RT of *in vitro* poly(A) RNA fragments followed by intramolecular ligation, and the incorporation of dUTP during second-strand synthesis and digestion with uracil-*N*-glycosylase. (Podnar et al., 2014). Poly(A) mRNA removes ncRNAs and therefore retains information on protein-coding genes. On the other hand, removal of rRNA allows enrichment of poly(A) mRNAs, ncRNAs, and intermediates or by-products of RNA biogenesis, but demands complicated downstream analysis (Podnar et al., 2014). A comparison of RNAse R- and rRNA-treated samples can yield evidence of real circRNA enrichment (Barrett and Salzman, 2016).

The first step in library preparation is fragment size selection depending on the RNA species to be investigated. The next generataion sequencing (NGS) platform can analyse millions of short fragments ranging from 25–450 bp in a single run, allowing data outputs of up to 50 GB (Mutz et al., 2013). The read depth varies according to the platform used. For example, the Illumina platform can allow read lengths of 30–100 bp (Marguerat and Bähler, 2010). The target library insert length is achieved by time-controlled heated digestion of RNA in the presence of magnesium or zinc cations (Head et al., 2014).

Once the RNA fragments are generated, end repair is executed by blunting the ends. They are then phosphorylated at their 5’ ends, as well as A-tailed at their 3’ ends to permit the ligation of adaptors, and purified using beads (Head et al., 2014; Podnar et al., 2014). The final library always consists of fragments ligated to ~120-bp adaptors at their 5’ and 3’ ends, and this step is followed by the hybridization of an RT primer to allow RT (Podnar et al., 2014). The library is then fed onto beads or into flow cells to allow fragments to hybridize on the flow cell surface, and amplified as a clonal cluster through bridge amplification by PCR to amplify the cDNA (Podnar et al., 2014; Marguerat and Bähler, 2010). Adaptor dimers and other artefactual by-products are generally cleaned up using beads or agarose gels (Head, 2015). In order to compare differential expression between groups or samples, different barcoded adaptors are used in each sample or are introduced using barcoded PCR primers during PCR amplification (Head et al., 2014).

NGS technology involves fluorescent signals being emitted at each sequencing cycle, when bases matching the template sequence are incorporated into the sequencing reaction. These signals are converted from raw outputs to short base-read sequences in FASTQ format in the form of images by base-calling algorithms. These images of short sequences are used for base calling in downstream analysis (Podnar et al., 2014). The sequences are aligned to a reference genome as transcriptome data are not easily available. Spliced read-mapping software splits unmapped read fragments and aligns them independently, in order to take into account genomic intron–exon structure (Mutz et al., 2013).

RNA-seq library preparation was done by Dr Karen Moore and RNA-seq analysis was performed by DR Ryan Ames as described below. To generate a circRNA profile, we subjected our samples to ribosomal removal and RNase R treatment to exclude linear mRNAs. In this study, circular RNA profiles were generated using a modified 'CircleSeq' procedure (Lopez-Jimenez et al., 2018), carried out by the Exeter sequencing service. Circle-Seq involves RNase R treatment of the samples before the library preparation to eliminate linear RNAs leaving the circRNAs intact. However higher amount of total RNA is needed in this protocol. So, in addition rRNA-depletion is done for high-throughput sequencing after which reads are directly mapped to de novo genomic positions to identify backspliced reads. Breifly, the RNA samples were in BR5 buffer containing RNAse inhibitor. Riborsomal RNA was removed using rRNA depletion magnetic beads (Illumina Ribo-Zero, Illumina, Inc., USA) which bind rRNA. The remaining cirRNA and mRNA was concentrated using RNAClean beads. The samples were cleaned using RNAClean beads in order to remove this buffer and replace with for water before moving to the next step of RNAseR digestion since the BR5 buffer with inhibitor would otherwise limit the RNAseR lead digestion of linear transcript. The quality of the cleaned and concentrated RNA was checked on the Tapestation before digestion. This method is an enriched bias-free unlike a candidate-based approach and permits the identification of novel circRNAs. This is because this approach additionally allows the alignment by considering the two terminations of a single read for mapping them separately based on the backsplice properties of the sequences for example of sequences flanked by GT/AG splice site.

Figure 8 Steps for the preparation of sample for RNA-Seq. *Samples are prepared from total RNA for enrichment of circular RNAs with RNAse R treatment after ribosomal depletion for sequencing processing and subsequently data analysis. (López-Jiménez, Rojas, and Andrés-León 2018).*

Each RNA sample was divided into two aliquots. One aliquot was treated with RNAse R (Epicentre, Madison, USA) at 30°C for 30 min to remove linear RNA, while the other was treated with RNase-free water as a mock-treated sample. Both aliquots were cleaned and concentrated using RNA Clean beads (Beckman Coulter, Indianapolis, USA) to remove RNAse R. The high sensitivities of RNA samples were confirmed with screentape (Agilent, Santa Clara, USA). rRNA was removed, and the concentrations of indexed sequencing libraries determined by qPCR and adjusted for size using Tapestation D1000 analysis (Agilent, Santa Clara, USA). Libraries were denatured, diluted, clustered and sequenced using TruSeq SBS reagents (V3) on the Illumina platform.

2.18 Analysis of circRNA profiles

In our study, RNase R and mock-treated sequence data were assembled against the reference human genome (hg19), and putative circular RNAs were identified using PTESFinder (Izuogu et al., 2016) using Tophat v2.1.0 with pre-set sensitive alignment parameters in paired-end mode (Trapnell et al., 2009).

(PTES) is a term used to describe RNA entities that harbour unusual splice junctions (Izuogu et al., 2016). PTESFinder analyses reads that fail to fully map to reference sequences. It splits such unmapped reads in to two or more segments, and aligns the split reads to unlock the rearranged splice junctions by genome-wide alignment or by comapring the two paired-end reads that map in an unusual configuration to reference transcriptomes (Izuogu et al., 2016).The numbers of reads mapping to each exon of each gene were calculated using FeatureCounts v2.0.0 (Liao et al., 2013; Liao et al 2014). In addition to circular RNA detection using PTESFinder, reads from all samples were also mapped to the human genome reference (hg19) obtained from iGenomes using Tophat v2.1.0 with the pre-set sensitive alignment parameters in paired-end mode (Trapnell et al., 2009). The number of reads mapping to each exon of each gene was then calculated using FeatureCounts v2.0.0 with parameters for unstranded alignment, paired reads, count multimapping reads and assigning reads to overlapping features (Liao et al., 2013; Liao et al., 2014). To calculate a comparable measure of circular RNA abundance between samples, we used a measure termed back-spliced reads per million mapped reads (bpm) for each circular RNA. This measure is designed to be similar to the commonly used reads per kilobase per million mapped reads (RPKM) metric used regularly to estimate each exon expression from RNA-Seq data across samples.

2.19 Pathway analysis of genes generating the circRNAs

The plug-in ClueGO (Cytoscape version 2.5.2) was used to assess pathways that could be affected by the host genes generating the top 10% of circRNAs in terms of abundance circRNAs (Bindea et al., 2009). The host genes generating 10% most abundant circRNAs in the circRNA profiles were queried against Kyoto Encyclopedia

of Genes and Genomes (KEGG_20.11.2017), REACTOME_Pathways_20.11.2017 and WikiPathways_20.11.2017. Outputs obtained from enrichment analyses were based on a two-sided hypergeometric test with Bonferroni correction for p-values for the selected ontology reference set of candidate genes. The functional pathways were groups based on the gene ontology (GO) terms and the kappa score.

2.20 Whole-genome amplification

Whole-genome amplification was done using a REPLI-g® Mini Kit (QIAGEN, Hilden, Germany). The REPLI-g® technology uses isothermal multiple misplacement amplification (MDA) combined with a gentle alkaline denaturation step to uniformly amplify genomic loci. MDA involves the binding of random hexamers to denatured DNA followed by strand displacement synthesis at a constant temperature. The strand synthesis step is executed by a high-fidelity phage-derived Phi29 polymerase with 3'–5' proofreading exonuclease activity. This enzyme delivers 1000-fold higher-fidelity products compared with Taq DNA polymerase. Phi29 polymerase can generate fragments as big as 100 kb through its proofreading ability, can override secondary structures such as hairpin loops and does not dissociate during amplification.

Denaturation of genomic DNA is often achieved through harsh methods such as incubation at elevated temperatures or high alkalinity. However, the REPLI-g® Mini Kit denatures DNA via mild alkaline incubation, permits very low levels of DNA fragmentation and leads to the generation of longer amplified DNA fragments with high integrity. Additionally, in contrast to other whole-genome amplification protocols, which use heat-induced denaturation leading to the generation of damaged template DNA

and biased underrepresented fragments, the exonuclease-resistant primers and buffer system in the REPLI-g® protocol ensure high yields of long, unbiased genomic fragments.

Whole-genome amplification was done using genominc DNA that co-eluted during RNA extraction (2.5 µL) and 2.5 µL buffer D1 (0.5 µL reconstituted buffer DLB and 2.0 µL RNase-free dH_2O (Fisher Scientific, New Hampshire, USA), and incubated at 15–25°C for 3 min. Next, 5.0 µL of buffer N1 (0.7 µL stop solution and 4.3 µL RNase-free dH_2O (Fisher Scientific, New Hampshire, USA)) was added, the reaction mixed by brief vortexing and centrifuged briefly. Then, 15 µL of ice-cold master mix containing REPLI-g® mini reaction buffer (14.5 µL) and REPLI-g® mini DNA polymerase (0.5 µL) was added, making a final reaction volume of 20 µL. The reaction mix was incubated at 30°C for 16 h, followed by an inactivation period of 3 min at 65°C.

2.21 Genotyping

The TaqMan® Genotyping protocol can be used to amplify and detect specific SNP alleles using a 5' nuclease assay. TaqMan® genotyping (SNP) assays use a pair of unlabelled primers, a reporter VIC® dye at the 5' end of the allele 1 probe, a 6FAM™ dye at the 5' end of the allele 2 probe, and an MGB and nonfluorescent quencher (NFQ) on the 3' end. Each MGB probe anneals to the complementary sequence between the forward and reverse primers.

PCR amplification is done using a chemically modified form of AmpliTaq® DNA polymerase for efficient hot-start PCR (ThermoFisher Scientific, Waltham, MA, USA).

DNA polymerases can be active, although to a lesser degree, at temperatures lower than the ideal temperature range for extension, i.e. 68–72°C. Primers tend to bind non-specifically at temperatures below ideal annealing conditions, leading to non-specific amplification, even if reaction mixes are prepared on ice. This can be prevented by using polymerase inhibitors like antibodies, which dissociate from the DNA polymerase by denaturation only when a certain temperature is reached during hot-start PCR. The AmpliTaq Gold® DNA polymerase does not facilitate extension at room temperature, and thus prevents any extension or subsequent amplification that could otherwise occur due to low-stringency mispriming events at room temperature. When the AmpliTaq Gold® DNA polymerase reaches probes hybridized to the target sequence, it separates the reporter dye from the quencher dye. This separation leads to an increase in fluorescence of the reporter during PCR amplification, indicating the presence of an allele of the respective dye. The probes remain intact in the absence of a complementary target sequence. This keeps the quencher dye in close proximity to the reporter dye and prevents any emission of fluorescence. Thus, the fluorescent signal generated by PCR amplification corresponds to the allele in the sample.

Genotyping was done using TaqMan® Genotyping Master Mix (2.5 µL, ThermoFisher Scientific, Waltham, MA, USA), TaqMan® gene assay (0.25 µL, ThermoFisher Scientific, Waltham, MA, USA), dH_2O (1.75 µL, Fisher Scientific, New Hampshire, USA) and whole-genome amplified template (0.5 µL) in a 5-µL final reaction volume.

PCR was also used for genotyping. PCR amplifies and detects DNA sequences using DNA polymerase in the presence of magnesium buffer and nucleotides. It involves a three-phase cycle of denaturation, annealing and elongation for about 20–40 cycles.

The double-stranded DNA templates are heat-denatured to allow primers to anneal to single-stranded DNA strands. The DNA polymerase then extends along the template strand in the elongation phase, producing two copies from the original double-stranded template DNA strand in each cycle.

PCR performance can be affected by the GC content of the original template. A high GC content renders the template more stable, often due to the presence of secondary structures such as hairpin loops. Such structures may demand higher denaturation and annealing temperatures, and shorter annealing times, to prevent non-specific binding of GC-containing primers. Additional reagents like dimethyl sulfoxide (DMSO), glycerol and betaine can help to unlock GC-rich secondary structures and facilitate denaturation.

The advantage of using MegaMix-Royal to amplify DNA is that it is a complete, freeze/thaw-stable, high-performing master mix. It contains optimum amounts of all of the core components, including chemically modified Taq polymerase, $MgCl_2$ buffer, dNTPs, blue MiZN loading dye and an enzyme stabilizer. Since it contains a blue agarose gel loading dye, it enables easy visualization on electrophoresis gels following amplification. The dye does not inhibit restriction enzymes or fluoresce. The modified Taq polymerase also stays inactive until denaturation has taken place. Thus, it can prevent non-specific binding of primers and primer dimer formation.

Genotyping was done using a primer mix (2.4 µL, containing a 1:1 ratio of forward:reverse primers, ThermoFisher Scientific, Waltham, MA, USA), MegaMix-Royal (4 µL, Microzone^{u}, Brighton, UK) and cDNA (1.60 µL) in a final reaction volume

of 8 µL. Reaction conditions for PCR were 95°C for 12 min; 40 cycles consisting of 95°C for 30 s, annealing for 1 min and 72°C for 1 min; followed by a final phase of 72°C for 10 min.

Chapter 3-Data chapter

Circular RNAs expressed in human peripheral blood are associated with human ageing phenotypes, cellular senescence and mouse lifespan

Abstract

Circular RNAs (circRNAs) are an emerging class of non-coding RNA molecules that are thought to regulate gene expression and human disease. Despite the observation that circRNA are known to accumulate in older organisms, and have been reported in cellular senescence, their role in ageing remains relatively unexplored. Here, we have assessed circRNA expression in ageing human blood, and followed up age-associated circRNA in relation to human ageing phenotypes, mammalian longevity as measured by mouse median strain lifespan, and cellular senescence in four different primary human cell types. We found that circRNAs *circDEF6*, c*ircEP300, circFOXO3* and *circFNDC3B* demonstrate associations with parental longevity or hand grip strength in 306 subjects from the InCHIANTI study of ageing, and furthermore, *circFOXO3* and *circEP300* also demonstrate differential expression in one or more human senescent cell types. Finally, four circRNAs tested showed evidence of conservation in mouse. Expression levels of one of these, *circPlekhm1,* was nominally associated with lifespan. These data suggest that circRNA may represent a novel class of regulatory RNA involved in the determination of ageing phenotypes, which may show future promise as both biomarkers and future therapeutic targets for age-related disease.

3.1 Introduction

Ageing is a multifactorial process leading to gradual deterioration of physical and physiological functionality at the cellular, tissue and organ level. It is the primary risk factor for chronic ageing pathologies such as cancer, sarcopenia, diabetes, cardiovascular disorders and neurodegenerative illnesses that account for the bulk of morbidity and mortality in both the developed as well as developing world (Kirkland, 2016). Physiological parameters such as loss of muscle mass, frailty, immobility and cognitive impairment increases the risk of developing geriatric syndromes (Fabbri et al., 2016; Narici and Maffulli 2010). The molecular processes that decline with advancing age underpin the phenotypes of ageing. At the cellular level, hallmarks of ageing include genomic instability, telomere attrition, epigenetic alterations, loss of proteostasis, deregulated nutrient-sensing, mitochondrial dysfunction, cellular senescence, stem cell exhaustion and altered intercellular communication (Lopez-Otin et al., 2013).

Changes in gene expression have been reported in many age-related diseases (Yang et al., 2015). In addition to an increase in transcriptional noise and aberrant production and maturation of mRNA transcripts (Bahar et al., 2006; Harries et al., 2011), studies report associations between gene expression and the development of age-associated syndromes of the muscle (Welle et al., 2004) as well as neurodegenerative conditions such as Alzheimer's disease and Parkinson's disease (Miller et al., 2017; Shamir et al., 2017). Differential expression of genes involved in inflammatory, mitochondrial and lysosomal degradation in ageing tissues has also been reported (de Magalhaes et al., 2009). Gene expression is regulated at many levels. Changes in the regulation and pattern of alternative splicing are associated with age in several human populations and are also evident in senescent cells of different lineages, where they may drive

cellular senescence, since restoration of levels reverses multiple senescence phenotypes (Latorre et al., 2017; Latorre et al., 2018a; Latorre et al., 2018b; Latorre et al., 2018c; Lye et al., 2019). Notably, non-coding RNAs also demonstrate associations with ageing or senescence and may be of equal importance (Abdelmohsen et al., 2012; Boulias and Horvitz, 2012; Gorospe and Abdelmohsen 2011).

Circular RNAs (circRNAs) are a recently discovered class of non-coding RNA molecules that are thought to have important roles in regulation of gene expression and human disease (Haque and Harries, 2017). CircRNAs are formed by the back splicing of downstream exons to the 3' acceptor splice site of upstream exons and result in a covalently closed circular structure containing one or more exons. They have been proposed to be key regulators of gene expression by various mechanisms including sequestration of RNA-binding proteins and miRNAs or by acting as a competitor of linear splicing of their cognate genes (Memczak et al., 2013). The possibility that a single circRNA could sequester several such RNA regulators suggests that these class of non-coding RNAs could modulate many cellular and physiological processes through multiple pathways. CircRNAs are known to accumulate in older organisms (Gruner et al., 2016), and some have been reported to be implicated in cellular senescence (Du et al., 2017; Du et al., 2016). Despite these promising findings, their role in ageing remains relatively unexplored.

We hypothesized that expression of some circRNAs may be associated with advancing age, ageing phenotypes, lifespan or cellular senescence. Changes in circRNA expression over a five-year period were assessed in relation to age,

combined parental longevity score (PLS) and hand grip strength. We then assessed expression levels of 15 circRNAs in early passage and late passage primary human dermal fibroblasts, cardiomyocytes, astrocytes and vascular endothelial cells. Finally, the junction sequences of relevant exons were examined for conservation between mouse and humans and where evidence was present that the back-spliced junction, and thus the circular RNA were conserved, we assessed expression in relation to longevity in 6 strains of mice with differential median strain longevities.

We present here evidence that although effects on age itself did not replicate in the wider sample set, the expression levels of *circEP300* (β=-0.065, p= 0.001) and *circFOXO3* (β=-0.060, p= 0.002) were negatively associated with parental longevity score. *CircDEF6* was positively associated with parental longevity score (β=0.070, p= 0.024) although this did not reach multiple testing thresholds. *CircFNDC3B* was also nominally associated with hand grip strength (β=0.004, p= 0.039). 7/12 (58%) circRNAs expressed in senescent human primary astrocytes, endothelial cells, fibroblasts or cardiomyocytes also demonstrated dysregulated expression in one or more cell types. Comparative sequence analysis suggested that four circRNA may be conserved in mice. When assessed, c*ircPlekhm1* transcript level in spleen was also demonstrated to be positively-associated with mouse median strain lifespan (β = 0.0025; p = 0.017). These results suggest that some age-related circRNAs may play roles in molecular drivers of ageing such as cellular senescence, and hence may represent potential contributors to lifespan or other human ageing phenotypes.

3.2 Methods

3.2.1 InCHIANTI cohort and selection of participants

The InCHIANTI study of Ageing is a population study of ageing (Ferrucci et al., 2000). The present study used participants from the third and fourth follow-up visits (FU3 and FU4). RNA samples and clinical/phenotypic data were already available for 698 participants at FU3. During the FU4 interviews in 2012/13, blood and clinical/phenotypic data were collected from 455 study participants. These data were cross-checked against RNA samples and clinical/phenotypic data already held from FU3, to ensure that sample and phenotypic data was available from both collections. Sample-associated data included measures of potential confounding factors. Characteristics of the study population are given in Table 2. Informed consent and ethical approval were obtained from all participants and the Instituto Nazionale Riposo e Cura Anziani institutional review board, Italy respectively.

Table 2 Participant demographics. *Population demographics and clinical characteristics of InCHIANTI study participants assessed in this work. A. Demographics B. Clinical characteristics.*

A	n	%
Participants	306	100
Age (years)		
30–39	24	7.84
40–49	37	12.09
50–59	31	10.13
60–69	32	10.46
70–79	116	37.91
80–89	63	20.59
90–100	3	0.98
Gender		
Male	143	46.73
Female	163	53.27
Pack years smoked (lifetime)		
None	164	53.59
<20	79	25.82
20–39	43	14.05
40 +	20	6.54
Study site		
Greve	146	47.71
Bagno	160	52.29
Education level attained		
Nothing	22	7.19
Elementary	124	40.52
Secondary	56	18.30
High school	50	16.34
Professional school	34	11.11
University or equivalent	20	6.54

B	n	Mean	SD	Min	Max
Age (years)	306	66.96	16.06	30.00	94.00
BMI	305	27.15	4.35	15.01	42.99
White blood cell count (n, K/ul)	305	6.40	1.59	2.10	13.00
Neutrophils (%)	305	56.59	8.35	34.20	81.20
Lymphocytes (%)	304	31.69	7.67	9.80	51.20
Monocytes (%)	304	8.04	2.20	3.90	21.30

Eosinophils (%)	304	3.18	2.17	0.00	21.50
Parental longevity score	206	-0.02	0.81	-2.46	1.71
Mean hand-grip strength (Kg)					
Follow-up3	305	29.65	12.49	2.50	70.75
Follow-up4	291	28.66	12.30	5.00	65.50

3.2.2 Generation of circRNA profiles from old and young human peripheral blood

Circular RNA profiles were initially generated in parallel from two sets of pooled peripheral blood total RNA samples using a modified 'CircleSeq' procedure (Lopez-Jimenez et al., 2018). 2 µg RNA (RNA integrity number; RIN = 6.4) was assessed in two separate pools from 20 'young' samples (median age=33 years, range 30-36 years, 55% female, 45% male; RIN 5.6) and 20 'old' samples (median age 87 years, range 86-95 years, 90% female 10% male, RIN 7.7). Each pooled sample was divided into two aliquots; one of which was treated with 20 units RNAse R (Epicentre, Madison, USA) at 30˚C for 30 minutes to remove linear RNA, the other sample being mock-treated using 1 µl RNase-free water in place of the enzyme. Both aliquots were cleaned and concentrated using 2 volumes of RNA Clean beads (Beckman Coulter, Indianapolis, USA) to remove the enzyme. The results of the RNase R treatment were confirmed on a high sensitivity RNA screentape (Agilent, Santa Clara, USA). Ribosomal RNA was removed and indexed sequencing libraries made using the libraries was determined by qPCR and adjusted for size using Tapestation D1000 analysis (Agilent, Santa Clara, USA). Ribosomal RNA was removed and indexed sequencing libraries made using the Illumina RNASeq protocol. The libraries concentrations were determined by qPCR and adjusted for size using the data from the Tapestation D1000 analysis. Libraries were pooled in equimolar quantities,

denatured and diluted to 12.0 pM + 1% PhiX for clustering and then underwent 125 paired-end Illumina sequencing in four lanes using TruSeq SBS reagents (V3).

3.2.3 Analysis of circRNA profiles

RNase R and mock-treated sequence data were assembled and putative circular RNAs were identified using PTESFinder (Izuogu et al., 2016) with the human genome (hg19) reference files provided with the software, a segment size of 65 and a uniqueness score of 7. The remaining parameters were left to default settings. To calculate a comparable measure of circular RNA abundance between samples we used a measure termed back spliced reads per million mapped reads (bpm) for each circular RNA i is defined as:

$$bpm_i = \left(\frac{j_i}{\sum_{a=1}^{n} j_a + \sum_{b=1}^{n} c_b} \right) . 10^6$$

Where J_i *i*s the number of reads mapped to the backspliced junction of the circular RNA, *c* is the number of reads mapped to canonical sites of the gene with the circular RNA and *n* is the number of circular RNAs identified. This measure is designed to be similar to the commonly used reads per kilobase per million mapped reads (RPKM) metric used regularly to estimate gene expression from RNA-Seq data.

In addition to circular RNA detection using PTESFinder, reads from all samples were also mapped to the human genome reference (hg19) obtained from iGenomes using Tophat v2.1.0 with the pre-set sensitive alignment parameters in paired end mode (Trapnell et al., 2009). The number of reads mapping to each exon of each gene was

then calculated using FeatureCounts v2.0.0 with parameters for unstranded alignment, paired reads, count multimapping reads and assigning reads to overlapping features (Liao et al., 2013; Liao et al., 2014). Counts were used to calculate RPKM per exon using the standard method to compare the expression of each exon across samples.

3.2.4 Pathway analysis of differentially-regulated circRNA host genes

CircRNAs showing expression differences between the pooled old and the pooled young samples were ranked by RPKM and fold change. To assess whether circRNAs demonstrating expression differences between 'young' and old' pools were enriched in genes derived from specific molecular or biochemical function groups, we carried out a Cytoscape version 2.5.2 plug-in ClueGO analysis. This platform queries over-representation of query genes in specific KEGG, REACTOME and WikiPathways (Bindea et al., 2009). The linear genes hosting the top 10% most abundantly-expressed circRNAs in 'young' and 'old' pools for the circRNA profile were queried against KEGG_20.11.2017, REACTOME_Pathways_20.11.2017 and WikiPathways_20.11.2017. Outputs were selected based on 'enrichment/depletion' through a two-sided hypergeometric test with Bonferroni step down for p-value correction with the selected ontology reference set of chosen genes. The GO terms were used to group functional pathways and the leading functional grouping was based on highest significant kappa score.

3.2.5 Design of qPCR assays for circRNA validation

Levels of individual circRNA in 'young' and 'old' pools were ranked by abundance. CircRNAs demonstrating evidence of altered expression with age fell into three classes: those expressed exclusively in old, those expressed exclusively in young, and those expressed in both young and old, but with evidence that levels were different between the pools. We selected 5 circRNAs exclusively expressed in young (*circITGAX, circPLEKHM1, circDEF6, circATP6V0A1* and *circASAP1*), 5 exclusively expressed in the old (*circFOXO3, circFNDC3B, circAFF1, circCDYL* and *circXPO7)*, as well as 5 expressed in both pools but demonstrating evidence of altered expression (*circMIB1*, *circMETTL3*, c*ircBCL11B*, *circZC3H18* and *circEP300*), where sequence and assay design constraints allowed for to design specific assays to unique back spliced junction for qRTPCR follow up. Standard curves for the assays are shown in appendix (Fig A1).

3.2.6 CircRNA probe design

Custom designed qRTPCR assays for quantification of relative expression were designed to unique backspliced circRNA junctions (Thermo Fisher, Foster City, USA), the sequences of which are given. Each target sequence was checked for the presence of single nucleotide polymorphisms in potential primer or probe binding regions prior to ordering. Assays were ordered as custom single tube assays from Thermo Fisher (Foster City, USA). Each circRNA probe was validated using standard curve analysis using 1:10 serial dilutions of synthetic oligonucleotides homologous to the back spliced junctions.

Table 3 Assay information for age-associated circRNA assessed in this study.

CircRNA	Forward primer	Probe	Reverse primer
CircAFF1	CCTGCCAAAGCCAAGCT	TCTCAGTCAGTTGAGTTTGT	AGCAGGTTTCTGTCGTCATTGT
CircASAP1	AGGAGGAAGTGTTCAGTCAAGAATG	CACATGCCACATTTCT	ACTTATCAGCTGTTTTCAAGCCATCT
CircATP6V0A1	CGCCGTCAGTATTTGAGGAGAAA	CTTCTTGAAATAGCAAATGC	AGCCAAACAAAGAGGTCATGAAGAT
CircBCL11B	AAAGGCATCTGTCCCAAGCA	CAGCCTCTGCAATGTT	GCGGCCTCCACATGGT
CircCDYL	CATGGCCACAGGCTTAGCT	CAATCCTTTCAACCTTTCCC	CGAACCAAATACTCTGTCTTCCCTTTT
CircDEF6	GGGAGTGAAGAGTGCAAAGAGAAA	TCCACCTCCACGCAGCAG	GCTGAGTACCTTTTTCAGCAGGTAT
CircEP300	GTTGCATATGCTCGGAAAGTTGAAG	CATTCCCATTCGATTGTTTG	GCTGTCCAGGATTCTGAGTATATGG
CircFNDC3B	AGCCCAAAGTCGAATGATTCAGA	TTGCAAGGTGATTGAAGATA	CCGGCGGACTCCAGTAC
CircFOXO3	AGGCTGAAGGATCACTGAGGAA	ATGGAGTTCTGCTTTGCC	CGACTATGCAGTGACAGGTTGT
CircITGAX	GAGGATGAAGGCCGAAGTCA	CCGTACCTGAGTCCCC	TCGAAGGAGCTACTGCTTGTG
CircMETTL3	GAACCAACAGTCCACTAAGGAACAA	CAGAGCAAGAAGATCTAC	ACAATGCTGCCTCTGGATTCC
CircM1B1	GGCATTGATGAAGATCATGACATTGT	ATGCTTGATGCCTATTGCC	TTGCTGGCGGCAGGTAT
CircPLEKHM1	CTGGGCACAGCAAATGCT	CTGCAAGAACACATCATC	CGTCAGGTGCTCCAACTCT
CircXPO7	TGTTGATGGTGTTAAACGAATACTGGAA	CCCACAGGCAGACACC	AGAGGCTATTTTTCTGTGCTTGGT
CircZCH3H18	GGAGCGGGAGAAGGAGAAG	CAGCCGCCAAGACTCG	CCAAAACCGCTCAATTTCATAGTCATAA

Endogenous controls	Assay ID	Supplier
IP08	Hs00183533_m1	Thermofisher Scientific
P0L2RA	Hs00172187_m1	Thermofisher Scientific
TFRC	Hs00174609_m1	Thermofisher Scientific

3.2.7 Assessment of associations between circRNA expression and ageing phenotypes in the InCHIANTI cohort.

RNA samples and phenotypic data were available from 306 individuals at both follow up 3 (FU3) and follow up 4 (FU4) of the InCHIANTI study of Ageing. Characteristics of participants are given in Table 2. We assessed the expression of 15 age-associated circRNAs demonstrating the most marked differential expression with age between young and old pools as described above. Ageing parameters assessed were age itself, parental longevity score (PLS) and hand grip strength. Participants aged 65+ years were categorised for PLS based on the age at death of their parents. Short, intermediate and long-lived cut-offs were calculated separately for mothers and fathers based on the normal distribution of age-at-death in the cohort, as described in (Dutta et al., 2013a). Mothers and fathers aged <49 years or <52 years at death respectively were classed as premature and excluded. To standardize parental age of death, a Z-score was generated for combined maternal and paternal measures of parental longevity. Hand-grip strength was measured in kilograms using a dynamometer, with repeated measurements at both FU3 and FU4.

3.2.8 Reverse transcription and pre-amplification of circRNAs in human peripheral blood RNA

cDNA synthesis was carried out using 100ng total RNA using the High-Capacity cDNA Reverse Transcription Kit (Thermo Fisher, Foster City, USA) according to manufacturer's instructions (Fisher Scientific New Hampshire, United States) in a final reaction volume of 10.0µL per sample. Reactions (samples in 96-well plates) were run at 25°C for 10min, 37°C for 120 min, 85°C for 5 min followed by an inactivation period

for 95°C for 10 min. Pre-amplification of circRNA expression was carried out using 5µl TaqMan PreAmp master mix (Thermo Fisher, Foster City, USA), 2.5µL pooled assay mix and 2.5µL cDNA in a final reaction volume of 10µL per sample. Cycling conditions were one cycle of 95°C for 10 min followed by 14 cycles of 95°C for 15 sec with 60°C for 4 min followed by 95°C for 10min. Pre-amplified samples were then diluted 1:10 and maintained on ice prior to analysis.

3.2.9 Assessment of associations between circRNA expression in peripheral blood RNA and human ageing phenotypes

The expression profiles of selected circRNAs were then measured in total peripheral blood mRNA using custom-designed OpenArray® plates on the Thermo Fisher 12K Flex platform (Thermo Fisher, Foster City, USA). The differential expression of circRNA measured in a customized open array platform allowed a maximum of 18 probes to be assessed. Therefore, there was no room for linear assays to be assessed in this part of the thesis**.** The differential expression of circRNA in the RNA-Seq profile was assessed in 20 samples pooled from young and old participants. Based on this initial difference in expression, a follow-up, on a larger cohort which was not pooled, was assessed using blood samples. Reaction mixes contained 2.5 µl 2× OpenArray® Real-Time Master mix, diluted pre-amplified cDNA (1.2µL) and RNase-free dH_2O (1.3µL) (Thermo Fisher, Foster City, USA). CircRNA expression was measured relative to the geometric mean of the entire set of transcripts, with the expression of each individual circRNA normalised to the global mean of expression of that circRNA across the samples. Samples were run in 3 technical triplicates. Association of circRNAs with age in InCHIANTI was carried out by multivariate linear regression,

adjusted for potential confounders BMI, sex, level of education (none, elementary, secondary, high school and university), study site, smoking and white blood counts (neutrophil, lymphocyte, monocyte, eosinophil percentages) while age was additionally adjusted for all other measures of association in the ageing human cohort. We assessed association of circRNA with hand grip strength and parental longevity score (PLS) (Dutta et al., 2013b; Dutta et al., 2013c) as a proxy measure of longevity in humans. Statistical analysis was completed using StataSE15 (StataCorp, Texas, USA). Figures were generated using GraphPad Prism 8.1.2 (GraphPad Software, San Diego, USA).

3.2.10 Assessment of circRNA expression in human primary senescent cells of different lineages

The expression levels of the 15 candidate circRNAs analysed above were also assessed in relation to cellular senescence, in senescent and early passage primary human primary fibroblasts, endothelial cells, astrocytes and cardiomyocytes using high-throughput qRTPCR on the 12K Flex OpenArray platform (Thermo Fisher, Foster City, USA). Samples were run in 3 biological replicates and 3 technical replicates. Senescent cells had been generated and characterised in previous work by our group, and culture conditions and details of assessment of senescence are reported elsewhere (Latorre et al., 2017; Latorre et al., 2018a; Latorre et al., 2018b; Latorre et al., 2018c; Lye et al., 2019). RNA samples from this work were available for use. CircRNA levels were assessed in three biological and three technical replicates from early and late passage human primary cells of 4 different cell types. Early passage 'young' cells were at population doubling (PD) of 24 for astrocytes, 28 for

cardiomyocytes, 24 for endothelial cells and 25 for fibroblasts, whilst late passage senescent cells were at PD = 84 for astrocytes, 75 for cardiomyocytes, 65 for endothelial cells and 63 for fibroblasts. Senescent cell load in these samples was ~75% for fibroblasts, ~55% for endothelial cells, ~38% for cardiomyocytes and ~36% for cardiomyocytes (Latorre et al., 2017; Latorre et al., 2018a; Latorre et al., 2018b; Latorre et al., 2018c; Lye et al., 2019). In all cases, growth of the culture had slowed to less than 0.5 PD/week. Differential circRNA expression in senescent cells was then assessed by one-way ANOVA using StataSE15 (StataCorp, Texas, USA). Figures were generated using GraphPad Prism 8.1.2 (GraphPad Software, San Diego, USA).

3.2.11 Assessment of circRNA conservation between mouse and human

We assessed whether the 15 circRNAs identified in our human study were likely to be conserved in mouse by aligning the mouse and human exon junction sequences using the Blat tool in the UCSC genome browser (https://genome.ucsc.edu). Quantitative real-time PCR assays were developed to unique back-spliced junctions of conserved circRNAs. Probe and primer sequences are given. CircRNA expression was then measured in mouse spleen and muscle tissue and assessed in relation to lifespan by analysis of levels in 6 strains of male mice (A/J, NOD.B10Sn-H2^{b}/J, PWD/PhJ, 129S1/SvlmJ, C57BL/6J and WSB/EiJ) selected on the basis of divergent median strain longevity lifespan ranging from 623 to 1005 days (Yuan et al., 2009). Samples from male mice were obtained from Jackson Laboratory Nathan Shock Center of Excellence in the Basic Biology of Ageing for this study. Animal husbandry, handling, animal characteristics and sample preparation protocols have been previously described (Lee et al., 2016). Tissue samples were obtained from cross-sectional study

conducted in the same compartment and in the same period of time as described in (Yuan et al., 2009). At the age of 6 and 20/22 months, CO_2 asphyxiation was used to euthanize the animals. Spleen and quadriceps muscles tissues were excised immediately after sacrifice and shipped from the Jackson Laboratory using RNAlater-ICE Collection protocol (Life Technologies, Carlsbad, CA). In this method, tissues are submerged in RNAlater® stabilization solution, an aqueous tissue storage reagent used to rapidly permeate tissues and stabilize RNA from fresh specimens and stored at –20°C or below for later use.

Table 4 Assay details for mouse circRNAs assessed in this work.

CircRNA	Forward primer	Probe	Reverse primer
CircMib1	AACTACAACTCGAACCGTCTG	CCAAGTGGCAATAGGCATCAAGCA	CGGCAGGTATCACACATAGTT
CircPlekhm1	TCTGAGGAACCCATGTCCTAT	CCGACAGGTCTCTGCAAGAACACA	AAGACCAGGTGCTCCAAATC
CircXpo7	GGCCAACTTTCTCTCTCATCTT	TCCACAGGCAGACACAACTCATCC	GTCTCGGAAAGAAGAGGCTATTT
CircFoxo3	CTGAAGGATCACTGAGGAAAGG	TGGAGTTCTGCTTGCCCATTTCC	TCATTCTGAACGCGCATGA

Endogenous controls	Assay ID	Supplier
Ip08	Mm.PT.39a.22214844	Integrated DNA Technologies
Pol2ra	Mm.PT.39a.22214849	Integrated DNA Technologies
Tfrc	MM.PT.39a.22214833.g	Integrated DNA Technologies

3.2.12 RNA extraction and reverse transcription from mouse tissues

Total RNA was extracted using the TRI®reagent/ chloroform phase separation according to manufacturer's instructions. Briefly, tissues stored in RNA later were drained, and then placed in 1 mL TRI Reagent® solution containing 10 mM $MgCl_2$. Samples were homogenized for 15mins (spleen) or 30mins (muscle) using bead mills (Retsch Technology GmbH, Haan, Germany). This was followed by a phase separation using chloroform. Total RNAs in the separated RNAs were precipitated from the aqueous phase through overnight incubation with isopropanol at −20 °C. The following morning, RNA pellets were washed twice with ethanol and resuspended in RNase-free dH_2O. Complementary DNA (cDNA) was generated from 100ng RNA using the Evocript® Universal cDNA Master Synthesis kit according to the manufacturer's instructions (Roche, Switzerland).

3.2.13 Assessment of circRNA expression in mouse spleen and *muscle*

CircRNAs selected on the basis of inter-species sequence conservation were validated in mouse spleen and muscle tissue. Considering, grips-strength as a measure of frailty was assessed in the human cohort, the effect of expression in mice models of different longevity was also assessed. While the differential expression of circRNAs was measured in human, in the absence of blood samples in mice models, spleen which is rich in cells of the vascular system was used. Expression levels of conserved circRNAs were assessed in relation to median strain lifespan by relative quantification. Quantitative qRTPCR was carried out for circRNAs (*circFoxo3, circMib1, CircPlekhm1* and *circXpo7)* in relation to the *Pol2ra*, *Trfc* and *Ipo8* endogenous control genes, selected on the basis of lack of age-association in a

previous study (Harries et al., 2011). Reaction mixes contained cDNA (0.5 µL) , Taqman® Universal PCR mastermix II (2.5 µL, no AmpErase® UNG, (Thermo Fisher, Foster City, USA), dH_2O (1.75 µL, Fisher Scientific , United States), and Taqman®gene assay (0.25 µL, Thermo Fisher, Foster City, USA) in a 5 µL final reaction volume. The reaction mixes were centrifuged at 3000 rpm, vortexed and centrifuged again at 3000 rpm and transferred to 384 well qRTPCR plates. qRTPCR was run at 50 °C for 2 min, 95 °C for 10 min and 50 cycles of 15 s at 95 °C for 30 s and 1 min at 60 °C. Each sample assay was conducted in 3 technical triplicates. Expression levels of circRNAs in young and old mouse tissues were measured relative to the geometric mean of the entire set of transcripts, with the expression of each individual circRNA normalised to the global mean of expression of each circRNA across the samples. Linear regression analysis was carried out to assess the association of expression of circRNA using StataSE15 (StataCorp, Texas, USA).

3.3 Results

3.3.1 CircRNA profile in peripheral blood of ageing humans

166-167M reads were obtained from the RNAse R-treated pools and 157-163M reads from the mock-treated pools with a mean Q score of 34.6-35.1 and total error rate of 0.47-0.53%. A total of 2207 circRNAs were expressed in human peripheral blood. Of these, 184 circRNAs were found in both the young and old samples, 431 were exclusively expressed in the ‘young’ sample pool and 1592 were exclusively expressed in the ‘old’ sample pool (Online Resource 1). We selected 15 circRNAs for further analysis; 5 expressed exclusively in the young pool, 5 expressed exclusively in the old pool, and 5 expressed in both pools but showing the most discrepant

expression for further study. These were *circITGAX, circPLEKHM1, circDEF6, circATP6V0A1* and *circASAP1* which showed exclusive expression in the young; *circFOXO3, circFNDC3B, circAFF1, circCDYL* and *circXPO7* which showed exclusive expression in the old; *circMIB1*, *circMETTL3*, *circEP300*, *circZC3H18* and *circBCL11B* that were expressed, but differentially so in both sample pools.

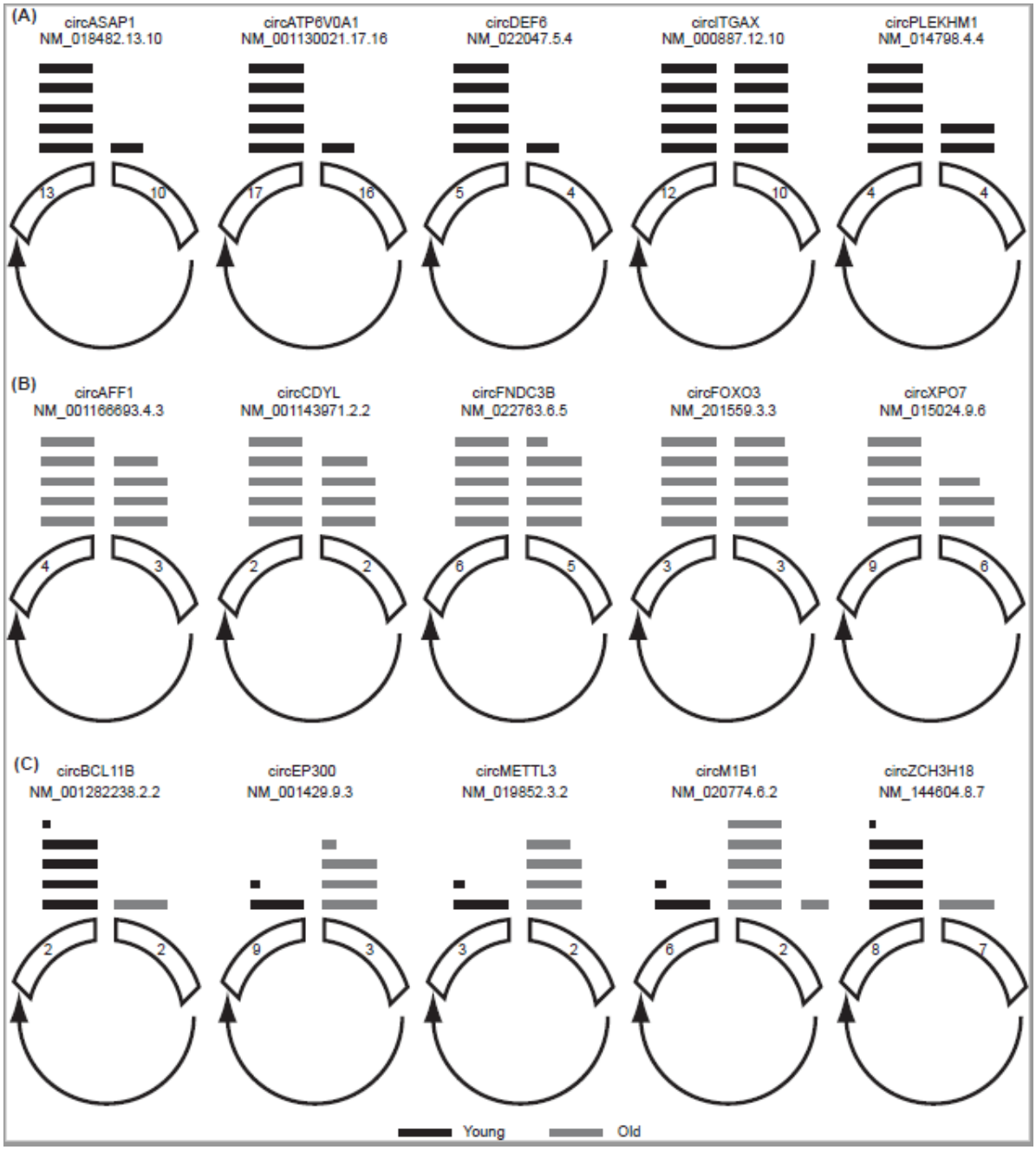

Figure 9 Circular RNA junction schematics for the top 5 most abundant circular RNAs uniquely found in young (A) and old samples (B). *Also shown, are junction schematics for the top 2 and 3 most abundant common circular RNAs found in young (n=20) and old samples (n=20) respectively (**C**). Each schematic shows the identified*

backsplicedd exon or exons. The relative read depth at each backsplicedd junction is shown by the number of bars above each junction and is scaled by linear interpolation, where the backsplicedd junctions with 1 and 10 bars represent the junctions with the lowest and highest read depth respectively. Black and grey bars show relative read depth at junctions in young and old samples respectively.

3.3.2 Pathway analysis of circRNA expressed in ageing humans

Pathway enrichment for the genes hosting the top 10% most abundant circRNAs in each of young and old pooled peripheral blood samples was performed using ClueGO cytoscape (Bindea et al., 2009). In the young peripheral blood, the top 10% most abundant circRNAs derived from genes associated with negative regulation of ATP metabolic processes and in transmission of synaptic signals. The leading-edge genes hosting circRNAs for negative regulation of ATP processes were *SNCA*, *STAT3* and *UFSP2*, whilst those associated with synaptic vesicle endocytosis were *FCH02*, *PICALM*, *PIP5K1C* and *SNCA*. Genes hosting circRNAs were primarily localised in pathways involved in phagocytosis, circadian regulation, cancer pathways and golgi-associated vesicle budding in the blood from aged donors (Table 5).

Table 5 Pathways enriched in age-associated circRNAs *The ClueGo pathways results for pathways potentially targeted by genes generating the top 10% of circRNAs differentially expressed with age are presented here aligned to the hg19 genome alignment. Number of genes = number of differentially-expressed genes in each pathway.*

Pathway	p-value	Number Of Genes	Genes
Expressed only in old			
Fc gamma R-mediated phagocytosis	0.005	4	*ARPC1B, ASAP1, PIP5K1C, VASP*
Exercise-induced Circadian Regulation	0.006	3	*CRY2, NCOA4, TAB2*
Pathways Affected in Adenoid Cystic Carcinoma	0.018	4	*ERBB2, FOXO3, KANSL1, MGA*
Endometrial cancer	0.041	3	*AXIN1, ERBB2, FOXO3*
trans-Golgi Network Vesicle Budding	0.035	3	*DNAJC6, IGF2R, PICALM*
Clathrin derived vesicle budding	0.049	3	*DNAJC6, IGF2R, PICALM*
Golgi Associated Vesicle Biogenesis	0.069	3	*DNAJC6, IGF2R, PICALM*
Cargo recognition for clathrin-mediated endocytosis	0.062	5	*FCHO2, IGF2R, PICALM, REPS1, UBQLN1*
Clathrin-mediated endocytosis	0.049	8	*DNAJC6, FCHO2, GAPVD1, IGF2R, PICALM, PIP5K1C, REPS1, UBQLN1*
Expressed only in young			
Negative regulation of ATP metabolic process	0.004	3	*SNCA, STAT3, UFSP2*
Synaptic vesicle recycling	0.009	4	*FCHO2, PICALM, PIP5K1C, SNCA*
Presynaptic endocytosis	0.018	4	*FCHO2, PICALM, PIP5K1C, SNCA*
Synaptic vesicle endocytosis	0.017	4	*FCHO2, PICALM, PIP5K1C, SNCA*
Expressed in both old and young, but demonstrating differential expression			
Huntington's disease_Homo sapiens_hsa05016	0.014	2	*ATP5C1, EP300*
Pyruvate metabolism_Homo sapiens_hsa00620	0.037	1	*HAGH*
Notch signaling pathway_Homo sapiens_hsa04330	0.045	1	*EP300*

3.3.3 CircPLEKHM1, circMETTL and CircFNDC3B expression levels are associated with ageing phenotypes in humans

The structures of the 15 circRNAs selected for follow up were predicted based on the sequencing read depth for each exon and are presented in Fig. 9. Although we demonstrated no associations with age itself, we did identify associations between some circRNAs and human ageing phenotypes. *CircEP300* and *circFOXO3* both demonstrated negative associations with combined parental longevity score (β=-0.065 and -0.060; p = 0.001 and 0.002 respectively), after adjustment for multiple testing. *CircDEF6* was positively correlated with parental longevity scores but demonstrated nominal significance only (β=0.070, p= 0.024) (Table 6, Fig. 10). A positive association was also identified both cross-sectionally (β=0.004, p=0.039) and longitudinally (β=0.004, p=0.038) between *circFNDC3B* expression and hand grip strength (Table 7, Fig. 11), although these were nominal only.

Table 6 CircRNA expression in relation to combined parental longevity score.
Beta co-efficients, p values and 95% confidence intervals (95% CI) are given for associations between circRNAs expression and combined parental longevity (PLS) score from multivariate regression analysis. 291 samples were assessed. Genes demonstrating statistically significant results below the multiple testing limit of 0.003 are indicated in bold, underlined type, whilst those demonstrating nominal associations only are given in bold type.

CircRNA	β-coefficient	p-value	95 % CI		
CircAFF1	-0.012	0.485	-0.048	-	0.023
CircASAP1	-0.044	0.064	-0.090	-	0.003
CircATP6V0A1	0.036	0.223	-0.022	-	0.094
CircBCL11B	0.042	0.136	-0.013	-	0.097
CircCDYL	-0.030	0.109	-0.067	-	0.007
CircDEF6	**0.070**	**0.024**	**0.009**	-	**0.131**
CircEP300	**-0.065**	**0.001**	**-0.103**	-	**-0.026**
CircFNDC3B	0.025	0.239	-0.016	-	0.066
CircFOXO3	**-0.060**	**0.002**	**-0.098**	-	**-0.021**
CircITGAX	0.019	0.440	-0.030	-	0.068
CircMETTL3	0.007	0.730	-0.034	-	0.049
CircMIB1	-0.018	0.310	-0.052	-	0.017
CircPLEKHM1	-0.009	0.493	-0.035	-	0.017
CircXPO7	0.038	0.162	-0.016	-	0.093
CircZC3H18	-0.036	0.078	-0.077	-	0.004

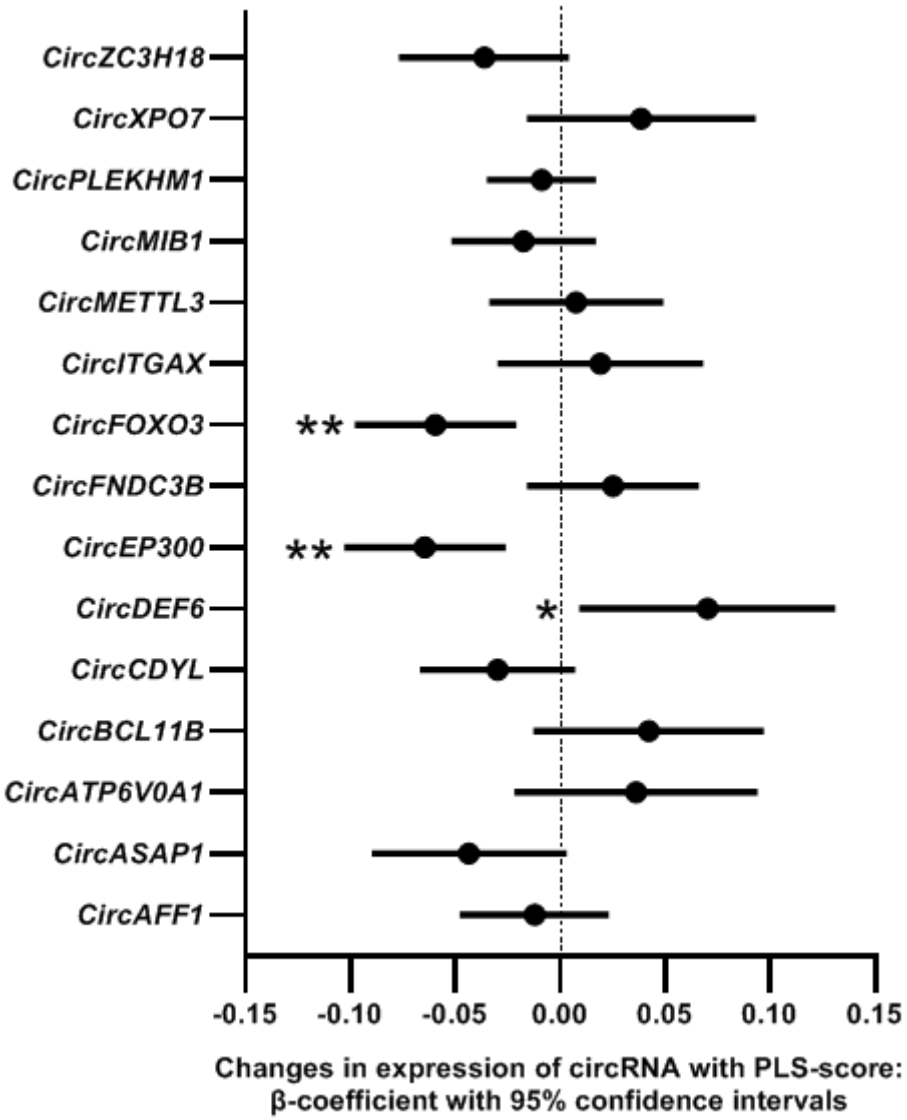

Figure 10 CircRNA expression is associated with combined parental longevity. *Forest plot illustrating the association between peripheral blood circRNA expression and combined human parental longevity score (PLS) in participants from the InCHIANTI study of* Ageing*. N= 291 individuals. The beta coefficient of the association measured by multivariate regression analysis is given on the X-axis and the identity of the gene is given on the Y axis. Lines attached to each data point represent 95% Confidence intervals (95% CI). Statistical significance is indicated by stars. * = <0.05, ** = <0.005.*

Table 7 CircRNA expression in relation to grip strength *Beta co-efficients, p values and 95% confidence intervals (95% CI) are given for associations between circRNAs expression and hand grip strength. 306 individuals were assessed. Associations were assessed cross-sectionally using multivariate regression (Expression data FU3 and clinical outcome FU3) and longitudinally (Expression data FU3, clinical outcome FU4). All associations identified here were nominal only and are given in bold type.*

CircRNA	Grip-strength	β-coefficient	p-value	95 % CI
CircAFF1	cross-sectional	-0.001	0.508	-0.004 - 0.002
	longitudinal	-0.003	0.081	-0.007 - 0.000
CircASAP1	cross-sectional	-0.001	0.713	-0.005 - 0.004
	longitudinal	0.000	0.854	-0.005 - 0.004
CircATP6V0A1	cross-sectional	0.000	0.965	-0.005 - 0.005
	longitudinal	-0.002	0.403	-0.008 - 0.003
CircBCL11B	cross-sectional	0.002	0.443	-0.003 - 0.007
	longitudinal	0.000	0.914	-0.006 - 0.005
CircCDYL	cross-sectional	-0.001	0.665	-0.004 - 0.003
	longitudinal	0.000	0.828	-0.004 - 0.003
CircDEF6	cross-sectional	0.000	0.903	-0.005 - 0.006
	longitudinal	0.002	0.599	-0.004 - 0.008
CircEP300	cross-sectional	-0.004	0.060	-0.007 - 0.000
	longitudinal	-0.003	0.112	-0.007 - 0.001
CircFNDC3B	**cross-sectional**	**0.004**	**0.039**	**0.000 - 0.008**
	longitudinal	**0.004**	**0.038**	**0.000 - 0.008**
CircFOXO3	cross-sectional	0.002	0.402	-0.002 - 0.005
	longitudinal	0.000	0.834	-0.004 - 0.003
CircITGAX	cross-sectional	0.000	0.997	-0.004 - 0.004
	longitudinal	-0.001	0.658	-0.006 - 0.004
CircMETTL3	cross-sectional	-0.003	0.139	-0.007 - 0.001
	longitudinal	-0.001	0.680	-0.005 - 0.003
CircMIB1	cross-sectional	0.000	0.906	-0.003 - 0.003
	longitudinal	0.002	0.305	-0.002 - 0.005
CircPLEKHM1	cross-sectional	0.000	0.799	-0.002 - 0.003
	longitudinal	-0.001	0.614	-0.003 - 0.002
CircXPO7	cross-sectional	-0.003	0.236	-0.008 - 0.002
	longitudinal	-0.004	0.139	-0.009 - 0.001
CircZC3H18	cross-sectional	0.001	0.761	-0.003 - 0.004
	longitudinal	-0.002	0.374	-0.006 - 0.002

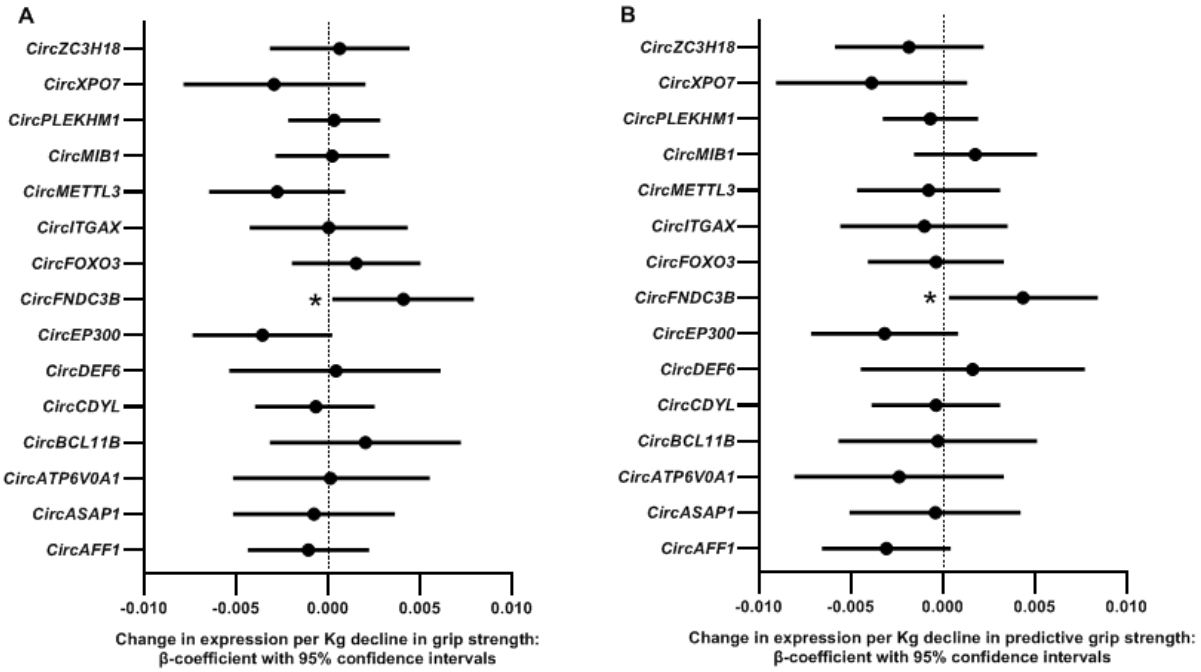

Figure *11 Peripheral blood circFNDC3B expression is nominally associated with hand grip strength.* *Forest plot illustrating the association between circRNA expression and hand grip strength in participants from the InCHIANTI study of* Ageing*. Associations with grip strength from multivariate regression analysis are shown both* ***(A)*** *cross-sectionally from follow up 3 (FU3) and* ***(B)*** *longitudinally, from follow up 4 (FU4). N = 306 individuals. The beta coefficient of the association is given on the X-axis and the identity of the gene is given on the Y axis. Lines attached to each data point represent 95% Confidence intervals (95% CI). Statistical significance is indicated by stars. * = <0.05, ** = <0.005.*

3.3.4 CircRNAs are differentially expressed in early passage and late passage cells

12 of 15 circRNAs tested were expressed in astrocytes, endothelial cells, fibroblasts or astrocytes. 7 (58%) of these demonstrated differential expression between early and late passage cells of one or more cell type (Table 8, Fig. 12). *CircAFF1* and *circFOXO3* demonstrated associations in more than one cell type although direction of effect was concordant only for *circFOXO3* (in cardiomyocytes and fibroblasts). *CircCDYL*, *circEP300, circMIB1*, *CircZC3H18* and *circMETTL3* were differentially-

expressed in only one cell type. *CircBCL11B, CircDEF6 and CircITGAX* were not expressed in any cell type tested.

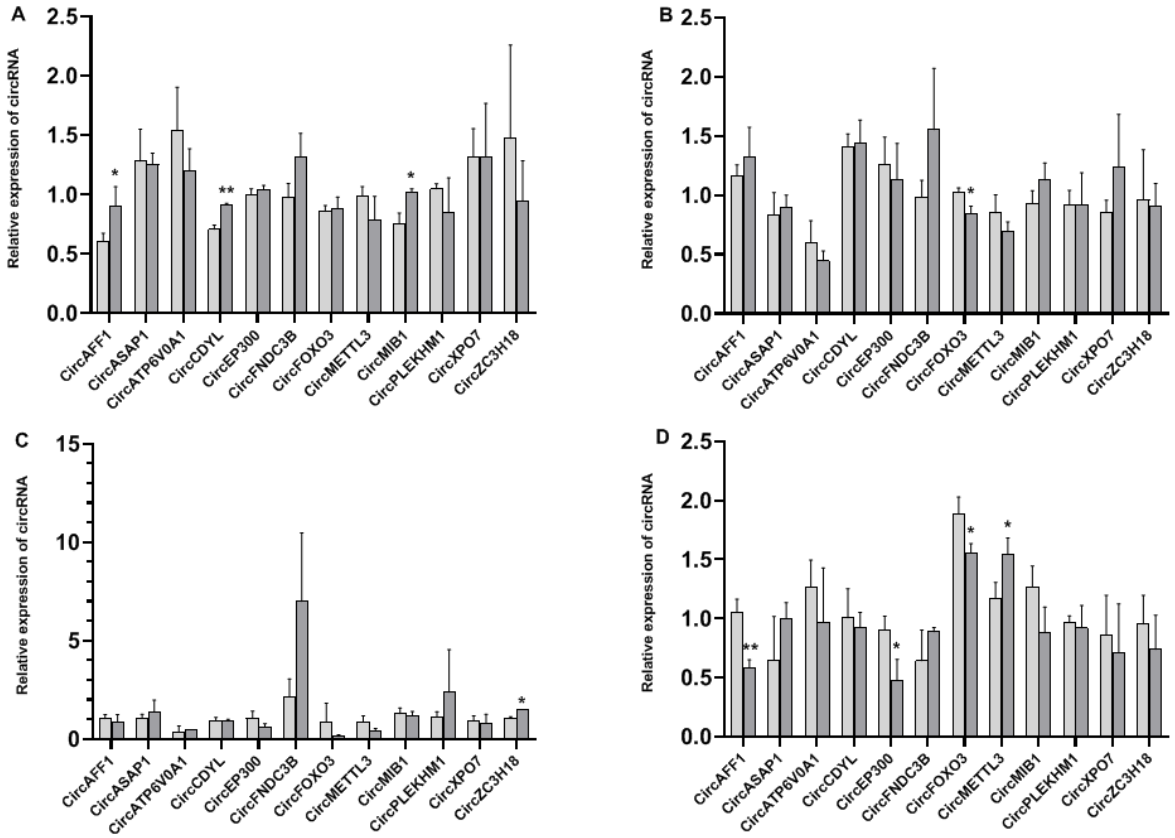

Figure 12 Differential expression of circRNAs in senescent cells of various lineages. *CircRNAs are dysregulated in senescent astrocytes **(A)**, cardiomyocytes **(B)**, endothelial cells **(C)** and fibroblasts **(D).** Some circRNAs are dysregulated in multiple cell types. Differential expression assessed by one-way ANOVA. N = 6 samples. CircRNA is shown on the X-axis and the relative expression of the circRNA is given on the Y axis. Statistical significance is indicated by stars. * = <0.05, ** = <0.005.*

Table 8 CircRNA expression in early and late passage primary human cells *IQR = interquartile range of gene expression. N=6 samples. Results reaching statistical significance from one-way ANOVA analysis are indicated in bold underlined typeface.*

CircRNA	Median (IQR)		p-value
	Early passage	Late passage	
Astrocytes			
CircAFF1	**0.58 (0.55-0.68)**	**0.84 (0.79-1.09)**	**0.040**
CircASAP1	1.39 (0.97-1.48)	1.22(1.18-1.36)	0.878
CircATP6V0A1	1.60 (1.14-1.87)	1.14 (1.05-1.41)	0.229
CircCDYL	**0.71 (0.67-0.74)**	**0.90 (0.90-0.93)**	**0.001**
CircEP300	1.01 (0.95-1.04)	1.05 (1.00-1.07)	0.329
CircFNDC3B	0.96 (0.85-1.10)	1.38 (1.20-1.48)	0.059
CircFOXO3	0.88 (0.80-0.89)	0.89 (0.80-0.98)	0.646
CircMETTL3	0.97(0.92-1.08)	0.69 (0.66-1.02)	0.180
CircMIB1	**0.71(0.69-0.86)**	**1.03 (0.99-1.04)**	**0.008**
CircPLEKHM1	1.05 (1.00-1.09)	0.76 (0.61-1.17)	0.306
CircXPO7	1.25 (1.12-1.58)	1.54 (0.81-1.62)	0.987
CircZC3H18	1.50 (0.67-2.24)	0.88 (1.00-1.07)	0.346
Cardiomyocytes			
CircAFF1	1.15 (1.09-1.26)	1.42 (1.04-1.52)	0.357
CircASAP1	0.74 (0.71-1.05)	0.84 (0.83-1.02)	0.643
CircATP6V0A1	0.57 (0.44-0.80)	0.41 (0.39-0.54)	0.249
CircCDYL	1.47 (1.29-1.48)	1.42 (1.25-1.64)	0.855
CircEP300	1.27 (1.02-1.48)	1.10 (0.84-1.45)	0.596
CircFNDC3B	1.03 (0.83-1.09)	1.93 (0.96-1.97)	0.139
CircFOXO3	**1.00(0.99-1.07)**	**0.82 (0.79-0.92)**	**0.015**
CircMETTL3	0.88(0.69-0.99)	0.66 (0.63-0.79)	0.186
CircMIB1	0.96 (0.81-1.02)	1.16 (0.97-1.25)	0.129
CircPLEKHM1	0.85 (0.84-1.05)	0.82(0.71-1.22)	0.983
CircXPO7	0.89 (0.74-0.94)	1.32 (0.75-1.63)	0.227
CircZC3H18	0.83 (0.63-1.43)	0.85 (0.77-1.12)	0.862
Endothelial cells			
CircAFF1	0.94 (0.91-1.27)	1.07 (0.49-1.11)	0.548
CircASAP1	1.03 (0.94-1.28)	1.69 (0.68-1.76)	0.467
CircATP6V0A1	0.37 (0.16-0.58)	0.48 (0.48-0.48)	0.821
CircCDYL	0.90 (0.76-1.11)	0.89 (0.84-1.02)	0.942
CircEP300	0.99 (.75-1.45)	0.58 (0.53-0.80)	0.128
CircFNDC3B	1.74 (1.49-3.18)	7.84 (3.18-9.97)	0.080
CircFOXO3	0.38 (0.20-1.98)	0.14 (0.04-0.22)	0.275
CircMETTL3	1.02 (0.54-1.08)	0.39 (0.39-0.56)	0.072
CircMIB1	1.36 (0.98-1.54)	1.11 (1.03-1.43)	0.640
CircPLEKHM1	1.02 (0.99-1.42)	1.47(0.83-4.85)	0.380
CircXPO7	0.97 (0.72-1.18)	0.87 (0.31-1.22)	0.620
CircZC3H18	**1.02 (0.98-1.15)**	**1.51 (1.51-1.51)**	**0.047**
Fibroblasts			
CircAFF1	**1.06 (0.95-1.16)**	**0.58 (0.52-0.65)**	**0.003**
CircASAP1	0.51 (0.38-1.07)	1.05 (0.85-1.10)	0.196
CircATP6V0A1	1.39 (1.00-1.41)	1.10 (0.46-1.35)	0.375
CircCDYL	1.13 (0.72-1.17)	0.90 (0.81-1.06)	0.640
CircEP300	**0.96 (0.78-0.98)**	**0.38 (0.38-0.69)**	**0.023**
CircFNDC3B	0.50(0.48-0.94)	0.90 (0.85-0.91)	0.182
CircFOXO3	**1.91 (1.72-2.01)**	**1.60 (1.47-1.61)**	**0.025**
CircMETTL3	**1.23(1.00-1.26)**	**1.39 (1.58-1.66)**	**0.030**
CircMIB1	1.20 (1.14-1.47)	0.85 (0.69-1.11)	0.072
CircPLEKHM1	1.00(0.90-1.00)	0.84 (0.79-1.14)	0.716
CircXPO7	1.03(0.48-1.08)	0.57 (0.39-1.18)	0.645
CircZC3H18	0.93 (0.72-1.21)	0.74 (0.53-0.94)	0.432

3.4.5 Differential expression of circRNAs between mice of different median strain longevities

In silico analyses suggested that 4 circRNAs (*circFoxo3, circMib1, CircPlekhm1* and *circXpo7*) may have conserved back-spliced junction in the mouse. Associations with longevity were then assessed in spleen and muscle tissue from young (6 months) and old (20-22 months) mouse strains of 6 different median strain longevities. *CircMib1* and *circXpo7* were expressed only in spleen, whereas *circFoxo3 and circPlekhm1* was expressed in both tissues (Table 9). The expression of *circPlekhm1* demonstrated a nominal positive correlation with median lifespan in young and old (β =0.0013, p=0.016) as well as in spleen of young mice (β =0.0025, p=0.017), although these were not significant after adjustment for multiple testing (threshold p = 0.013). No associations were seen between muscle circRNA expression levels and median strain longevity.

Table 9 Differential expression of conserved circRNAs in mice of differential median strain longevities. *CircRNA expression is reported here in relation to median strain longevity. Data are assessed separately for young and old animals of each strain. N=67 (muscle); 90 (spleen). IQR = interquartile range. ND = Not detected. Results reaching statistical significance from regression analysis are indicated in bold underlined typeface.*

CircRNA	Tissue	β-coefficient	p-value	95% CI	
CircFoxo3	muscle	0.00	0.403	-0.0010	0.0024
	young (muscle)	0.0001	0.936	-0.0028	0.0031
	old (muscle)	0.0008	0.478	-0.0015	0.0031
	spleen	-0.0003	0.815	-0.0027	0.0021
	young (spleen)	0.0002	0.922	-0.0039	0.0043
	old (spleen)	-0.0005	0.757	-0.0037	0.0027
CircMib1	muscle	ND	ND	ND	ND
	young (muscle)	ND	ND	ND	ND
	old (muscle)	ND	ND	ND	ND
	spleen	0.0001	0.924	-0.0023	0.0026
	young (spleen)	-0.0018	0.150	-0.0044	0.0008
	old (spleen)	0.0021	0.299	-0.0020	0.0062
CircPlekhm1	muscle	0.0003	.813	-0.0022	0.0028
	young (muscle)	-0.0022	0.161	-0.0054	0.0010
	old (muscle)	0.0016	0.365	-0.0020	0.0053
	spleen	***0.0013***	***0.016***	***0.0002***	***0.0024***
	young (spleen)	***0.0025***	***0.017***	***0.0005***	***0.0046***
	old (spleen)	0.00001	0.967	-0.0008	0.0009
CircXpo7	muscle	ND	ND	ND	ND
	young (muscle)	ND	ND	ND	ND
	old (muscle)	ND	ND	ND	ND
	spleen	0.0009	0.509	-0.0019	0.0038
	young (spleen)	0.0003	0.894	-0.0040	0.0045
	old (spleen)	0.0020	0.333	-0.0023	0.0063

3.5 Discussion

Circular RNAs (circRNAs) are an emerging class of regulatory RNA molecule thought to play a role in human disease (Haque and Harries, 2017). These molecules have no free ends, and as such are exonuclease resistant. CircRNAs accumulate in aged organisms (Gruner et al., 2016) and have been suggested to play a role in cellular senescence (Du et al., 2017; Du et al., 2016). We hypothesised that the human circRNAome may differ in aged humans compared with younger subjects, and that these changes may also be associated with cellular senescence, or with longevity in animal models. We identified >2000 circRNAs in total RNA from human blood, some of which were expressed exclusively in samples from older donors. GSEA pathways enrichment analysis of genes hosting the top 10% most abundant circRNAs in elderly donors suggested that pathways involved in phagocytosis, circadian regulation, cancer pathways and golgi-associated vesicles were the most enriched in these genes. We demonstrated that 3 circRNAs (*circDEF6*, *circFOXO3* and *circEP300*) were associated with measures of parental longevity, and one (*circFNDC3B*) was associated with hand grip strength both longitudinally and cross-sectionally. Furthermore, 7/12 circRNAs expressed in human senescent cells of different cell types demonstrated dysregulated expression in one or more cell type and 1/4 circRNAs demonstrating conserved expression were associated with median strain longevity in spleen tissue from young mice. These findings are consistent with the hypothesis that some circRNAs have roles in molecular ageing and the determination of mammalian ageing phenotypes.

CircRNAs generated from the *FOXO3* and *EP300* genes were negatively associated with measures of human parental longevity, and also demonstrated dysregulated expression in human senescent cells. CircRNAs deriving from the *FOXO3* gene have

previously been demonstrated to regulate cell cycle when manipulated by gene knockdown in mouse embryonic fibroblasts, cardiac fibroblasts or mammary cancer cell lines (Du et al., 2016). Furthermore, *FOXO3* circular RNAs also demonstrate elevated expression and association with cellular senescence in the heart tissue of mice and humans (Du et al., 2017). It is not clear whether the previously reported circular *FOXO3* transcripts have the same structure as the one we have identified, since previous studies do not give its exon structure. A circRNA from the *FOXO3* gene identical to the one we have identified has also previously been demonstrated to inhibit myoblast differentiation in mouse cells (Li et al., 2019). Genetic variation in the *FOXO3* gene itself has previously been associated with extreme longevity (Flachsbart et al., 2017; Fuku et al., 2016), and has also been associated with maintenance of telomere length (Davy et al., 2018).

CircRNAs deriving from the *EP300* gene have not been previously reported. *EP300* encodes the repressor histone acetyltransferase protein p300, which also has roles as a transcriptional corepressor protein. EP300 has been implicated in modulation of *FOXO3* activity (Mahmud et al., 2019) and in antagonism of the FOX03a/SIRT1 signalling axis (Jeung et al., 2016). Inhibition of EP300 has been shown to mimic calorific restriction in human and mouse cells (Pietrocola et al., 2018); calorific restriction is of course a well-known modifier of lifespan in many species (Austad, 1989; Hansen et al., 2008; Kapahi et al., 2004; Mitchell et al., 2010). This protein is also a master regulator of autophagy, which is a pivotal factor in stem cell maintenance and evasion of cellular senescence (Vijayakumar and Cho, 2019).

CircFNDC3B was positively associated with hand grip strength. Although these associations were nominal only, they were present both cross-sectionally and longitudinally. An average person may lose ~20-40% of skeletal muscle mass as well as muscle strength from by the time they reach 80 years of age (Carmeli et al., 2002; Doherty, 2003) and decline in skeletal muscle strength is predictive of disability and mortality in humans (Giampaoli et al., 1999; Rantanen et al., 1999; Rantanen et al., 2012). Circular RNAs originating from this gene have been reported previously, and suggested to possess tumour suppressor activity (Liu et al., 2018).

The results generated from our mouse data suggest that *circPlekhm1*, which was associated with median strain longevity may drive longevity, rather than being consequential to it, since the associations are present in the spleen RNA of young mice alone. The *Plekhm1* gene encodes a multivalent adaptor protein that integrates endocytic and autophagic pathways at the lysosome (McEwan and Dikic, 2015). Its role in lifespan may therefore stem from moderation of lysosomal trafficking since lysosomes play a critical part in successful ageing and longevity (Carmona-Gutierrez et al., 2016; Simonsen et al., 2007).

Our study has both strengths and weaknesses. It represents one of the first circRNA profiles in ageing human peripheral blood, and provides data not only population-level epidemiological evidence for a role in human ageing phenotypes, or mammalian lifespan, but also *in vitro* evidence that some circRNA may influence cell senescence phenotypes. Weaknesses include a relatively low power to detect effects of in the population study, which might be attributed to the biological variation in circRNA levels and limitations in samples size and power. While differential expression of circRNA by

sex has been mentioned in a study on patients with sporadic parathyroid adenomas suggesting the role of epigenetics in the gender specific differences of these patients (Yavropoulou et al., 2018). Another study shows sexual dimorphism of circRNAs in 6 organs of the 8 organs i.e brain, heart, lung, liver, kidney, muscle, testes and thymus in rats. However, liver was relatively devoid of such sexual dimorphism (Mahmoudi and Cairns, 2019). Sex-related circRNA expression is also found in rhesus macaque brain like in the rat brain from the previous study (Xu et al., 2018). Gender-specific expression changes were also observed with the expression of circRNAs derived from male-specific host genes including circCD99, circPREX1, and circTSPAN15. Additional gender-specific circRNAs included circEFCAB2 for males and circPCTP and circZNF484 for females (Sekar and Liang 2019). Another study reveals that approximately 50% of circRNAs between both sexes are common in nonsex organs, indicating not all circRNAs might serve as biomarkers for both sexes. However, the study also shows that the number of common circRNAs between both sexes increased with age for most organs except heart, spleen, and thymus in rats (Gong et al., 2011). In this study, we presented here data and selected candidate circRNAs for follow-up from pooled male and female samples.

The circRNA profile was also generated from RNA samples with relatively low RNA integrity number (RIN) value. RNA sequencing is widely used for generating gene expression profiles. Prior to such RNA sequencing, the quality of the RNA is assessed using RIN. RIN affects the gene coverage and false positives in differential expression. Ideally, high RIN of 8 would be used for RNA sequencing experiments. However, RNA is susceptible to degradation and obtaining high quality RNA from certain clinical tissues is often impossible or when samples collected in a certain way is the sole

source for addressing specific questions. This is important since not all transcripts are degraded at the same rate and therefore it is not possible to have a linearly reduced library size that can be corrected solely by normalization. One study revealed that RIN introduce inter-run variation because degradation introduces of variance in the RNAseq outputs reducing library complexity when assessing profile for linear transcripts, using a protocol that does not rely on PolyA selection or RiboZero or by using 3' Tag Counting (Sigurgeirsson, Emanuelsson, and Lundeberg 2014). However, in another study, it was shown that standard normalizations fails to compensate for the effects of degradation but using a linear model framework can compensate for the majority of these effects and therefore extract biologically meaningful data from degraded samples having low RIN value (Gallego Romero et al., 2014). This is important since excluding rare samples would leave those questions unanswered or result in low power in studies than having to globally correct for RIN values to only include samples with high RIN.

Nevertheless, we were able to identify some interesting associations, which likely represent the largest effects. Future work could include validation of epidemiological data in larger sample sets, and also functional delineation of the molecular effects of the circRNA in question. Our data provide evidence that circRNAs may play an important role in the determination of mammalian ageing phenotypes. CircRNAs are inherently stable, due to their exonuclease resistance, and are found not only in tissues relevant to human diseases, but also in the circulation, raising the possibility that they may prove useful as biomarkers of disease or targets for molecular therapies in the future.

Chapter 4 – Data chapter

Islet-expressed circular RNAs are associated with type 2 diabetes status in human primary islets

Abstract

Circular RNAs are an emerging class of non-coding RNA molecule with gene regulatory potential; dysregulation of circRNAs has been reported in association with several human diseases. Here we aimed to produce an enriched circRNA profile for human pancreatic islets, and explore the relationship between circRNA expression, diabetes status, genotype at T2D risk loci and measures of glycaemia (insulin secretory index; SI and HbA1c) in human islet preparations from healthy control donors and donors with type 2 diabetes. We also assessed the effect of elevated glucose, cytokine and lipid and hypoxia on circRNA expression in the human beta cell line EndoC-βH1. We identified over 2600 circRNAs present in islets, of which 47 had not been previously described in other tissues. Of the five most abundant circRNAs in human islets, four (*circCIRBP*, *circZKSCAN1*, *circRPH3AL* and *circCAMSAP1*) demonstrated marked associations with diabetes status. C*ircCIRBP* also demonstrated an association with insulin secretory index in isolated human islets and *circCIRBP* and *circRPH3AL* displayed altered expression with elevated fatty acid in treated EndoC-βH1 cells. No associations between circRNA expression and genotype at T2D risk loci were identified in our samples. Our data suggest that circRNAs are abundantly expressed in human islets, are differentially regulated in the islets of donors with type 2 diabetes, and some may derive from genes with roles in exocytosis or stress resilience.

4.1 Introduction

One of the key difficulties in dissecting the factors driving progression of multifactorial polygenic chronic diseases such as type 2 diabetes (T2D) is the degree of heterogeneity that it presents. Although the development of diabetes like other common chronic disorders has a large lifestyle contribution, there is a substantial genetic component (Xue et al., 2018). 70% of individuals with prediabetes eventually develop diabetes (Bansal, 2015; Tabak et al., 2012), with increasing evidence suggesting that diabetic complications such as peripheral nephropathy and retinopathy may initiate at the pre-diabetic stage (Tabak et al., 2012). Identifying people at risk of type 2 diabetes, or those likely to progress from impaired glucose tolerance to overt disease is thus an important aim. Understanding the molecular causes of T2D, and identification of sensitive and specific biomarkers to indicate those at risk of pre-diabetes, or of transition from pre-diabetes to overt disease is therefore a key aim for research.

Genome wide association studies (GWAS) for T2D have identified over 143 risk loci associated with susceptibility to T2D (Xue et al., 2018). More than 85% of these disease-associated variants reside in non-coding regions of the genome (Edwards et al., 2013). Over 80% of the human genome is predicted to display some degree of functionality (Qu and Fang, 2013), so it is likely that the many of the diabetes-associated genetic variants may act via dysregulation of gene expression. Disruption of the activity or function of non-coding RNAs that moderate gene activity, such as microRNA (miRNA) or long non-coding RNA (lncRNA) may have particular relevance (Hrdlickova et al., 2014).

Circular RNAs (circRNAs) are an emerging class of non-coding RNA (ncRNA) generated by the back splicing of downstream exons to the 3' acceptor splice site of upstream exons and result in a covalently closed circular structure containing one or more exons (Haque and Harries, 2017). Their mode(s) of action remain to be fully elucidated but they have been suggested to manipulate gene expression by moderation of transcription (Bose and Ain, 2018), interaction with cellular proteins (Luo et al., 2019), sequestration of RNA-binding proteins (Zang et al., 2018) or sponging miRNA (Kulcheski et al., 2016). Their covalently closed structure means that they are resistant to exonucleases; accordingly, they have half-lives on average 19-24 hours (Enuka et al., 2016), being significantly more stable than linear mRNAs from their cognate genes which have half-lives typically in the region of 4-9 hours (Schwanhausser et al., 2011). Data on circRNA abundance can be extracted from conventional NGS data, but such data may also include aberrant back spliced sequences from linear transcripts as well as genuine circRNAs.

Cell-type specific circRNA expression has previously been reported in human pancreatic β, α and δ cells (Kaur et al., 2018), but these profiles were not circRNA-specific, being extracted from published NGS data in the absence of RNAse R treatment to remove linear RNA. Other human islet circRNA profiles have been generated using microarray approaches, which will capture only known circRNAs (Stoll et al., 2018).

We present here an enriched whole circRNAome profile from primary human pancreatic islets which we have generated using a modified circleSeq technique (Lopez-Jimenez et al., 2018). This included an RNAse R step to remove linear RNA

and enrich for circRNAs. We then aimed to determine firstly whether expression of the most abundantly-expressed islet circRNAs were associated with insulin secretory index (SI), donor HbA1c or donor diabetes status in human primary islets. Secondly, we aimed to determine whether circRNAs localising to the genomic regions encompassing the GWAS association signals for type 2 diabetes were differentially-expressed according to donor risk genotype. Thirdly, we aimed to explore whether abundantly-expressed circRNAs were responsive to diabetomimetic stimuli (hypo- or hyperglycaemia, hypoxia, elevated fatty acids or inflammatory cytokines), in the human beta cell line EndoC-βH1.

4/5 circRNAs most abundant in human islets *(circCAMSAP1, circCIRBP, circRPH3AL* and *circZKSCAN1*) were differentially-expressed in the islets of patients with type 2 diabetes compared with control samples. The linear transcripts of *CAMSAP1, CIRBP* and *ZKSCAN1* also demonstrated associations with T2D status, as did the linear transcript of *RHOBTB3*. 1 of 5 of the most abundantly-expressed circRNA species in primary human islets *(circCIRBP)* demonstrated a nominal inverse correlation with insulin secretory index in islets from non-diabetic donors. No circRNA mapping to T2D GWAS loci however demonstrated associations between their expression and T2D risk genotype and associations with donor HbA1c were identified. 2 of the 5 most abundantly expressed circRNAs (*circCIRBP* and *circRPH3AL*) also demonstrated differential expression in response to elevated free fatty acids in treated EndoC-βH1 cells. To conclude, we have produced the first global circRNA-only profile in human pancreatic islets and provide evidence that some of these are responsive to the diabetic microenviroment.

4.2 Methods

4.2.1 Pancreatic islet preparations

Snap-frozen islet preparations were purchased from ProCell Biotech (Newport Beach, CA, USA) where islets had been collected with ethical permission at source. Islet purity and viability was determined by dithizone and fluorescein diacetate/propidium iodide staining, respectively. RNAlater-ICE (Life Technologies, Carlsbad, CA, USA) was used to transition the tissue to a state where RNA could be extracted using the miRVana miRNA isolation kit, as per the manufacturers' instructions and using the total RNA extraction protocol. RNA Integrity Number (RIN) was determined for all samples using an Agilent Bioanalyser (Agilent, Santa Clara, USA). 53 islet samples were available from healthy donors, and 20 from donors with T2D. Islet donor characteristics are given in table 10.

4.2.2 Generation of human primary islet circRNA profile

Circular RNA profiles were initially generated from 5 individual islet total RNA samples from individuals without T2D which were pooled and profiled for circRNA expression using a modified 'CircleSeq' procedure. Samples derived from 3 females and 2 males, with an average age of 50.2 years and an average BMI of 26.4. Islet preparations had, an average viability 94.4% and an average purity of 81%. 2 µg RNA (RIN 6.4) was divided into two aliquots; one aliquot was treated with 20 units RNAse R (Epicentre, Madison, USA) at 30˚C for 30 minutes to remove linear RNA, one samples was mock-treated using 1 µl RNase-free water in place of the enzyme. Both aliquots were processed in parallel using 2 volumes RNAClean beads (Beckman Coulter, Indianapolis, USA) to remove the enzyme. The results of the RNase R treatment were

confirmed on a high sensitivity RNA screentape (Agilent, Santa Clara, USA). Ribosomal RNA was removed and indexed sequencing libraries made using the TruSeq direction library preparation kit with Ribozero depletion (Illumina, San Diego, USA). Concentration of the final libraries was determined by qPCR and adjusted for size using Tapestation D1000 analysis (Agilent, Santa Clara, USA). Libraries were pooled in equimolar quantities, denatured and diluted to 9.0 pM + 1% PhiX for clustering and 100 paired-end Illumina sequencing in a single lane using HiSeq Rapid SBS reagents (V2). 62M reads were obtained from the RNAse R-treated sample and 41M reads from the mock-treated sample with a mean Q score of 38.9-39.1 and total error rate of 0.24%.

Table 10 Sample and donor characteristics for human pancreatic islet samples used in this work. A. *Characteristics of human islet preparations from donors with (n = 20) and without (n = 50) T2D for assessing association of gene expression with diabetic status in the islets. SD = standard deviation. Differences in parameters between islet groups was determined by t-test.* ***B****. Characteristics of human islets from non-diabetic donors (n=53) for association of gene expression with genotype in islets. SNP-1 = major alleles; SNP-2 = minor alleles.*

	Control (n=50)		T2D (n = 20)		p-value
	Mean	**SD**	**Mean**	**SD**	
Age	40.66	14.25	53.55	9.22	<0.001
BMI	28.30	6.83	33.05	10.31	0.027
SI	2.45	1.26	-	-	-
HbA1c	5.44	0.36	-	-	-
Purity	89.28	6.00	80.38	14.92	<0.001
Viability	93.53	4.80	89.73	4.54	0.003
Sex	F (40%);	M (60%)	F (45%)	M (55%)	0.706
Ethnicity	white (74%)	other (26%)	white (45%)	other (55%)	0.348

B.

	p-value	SNP-1		SNP-2	
		Mean	**SD**	**Mean**	**SD**
rs6819243 (*CTBP1*)					
Age	0.620	40.19	14.12	42.38	11.78
BMI	0.715	27.85	5.34	27.16	7.03
Purity	0.671	89.26	5.86	90.00	3.54
Viability	0.633	93.33	5.68	94.12	2.38
Sex	0.595	F (53 %)	M (47%)	F (38%)	M (62%)
Ethnicity	0.020	white (83%)	other (17%)	white (31%)	other (69%)
rs10758593 (*GLIS3*)					
Age	0.966	41.08	15.04	40.88	12.25
BMI	0.130	26.27	4.14	29.07	5.80
Purity	0.633	89.46	4.96	88.50	6.26
Viability	0.133	94.81	3.09	92.33	5.37
Sex	0.269	F (39%)	M (62%)	F (42%)	M (58%)
Ethnicity	0.916	white (69%)	other (31%)	white (73%)	other (27%)
rs7177055 (*HMG20A*)					
Age	0.371	39.97	13.95	43.69	12.35
BMI	0.355	27.83	5.63	29.87	9.46
Purity	0.998	89.13	5.18	89.13	6.18
Viability	0.986	93.37	4.03	93.34	6.70

Sex	0.547	F (47%)	M (53%)	F (38%)	M (63%)
Ethnicity	0.697	white (72%)	other (28%)	white (75%)	other (25%)
rs1111875 (*IDE*)					
Age	<0.001	48.58	9.95	33.43	12.20
BMI	0.088	30.05	8.52	26.50	4.80
Purity	0.175	88.61	4.91	90.57	4.73
Viability	0.374	94.57	3.30	93.57	4.20
Sex	0.056	F (58%)	M (42%)	F (30%)	M (70%)
Ethnicity	0.733	white (67%)	other (33%)	white (74%)	other (26%)
rs12427353 (*SPPL3*)					
Age	0.137	39.68	14.15	46.80	9.02
BMI	0.104	29.03	7.32	25.03	4.00
Purity	0.267	89.98	5.22	87.78	5.65
Viability	0.645	93.48	5.28	94.33	3.50
Sex	0.092	F (40%)	M (60%)	F (70%)	M (30%)
Ethnicity	0.949	white (68%)	other (33%)	white (80%)	other (20%)
rs10203174 (*THADA*)					
Age	0.802	42.18	13.62	43.36	13.38
BMI	0.155	29.07	7.54	25.54	5.13
Purity	0.754	89.64	4.50	89.09	6.25
Viability	0.565	93.85	4.25	94.64	2.46
Sex	0.546	F (47%)	M (53%)	F (36%)	M (64%)
Ethnicity	0.920	white (74%)	other (26%)	white (55%)	other (45%)

4.2.3 Analysis of circRNA profiles

RNase R and mock-treated sequence data were assembled and putative circular RNAs were identified using PTESFinder (Izuogu et al., 2016) with the human genome (hg19) reference files provided with the software, a segment size of 65 and a uniqueness score of 7. The remaining parameters were left to default settings. To calculate a comparable measure of circular RNA abundance between samples we

used a measure termed back spliced reads per million mapped reads (bpm) for each circular RNA i is defined as:

$$bpm_i = \left(\frac{j_i}{\sum_{a=1}^{n} j_a + \sum_{b=1}^{n} c_b} \right) . 10^6$$

Where J_i *i*s the number of reads mapped to the backsplicedd junction of the circular RNA, *c* is the number of reads mapped to canonical sites of the gene with the circular RNA and *n* is the number of circular RNAs identified. This measure is designed to be similar to the commonly used reads per kilobase per million mapped reads (RPKM) metric used regularly to estimate gene expression from RNA-Seq data.

In addition to circular RNA detection using PTESFinder, reads from all samples were also mapped to the human genome reference (hg19) obtained from iGenomes using Tophat v2.1.0 with the pre-set sensitive alignment parameters in paired end mode (Trapnell et al., 2009). The number of reads mapping to each exon of each gene was then calculated using FeatureCounts v2.0.0 with parameters for unstranded alignment, paired reads, count multi-mapping reads and assigning reads to overlapping features (Liao et al., 2013; Liao et al., 2014). Counts were used to calculate RPKM per exon using the standard method to compare the expression of each exon across samples.

4.2.4 Analysis of genes hosting differentially-regulated circRNA

To determine whether circRNAs to date identified only in islets, or those representing the top 10% most abundant demonstrated enrichment in specific gene ontology pathways, we carried out a Cytoscape version 2.5.2 plug-in ClueGO analysis which

incorporates KEGG, REACTOME and WikiPathways (Bindea et al., 2009). Outputs were selected based on 'enrichment/depletion' through a two-sided hypergeometric test with Bonferroni step down for p-value correction with the selected ontologies reference set of chosen genes. The GO terms were used to group functional pathways and the leading functional grouping was based on highest significant kappa score.

4.2.5 Selection of circRNAs for validation

CircRNAs were selected for follow up on two criteria. Firstly, levels of individual circRNAs in the islet were ranked by abundance. We selected the 5 most abundantly expressed circRNAs (*circCAMSAP1, circCIRBP, circRHOBTB3, circRPH3AL and circZKSCAN1*) for further analysis. We also assessed the expression of the linear reference transcript for each circRNA in each case. The second class of circRNAs selected for follow up were those mapping to the GWAS loci for T2D.

The circRNA profile in our study was mapped against the T2D susceptibility loci (Morris et al., 2012). The co-ordinates of the upstream and downstream exons predicted to constitute each circRNA were then cross-referenced against the T2D GWAS signals using Python 2.7 to determine whether any circRNAs co-localized within the recombination windows. Pythoon codes used are shown in (Fig A3).13 circRNAs fulfilled these criteria and were selected for follow up (*circCTBP1_1, circCTBP1_2, circGLIS3, circHMG20A, circIDE1, circIDE2, circSPPL3_1, circSPPL3_2, circTHADA1, circTHADA2, circTHADA3, circTHADA4 and circTHADA5*). The expression of both circRNA and their host linear transcripts were assessed.

4.2.6 Design of qPCR assays for circRNA validation

Custom designed quantitative qRTPCR assays for quantification of relative expression were designed to unique back-spliced circRNA junctions (ThermoFisher, Foster City, USA), the sequences of which are given in table 11. Each target sequence was checked for the presence of single nucleotide polymorphisms in potential primer or probe binding regions prior to ordering. Assays were ordered as custom single tube assays from ThermoFisher (Foster City, USA) or IDT (Iowa, USA). Each circRNA probe was validated for sensitivity and linearity using standard curves produced from 1:10 serial dilutions of synthetic oligonucleotides corresponding to each back spliced junction (ThermoFisher, Foster City, USA). Standard curves for the assays are shown in appendix (Fig A2).

Table 11 CircRNA probe and primer sequences

Circular RNA probes

CircRNA	Forward primer	Probe	Reverse primer
CircCAMSAP1	CTCGAGGATGCCATGGTGTT	CTGGATCAACAAGATAACA	GTCAACGTAGAAAGGGTCTCTGA
CircCRIBP	GGCGGGTCCTACAGAGACA	CCATCTACAGACGTAACTGT	GCCTGGTCTACTCGGATCTG
CircCTBP1_1	CGGCGCTGCCAGGAT	ATCGGACTTGTAAGACTTT	CCGCGGCAATCACTGAAG
CircCTBP1_2	CAGTGGTTTTGACAACATCGACATC	CAAAGTCTTACTAAATCCC	CCGCGGCAATCACTGAAG
CircGLIS3	CAGGAGTTTGGAAGCCCTTTTC	CTGGGAAAGGCTTATAACC	GGCAAAGTCCAATAAGTTATCCATGGT
CircHMG20A	CGGCAGGCCACTCATGAT	ATGAGCAACGAAGTAAAC	CTCTTTCTTCCTTTGGACCAACCT
CircIDE1	GATGGTTCTCGATAAACTCAGACCA	TTGGAAACGGACATTTT	GGCTGGATTATTCATTTTGCTGTAAGT
CircIDE2	GGAATCCTAAACACCCCTTCAGT	TTGGAAACTGTCCCAAATTT	GGCTGGATTATTCATTTTGCTGTAAGT
CircRHOBTB3	GGATGTTTCAAATGTAATCGAGAAAG	TTTTTCTTTCCTGGTGTTTTTA	TGACGCTTCAGCCTTTAAGACA
CircRPH3AL	GGCTGTGTAAGATCTGCAGTGA	AAAGAGAGATGTGACTCCC	GCCATGGCTCGGAGCA
CircSPPL3_1	TGGGTTCTCACTGGCCATTG	TAGGCCCATCCATGAGAAG	GAAATGTAGACACTTGACTGGAATCCA
CircSPPL3_2	TCGTCCTCATCTGGGTTCTCA	TTGGCTTCTCATGGATGGCATC	AGCCTGGGTAGAGTCAATTGTTTG
CircTHADA1	GGCTGCAATTCTGGGTTTTACAT	CTGGGCAGTAAAAGAAA	CTGGACTGCAAAAGGTGTTGTTTAA
CircTHADA2	TTCCGGCAAAACCACATTCATG	CTCCAGGTGCGAAATT	CAAGGCACTAAAGAGAAGTGTGGAT
CircTHADA3	AGGAGTGCGGCAACAGATC	CTTCTTAAAAAGGATTAAAGAGCC	TCCAGGATGCTAAGATTCTAGACAGA
CircTHADA4	TTCACCCGTCTGAAAAGATTCCTC	CAGAGGCACAATCAAAT	GTGGGATCACACATGCCATTTTTAT
CircTHADA5	GGCCTACAGATGACATACAGAGTAC	TCCCCCAGGTAAAAGA	CTGGACTGCAAAAGGTGTTGTTTAA
CircZKSCAN1	CGGAAACCCCGCCTCTT	ACAGTCACGAGGAATAG	TCCTGGGAGGTTTTATGATGTGTTT

Linear RNA assays

Gene	Assay ID	Supplier
Endogenous controls		
B2M	Hs00187782_m1	Thermofisher Scientific
GUSB	Hs00939627_m1	Thermofisher Scientific
PPIA	Hs04194521_s1	Thermofisher Scientific
B2M	Hs.PT.58v.18759587	Integrated DNA Technologies
GUSB	Hs.PT.39a.2214857	Integrated DNA Technologies
PPIA	Hs.PT.58v.38887593.g	Integrated DNA Technologies
Linear transcripts		
CIRBP	Hs00154457_m1	Thermofisher Scientific
CAMSAP1	Hs00251465_m1	Thermofisher Scientific
RHOBTB3	Hs00208554_m1	Thermofisher Scientific
RPH3AL	Hs01063755_m1	Thermofisher Scientific
ZKSCAN1	Hs00379174_m1	Thermofisher Scientific
CTBP1	Hs00972287_m1	Thermofisher Scientific
GLIS3	Hs00541450_m1	Thermofisher Scientific
HMG20A	Hs00217047_m1	Thermofisher Scientific
IDE	Hs00610452_m1	Thermofisher Scientific
SPPL3	Hs00293370_m1	Thermofisher Scientific
THADA	Hs00736554_m1	Thermofisher Scientific

4.2.7 Expression of islet circRNAs in other tissues

The expression of the 13 circRNAs co-localizing to T2D-GWAS loci and the 5 most abundant circRNAs expressed in pancreatic islets and their parent linear transcripts were assessed in 39 different commercially available RNA samples of various tissues by quantitative qRTPCR. Reaction mixes contained 2.5 µL Taqman® Universal PCR mastermix II, no AmpErase® UNG, (ThermoFisher, Foster City, USA), 1.75 µL dH_2O, 0.5 µL cDNA and 0.25 µL Taqman® gene expression assay (ThermoFisher, Foster City, USA) in a 5 µL final reaction volume on 384 well qRTPCR plates. qRTPCR was run at 50 °C for 2 min, 95 °C for 10 min and 50 cycles of 15 s at 95 °C for 30 s and 1 min at 60 °C on the QuantStudio 12K Flex Real-Time PCR System. Each sample assay was conducted in 3 technical replicates.

4.2.8 Reverse transcription of circRNAs in islet RNA and EndoC βH1 cells

cDNA synthesis for analysis of circRNA expression in islets and across a panel of tissues was carried out using the Superscript® VILO™ cDNA synthesis kit (ThermoFisher, Foster City, USA) according to manufacturer's instructions. Reactions contained 100 ng/μL RNA in a final reaction volume of 20μL. Reaction conditions were 25°C for 10 min, 42°C for 60min and 85°C for 5min.

4.2.9 Assessment of associations between the islet expression of abundant circRNAs, insulin secretory index (SI), HbA1c or T2D status

RNA samples and clinical data were available for islet preparation from 50 non-diabetic donors and from 20 donors with T2D. Islet donor characteristics are given in table 10. We assessed the expression of the 5 most abundant circRNAs expressed in pancreatic islets as well as their host linear transcripts in relation to insulin secretory index, HbA1c or diabetes status in these samples by quantitative qRTPCR. Reaction mix contained 2.5 μL Taqman® Universal PCR mastermix II, no AmpErase® UNG, (ThermoFisher, Foster City, USA), 1.75 μL dH_2O, 0.5 μL cDNA and 0.25 μL Taqman® gene expression assay (ThermoFisher, Foster City, USA) in a 5 μL final reaction volume on 384 well qRT-PCR plates. qRTPCR was run at 50 °C for 2 min, 95 °C for 10 min and 50 cycles of 15 s at 95 °C for 30 s and 1 min at 60 °C. Each sample assay was conducted in 3 technical replicates on the QuantStudio 12K Flex Real-Time PCR System. Differential expression by diabetic status was then assessed by one-way ANOVA using StataSE15 (StataCorp, Texas, USA), with adjustment made for potential confounders including age, sex, BMI and ethnicity.

4.2.10 Determination of donor genotype at T2D risk SNPs

Python programming was used to cross-match the coordinates of the exons at the backsplice junctions with the coordinates of the T2D GWAS-loci. This ensured if the coordinates of the circRNA overlapped or encompassed within the T2D loci. We then sought to relate genotype at the GWAS association loci for T2D with expression of circRNAs located in those regions. Small amounts of genomic DNA are co-eluted in RNA preparations upon RNA extraction. We used a whole genome amplification (WGA) approach to access this genomic DNA for genotyping using the REPLI-g Mini kit (Qiagen, Paisley, UK). WGA was carried out using 2.5µL RNA and was performed according to manufacturer's instructions. Genotype was then determined by Sanger Sequencing of PCR amplicons containing the SNP in question. PCR reaction mixes included 2.4µL primer mix containing a 1:1 ratio of forward: reverse primers (ThermoFisher, Foster City, USA), 4µL MegaMix-Royal (Microzoneų, Brighton, UK), 1.60µL cDNA in a final reaction volume of 8µL. Reaction condition for PCR were 95°C for 12 min, 40 cycles for 95°C for 30s, annealing for 1 min, 72°C for 1 min followed by 72°C for 10 min**.** In one case, sequence analysis proved inconclusive. In this case, genotype at the SNP in question was determined by qPCR with TaqMan® Genotyping assay. Reactions contained 2.5 µL TaqMan® Genotyping Master Mix (ThermoFisher, Waltham, MA, USA), 0.25 µL Taqman® genotyping assay (rs6819243) (ThermoFisher, Waltham, MA, USA), 1.75 µL dH_2O and 0.5 µL whole genome amplified template in a 5 µL final reaction volume.

RNA samples and phenotypic data were available from 53 non-diabetic islet donors. Characteristics of participants are given in table 10. The expression of 13 circRNAs co-localising to the genomic regions containing the GWAS association loci for T2D

was assessed in relation to genotype. Expression levels were quantified by qRTPCR as described earlier. Expression levels were then correlated with genotype of the islets was assessed by one-way ANOVA using StataSE15 (StataCorp, Texas, USA) with adjustment for age, sex, BMI and ethnicity.

Table 12 Genotyping primers

Target	Forward primer	Reverse primer
rs1111875	GCATTACTACAGACTTTCC	AACTGATCAACAGCACCA
rs71777055	CCAATAGAGTATGGCAGAA	CATGGACCCATTCATCAG
rs12427353	CATGAAGACGCAGAAGC	GGTAATAAATGCAGGTTGAA
rs6819243	CTGCTGCTCTTCCCACCTC	CTGGCCTTCATCCCCAGG
rs10203174	TTCTCCCTCAGTGTTGAGG	GCTGAGATGTTGCAGCTC
rs10758593	ATGGCAAGGGAGAAGAGG	ATGGACCACCAATGAATTG

4.2.11 Assessment of circRNA expression in EndoC βH1 under diabetomimetic conditions

The expression levels of the 5 circRNAs chosen on the basis of islet abundance and their linear transcripts were also assessed in the human pancreatic beta cell line EndoC-βH1, following exposure to dysregulated glucose (2.5mM and 25mM), hypoxia (1% $O_{2)}$, dyslipidaemia (0.5mM palmitic acid) or proinflammatory cytokines (TNFα (1000 U/ mL, INFγ (750 U/ mL) and IL1β (75 U/ mL) as previously described (Jeffery et al., 2019). CircRNA expression was measured using qRTPCR as described above on the QuantStudio 12K Flex platform (ThermoFisher, Foster City, USA). Samples were run in 3 biological replicates and 3 technical replicates. Differential circRNA expression in treated cells was then assessed by one-way ANOVA using StataSE15 (StataCorp, Texas, USA).

4.3 Results

4.3.1 CircRNA profiling in islets

2619 circRNAs were expressed in islet donors in the present study (online resource 1). 47 of these circRNAs not been previously identified in human data from human tissues (multiple brain regions, muscle, thyroid and liver), and multiple cell types (including stem cells, skin and lung fibroblasts, neurons, lung epithelia, hepatocytes, breast cancer cells, lymphocytes, muscle myoblasts, aortic and vascular endothelial cells) analysed using the circBase circRNA database (Glazar et al., 2014). The five circRNAs demonstrating the highest expression in human islets derived from the *CAMSAP1, CIRBP, RPH3AL, RHOBTB3* and *ZKSCAN1* loci. 13 circRNAs co-localized with the GWAS association signals for T2D; these comprised *GLIS3* and *HMG20A* (1 circRNA each), *CTBP1, IDE and SPPL3* (2 circRNAs each) and *THADA* (five circRNAs). We selected these 18 circRNAs for further follow up. CircRNA structures were predicted based on the sequencing read depth for each exon and are presented in Fig. 13.

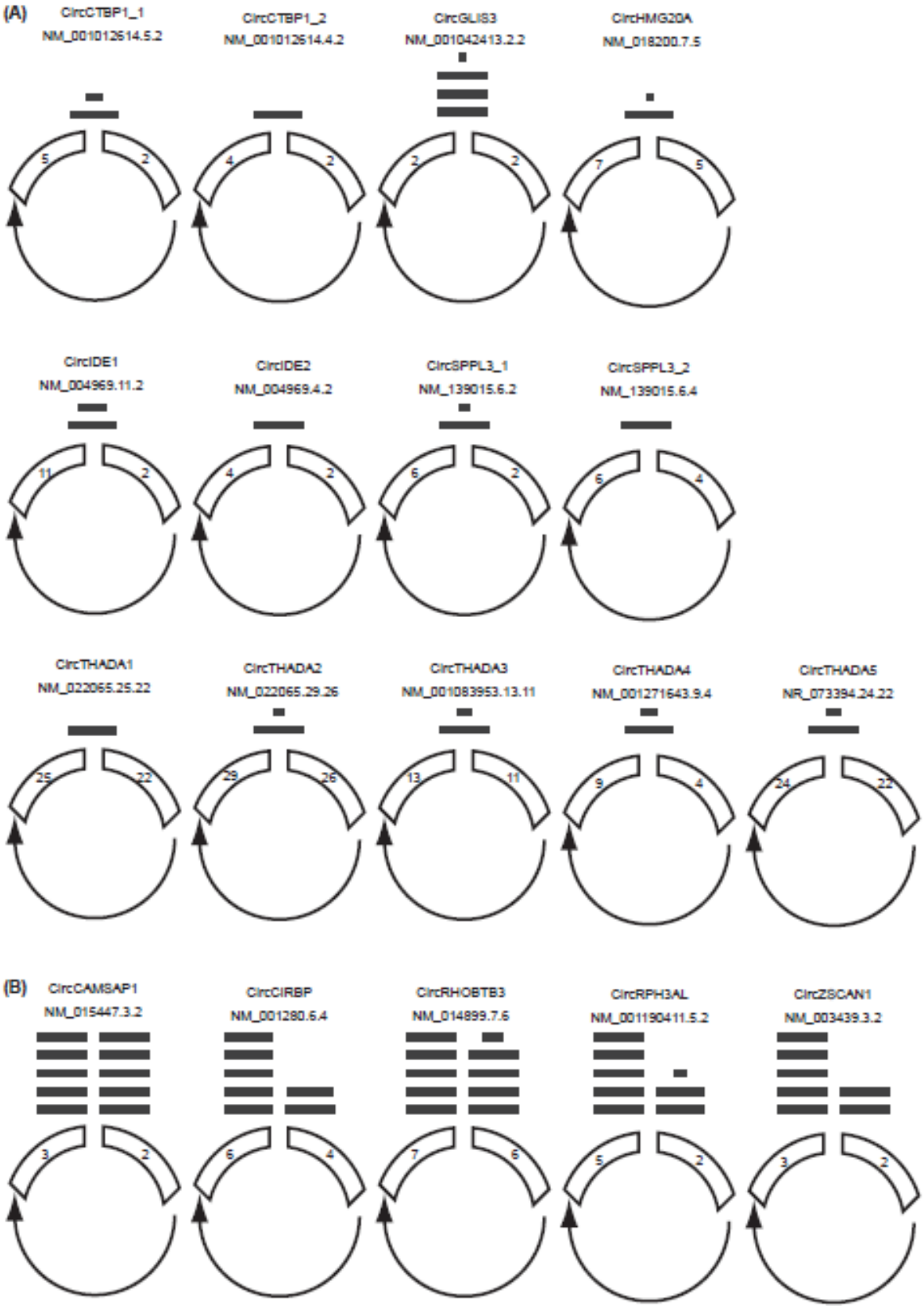

Figure 13 Predicted structures of circRNA expressed in the islets selected for this study. *CircRNA structures backsplice junctions were predicted based on the sequencing read depth for each exon from pooled samples from 5 non-daibetic islets. The relative read depth of each backspliced junction is shown by the number of bars above the respective backsplice junction.*

4.3.2 Pathway Analyses for genes generating islet-specific or abundant circRNAs

Pathway enrichment analysis was carried out to determine whether the genes hosting the 47 'islet-specific' circRNAs were enriched in any specific gene ontology (GO) pathways. A similar analysis was also carried out the genes hosting the top 10% most abundant circRNAs. Pathways analysis was performed using ClueGO cytoscape (Bindea et al., 2009). The circRNAs that so far seemed to be exclusively identified in islets unsurprisingly demonstrated enrichment for genes in the 'pancreatic secretion' pathway ($p = <0.001$). The 10% most abundantly expressed circRNAs were derived from genes demonstrating enrichment in the lysine degradation ($p = 0.03$), attenuation phase ($p = 0.02$), RUNX3 ($p = 0.02$) carcinoma ($p = 0.01$) and stem cell gene regulation ($p = <0.001$) pathways (table 13).

Table 13 Enrichment analysis of potential pathways targeted by genes generating circRNAs expressed predominantly in human pancreatic islets. *GO pathways analysis was carried out on A. 'islet-specific' circular RNAs and B. the top 10% most abundantly expressed circRNAs in human islets are presented here aligned to the hg19 genome alignment. Number of genes = number of differentially-expressed genes in each pathway.*

A.

Pathways enriched in genes hosting circRNAs expressed predominantly in islets

Pathway	p-value	Number of Genes	Genes
Pancreatic secretion	<0.0001	5	*CELA3A, CFTR, CPA1, KCNQ1, PNLIPRP2*

B.

Pathways enriched in genes generating the top 10% most abundantly-expressed circRNAs in islets

Pathway	p-value	Number of Genes	Genes
Hematopoietic Stem Cell Gene Regulation	<0.0001	4	*CREBBP, EP300, FOXO3, GABPB1*
Pathways affected in Adenoid Cystic Carcinoma	0.010	6	*CREBBP, EP300, FOXO3, KANSL1, KMT2C, MAML3*
Attenuation phase	0.020	3	*CREBBP, DNAJB1, EP300*
RUNX3 regulates NOTCH signaling	0.020	3	*CREBBP, EP300, MAML3*
Lysine degradation	0.030	5	*ASHIL, EHMT1, KMT2C, PLOD1, SETD3*

4.3.3 CircRNAs are differentially expressed in a tissue-specific pattern

We assessed the expression patterns of the 18 circRNAs selected for further analysis across a panel of human tissues. We demonstrated that the expression patterns of circRNAs did not always correlate with levels of their corresponding linear transcripts. The expression levels of circular and linear forms of the gene were sometimes divergent, indicating that the circRNAs are regulated independently from the mRNAs also deriving from the parental linear gene (Fig. 14). For instance, while *circSPPL3_2* was upregulated in most tissues compared to its linear gene, both *circCAMSAP1* and *circRHOBTB3* roughly followed the pattern of expression of their linear transcript levels across divergent tissues.

A.

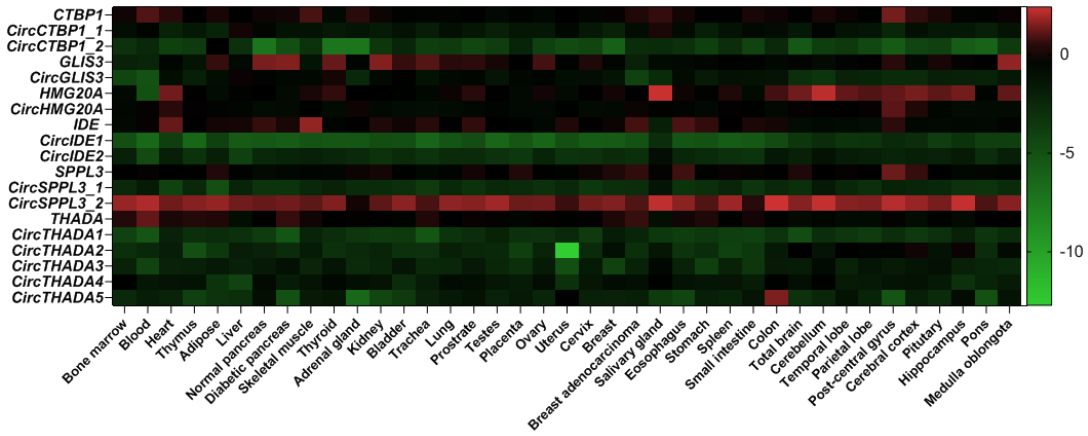

B.

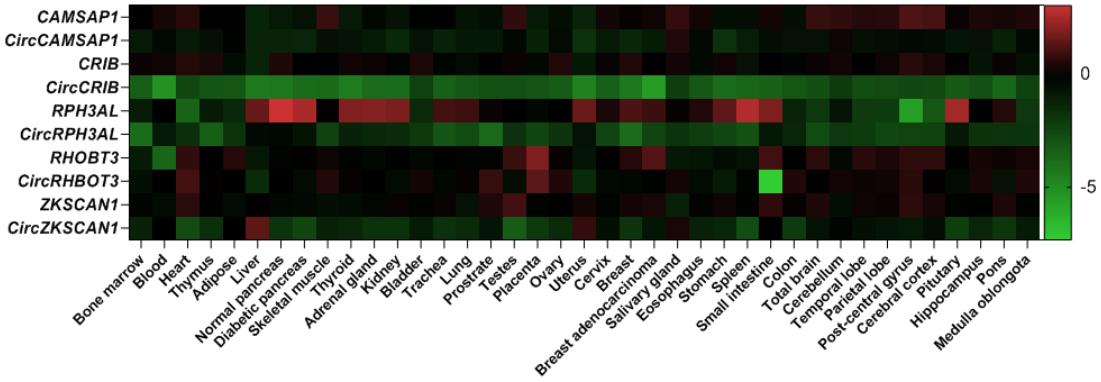

Figure 14 Tissue profile of islet and GWAS-located circRNAs. *Relative expression of circRNAs and their cognate transcripts have been assessed in 39 different commercially available tissue samples. The expression profile of 13 GWAS-localizing circRNAs are shown in* ***(A)*** *and 5 most abundant circRNAs are shown in* ***(B)*** *alongside their cognate RNA.*

4.3.4 The most abundant islet circRNAs are associated with insulin secretory index (SI) or T2D status in human islets

4/5 circRNAs that showed marked expression in the islets demonstrated an association with T2D status (Fig. 15; table 14). Three of these circRNAs, *circCAMSAP1*, *circCIRBP* and *circRPH3AL* satisfied the multiple testing threshold (p = <0.001, <0.001 and <0.001 respectively). *CircZKSCAN1* showed nominal association with T2D status in islet donors (p=0.030). Of these, the expression of the linear transcripts genes of three of these circRNAs, *CAMSAP1, CIRBP* and *ZKSCAN1* were also significantly associated with diabetic status (p = <0.001, <0.001 and <0.001 respectively). *RHOBTB3* (p<0.001) also demonstrated significant association with T2D status although its circRNA showed no association. The majority of these were positive associations, with the exception of *CIRBP* and *circCIRBP*, which were negatively correlated with T2D status. In addition, one circRNA (*circCIRBP*) demonstrated a nominal negative association with insulin secretory index (p = 0.028; table 14). No associations were identified between islet circRNA expression and donor HbA1c.

Table 14 Differential expression of the 5 most abundant islet circRNAs with insulin secretory index (SI), donor HbA1c or T2D status. *We measured the expression of the 5 most abundantly-expressed circRNAs and their linear counterparts in human pancreatic islet preparations using regression analysis with respect to* ***A.*** *Insulin secretory index (n = 50),* ***B****. Donor HbA1c (n = 18) or* ***C.*** *T2D status (n = 50 control islets and 20 islets from T2D donors). SD = Standard Deviation. 95% CI = 95% confidence intervals. Transcripts demonstrating associations with glycaemic parameters that are significant in regression analysis following adjustment for multiple testing are given in bold underlined type. Those demonstrating nominal associations only are indicated in bold italic type and asterisks.*

A

CircRNA	β-coefficient	p-value	95% CI		
CAMSAP1	0.051	0.444	-0.184	-	0.082
CircCAMSAP1	0.060	0.101	-0.133	-	0.012
CIRBP	0.007	0.894	-0.112	-	0.098
CircCIRBP*	***-0.153***	***0.029***	***-0.289***	***-***	***-0.017***
RHOBTB3*	***0.083***	***0.044***	***0.003***	***-***	***0.164***
CircRHOBTB3	-0.017	0.64	-0.088	-	0.055
RPH3AL	0.026	0.626	-0.133	-	0.081
CircRPH3AL	0.034	0.532	-0.075	-	0.143
ZKSCAN1	0.085	0.272	-0.069	-	0.239
CircZKSCAN1	0.028	0.357	-0.033	-	0.090

B

CircRNA	β-coefficient	p-value	95% CI		
CAMSAP1	-0.297	0.368	-1.005	-	0.412
CircCAMSAP1	0.128	0.582	-0.379	-	0.635
CIRBP	-0.423	0.325	-1.342	-	0.496
CircCIRBP	-0.024	0.977	-2.084	-	2.035
RHOBTB3	0.237	0.429	-0.410	-	0.884
CircRHOBTB3	-0.228	0.420	-0.837	-	0.382
RPH3AL	0.25	0.423	-0.424	-	0.925
CircRPH3AL	0.067	0.873	-0.858	-	0.992
ZKSCAN1	-0.096	0.872	-1.402	-	1.210
CircZKSCAN1	0.067	0.793	-0.490	-	0.623

C.

CircRNA	Mean	SD	Mean	SD	p-value
CAMSAP1	**0.049**	**0.550**	**0.658**	**0.424**	**<0.001**
CircCAMSAP1	**-0.010**	**0.302**	**1.341**	**0.405**	**<0.001**
CIRBP	**-0.007**	**0.454**	**-2.218**	**0.434**	**<0.001**
CircCIRBP	**0.070**	**0.530**	**-1.996**	**0.266**	**<0.001**
RHOBTB3	**0.000**	**0.428**	**-0.034**	**0.380**	**<0.001**
CircRHOBTB3	-0.009	0.425	0.823	0.494	0.419
RPH3AL	0.000	0.333	0.452	0.274	0.891
CircRPH3AL	**-0.048**	**0.303**	**-0.001**	**0.377**	**<0.001**
ZKSCAN1	**-0.216**	**0.663**	**0.907**	**0.510**	**<0.001**
CircZKSCAN1*	***0.019***	***0.267***	***0.211***	***0.537***	***0.012***

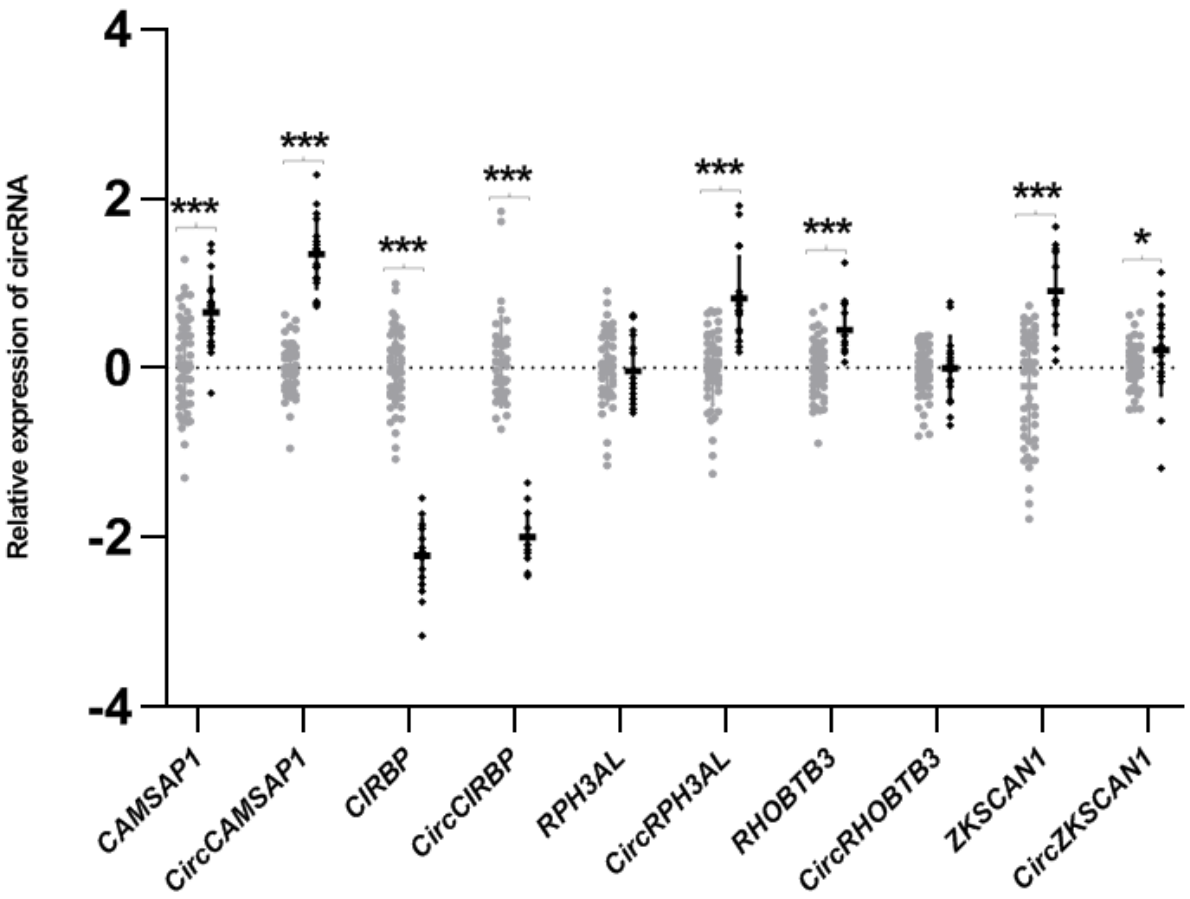

Figure 15 Differential expression of circCAMSAP1, circCIRBP, circRPH3AL and circZKSCAN1 in diabetic islets. *Expression levels of circular and linear transcripts of the top 5 most abundant circRNAs in human islets are given here in relation to T2D status. Islets from non-diabetic individuals are given in grey (n = 50), those from individuals with T2D are given in black (n = 20). Relative expression of each linear or circular RNA is given on the Y axis. Statistical significance in difference of expression assessed by one-way ANOVA between islets from donors with or without T2D is indicated by stars. * = <0.05, ** = <0.005, *** = <0.001.*

4.3.5 CircRNA expression is not driven by genotype

We next assessed the expression of circRNAs located in regions of the genome linked to risk of T2D. 13 circRNAs co-localised with the genomic regions encompassing the GWAS association signals for T2D; 2 circRNAs from the *CTBP1* gene (in rs6819243 region), one circRNA from the *GLIS3* gene (rs10758593), one circRNA from the *HMG20A* gene (rs7177055), two circRNAs from the *IDE* gene (rs1111875), two

circRNAs from the *SPPL3* gene (rs12427353) and five circRNAs deriving from the *THADA* gene (rs10203174). We identified no associations between any of these circRNAs and genotype at these loci (table15).

Table 15 Association of expression of circRNAs mapping to T2D-GWAS loci and their parental transcripts with genotype in primary non-diabetic islets. *The association assessed by one-way ANOVA between circRNA/linear transcript expression and genotype for circRNAs located to GWAS loci for T2D are given. Heterozygous samples and minor allele homozygotes are combined into one category. N=53. SD = standard deviation. Genotypes: GG = most common allele observed. Gg = heterozygotes, gg = minor allele heterozygotes.*

Transcript		GG		Gg and gg	
	p-value	Mean	SD	Mean	SD
rs6819243					
CTBP1	0.781	-0.11	0.32	-0.04	0.34
CircCTBP1_1	0.274	-0.03	0.65	0.09	0.37
CircCTBP1_2	0.293	0.00	0.85	0.11	0.85
rs10758593					
GLIS3	0.139	-0.19	0.37	0.02	0.36
CircGLIS3	0.535	0.03	0.37	0.04	0.41
rs7177055					
HMG20A	0.502	-0.03	0.38	0.09	0.37
CircHMG20A	0.952	0.03	0.36	0.03	0.38
rs1111875					
IDE	0.578	-0.66	0.39	-0.46	0.35
CircIDE1	0.953	-0.02	0.40	0.04	0.45
CircIDE2	0.937	-0.02	0.23	0.02	0.36
rs12427353					
SPPL3	0.808	-0.01	0.48	0.05	0.43
CircSPPL3_1	0.677	-0.02	0.45	0.06	0.34
CircSPPL3_2	0.595	0.01	0.48	0.21	0.48
rs10203174					
THADA	0.369	-0.02	0.61	0.22	0.50
CircTHADA1	0.672	0.05	0.40	0.10	0.42
CircTHADA2	0.282	-0.01	0.86	-0.33	0.96
CircTHADA3	0.133	0.11	0.32	0.16	0.45
CircTHADA4	0.319	0.06	0.39	-0.24	0.46
CircTHADA5	0.651	0.14	0.59	0.27	0.40

4.3.6 CircRNAs are differentially expressed upon exposure to stress conditions in EndoC-βH1 cells

Although the 5 most abundant circRNAs expressed in human islets did not show overt responsiveness to altered glucose, hypoxia or pro-inflammatory cytokines when tested in the human beta cell line EndoC-βH1, two (*circCIRBP* and *circRPHAL3*) did demonstrate changes in expression following treatment with 0.5mM palmitate. *CircCIRBP* expression was increased following treatment ($p = 0.021$) whereas *circRPHAL3* demonstrated reduced expression ($p = 0.022$; table 16). The expression of the linear transcripts from the *RHOBTB3* and *ZKSCAN1* genes also demonstrated increased expression in EndoC-βH1 cells treated with palmitic acid, in the absence of effects of their respective circRNAs.

Table 16 Expression of most abundantly expressed circRNAs and their parental transcripts in EndoC-βH1 cells treated with diabetes-related stresses. *We assessed the effect of diabetes-related cellular stresses (low/high glucose, elevated fatty acid, hypoxia and exposure to pro-inflammatory cytokines) on the expression of the 5 most abundant islet circRNAs in the EndoC-βH1 human beta cell line by one-way ANOVA. N=9 sapmles for each treatment conditions. IQR = interquartile range. Results meeting the threshold for 4 test conditions are given in bold underlined type, those presenting nominal associations only are indicated in bold italic type.*

Transcript	Treatment	p-value	Median (IQR)
CAMSAP1	Control		1.11 (0.95-1.39)
	2.5mM glucose	0.313	1.03 (0.92-1.05)
	25mM glucose	0.444	0.96 (0.95-1.17)
	Control		0.92 (0.89-1.06)
	1% O_2	0.694	0.97 (0.73-1.04)
	3% O_2	0.347	0.88 (0.63-0.99)
	Control		1.05 (0.95-1.08)
	Palmitic acid	0.062	0.89 (0.77-0.94)
	Control		0.93 (0.25-1.21)
	Cytokines	0.635	0.95 (0.90-0.99)
CircCAMSAP1	Control		0.84 (0.79-1.11)
	2.5mM glucose	0.762	1.02 (0.75-1.12)
	25mM glucose	0.681	0.92 (0.78-1.29)
	Control		0.98 (0.92-1.14)
	1% O_2	0.136	0.89 (0.76-0.93)
	3% O_2	0.292	0.83 (0.63-1.07)
	Control		1.04 (1.02-1.23)
	Palmitic acid	0.090	0.82 (0.65-1.00)
	Control		0.77 (0.27-1.14)
	Cytokines	0.555	0.99 (0.69-1.02)
CIRBP	Control		1.06 (0.83-1.08)
	2.5mM glucose	0.080	1.38 (1.10-1.53)
	25mM glucose	0.077	1.30 (1.14-1.56)
	Control		1.01 (0.99-1.09)
	1% O_2	0.146	0.79 (0.39-0.97)
	3% O_2	0.129	0.84 (0.74-1.02)
	Control		0.88 (0.65-1.09)
	Palmitic acid	0.907	0.91 (0.64-1.15)
	Control		0.90 (0.03-1.34)
	Cytokines	0.593	0.95 (0.93-1.06)
CircCIRBP	Control		0.77 (0.61-1.42)
	2.5mM glucose	0.844	0.86 (0.32-1.37)
	25mM glucose	0.652	0.77 (0.72-0.94)
	Control		1.10 (1.00-1.23)
	1% O_2	0.955	0.86 (0.56-2.00)
	3% O_2	0.726	0.89 (0.68-1.48)
	Control		0.75 (0.72-1.04)
	Palmitic acid	***0.021***	***1.69 (1.30-1.98)***

	Control		1.17 (1.00-1.33)
	Cytokines	0.180	0.73 (0.69-1.06)
RPH3AL	Control		1.05 (0.93-1.06)
	2.5mM glucose	0.503	0.99 (0.75-1.07)
	25mM glucose	0.441	0.93 (0.80-1.08)
	Control		1.09 (1.06-1.37)
	1% O_2	0.357	1.55 (1.04-1.56)
	3% O_2	0.205	1.32 (1.28-1.81)
	Control		0.95 (0.87-0.99)
	Palmitic acid	0.102	0.84 (0.70-0.87)
	Control		0.98 (0.02-1.01)
	Cytokines	0.354	1.02 (0.91-1.12)
CircRPH3AL	Control		1.00 (0.45-1.00)
	2.5mM glucose	0.941	0.85 (0.58-0.97)
	25mM glucose	0.867	0.76 (0.73-0.86)
	Control		1.09 (1.06-1.37)
	1% O_2	0.357	1.55 (1.04-1.56)
	3% O_2	0.205	1.32 (1.28-1.81)
	Control		1.66 (1.32-1.85)
	Palmitic acid	***0.022***	***0.97 (0.95-1.11)***
	Control		0.68 (0.47-0.77)
	Cytokines	0.295	0.97 (0.55-1.02)
RHOBTB3	Control		1.24 (1.23-1.31)
	2.5mM glucose	0.188	1.11 (1.00-1.27)
	25mM glucose	0.117	1.20 (0.72-1.14)
	Control		0.95 (0.69-1.06)
	1% O_2	0.949	0.97 (0.77-0.98)
	3% O_2	0.353	0.67 (0.65-0.93)
	Control		0.80 (0.72-0.90)
	Palmitic acid	***0.003***	***1.18 (1.15-1.21)***
	Control		1.17 (0.29-1.35)
	Cytokines	0.186	1.59 (1.22-1.72)
CircRHOBTB3	Control		0.74 (0.73-1.00)
	2.5mM glucose	0.836	0.89 (0.65-1.02)
	25mM glucose	0.351	0.77 (0.57-0.78)
	Control		1.04 (0.72-1.08)
	1% O_2	0.182	0.78 (0.74-0.78)
	3% O_2	0.288	0.79 (0.77-0.86)
	Control		1.16 (0.99-1.27)
	Palmitic acid	0.306	1.03 (0.83-1.13)
	Control		1.01 (0.95-1.08)
	Cytokines	0.628	0.97 (0.89-1.06)
ZKSCAN1	Control		1.24 (1.18-1.33)
	2.5mM glucose	0.632	1.23 (1.05-1.87)
	25mM glucose	0.997	1.23 (1.16-1.36)
	Control		0.93 (0.86-1.08)

	1% O_2	0.388	1.06 (0.94-1.12)
	3% O_2	0.218	0.72 (0.66-0.98)
	Control		0.50 (0.39-0.55)
	Palmitic acid	***0.001***	***1.01 (0.94-1.12)***
	Control		1.29 (0.24-1.33)
	Cytokines	0.378	1.30 (1.27-1.35)
CircZKSCAN1	Control		0.86 (0.81-1.17)
	2.5mM glucose	0.490	0.91 (0.83-1.17)
	25mM glucose	0.505	0.88 (0.83-1.28)
	Control		1.11 (0.99-1.42)
	1% O_2	0.060	1.65 (1.41-1.79)
	3% O_2	0.631	1.24 (1.02-1.57)
	Control		1.01 (0.81-1.45)
	Palmitic acid	0.252	0.83 (0.75-0.91)
	Control		1.05 (0.10-1.13)
	Cytokines	0.292	1.16 (1.13-1.18)

4.4 Discussion

We present here the first enriched circRNA profile from human primary pancreatic islet RNA produced from a modified NGS ciiscrcleSeq protocol with enrichment for circRNAs. We have identified 2619 circRNAs expressed in human islets, including 47 circRNAs which were not identified in profiles from multiple other tissues in circBase. As mentioned earlier, the circRNA profile was generated from pooled samples of RNA from 5 non-diabetic islet donor. After selection of circRNAs from the circRNA profile based on their abundance in the RNA-Seq circRNA profile, five circRNAs were followed up in islets of a diabetic human cohort.

Of the 18 circRNAs selected for follow up on the basis of abundance or co-localisation to the GWAS association signals for T2D, many also show evidence of regulation independent of their parent gene. 4 out of 5 of the most abundant circRNAs in human islets demonstrate strong evidence of dysregulated expression in the islets of human donors with T2D, with one (*circCIRBP*) demonstrating an association with insulin

secretory index. 2 out of 5 also show dysregulated expression in human EndoC-βH1 beta cells treated with fatty acids although direction of effect was not conserved.

It is interestsing that both EP300 and FOXO3 are amongst the most abundance candidate circRNAs in the circRNA profile for peripheral blood as well as islets in this thesis. rs7903146 *TCF7L2* variant display genotypic association in diabetic patients. Interactome analysis reveal this variant interacts with Ep300 which is a histone acetyltransferase and regulates transcription via chromatin remodelling that play a fundamental role in susceptibility to diabetes and other age related disorders (Garagnani et al., 2013). FOXO is a mediator of the effects of insulin and insulin-like growth factors affecting several cellular processes such as proliferation, apoptosis, metabolism and response to oxidative stress. *FOXO3* variants rs13217795, rs2764264, and rs2802292 were associated with lower blood glucose level in T2D elderly women (Mao et al., 2019). DAF-16 increases the expression of manganese superoxide dismutase which confers protection against free radicals and thereby ageing FoxO3 is also a driver in maintaining stem cell pool in mammals, exhaustion of which is a key hallmark of ageing (Morris et al., 2015; Willcox et al., 2008) . FOXO may mediate insulin effects on metabolism, control response to ROS and maintain stem cells and these may cumulatively influence longevity through multiple mechanisms in humans.

To date, there have been two circRNA profiles generated from human pancreatic endocrine cells or intact islets. The first provides a circRNA profile generated from publically-available NGS data from isolated β, α and δ cell transcriptomes (Kaur et al., 2018). This study reported 10,832 putative circRNAs expressed in total, with 382

shared across cell types. This study reports more islet circRNAs than identified in our dataset, but this profile is derived from conventional NGS data, with no pre-treatment to remove linear sequences. Back splicing events can be generated from tandem DNA duplications within genes, or from trans-splicing events during linear splicing (Izuogu et al., 2016), so it is likely that profiles derived from conventional NGS contain 'circRNAs' that in fact represent aberrantly spliced linear transcripts rather than genuine circRNAs. Differences will also arise in that this previous circRNA profile derives from isolated β, α and δ cell populations, whereas ours is a profile derived from intact islets. Differences in gene expression patterns may thus reflect the effects of cell:cell crosstalk as occurs in vivo. Nevertheless, there was considerable overlap between our circRNA and the beta cell circRNA profile reported earlier; >25% of the top 20 circRNAs in the beta cell profile have counterparts generated from the same genes in the top 20 most abundant circRNAs in our profile.

A second islet circRNA profile has also been reported (Stoll et al., 2018). This profile was based on a microarray approach, identified 3441 islet circRNAs from a study of 3 human islet samples (two female and one male donor). Since this is a microarray-based profile, it will only contain circRNAs that have been already annotated. The most abundant circRNA in this study derived from the *HIPK3* gene. We also identified a circRNA deriving from this gene in the top 75 most abundant circRNA transcripts in our profile. This study differs from ours in that follow up work on circRNA expression in cell lines and in relation to T2D status occurred in animal models and not in human cells and tissues.

Our data, like those reported in previous islet studies (Kaur et al., 2018; Stoll et al., 2018) suggests that many of the circRNAs we have identified are regulated independently of their linear counterparts; the expression pattern of circular transcripts does not always echo that of their linear counterparts (Fig. 14). In some cases, we have identified associations between cell treatments or T2D status with circRNAs in the absence of apparent effects on their linear transcripts. Comparison of circRNA expression across tissues showed expression patterns of many circRNAs were often higher in brain tissues compared to other tissues, which is in line with existing knowledge that circRNAs accumulate in the brain (Gokool et al., 2019).

Some of our circRNAs are associated with glycaemic traits in human islets. The expression of *circCIRBP* demonstrates a negative association with insulin secretory index (SI) of the donor islets, is elevated in human EndoC-βH1 beta cells treated with palmitic acid and is reduced in islets from donors with T2D. The parent gene *CIRBP* (Cold Inducible RNA Binding Protein) has roles in genotoxic stress response, not only from cold, but also from other cellular stressors such as hypoxia (Lee et al., 2015). Elevated levels have been associated with maintenance of glucose metabolism and protection from cold exposure through effects on the AKT pathway (Liu et al., 2019). The elevated levels we demonstrate in the human beta cell line EndoC-βH1 treated with palmitate may therefore represent an acute stress response to altered lipid. The lower levels in the islets of individuals with T2D may reflect lower stress tolerance in diabetic islets, and the inverse correlation with SI may reflect a compensatory effort to maintain insulin secretion in the face of increased insulin resistance in individuals with T2D.

We also identified elevated levels of both *circCAMPSAP1* and its host gene *CAMSAP1* in the islets of donors with T2D. CAMSAP1 encodes an organisation protein involved in microtubule dynamics and localisation (Baines et al., 2009). The dynamics of microtubule assembly and disassembly has an impact on the insulin secretion machinery; translocation of insulin granules along microtubules can influence their availability for secretion and failure to disassemble can impede docking. Microtubule density is higher in the islets of diabetic mice compared with non-diabetic littermates (Zhu et al., 2015). CAMSAPs are active in multiple tissues, and also have roles in white blood cells, which rely on the tubulin-microtubule system for lymphocyte activation (Sherline and Mundy, 1977). ZKSCAN1 and its circular RNA *circZKSCAN1* have been described as inhibitors of cellular proliferation and survival (Yao et al., 2017). Both transcripts demonstrate elevated expression in islets from donors with T2D, which may perhaps reflect adverse effects on beta cell survival. *CircRPH3AL* was also upregulated in diabetic islets. Linear transcripts from *RPH3AL* are highly expressed in β-cells and have roles in calcium-dependent exocytosis during granule maturation and insulin secretion (Matsunaga et al., 2017).

We hypothesised that dysregulation of circRNA expression may underpin some of the GWAS association signals for T2D. 13 circRNAs colocalise to the recombination windows surrounding the 6 of the GWAS index loci, but none of these demonstrated differential expression by risk genotype. This suggests that the genetic associations between individual genetic variants and T2D is probably not mediated by dysregulation of islet circRNAs.

We acknowledge that at present our data are largely correlative, and do not offer information on causality, definitive mechanistic proof or insight into the regulatory relationships between circRNAs and their host genes. CircRNAs can have effects *in cis* by regulating the transcription, linear splicing or translation of linear transcripts from their host genes (Abdelmohsen et al., 2008; Ashwal-Fluss et al., 2014; Chao et al., 1998; Grigull et al., 2004; Gualandi et al., 2003; Jeck et al., 2013). In our data, we observe similar responses of linear and circular transcripts in response to challenge (*CAMSAP1/circCAMSAP1*, *CIRBP/circCIRBP, ZKSCAN1/circZKSCAN1*). This may be a manifestation of effects on transcription of common pre-RNAs from which both forms can be expressed. Other circRNAs show dysregulated expression for the circRNA alone (*circRPH3AL*). This suggests that the effect of circRNA regulation is post-transcriptional in these cases. CircRNAs can also act *in trans*, by virtue of sponging of other non-coding (nc) RNAs or RNA binding proteins (Abdelmohsen et al., 2017; Piwecka et al., 2017; Zheng et al., 2016). In these cases, it is impossible to deduce from our data what the molecular targets of dysregulated islet circRNAs may be.

There can also be issues of uneven degradation of linear trasncipts. Washing cells from tissue culture with PBS before extraction with Trizol and adding beta-mercaptoethanol to the lysis buffer can stabilize the tissues during extraction by inactivating RNAase and therefore minimize uneven degradation of linear transcripts or rRNA. The use of RNase inhibitors as has been done in this project to generate RNASqeq data to prevent degradation by endogenous RNase. Storing in RNase-free water or TE buffer at -80ºC for 1 year, as done in this thesis, or as ethanol precipitates

at -20°C. However, the use of ethanol should be avoided because RNA cannot be dispersed evenly in solution and used for direct quantitative experiments.

In conclusion, we present here an enriched circular RNA profile in human pancreatic islets. Although we find no evidence that the associations between T2D and genetic variation are underpinned by effects on the circRNA milieu, we demonstrate that the majority of the most abundant islet circRNAs display associations between their expression and aspects of glucose homeostasis in human donors. Furthermore, two of the top 5 most abundant circRNAs derive from genes with known roles in the mechanics of insulin exocytosis. We propose therefore that the circular RNA milieu in pancreatic islets may contribute to the regulation of genes with endocrine function.

Chapter 5 – Data Chapter

Islet-expressed circular RNAs are associated with type 2 diabetes status in peripheral blood

Abstract

The prevalence and incidence of T2D is expected to rise to 629 million by 2045. Intervention through lifestyle changes like healthy diet and physical activity during the early stages of T2D can improve insulin sensitivity. However, the management of insulin resistance by diet ought to be very carefully assessed because of the risk collapsing due to hypoglycaemia. Therefore, biomarkers to predict those at risk for T2D can enable physicians to offer dietary alterations early on in order to delay the onset of T2D and its associated co-morbidities. Many biomarkers for T2D show associations with diabetes status. However, the associations seem to be due to manifestation of confounding factors rather than causality. Given the chronic and heterogeneity manner of this disease, the use of biomarkers may better characterize risk and greatly assist healthcare decision making. In addition to using biomarkers for future risk assessment, it is essential that they can also be used to identify causal pathways even in cases where the associations might be comparatively weak. This can throw light into the development of new drug targets for preventive or individualized targeted therapeutic interventions. An important pre-requisite for this is the characterisation of circRNA sequences in diabetes-relevant tissues such as pancreatic islets and in more accessible tissues such as peripheral blood. CircRNAs are highly nuclease-resistant and thus more stable than linear transcripts, by virtue of their covalently closed bonds at the backspliced junctions. The half-lives of circRNAs are approximately 2.5 times that of the median half-lives of their linear transcripts. Many circRNAs are enriched in blood compared to the level of expression of their linear mRNAs. I assessed whether any of the circRNAs differentially in the islets were similarly dysregulated in the peripheral blood of individuals with pre-diabetes or overt disease. 3/5 of the most abundant islet circRNAs were expressed in blood. Of these, *circCAMSAP1* showed a nominal association with T2D status in the peripheral blood

of patients with T2D. It may have the potential as a biomarker as future molecular targets for novel diabetes therapeutics after further investigation in longitudinal study.

5.1 Introduction

Biomarkers are molecular entities that can predict intermediate outcomes or endpoints of disease states. The use of these entities makes it easier and quicker through cheaper approaches to assess risk of diseases or stages of disease than that would be possible from direct measurement of clinical endpoint often in inaccessible tissues. They can be used to predict the onset or progression of diseases, for screening, diagnosis and prognosis to determine outcomes or predict mortality which can often help make decision on individualized targeted therapeutic interventions (Aronson and Ferner, 2017).

The prevalence and incidence of diabetes is expected to rise from 463 to 700 million by 2045 (Atlas 2019). Although, intervention through lifestyle changes like healthy diet and physical activity during the early stages of T2DM can improve insulin sensitivity, the management of insulin resistance by diet ought to be very carefully assessed because of the risk collapsing due to hypoglycaemia. Biomarkers to predict those at risk for T2D can enable physicians to offer dietary alterations early on in order to delay the onset of T2D and its associated co-morbidities.

A successful biomarker should show minimal variability, surpass the effect on confounding factors sometimes and change proportionately in response to changes in disease states or upon response to therapeutic intervention (Aronson and Ferner, 2017). It is often very cumbersome to determine a good candidate biomarker due to the pathophysiological complexities and the technical difficulties in validating diagnostic, prognostic or therapeutic-response biomarkers and standardizing methods

for sampling handling to cover broad spectrum patients with different genetic background and environmental factors.

Many biomarkers for T2D are not assessed based on the measurement of fasting glucose, 2-hour glucose or HbA1c levels leading to underestimation of incident cases of T2D. In other cases, the potential mechanisms leading to the T2D has remained unanswered especially in relation to impaired β-cell function which is the key to pathogenesis of T2D. Only 35 biomarkers have been reported in large scale studies with sample size of more than 1000 T2D cases of which none has strong evidence of association from genetic association studies that explaining underlying causal association (Abbasi et al., 2016). Many biomarkers like adiponectin (Dastani et al., 2012; Yaghootkar et al., 2013), C-reactive protein (Brunner et al., 2008; Jensen et al., 2013), triglycerides (De Silva et al., 2011), vitamin D (Ye et al., 2015; Buijsse et al., 2013), IL-1Ra (Anon, 2015) and uric acid (Pfister et al., 2011) which show associations with diabetes, seem to be due to manifestation of confounding rather than a causality.

Given the chronic and heterogeneity manner of this disease, the use of biomarkers may better characterize risk and greatly assist healthcare decision making (Yach et al., 2004; Biomarkers Definitions Working Group. 2001). Many studies predicting of future risk to diabetes have included people with existing undiagnosed diabetes at baseline and thus may not have addressed the problem of potential reverse causality (Abbasi et al., 2012; Kengne et al., 2014). Molecular entities expressed in easily accessible body fluids such as blood may play a role in quantifying the future risk of T2D and in understanding possible aetiological factors affecting the disease

process. In addition to using biomarkers for future risk assessment, it is essential that they can also be used to identify causal pathways even in cases where the associations might be comparatively weak. This can throw light into the development of new drug targets for preventive or targeted therapeutic interventions (Biomarkers Definitions Working Group. 2001)

CircRNAs are highly nuclease-resistant and thus more stable than linear transcripts, by virtue of their covalently closed bonds at the backspliced junctions (Suzuki et al., 2006; Lasda and Parker, 2016a). The half-lives of circRNAs are approximately 2.5 times that of the median half-lives of their linear transcripts. The half-lives of circRNAs can be as long as 50 hrs. (Enuka et al., 2016).

Many circRNAs are enriched in blood compared to the level of expression of their linear mRNAs. This makes them useful tools for non-invasive diagnostics assays using samples from otherwise inaccessible tissues (Memczak et al., 2015). CircRNAs may have potential as biomarkers for the development of diabetes or as future molecular targets for novel diabetes therapeutics (Fang et al., 2018; Wu et al., 2019; Zhang et al., 2017). An important pre-requisite for this would be the characterisation of circRNA sequences in diabetes-relevant tissues such as pancreatic islets and in more accessible tissues such as peripheral blood.

We aimed to determine whether abundant islet circRNAs were differentially expressed in the peripheral blood of individuals with pre-diabetes or overt disease. 3/5 of the most abundant islet circRNAs were also expressed in blood, and the expression of one, *circCAMSAP1* demonstrating a nominal association with T2D status in the peripheral

blood of patients with T2D, but not impaired glucose tolerance (IGT). These may have future potential as biomarkers of disease. This circRNA can perhaps be considered for further complex longitutdinal studies adjusting for the time at diagnosis, amount of physical acivity and lifestyle habits and other factors that may influence response in the pre-diabetic phase or after diagnosis.

5.2 Methods

5.2.1 RNA extraction from peripheral blood samples from control donors, donors with IGT and those with T2D

We assessed the expression of the 5 most abundant islet circRNAs in relation to diabetes status in RNA extracted from 285 peripheral blood samples from the Exeter 10K study. Our sample set consisted of 133 non-diabetic patients (fasting glucose <100.8 mg/dL), 46 individuals with impaired glucose tolerance (fasting glucose 100.8 to 122.4 mg/dL) and 106 patients with overt diabetes (fasting glucose >122.4mg/dL). Participant characteristics are given in table 17. This collection is a cross sectional population study consisting of samples collected from volunteer individuals living in the South West of England and recruited since 2010. Whole blood samples were collected in 2011/2012 using the PAXgene system (Debey-Pascher et al., 2009) and extracted using the PAXgene Blood RNA kit (Qiagen, Paisley, UK). Written informed consent was obtained for all participants and ethical permission was granted through the National Institute for Health Research (NIHR) Clinical Facility (REC 09/H0106/75).

Table 17 Participant characteristics for circRNA expression in peripheral blood.
A. Anthropometric characteristics of peripheral blood donors with normal blood glucose (n = 133) and those with impaired glucose tolerance (IGT; n = 46) B. Anthropometric characteristics of peripheral blood donors with normal blood glucose (n = 133) and those with overt T2D (n = 106). Differences in parameters between islet groups was determined by t-test.

A.

	p-value	Control		IGT	
		Mean	SD	Mean	SD
Age	0.016	52.45	17.08	59.26	14.31
BMI	<0.001	26.51	4.13	28.93	3.68
HbA1c	-	5.61	0.34	-	-
Glucose	-	4.85	0.40	-	-
Sex	0.004	F (60%);	M (40%)	F (40%)	M (60%)
Ethnicity	0.611	white (99%)	other (1%)	white (100%)	other (0%)

B.

	p-value	Control		T2D	
		Mean	SD	Mean	SD
Age	<0.001	52.45	17.08	68.74	10.65
BMI	<0.001	26.51	4.13	30.61	5.99
HbA1c	-	5.61	0.34	-	-
Glucose	-	4.85	0.40	-	-
Sex	0.001	F (60%);	M (40%)	F (57%)	M (43%)
Ethnicity	0.445	white (99%)	other (1%)	white (99%)	other (1%)

5.2.2 Design of qPCR assays for circRNA validation

Custom designed quantitative qRTPCR assays for quantification of relative expression were designed to unique back-spliced circRNA junctions (IDT, Iowa, USA). Each target sequence was checked for the presence of single nucleotide polymorphisms in potential primer or probe binding regions prior to ordering. Assays were ordered as custom single tube assays from IDT (Iowa, USA).

5.2.3 Assessment of circRNA expression in peripheral blood of pre-diabetic and diabetic participants

The expression levels of the 3 circRNAs chosen on the basis of their differential expression in donor islets. CircRNA expression was measured using qRTPCR. Reaction mix contained 2.5 µL Taqman® Universal PCR mastermix II, no AmpErase® UNG, (ThermoFisher, Foster City, USA), 1.75 µL dH_2O, 0.5 µL cDNA and 0.25 µL Taqman® gene expression assay (ThermoFisher, Foster City, USA) in a 5 µL final reaction volume on 384 well qRT-PCR plates. qRTPCR was run at 50 °C for 2 min, 95 °C for 10 min and 50 cycles of 15 s at 95 °C for 30 s and 1 min at 60 °C. Each sample assay was conducted in 3 technical replicates on the QuantStudio 12K Flex Real-Time PCR System. Differential expression by diabetic status was then assessed by one-way ANOVA using StataSE15 (StataCorp, Texas, USA), with adjustment made for potential confounders including age, sex, BMI and ethnicity.

5.2.4 Assessment of associations between the islet expression of abundant circRNAs, insulin secretory index (SI), HbA1c or T2D status

RNA samples and phenotypic data were available for the 133 non-diabetic patients, 46 individuals with impaired glucose tolerance and 106 patients with overt diabetes. The expression of the 3 circRNAs were quantified by qRTPCR as described earlier. We assessed the expression in the peripheral blood were correlated with HbA1c or diabetes status in the study cohort by one-way ANOVA using StataSE15 (StataCorp, Texas, USA) with adjustment made for confounders like age, sex, BMI and ethnicity.

5.3 Results

5.3.1 CircCAMSAP1 is differentially expressed in T2D peripheral blood

Of the 4 circRNAs demonstrating evidence of altered expression in the islets of donors with T2D, two (*circIDE1* and *circRPH3AL)* were not expressed in peripheral blood. Of the three remaining circRNAs which did have expression in peripheral blood (*circCAMSAP1*, *circCIRBP* and *circZKSCAN1*), *circCAMSAP1* demonstrated a nominal negative association with diabetes status in the peripheral blood of patients with T2D (Fig. 16; table 18). No difference in expression was detected for any circRNA between control patients and those with IGT, or between those with IGT and those with T2D). No associations were evident between circRNA expression in peripheral blood and either participant fasting glucose or HbA1c.

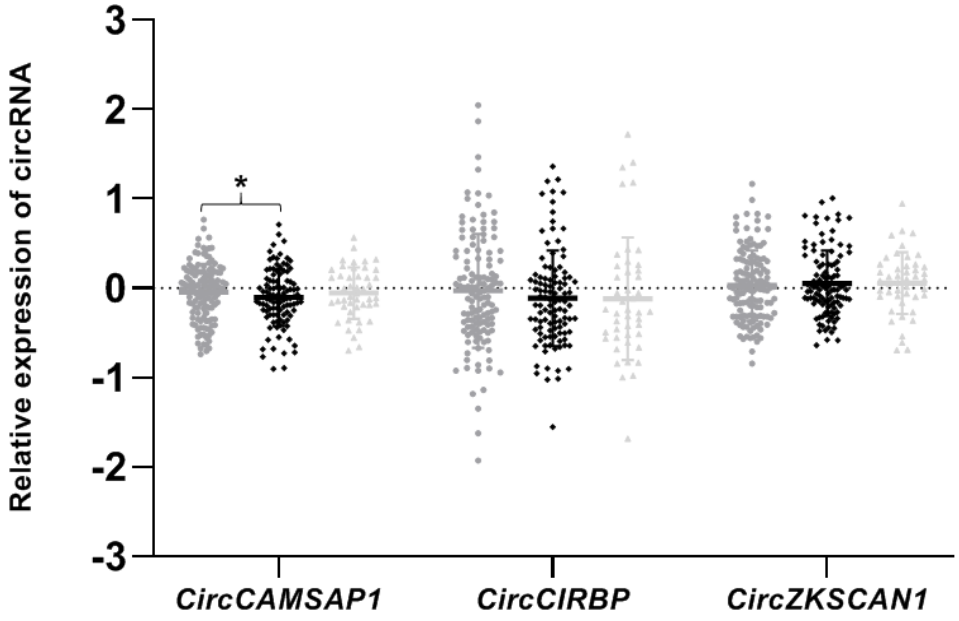

Figure 16 Differential expression of circCAMSAP1 in peripheral blood of T2D participants. *Peripheral blood circRNA levels are given here for non-diabetic samples (labelled in mid-grey; n=133), samples from individuals who have overt diabetes (labelled in black; n = 106) and those with impaired glucose tolerance IGT (labelled in light grey; n = 46). Relative expression of circRNAs is given on the Y axis. Statistical significance, from one-way ANOVA analysis, in difference of expression between early and late passage cells is indicated by stars. * = <0.05.*

Table 18 The expression of islet circRNAs according to diabetes status in the peripheral blood of individuals with IGT or overt T2D, compared with non-diabetic controls. *The expression of the circCAMSAP1, circCIRBP and circZKSCAN1 circRNAs is given here in relation to A. fasting blood glucose (n = 130) and B. HbA1c (n = 80) in the peripheral blood of non-diabetic controls. C. The expression of the* circCAMSAP1, circCIRBP and circZKSCAN1 *circRNAs is also given in relation to diabetes status in the peripheral blood of patients without disease (n =133), those with IGT (Impaired glucose tolerance; n = 46) and those with overt T2D (n = 106). Association of circRNA expression levels with fasting blood glucose level (**A**) and HbA1c **(B)** was assessed by linear regression and relation of circRNA expression levels with diabetes status **(C)** was assessed by ANOVA. SD = Standard deviation. Results showing statistical significance are indicated in bold italic type.*

A

CircRNA	β-coefficient	95% CI			p-value
CircCAMSAP1	0.069	-0.085	-	0.222	0.378
CircCIRBP	0.039	-0.276	-	0.353	0.808
CircZKSAN1	0.052	-0.135	-	0.238	0.585

B.

CircRNA	β-coefficient	95% CI			p-value
CircCAMSAP1	-0.012	-0.269	-	0.245	0.928
CircCIRBP	0.303	-0.105	-	0.710	0.143
CircZKSAN1	-0.257	-0.558	-	0.044	0.093

C.

		Control		Case	
Transcript	**p-value**	**Mean**	**SD**	**Mean**	**SD**
		Control vs T2D			
CircCAMSAP1	***0.029***	***-0.04***	***0.32***	***-0.10***	***0.32***
CircCIRBP	0.260	-0.03	0.64	-0.11	0.53
CircZKSCAN1	0.054	0.03	0.39	0.05	0.37
		Control vs IGT			
CircCAMSAP1	0.606	-0.04	0.32	-0.05	0.29
CircCIRBP	0.913	-0.03	0.64	-0.12	0.68
CircZKSCAN1	0.987	0.03	0.39	0.06	0.34
		IGT vs T2D			
CircCAMSAP1	0.495	-0.05	0.29	-0.10	0.32
CircCIRBP	0.281	-0.12	0.68	-0.11	0.53
CircZKSCAN1	0.089	0.06	0.34	0.05	0.37

5.4 Discussion

Because of their stability and sustained expression in easily accessible body fluids (Enuka et al., 2016), circRNAs have the potential to serve as biomarker for diagnostic and therapeutic procedures. They may also contribute to the alternative isoforms profile during the progression of disease. An exonic circRNA *circ-UBR5* has been suggested to be a potential regulator of RNA splicing. It is thought that circ-UBR5 may bind to the KH domain containing RNA binding of splicing regulatory factor QKI and NOVA alternative splicing regulator 1 (NOVA1) and U1 small nuclear RNA (snRNA) in the nucleus (Qin, Wei, and Sun, 2018). Thus, their differential expression may imply the dysregulation of key genes through alternative splicing in diseases as well. This chapter addresses the query if circRNAs, whose expression in the islets are associated diabetic status, show a similar pattern of dysregulation in the peripheral blood of pre-diabetic and diabetic patients. Of the 4 most abundant circRNAs that were differentially expressed in the islets, 3 circRNAs were expressed in blood. One circRNA was associated with diabetic status in the current study. While there is nominal difference in expression of circRNA between control and T2D, this needs to be studied in a longitudinal satudy with a bigger sample size to ensure if the circRNA could be used to predict diabetic status. This will allows us to counteract for the confounding effect of lifestyle changes made at the pre-diabetic stage or in general including bacis physical acivity, eating habits and depending on the cohort on the ethnicity which might affect the risk alleles.

One study which reported a circRNA as a predictor of pre-diabetes (Zhao et al., 2017). The circRNA was selected from the pre-annotated circRNAs in a microarray platform from peripheral blood from six healthy individuals and six T2D which were followed up

in a very smaller cohort of 20 normal cases, 20 pre-diabetes patients and 20 T2DM patients and then followed up finally in a small cohort of 60 control, 63 pre-diabetes, and 64 T2DM participants. In contrast, in this thesis, circRNAs were chosen based most differentially expression in islet using RNA-Seq enrichment method for circRNA and more islets and finally followed up in the peripheral blood of a reasonably larger cohort.

Various stimulants mimicking the diabetic milieu is associated with dysregulation of circRNA expression. For instance, one study showed high glucose exposure leads to differential expression of 95 circRNAs in human endothelial cells (Shang et al., 2018). High glucose-induced human umbilical vein endothelial cells (HUVECs) also have 214 differentially expressed *circRNAs including hsa_circ_0008360, hsa_circ_0005741, hsa_circ_0003250, hsa_circ_0045462, hsa_circ_0064772, hsa_circ_0007976*, and *hsa_circ_0005263* (Jin et al., 2019). Other studies show high glucose induced RSC96 cell have circRNA *ACR* sequestering miR-145-3p and activating PI3K/AKT/mTOR that lead to cell apoptosis and autophagy (Liu et al., 2019). Other findings show high glucose stimulates glomerular endothelial cells (GECs) to secrete exosomes enriched in circRNAs compared with normal glucose GECs. *CircRNF169* and *circSTRN3* in the exosomes enhances α-smooth muscle actin (α-SMA) expression and inhibits proliferation leading to epithelial-mesenchymal transition in glomerular mesangial cells implying the role of intercellular transfer of circRNAs in diabetic nephropathy (Ling et al., 2019). In addition, high-glucose exposed cardiomyocytes have enhanced expression of circRNA *CACR* like that of the serum of diabetic patients. It modulates miR-214-3p regulated expression of caspase-1 silencing pyroptosis i.e. the programmed death which is markedly upregulated in cardiomyocytes and aggravates

inflammation leading to cardiac hypertrophy and fibrosis in diabetic cardiomyopathy (Yang et al., 2019). *CircRNA_15698* modulates expression of miR-185/TGF-β1 and promotes extracellular matrix related protein synthesis in mesangial cells in diabetic nephropathy mice. It is upregulated in high glucose induced mouse mesangial cells and diabetic mice (Hu et al., 2019, 1). *CircACTR2* is also upregulated in high glucose-induced cells and regulate cell death and inflammation as its knockdown causes decreased pyroptosis, interleukin (IL)-1β release and collagen IV and fibronectin production (Wen et al., 2020).

Apart from hyperglycaemia exposure, *β*-cells isolated from rat islets of high fat and high sugar diet induced T2D in rat model have 825 differentially expressed circRNA of which 388 are upregulated and 437 downregulated. Pathways analysis indicate these circRNAs, including *rno_circRNA_008565*, may regulate of *β*-cell autophagy (Bai et al., 2019). One circRNA, *circHIPK3*, has been shown to contribute to hyperglycaemia and insulin resistance in a miR-192-5p-dependent manner. Fatty acid oleate stimulation leads to upregulation of *circHIPK3* which enhances the stimulatory effect of oleate on adipose deposition as well as increases triglyceride and cellular glucose content in HepG2 cells. *CircHIPK3* asserts its effect by decreasing miR-192-5p and thereby increasing transcription factor forkhead box O1 (FOXO1) which is a downstream regulator of miR-192-5p. These cells have increased levels of forskolin/dexamethasone (FSK/DEX) , phosphoenolpyruvate carboxykinase (PEPCK) and glucose 6-phosphatase (G6Pase) which is inhibited by miR-192-5p.(Cai et al., 2019).

Other studies indicate differential expression of several circRNAs in diabetes-related complications. For example, *hsa_circRNA_103410* upregulated in diabetic retinopathy patients and is thought to promote endothelial injury in the retina, while *hsa_circRNA_100192*, could, by sequestering miR-146, promote NF-κB activation, adenosine deaminase-2 expression and inflammatory cytokines (Gu et al., 2017). Another circRNA, c*ircHIPK3* is thought to lead to miR-30a-3p dependent elevation in expression levels of *VEGFC*, *FZD4*, and *WNT2* in diabetic retinas (Shan et al., 2017). Downregulation of *circDNMT3B* associated with vascular dysfunction in retinas of diabetic patients and *in vitro* models in a miR-20b-5p and BMBI dependent manner (Zhu et al., 2019). Other reports indicate more than 1000 circRNAs are differentially expressed in diabetic cataract tissues. (Fan et al., 2019) . 183 circRNAs are upregulated while 64 downregulated in the T2D depressed patients compared those who are T2D without depression (Jiang et al., 2017). Another study shows *hsa_circ_0084443*, in the cytoplasm of human epidermal keratinocytes, is upregulated in diabetic foot ulcer. It reduces motility while enhancing the growth of keratinocytes (Wang et al., 2020).

Other studies related to diabetic complication show *circRNA cPWWP2A* disrupts the crosstalk between vascular pericytes and endothelial cells and causes lethal vascular damage in diabetes as a result of disrupted microvascular stabilization and remodelling. Overexpression of circRNA and subsequent miR-579 inhibition leads to decreased expression of angiopoietin 1, occludin, and SIRT1 which alleviates diabetes -induced retinal vascular dysfunction (Liu et al., 2019) . *Circ_0005015* is also upregulated in the plasma and fibrovascular membranes of diabetic retinas and inhibit miR-519d-3p activity, leading to increased MMP-2, XIAP,

and STAT3 expression in patients. *Circ_0005015* is thus thought to facilitate retinal endothelial angiogenic function via regulating endothelial cell proliferation, migration, and tube formation (Zhang et al., 2017).

As many as 227 circRNAs are up-regulated and 255 circRNAs are down-regulated in diabetic pregnancy (Yan et al., 2018). Hsa_cirRNA_0054633 expression, amongst others, associate with gestational HBA1c levels in maternal blood , placental tissue and umbilical cord blood samples during various stages of gestational diabetes (Wu et al., 2019). Other circRNAs like *circ_5824, circ_3636, and circ_0395* are downregulated in gestation diabetics (Wang et al., 2019).

Recent findings imply as many as 497 circRNAs are conserved in mouse and human islets. Of these at least, *circHIPK3* and *ciRS-7/CDR1as* are downregulated in the islets of diabetic diabetic mouse islets, impair insulin secretion, reduce β-cell proliferation, and survival. *CircHIPK3* sequesters miR-124-3p and miR-338-3p resulting in modulation of expression of key β-cell genes like as Slc2a2, Akt1, and Mtpn (Stoll et al., 2018) . *CircHIPK3* is downregulated in HUVECS and primary aortic endothelial cells from diabetic patients. It modifies miR-124 expression and inhibits high glucose-induced cell death and apoptosis in HUVECs and prevents high glucose-induced vascular endothelial cell injury (Cao et al., 2018). C*ircHIPK3* blocks miR-30a and enhances proliferative retinopathy and vascular dysfunction in diabetes related retinal vascular dysfunction (Shan et al., 2017). It is also upregulated in serum from diabetics with neuropathic pain and is positively associated with the grade of neuropathic pain in patients. It is also upregulated in in dorsal root ganglion and contributes to pain and neuroinflammation in diabetic rats (Wang et al., 2018) . Another circRNA, *Cdr1as,* modulate expression of Myrip in a miR-7-depenent manner pathway to enhance

insulin, content and secretion in islet cells. It also modulates Pax6 expression to enhance insulin transcription (Xu et al., 2015). Additionally, electroacupuncture which is known to reduce islet β-cell apoptotic rate in T2DM mice also lead to 165 differential expression of circRNAs in plasma exosomes and thus may be involved in preserving islet function in T2DM mice (Shou et al., 2019) .

As many as 30 circRNAs are upregulated in the serum of diabetic retinopathy which includes *hsa_circRNA_063981, hsa_circRNA_ 404457, hsa_circRNA_100750, hsa_circRNA_406918, hsa_ circRNA_104387, hsa_circRNA_103410* and *hsa_circRNA_ 100192* (Gu et al., 2017). Recent study shows 489 circRNAs are differentially expressed in the peripheral blood of patients with T2D while another suggest almost differential expression of 900 circRNA in T2D. Of them circRNA *hsa_circ_0054633* seem to have a predictive potential for diagnosing pre-diabetes (Zhao et al., 2017c). Findings from this chapter indicate *CircCAMSAP1* have the potential to be used for diagnostics using relatively non-invasive procedures with peripheral blood. The observations from this chapter raise the exciting possibility that circRNAs expressed in accessible tissues may be useful markers of disease in inaccessible organs such as pancreas.

Microtubules are cellular polymers that are important for cargo transport and mitotic spindle formation in cells. Different CAMSAPs can bind to the end of microtubules and allow the addition of new tubulins at different rates. CAMSAPs are involved in multiple processes in the cell which include promoting cell polarity, regulation of neuronal differentiation and axonal regeneration as well as definition of spindle organization and asymmetry through the regulation of microtubule dynamics (Atherton

et al., 2019). While CAMSAP2 and CAMSAP3 remain tightly bound to the microtubules after tubulin incorporation, CAMSAP1 dissociate after allowing tubulin incorporation and microtubule elongation (Hendershott and Vale, 2014). CAMSAPs are active in multiple tissues, and also have roles in white blood cells, which rely on the tubulin-microtubule system for lymphocyte activation (Sherline and Mundy, 1977). We identified an association between the expression of circRNA generated from *CAMSAP1*, *circCAMSAP1*, and diabetes status in the peripheral blood of individuals with T2D, although this was the inverse of that seen in islets mentioned in the previous chapter.

In conclusion, we present here an evidence that circRNAs have tissue-specific pattern of expression. We also report that some circRNAs, that are dysregulated in disease-relevant tissue, are similarly dysregulated in easily accessible body fluid. However, this study is limited by samples size and power. It is possible that beside *circCAMSAP1*, *circZSCAN1* could also be used as diagnostics (p=0.054) which we did not detect. Despite that, *circCAMSAP1* seems to have potential to serve as biomarkers using relatively non-invasive procedures for predictive and therapeutic purposes. These circRNA may be further followed-up up in longitudinal studies accounting for pre and post phases of T2D diagnosis and by monitoring the effect of lifestyle changes in the pre-diabetes phase.

Chapter 6

Discussion

Ageing is a gradual decline of physical and physiological homeostasis at the cellular, tissue and organ levels over the course of an organism's life. It is the main risk factor for chronic diseases of ageing such as cancer, sarcopenia, diabetes, and cardiovascular and neurodegenerative illnesses (Goldman et al., 2013; Kirkland, 2016). Although, improvements in medical technologies and healthcare have resulted in an increase in lifespan, a vast proportion of long-lived people continue to suffer from multiple comorbidities and thus have reduced disability-adjusted life years (Kehler, 2019). The processes that decline with advancing age can cumulatively affect phenotypes that become evident in ageing and ageing-related chronic diseases such as T2D. NcRNAs have been shown to modulate gene expression and are dysregulated in ageing. Despite the fact that circRNAs accumulate in older organisms (Gruner et al., 2016) and have been implicated in cellular senescence (Du et al., 2017; Du et al., 2016), their role in ageing has been largely unexplored. In this thesis, I investigated the potential role of circRNAs in ageing and T2D, an ageing-related chronic outcome.

Chapter 3 CircRNAs expressed in human peripheral blood are associated with human ageing phenotypes, cellular senescence and mouse lifespan

The primary objective of this chapter was to determine whether circRNAs are dysregulated during normal ageing. I addressed this question by assessing the expression of the 15 most dysregulated circRNAs in a study of ageing and the pathways they might be involved in. Our NGS data from young and old donors from the ageing cohort showed that >2000 circRNAs are expressed in human blood. Some of these were expressed exclusively in samples from younger and older donors.

Pathway enrichment analysis of genes hosting the top 10% most abundant circRNAs in aged donors indicated their involvement in phagocytosis and cancer pathways.

I further investigated the 15 most dysregulated circRNAs and assessed their expression in the ageing human cohort to determine if they are associated with ageing and measures of ageing. I found that four circRNAs correlated with each measure of ageing. Of the four, *circFOXO3* and *circEP300* negatively associated with parental longevity score, while *CircDEF6* positively (although nominally) associated with parental longevity score. In our study*, circFNDC3B* also nominally associated with another measure of ageing, i.e. hand grip strength. In contrast to a circRNA from *FOXO3*, which has been reported before, this study reports *circEP300* for the first time. It is possible that *circEP300* may modulate the expression of its host gene or downstream *FOXO*, and thereby serves to modify lifespan in humans through a variety of modes of action by affecting the performance of the immune system, and playing a role in stem cell exhaustion and senescence.

Because ncRNAs have been reported to be involved in senescence, I determined whether any of the 15 circRNAs were differentially expressed in human peripheral blood or were dysregulated in other tissues relevant to ageing. To do this, I assessed their expression during senescence using *in vitro* cultures of senescent human primary astrocytes, endothelial cells, fibroblasts and cardiomyocytes. I found that while three circRNAs were not expressed, seven circRNAs demonstrated dysregulated expression in one or multiple cell types. Interestingly, most circRNAs were upregulated in astrocytes, somewhat reflecting previous findings that circRNAs accumulate in the ageing brains of mammals.

Since mice are good *in vivo* models for the study of ageing and ageing-related disorders, I investigated whether the expression of circRNAs that are differentially expressed in humans in mouse models would mirror the median lifespans observed, and therefore serve as a model to dissect the role of circRNAs *in vivo*. I found that four circRNAs were conserved in mice. C*ircPlekhm1* expression in spleen associated with median lifespan, but only in young mice. This suggests that *circPlekhm1* may be a driver of longevity instead of being a result of ageing. Since this circRNA was found in spleen, it is possible that it drives the ageing process though modulation of the immune responses of lymphocytes and phagocytes. It is possible that the differential expression observed in peripheral blood from the human cohorts reflects dysregulation in disease-relevant inaccessible tissues, since some of these were also differentially expressed in *in vitro* models.

Importance

In summary, the findings of this chapter make available one of the first comprehensive circRNA profiles for the peripheral blood of ageing humans. In addition, evidence of differential expression of circRNAs in the blood is presented, as is their predictive potential and dysregulation in various *in vitro* models of senescence, which itself is one of the hallmarks of ageing. I also demonstrate that mouse models can be used to explore the roles of some circRNAs in mammalian lifespan, and hence ageing outcomes. These circRNAs may have potential as diagnostic targets, or predictive biomarkers of ageing and ageing-related outcomes.

Future work

In this study we determined circRNA expression in some samples from the InChianti study of ageing. Future work would focus on characterising circRNA expression in even more samples comparable to other large epidemiological data sets. In the future, it may be useful to assess the association of circRNAs with ageing in a larger ageing population sample, perhaps with various ageing-related diseases. This may lead us to not only reaffirm the findings of this study, but also investigate whether any of these circRNAs could represent potential biomarkers of ageing-associated disorders. Whether the dysregulation of circRNAs is a consequence or a driver of ageing, or ageing-related outcomes, could be validated though manipulation of *in vitro* and *in vivo* models. CircRNAs may enforce multilayered control of gene expression, including transcriptional, post-transcriptional and translational events. It would also be interesting to investigate how circRNA profiles correlate with the expression of their host gene isoforms, RBPs or miRNAs, since these are thought to be avenues through which circRNAs exercise their *cis*/*trans*-regulatory effects on gene expression. In the human cohort, it would be interesting to know if the host isoforms expressed predominantly exclude exons within in the circRNAs or have an inverse relationship with linear isoforms containing the same exons.

In this study, differential expression of circRNA with median lifespan was asseses in mouse of 6 different strains in a diversity of tissue samples tested, i.e. spleen and muscle. It would be interesting if we could unravel whether tissue-specific dysregulation of circRNAs is relevant to other ageing outcomes for tissues such as brain, heart or kidney in the current work. It is also noteworthy that while we assessed differential expression in human peripheral blood. It would be interesteting to

determine the same in blood samples for the mouse models when samples are available. It is also possible that we did not detect effects caused by the genetic backgrounds of each strain, as we did not assess background levels of expression of these entities in young animals or compare them with older animals for each strain.

Chapter 4 Islet-expressed circular RNAs are associated with type 2 diabetes status in human primary islets

The findings from the first chapter show that circRNAs are differentially expressed in an ageing cohort, senescent cells and in mouse models with varying median lifespans. Therefore, I wanted to determine whether circRNA expression would be similarly dysregulated in a chronic disease of ageing. As an exemplary chronic disease of ageing, I investigated the expression patterns of circRNAs in T2D and their potential role in the pathology of T2D. In order to address my queries, I generated a tissue panel to assess how circRNAs align with the expression of their host genes in a wide variety of tissues. Then, I assessed the differential expression of circRNAs in diabetic and non-diabetic islets, and determined whether their expression correlated with measures of glycaemia. Finally, I determined if these circRNAs were differentially expressed in human β-cells exposed to various diabetomimetic stresses to explore their potential modes of action in the diabetic pancreas.

Through this work, we present one of the first comprehensive circRNA profiles from human pancreatic islets. Of these circRNAs, 47 are exclusively expressed in the islets. Data from the tissue expression profile indicate that these circRNAs have a tissue-specific pattern of expression and may be regulated independently of their host genes.

The expression patterns of many circRNAs in this study were often higher in brain tissues compared to other tissues. This somewhat reflects existing knowledge that circRNAs accumulate in the brain.

Of the five most abundant circRNAs in human islets, four demonstrated significant correlation with diabetic status. Three of their host genes also demonstrated association with diabetic status, although the other one did not. As such, some of these associations were irrespective of a relationship of the host gene with diabetic status. Of the three, the expression of *circCAMPSAP1* in peripheral blood also associated with diabetic status in a human cohort. Another circRNA, c*ircCIRBP*, correlated with the insulin secretory index in human islets. This circRNA, along with *circRPH3AL*, displayed altered expression with elevated fatty acids in treated β-cells. It is possible that these differentially regulated circRNAs operate by regulating genes involved in insulin function and β-cell survival.

Importance

Through this research, we report one of the most comprehensive global circRNA profiles of human islets. Two other studies have previously reported circRNA profiles of islets (Izuogu et al., 2016 , Kaur et al., 2018). However, unlike in this study, they either did not include pre-treatment to exclude linear RNAs or only included previously annotated circRNAs in their profiles. Thus, the islet circRNA profile generated as part of the current study is the first global circRNA profile of human islets. I also report that the expression of many of these circRNAs is associated with different aspects of glucose homeostasis in human islets. Thus, they could be key regulators of

transcription through various mechanisms and may affect the performance of endocrine function in human islets.

Future work

In this study, I present evidence that while some circRNAs are dysregulated alongside their host genes in islets or β-cells, others are dysregulated irrespective of the host genes. In the future, these circRNAs could be taken forward to investigate whether they have modulate transcription by affecting the transcriptional or post-trancriptional events of their host genes or other genes. This may also help us understand whether they are responsible for driving, or are after-effects of, diabetic pathology.

Chapter 5 Islet-expressed circular RNAs are associated with type 2 diabetes status in peripheral blood

Having found that circRNAs are dysregulated in diabetic islets and under diabetomimetic stress in human β-cells, I investigated whether any of these circRNAs were differentially expressed in the peripheral blood of humans with pre-diabetes or T2D. *CircCAMSAP1* was differentially expressed in peripheral blood samples from the diabetic cohort. However, the effect was in the opposite direction to that seen in human islets. It is possible that this circRNA is engaged in two distinct modes of function in a tissue-specific manner, i.e. immune function and different aspects of insulin secretion in islets of diabetic patients.

Importance

Most pre-diabetic individuals eventually develop diabetes, and diabetic complications can develop at the pre-diabetic stage almost a decade before actual T2D diagnosis. It is important that we find novel biomarkers that can identify people who are at risk via a minimally invasive approach (Bansal, 2015; Tabak et al., 2012). We know that circRNAs are almost 2.5 times more stable than linear RNAs because of their closed covalent structures. In addition, they are exonuclease-resistant (Cocquerelle et al., 1993; Schwanhausser et al., 2011; Jeck et al., 2013; Lan et al., 2016; Lasda and Parker, 2016b). The fact that I have shown that *circCAMSAP1* is dysregulated in the islets as well as in the blood suggests that it may have potential as a diagnostic biomarker for diabetic patients via routine screening. A longitudinal study with a larger sample size could done to ensure its potentiality as a biomarker for diabetes.

Future work

In order to ensure that our findings could be applied to all ethnic groups, future work would focus on increasing the sample size. The sample cohort in this study was predominately one ethnic group. Therefore, the findings after adding more ethnic groups, perhaps, could be use to extrapolate to diabetics in all ethnic groups. In the future, we could conduct a follow-up study on a larger-sized population with diverse ethnicity to determine whether this circRNA is unanimously dysregulated in the peripheral blood of T2D patients.

Discussion of the thesis

Age-linked differential transcriptional noise has been reported by many groups as well as our own. Dysregulation of gene expression in cellular ageing can affect different aspects of cellular function such as the modulation of expression of genes engaged with mitochondrial proteins, protein synthesis machinery, the immune system, growth factor signalling and stress, as well as the DDR and mRNA processing. Regulation of gene expression by ncRNAs has already been established. CircRNAs have the potential to operate in multiple ways in modulating the expression of genes. These include serving as sponges for miRNAs and RBPs, and acting as transcriptional regulators. Hence, the circRNAs reported in this thesis may have regulatory roles in driving outcomes of ageing. They could also be used as potential predictive and diagnostic, or therapeutic, biomarkers for ageing and ageing-related outcomes.

Because circRNAs are closed structures, they are comparatively resistant to degradation. This makes them have longer half-lives than linear genes. They also demonstrate differential expression in a tissue specific manner and vary in time and state of cells. This makes them a good for prognostic tool of predicting the stages of diseases and a potential new diagnostic biomarker for predicting disease. For instance, *circFNDC3* seems not only be associated with handgrip cross-sectionally but also have predictive potential longitudinally. In other cases, circRNAs, which are differentially regulated in islets as well as peripheral blood like *circCAMSAP1*, can be used a therapeutic tool after validation in a longitudinal study with larger sample size as this would account for the personal changes in lifestyle changes, diet and other individual confounders.

Current publications on circRNA are predominantly on their use as biomarkers in different diseases. Not much is known about their mode of action in the cellular level. However, few circRNAs have the ability to sequester multiple miRNAs. Thus, one circRNA in some instances may be able to modulate multiple genes and pathways. Similar to miRNAs, they could also be sponging multiple RNA binding proteins and affect the expression of their own host genes or other genes. It is possible that by targeting one circRNA as a therapeutic machinery, we may be able to successfully optimize several pathways relevant to a disease.

The current study provides an insight into the potential role of non-coding circRNAs in ageing and in age-related diseases such as type 2 diabetes and provides the first comprehensive catalogue of circRNAs expressed in peripheral blood of ageing humans and human islets. RNA regulation is not only a good potential target for biomarkers, but also a potential area that could be used for targeted therapeutic intervention in the future for a healthier longer life span that could bring down the economic burden for treating the elderly population. Identification of circRNAs as biomarkers from easily accessible bodily fluid like blood would minimize the need for invasive procedures in ageing population and in individuals otherwise, not only making it more comfortable to patients but also reducing the cost of invasive diagnostic procedures for the healthcare.

Future work

In this study, I assessed the circRNA expression profile at one follow-up point of the InChianti study of ageing. It would be useful to confirm the pattern of the circRNA

profile at successive follow-up points from the same participants where RNA is available. Whether the dysregulation of circRNAs is a consequence or a driver of ageing, or ageing outcomes, could be validated through the manipulation of *in vitro* and *in vivo* models. The circRNAs may facilitate multilayered control of gene expression including transcriptional, post-transcriptional and translational events. It would also be interesting to investigate how the circRNA profile correlates with expression of the relevant host gene isoforms, RBPs or miRNAs, since these are thought to be avenues through which circRNAs exercise their *cis*/*trans*-regulatory effects on gene expression. In the human cohort, it would be interesting to know if the host isoforms expressed predominantly exclude exons within in the circRNAs or have an inverse relationship with linear isoforms containing the same exons.

Conclusion

This thesis provides insights into potential roles of circRNAs in normal ageing as well as ageing-associated chronic comorbidities in humans, cellular models and rodent models. It also presents two of the most comprehensive global circRNA profiles generated to date from different tissues from human donors. I have assessed the differential expression of circRNAs in the peripheral blood of a relatively healthy ageing cohort and shown their potential as predictors of measures of ageing. These differentially expressed circRNAs may be predictive biomarkers for the prediction of progression to future ageing outcomes through minimally invasive procedures that are common during routine clinical visits.

References

Abbasi, Ali, Linda M. Peelen, Eva Corpeleijn, Yvonne T. van der Schouw, Ronald P. Stolk, Annemieke M. W. Spijkerman, Daphne L. van der A, et al., 2012. "Prediction Models for Risk of Developing Type 2 Diabetes: Systematic Literature Search and Independent External Validation Study." *BMJ (Clinical Research Ed.)* 345 (September): e5900. https://doi.org/10.1136/bmj.e5900.

Abbasi, Ali, Anna-Stina Sahlqvist, Luca Lotta, Julia M. Brosnan, Peter Vollenweider, Philippe Giabbanelli, Derek J. Nunez, et al., 2016. "A Systematic Review of Biomarkers and Risk of Incident Type 2 Diabetes: An Overview of Epidemiological, Prediction and Aetiological Research Literature." *PloS One* 11 (10): e0163721. https://doi.org/10.1371/journal.pone.0163721.

Acosta, Juan Carlos, Ana Banito, Torsten Wuestefeld, Athena Georgilis, Peggy Janich, Jennifer P. Morton, Dimitris Athineos, et al., 2013. "A Complex Secretory Program Orchestrated by the Inflammasome Controls Paracrine Senescence." *Nature Cell Biology* 15 (8): 978–90. https://doi.org/10.1038/ncb2784.

"Advanced Genome Bioinformatics." n.d. Accessed April 14, 2020. http://comprna.upf.edu/courses/Master_AGB/Exercise_HMM_U12_BP/index.html.

Almog, Nava, Naomi Goldfinger, and Varda Rotter. 2000. "P53-Dependent Apoptosis Is Regulated by a C-Terminally Alternatively Spliced Form of Murine P53." *Oncogene* 19 (30): 3395–3403. https://doi.org/10.1038/sj.onc.1203673.

Alzheimer's Association. 2015. "2015 Alzheimer's Disease Facts and Figures." *Alzheimer's & Dementia: The Journal of the Alzheimer's Association* 11 (3): 332–84. https://doi.org/10.1016/j.jalz.2015.02.003.

Andrew, Toby, Abraham Aviv, Mario Falchi, Gabriela L. Surdulescu, Jeffrey P. Gardner, Xiaobin Lu, Masayuki Kimura, Bernet S. Kato, Ana M. Valdes, and Tim D. Spector. 2006. “Mapping Genetic Loci That Determine Leukocyte Telomere Length in a Large Sample of Unselected Female Sibling Pairs.” *American Journal of Human Genetics* 78 (3): 480–86. https://doi.org/10.1086/500052.

Anisimov, Vladimir N., Lev M. Berstein, Peter A. Egormin, Tatiana S. Piskunova, Irina G. Popovich, Mark A. Zabezhinski, Irina G. Kovalenko, et al., 2005. “Effect of Metformin on Life Span and on the Development of Spontaneous Mammary Tumors in HER-2/Neu Transgenic Mice.” *Experimental Gerontology* 40 (8): 685–93. https://doi.org/10.1016/j.exger.2005.07.007.

Ar, Brooks-Wilson. 2013. “Genetics of Healthy Aging and Longevity.” *Human Genetics* 132 (12): 1323–38. https://doi.org/10.1007/s00439-013-1342-z.

Aronson, Jeffrey, and Robin Ferner. 2017. “Biomarkers-A General Review.” In *Current Protocols in Pharmacology*, 2017:9.23.1-9.23.17. https://doi.org/10.1002/cpph.19.

Atherton Joseph, Luo Yanzhang, Xiang Shengqi, Yang Chao, Rai Ankit, Jiang Kai, Stangier Marcel, Vemu Annapurna, Cook Alexander D., Wang Su, Roll-Mecak Antonina, Steinmetz Michel O., Akhmanova Anna, Baldus Marc and Moores Carolyn A. 2019. “Structural Determinants of Microtubule Minus End Preference in CAMSAP CKK Domains | Nature Communications.” n.d. Accessed March 20, 2020. https://www.nature.com/articles/s41467-019-13247-6.

Atzmon, Gil, Marielisa Rincon, Clyde B. Schechter, Alan R. Shuldiner, Richard B. Lipton, Aviv Bergman, and Nir Barzilai. 2006. “Lipoprotein Genotype and

Conserved Pathway for Exceptional Longevity in Humans." *PLoS Biology* 4 (4): e113. https://doi.org/10.1371/journal.pbio.0040113.

Aubert, Geraldine, and Peter M. Lansdorp. 2008. "Telomeres and Aging." *Physiological Reviews* 88 (2): 557–79. https://doi.org/10.1152/physrev.00026.2007.

Avrahami, Dana, Changhong Li, Jia Zhang, Jonathan Schug, Ran Avrahami, Shilpa Rao, Michael B. Stadler, et al., 2015. "Aging-Dependent Demethylation of Regulatory Elements Correlates with Chromatin State and Improved β Cell Function." *Cell Metabolism* 22 (4): 619–32. https://doi.org/10.1016/j.cmet.2015.07.025.

Bachmayr-Heyda, Anna, Agnes T. Reiner, Katharina Auer, Nyamdelger Sukhbaatar, Stefanie Aust, Thomas Bachleitner-Hofmann, Ildiko Mesteri, Thomas W. Grunt, Robert Zeillinger, and Dietmar Pils. 2015. "Correlation of Circular RNA Abundance with Proliferation – Exemplified with Colorectal and Ovarian Cancer, Idiopathic Lung Fibrosis, and Normal Human Tissues." *Scientific Reports* 5 (January). https://doi.org/10.1038/srep08057.

Bai, Chao, Wenwen Yang, Yao Lu, Wei Wei, Zongbao Li, and Li Zhang. 2019. "Identification of Circular RNAs Regulating Islet β-Cell Autophagy in Type 2 Diabetes Mellitus." *BioMed Research International* 2019: 4128315. https://doi.org/10.1155/2019/4128315.

Baker, Darren J., Bennett G. Childs, Matej Durik, Melinde E. Wijers, Cynthia J. Sieben, Jian Zhong, Rachel A. Saltness, et al., 2016. "Naturally Occurring P16 Ink4a - Positive Cells Shorten Healthy Lifespan." *Nature* 530 (7589): 184–89. https://doi.org/10.1038/nature16932.

Baker, Darren J., Tobias Wijshake, Tamar Tchkonia, Nathan K. LeBrasseur, Bennett G. Childs, Bart van de Sluis, James L. Kirkland, and Jan M. van Deursen. 2011. “Clearance of P16Ink4a-Positive Senescent Cells Delays Ageing-Associated Disorders.” *Nature* 479 (7372): 232–36. https://doi.org/10.1038/nature10600.

Bareja, Akshay, David E. Lee, and James P. White. 2019. “Maximizing Longevity and Healthspan: Multiple Approaches All Converging on Autophagy.” *Frontiers in Cell and Developmental Biology* 7. https://doi.org/10.3389/fcell.2019.00183.

Barnes, Tammy M., Yolanda F. Otero, Amicia D. Elliott, Alicia D. Locke, Carlo M. Malabanan, Anastasia G. Coldren, Marcela Brissova, David W. Piston, and Owen P. McGuinness. 2014. “Interleukin-6 Amplifies Glucagon Secretion: Coordinated Control via the Brain and Pancreas.” *American Journal of Physiology - Endocrinology and Metabolism* 307 (10): E896–905. https://doi.org/10.1152/ajpendo.00343.2014.

Barrett, Steven P., and Julia Salzman. 2016. “Circular RNAs: Analysis, Expression and Potential Functions.” *Development* 143 (11): 1838–47. https://doi.org/10.1242/dev.128074.

Barzilai, Nir, Derek M. Huffman, Radhika H. Muzumdar, and Andrzej Bartke. 2012. “The Critical Role of Metabolic Pathways in Aging.” *Diabetes* 61 (6): 1315–22. https://doi.org/10.2337/db11-1300.

Baumgart, Mario, Steffen Priebe, Marco Groth, Nils Hartmann, Uwe Menzel, Luca Pandolfini, Philipp Koch, et al., 2016. “Longitudinal RNA-Seq Analysis of Vertebrate Aging Identifies Mitochondrial Complex I as a Small-Molecule-Sensitive Modifier of Lifespan.” *Cell Systems* 2 (2): 122–32. https://doi.org/10.1016/j.cels.2016.01.014.

Baur, Joseph A., Kevin J. Pearson, Nathan L. Price, Hamish A. Jamieson, Carles Lerin, Avash Kalra, Vinayakumar V. Prabhu, et al., 2006. “Resveratrol Improves Health and Survival of Mice on a High-Calorie Diet.” *Nature* 444 (7117): 337. https://doi.org/10.1038/nature05354.

Bays, Harold, Lawrence Mandarino, and Ralph A. DeFronzo. 2004. “Role of the Adipocyte, Free Fatty Acids, and Ectopic Fat in Pathogenesis of Type 2 Diabetes Mellitus: Peroxisomal Proliferator-Activated Receptor Agonists Provide a Rational Therapeutic Approach.” *The Journal of Clinical Endocrinology and Metabolism* 89 (2): 463–78. https://doi.org/10.1210/jc.2003-030723.

Beckman, K. B., and B. N. Ames. 1998. “The Free Radical Theory of Aging Matures.” *Physiological Reviews* 78 (2): 547–81. https://doi.org/10.1152/physrev.1998.78.2.547.

Beerman, Isabel, Deepta Bhattacharya, Sasan Zandi, Mikael Sigvardsson, Irving L. Weissman, David Bryder, and Derrick J. Rossi. 2010. “Functionally Distinct Hematopoietic Stem Cells Modulate Hematopoietic Lineage Potential during Aging by a Mechanism of Clonal Expansion.” *Proceedings of the National Academy of Sciences of the United States of America* 107 (12): 5465–70. https://doi.org/10.1073/pnas.1000834107.

Beroukhim, Rameen, Craig H. Mermel, Dale Porter, Guo Wei, Soumya Raychaudhuri, Jerry Donovan, Jordi Barretina, et al., 2010. “The Landscape of Somatic Copy-Number Alteration across Human Cancers.” *Nature* 463 (7283): 899–905. https://doi.org/10.1038/nature08822.

Biagi, Elena, Claudio Franceschi, Simone Rampelli, Marco Severgnini, Rita Ostan, Silvia Turroni, Clarissa Consolandi, et al., 2016. “Gut Microbiota and Extreme

Longevity.” *Current Biology: CB* 26 (11): 1480–85. https://doi.org/10.1016/j.cub.2016.04.016.

Biagi, Elena, Lotta Nylund, Marco Candela, Rita Ostan, Laura Bucci, Elisa Pini, Janne Nikkïla, et al., 2010. “Through Ageing, and Beyond: Gut Microbiota and Inflammatory Status in Seniors and Centenarians.” *PLoS ONE* 5 (5). https://doi.org/10.1371/journal.pone.0010667.

Bindea, Gabriela, Bernhard Mlecnik, Hubert Hackl, Pornpimol Charoentong, Marie Tosolini, Amos Kirilovsky, Wolf-Herman Fridman, Franck Pagès, Zlatko Trajanoski, and Jérôme Galon. 2009. “ClueGO: A Cytoscape Plug-in to Decipher Functionally Grouped Gene Ontology and Pathway Annotation Networks.” *Bioinformatics (Oxford, England)* 25 (8): 1091–93. https://doi.org/10.1093/bioinformatics/btp101.

Biomarkers Definitions Working Group. 2001. “Biomarkers and Surrogate Endpoints: Preferred Definitions and Conceptual Framework.” *Clinical Pharmacology and Therapeutics* 69 (3): 89–95. https://doi.org/10.1067/mcp.2001.113989.

Blackburn, Elizabeth H., Carol W. Greider, and Jack W. Szostak. 2006. “Telomeres and Telomerase: The Path from Maize, Tetrahymena and Yeast to Human Cancer and Aging.” *Nature Medicine* 12 (10): 1133–38. https://doi.org/10.1038/nm1006-1133.

Bloch, Konstantin, Julia Vennäng, Daniel Lazard, and Pnina Vardi. 2012. “Different Susceptibility of Rat Pancreatic Alpha and Beta Cells to Hypoxia.” *Histochemistry and Cell Biology* 137 (6): 801–10. https://doi.org/10.1007/s00418-012-0925-4.

Blüher, Matthias, Barbara B. Kahn, and C. Ronald Kahn. 2003. “Extended Longevity in Mice Lacking the Insulin Receptor in Adipose Tissue.” *Science (New York, N.Y.)* 299 (5606): 572–74. https://doi.org/10.1126/science.1078223.

Böni-Schnetzler Marianne, Boller Simone, Debray Sarah, Bouzakri Karim, Meier Daniel T, Prazak Richard, Kerr-Conte Julie, Pattou Francois, Ehses Jan A, Schuit Frans C and Donath Marc Y . 2009. “Free Fatty Acids Induce a Proinflammatory Response in Islets via the Abundantly Expressed Interleukin-1 Receptor I | Endocrinology | Oxford Academic.” n.d. Accessed April 13, 2020. https://academic.oup.com/endo/article/150/12/5218/2455772.

Borbolis, Fivos, and Popi Syntichaki. 2015. “Cytoplasmic MRNA Turnover and Ageing.” *Mechanisms of Ageing and Development* 152 (December): 32–42. https://doi.org/10.1016/j.mad.2015.09.006.

Bose, Rumela, and Rupasri Ain. 2018. “Regulation of Transcription by Circular RNAs.” *Advances in Experimental Medicine and Biology* 1087: 81–94. https://doi.org/10.1007/978-981-13-1426-1_7.

Brady, Colleen A., Dadi Jiang, Stephano S. Mello, Thomas M. Johnson, Lesley A. Jarvis, Margaret M. Kozak, Daniela Kenzelmann Broz, et al., 2011. “Distinct P53 Transcriptional Programs Dictate Acute DNA-Damage Responses and Tumor Suppression.” *Cell* 145 (4): 571–83. https://doi.org/10.1016/j.cell.2011.03.035.

Brandt, Tobias, Arnaud Mourier, Luke S Tain, Linda Partridge, Nils-Göran Larsson, and Werner Kühlbrandt. n.d. “Changes of Mitochondrial Ultrastructure and Function during Ageing in Mice and Drosophila.” *ELife* 6. Accessed December 16, 2019. https://doi.org/10.7554/eLife.24662.

Brunner, Eric J., Mika Kivimäki, Daniel R. Witte, Debbie A. Lawlor, George Davey Smith, Jackie A. Cooper, Michelle Miller, et al., 2008. “Inflammation, Insulin Resistance, and Diabetes--Mendelian Randomization Using CRP Haplotypes Points Upstream.” *PLoS Medicine* 5 (8): e155. https://doi.org/10.1371/journal.pmed.0050155.

Buchan, J. Ross, Regina-Maria Kolaitis, J. Paul Taylor, and Roy Parker. 2013. “Eukaryotic Stress Granules Are Cleared by Autophagy and Cdc48/VCP Function.” *Cell* 153 (7): 1461–74. https://doi.org/10.1016/j.cell.2013.05.037.

Buijsse, Brian, Heiner Boeing, Frank Hirche, Cornelia Weikert, Matthias B. Schulze, Marion Gottschald, Tilman Kühn, et al., 2013. “Plasma 25-Hydroxyvitamin D and Its Genetic Determinants in Relation to Incident Type 2 Diabetes: A Prospective Case-Cohort Study.” *European Journal of Epidemiology* 28 (9): 743–52. https://doi.org/10.1007/s10654-013-9844-5.

Cai, Huiyao, Zhengrong Jiang, Xinna Yang, Jiayu Lin, Qingyan Cai, and Xisheng Li. 2019. “Circular RNA HIPK3 Contributes to Hyperglycemia and Insulin Homeostasis by Sponging MiR-192-5p and Upregulating Transcription Factor Forkhead Box O1.” *Endocrine Journal*, December. https://doi.org/10.1507/endocrj.EJ19-0271.

Campisi, Judith, and Fabrizio d’Adda di Fagagna. 2007. “Cellular Senescence: When Bad Things Happen to Good Cells.” *Nature Reviews. Molecular Cell Biology* 8 (9): 729–40. https://doi.org/10.1038/nrm2233.

Cao, Ying, Guohai Yuan, Ye Zhang, and Rong Lu. 2018. “High Glucose-Induced CircHIPK3 Downregulation Mediates Endothelial Cell Injury.” *Biochemical and Biophysical Research Communications* 507 (1–4): 362–68. https://doi.org/10.1016/j.bbrc.2018.11.041.

"Cardiometabolic Effects of Genetic Upregulation of the Interleukin 1 Receptor Antagonist: A Mendelian Randomisation Analysis - PubMed." n.d. Accessed April 13, 2020. https://pubmed.ncbi.nlm.nih.gov/25726324/.

Carlsson, C., L. A. Borg, and N. Welsh. 1999. "Sodium Palmitate Induces Partial Mitochondrial Uncoupling and Reactive Oxygen Species in Rat Pancreatic Islets in Vitro." *Endocrinology* 140 (8): 3422–28. https://doi.org/10.1210/endo.140.8.6908.

Cersosimo, Eugenio, Curtis Triplitt, Carolina Solis-Herrera, Lawrence J. Mandarino, and Ralph A. DeFronzo. 2000. "Pathogenesis of Type 2 Diabetes Mellitus." In *Endotext*, edited by Kenneth R. Feingold, Bradley Anawalt, Alison Boyce, George Chrousos, Kathleen Dungan, Ashley Grossman, Jerome M. Hershman, et al., South Dartmouth (MA): MDText.com, Inc. http://www.ncbi.nlm.nih.gov/books/NBK279115/.

Chan, Leon Y, Christopher F Mugler, Stephanie Heinrich, Pascal Vallotton, and Karsten Weis. 2018. "Non-Invasive Measurement of MRNA Decay Reveals Translation Initiation as the Major Determinant of MRNA Stability." Edited by Alan G Hinnebusch, James L Manley, and Roy Parker. *ELife* 7 (September): e32536. https://doi.org/10.7554/eLife.32536.

Chandler-Laney, P. C., R. Phadke, W. M. Granger, J. R. Fernández, A. J. Muñoz, C. Dalla Man, C. Cobelli, F. Ovalle, and B. A. Gower. 2011. "Age-Related Changes in Insulin Sensitivity and β-Cell Function among European American and African American Women." *Obesity (Silver Spring, Md.)* 19 (3): 528–35. https://doi.org/10.1038/oby.2010.212.

Chen, I.; Chen, C.Y.; Chuang, T.J. 2015. Biogenesis, identification, and function of exonic circular RNAs. *Wiley Interdiscip. Rev. RNA 6*, 563–579.

Cheng, Jun, Kerstin C. Maier, Ziga Avsec, Petra Rus, and Julien Gagneur. 2016. “Cis-Regulatory Elements Explain Most of the MRNA Stability Variation across Genes in Yeast.” Preprint. Genomics. https://doi.org/10.1101/085522.

Childs, Bennett G, Matej Durik, Darren J Baker, and Jan M van Deursen. 2015. “Cellular Senescence in Aging and Age-Related Disease: From Mechanisms to Therapy.” *Nature Medicine* 21 (12): 1424–35. https://doi.org/10.1038/nm.4000.

Ciryam, Prajwal, Gian Gaetano Tartaglia, Richard I. Morimoto, Christopher M. Dobson, and Michele Vendruscolo. 2013. “Neurodegenerative Diseases and Widespread Aggregation Are Associated with Supersaturated Proteins.” *Cell Reports* 5 (3). https://doi.org/10.1016/j.celrep.2013.09.043.

Cochemé, Helena M., Caroline Quin, Stephen J. McQuaker, Filipe Cabreiro, Angela Logan, Tracy A. Prime, Irina Abakumova, et al., 2011. “Measurement of H2O2 within Living Drosophila during Aging Using a Ratiometric Mass Spectrometry Probe Targeted to the Mitochondrial Matrix.” *Cell Metabolism* 13 (3): 340–50. https://doi.org/10.1016/j.cmet.2011.02.003.

Codd, Veryan, Massimo Mangino, Pim van der Harst, Peter S Braund, Michael Kaiser, Alan J Beveridge, Suzanne Rafelt, et al., 2010. “Variants near TERC Are Associated with Mean Telomere Length.” *Nature Genetics* 42 (3): 197–99. https://doi.org/10.1038/ng.532.

Conboy, Irina M., and Thomas A. Rando. 2012. “Heterochronic Parabiosis for the Study of the Effects of Aging on Stem Cells and Their Niches.” *Cell Cycle* 11 (12): 2260–67. https://doi.org/10.4161/cc.20437.

Coppé, Jean-Philippe, Katalin Kauser, Judith Campisi, and Christian M. Beauséjour. 2006. “Secretion of Vascular Endothelial Growth Factor by Primary Human

Fibroblasts at Senescence." *The Journal of Biological Chemistry* 281 (40): 29568–74. https://doi.org/10.1074/jbc.M603307200.

Cornes, Eric, Montserrat Porta-De-La-Riva, David Aristizábal-Corrales, Ana María Brokate-Llanos, Francisco Javier García-Rodríguez, Iris Ertl, Mònica Díaz, et al., 2015. "Cytoplasmic LSM-1 Protein Regulates Stress Responses through the Insulin/IGF-1 Signaling Pathway in Caenorhabditis Elegans." *RNA* 21 (9): 1544–53. https://doi.org/10.1261/rna.052324.115.

Cruickshanks, Hazel A., Tony McBryan, David M. Nelson, Nathan D. VanderKraats, Parisha P. Shah, John van Tuyn, Taranjit Singh Rai, et al., 2013. "Senescent Cells Harbour Features of the Cancer Epigenome." *Nature Cell Biology* 15 (12): 1495–1506. https://doi.org/10.1038/ncb2879.

Danan-Gotthold, Miri, Regina Golan-Gerstl, Eli Eisenberg, Keren Meir, Rotem Karni, and Erez Y. Levanon. 2015. "Identification of Recurrent Regulated Alternative Splicing Events across Human Solid Tumors." *Nucleic Acids Research* 43 (10): 5130–44. https://doi.org/10.1093/nar/gkv210.

Dao, Vinh, Srilakshmi Pandeswara, Yang Liu, Vincent Hurez, Sherry Dodds, Danielle Callaway, Aijie Liu, Paul Hasty, Zelton D. Sharp, and Tyler J. Curiel. 2015. "Prevention of Carcinogen and Inflammation-Induced Dermal Cancer by Oral Rapamycin Includes Reducing Genetic Damage." *Cancer Prevention Research (Philadelphia, Pa.)* 8 (5): 400–409. https://doi.org/10.1158/1940-6207.CAPR-14-0313-T.

Dasgupta, Biplab, and Jeffrey Milbrandt. 2007. "Resveratrol Stimulates AMP Kinase Activity in Neurons." *Proceedings of the National Academy of Sciences* 104 (17): 7217–22. https://doi.org/10.1073/pnas.0610068104.

Dastani, Zari, Marie-France Hivert, Nicholas Timpson, John R. B. Perry, Xin Yuan, Robert A. Scott, Peter Henneman, et al., 2012. “Novel Loci for Adiponectin Levels and Their Influence on Type 2 Diabetes and Metabolic Traits: A Multi-Ethnic Meta-Analysis of 45,891 Individuals.” *PLoS Genetics* 8 (3): e1002607. https://doi.org/10.1371/journal.pgen.1002607.

Davies Karen M., Strauss Mike, Daum Bertram, Kief Jan H., Osiewacz Heinz D., Rycovska Adriana, Zickermann Volker, and Kühlbrandt Werner. 2011. “Macromolecular Organization of ATP Synthase and Complex I in Whole Mitochondria.” n.d. Accessed December 16, 2019. https://www.ncbi.nlm.nih.gov/pmc/articles/PMC3161574/.

De Silva, N. Maneka G., Rachel M. Freathy, Tom M. Palmer, Louise A. Donnelly, Jian’an Luan, Tom Gaunt, Claudia Langenberg, et al., 2011. “Mendelian Randomization Studies Do Not Support a Role for Raised Circulating Triglyceride Levels Influencing Type 2 Diabetes, Glucose Levels, or Insulin Resistance.” *Diabetes* 60 (3): 1008–18. https://doi.org/10.2337/db10-1317.

Debey-Pascher, Svenja, Daniela Eggle, and Joachim L. Schultze. 2009. “RNA Stabilization of Peripheral Blood and Profiling by Bead Chip Analysis.” *Methods in Molecular Biology (Clifton, N.J.)* 496: 175–210. https://doi.org/10.1007/978-1-59745-553-4_13.

Dechat, Thomas, Katrin Pfleghaar, Kaushik Sengupta, Takeshi Shimi, Dale K. Shumaker, Liliana Solimando, and Robert D. Goldman. 2008. “Nuclear Lamins: Major Factors in the Structural Organization and Function of the Nucleus and Chromatin.” *Genes & Development* 22 (7): 832–53. https://doi.org/10.1101/gad.1652708.

Dellago, Hanna, Abdulhameed Khan, Monika Nussbacher, Anna Gstraunthaler, Ingo Lämmermann, Markus Schosserer, Christoph Mück, et al., 2012. “ATM-Dependent Phosphorylation of SNEVhPrp19/HPso4 Is Involved in Extending Cellular Life Span and Suppression of Apoptosis.” *Aging (Albany NY)* 4 (4): 290–304.

Deschênes, Mathieu, and Benoit Chabot. 2017. “The Emerging Role of Alternative Splicing in Senescence and Aging.” *Aging Cell* 16 (5): 918–33. https://doi.org/10.1111/acel.12646.

Deursen, Jan M. van. 2014. “The Role of Senescent Cells in Ageing.” *Nature* 509 (7501): 439–46. https://doi.org/10.1038/nature13193.

Dimmeler, Stefanie, and Pierluigi Nicotera. 2013. “MicroRNAs in Age-Related Diseases.” *EMBO Molecular Medicine* 5 (2): 180–90. https://doi.org/10.1002/emmm.201201986.

Ding, Fangyuan, and Michael B. Elowitz. 2019. “Constitutive Splicing and Economies of Scale in Gene Expression.” *Nature Structural & Molecular Biology* 26 (6): 424–32. https://doi.org/10.1038/s41594-019-0226-x.

Dörr, Jan R., Yong Yu, Maja Milanovic, Gregor Beuster, Christin Zasada, J. Henry M. Däbritz, Jan Lisec, et al., 2013. “Synthetic Lethal Metabolic Targeting of Cellular Senescence in Cancer Therapy.” *Nature* 501 (7467): 421–25. https://doi.org/10.1038/nature12437.

Dunning, Beth Elaine, and John E. Gerich. 2007. “The Role of Alpha-Cell Dysregulation in Fasting and Postprandial Hyperglycemia in Type 2 Diabetes and Therapeutic Implications.” *Endocrine Reviews* 28 (3): 253–83. https://doi.org/10.1210/er.2006-0026.

Dutta, Ambarish, William Henley, Jean-Marie Robine, Kenneth M. Langa, Robert B. Wallace, and David Melzer. 2013. “Longer Lived Parents: Protective Associations with Cancer Incidence and Overall Mortality.” *The Journals of Gerontology Series A: Biological Sciences and Medical Sciences* 68 (11): 1409–18. https://doi.org/10.1093/gerona/glt061.

Dutta, Ambarish, William Henley, Jean-Marie Robine, David Llewellyn, Kenneth M. Langa, Robert B. Wallace, and David Melzer. 2014. “Aging Children of Long-Lived Parents Experience Slower Cognitive Decline.” *Alzheimer’s & Dementia: The Journal of the Alzheimer’s Association* 10 (5 Suppl): S315-322. https://doi.org/10.1016/j.jalz.2013.07.002.

Ellingsgaard, Helga, Jan A. Ehses, Eva B. Hammar, Leentje Van Lommel, Roel Quintens, Geert Martens, Julie Kerr-Conte, et al., 2008. “Interleukin-6 Regulates Pancreatic α-Cell Mass Expansion.” *Proceedings of the National Academy of Sciences of the United States of America* 105 (35): 13163–68. https://doi.org/10.1073/pnas.0801059105.

Errichelli, Lorenzo, Stefano Dini Modigliani, Pietro Laneve, Alessio Colantoni, Ivano Legnini, Davide Capauto, Alessandro Rosa, et al., 2017. “FUS Affects Circular RNA Expression in Murine Embryonic Stem Cell-Derived Motor Neurons.” *Nature Communications* 8 (March): 14741. https://doi.org/10.1038/ncomms14741.

Faggioli, Francesca, Tao Wang, Jan Vijg, and Cristina Montagna. 2012. “Chromosome-Specific Accumulation of Aneuploidy in the Aging Mouse Brain.” *Human Molecular Genetics* 21 (24): 5246–53. https://doi.org/10.1093/hmg/dds375.

Fan, Caixia, Xiaomin Liu, Wenfeng Li, Haiyan Wang, Yingli Teng, Jun Ren, and Yusen Huang. 2019. “Circular RNA Circ KMT2E Is Up-Regulated in Diabetic Cataract Lenses and Is Associated with MiR-204-5p Sponge Function.” *Gene* 710 (August): 170–77. https://doi.org/10.1016/j.gene.2019.05.054.

Ferrucci, L., S. Bandinelli, E. Benvenuti, A. Di Iorio, C. Macchi, T. B. Harris, and J. M. Guralnik. 2000. “Subsystems Contributing to the Decline in Ability to Walk: Bridging the Gap between Epidemiology and Geriatric Practice in the InCHIANTI Study.” *Journal of the American Geriatrics Society* 48 (12): 1618–25.

Figge, Marc Thilo, Andreas S. Reichert, Michael Meyer-Hermann, and Heinz D. Osiewacz. 2012. “Deceleration of Fusion-Fission Cycles Improves Mitochondrial Quality Control during Aging.” *PLoS Computational Biology* 8 (6): e1002576. https://doi.org/10.1371/journal.pcbi.1002576.

Fontana, Luigi, Linda Partridge, and Valter D Longo. 2010. “Dietary Restriction, Growth Factors and Aging: From Yeast to Humans.” *Science (New York, N.Y.)* 328 (5976): 321–26. https://doi.org/10.1126/science.1172539.

Forsberg, Lars A., Chiara Rasi, Hamid R. Razzaghian, Geeta Pakalapati, Lindsay Waite, Krista Stanton Thilbeault, Anna Ronowicz, et al., 2012. “Age-Related Somatic Structural Changes in the Nuclear Genome of Human Blood Cells.” *American Journal of Human Genetics* 90 (2): 217–28. https://doi.org/10.1016/j.ajhg.2011.12.009.

Foukas, Lazaros C., Benoit Bilanges, Lucia Bettedi, Wayne Pearce, Khaled Ali, Sara Sancho, Dominic J. Withers, and Bart Vanhaesebroeck. 2013. “Long-Term P110α PI3K Inactivation Exerts a Beneficial Effect on Metabolism.” *EMBO Molecular Medicine* 5 (4): 563–71. https://doi.org/10.1002/emmm.201201953.

Fraga, Mario F., and Manel Esteller. 2007. “Epigenetics and Aging: The Targets and the Marks.” *Trends in Genetics: TIG* 23 (8): 413–18. https://doi.org/10.1016/j.tig.2007.05.008.

Freitas, Alex A., and João Pedro de Magalhães. 2011. “A Review and Appraisal of the DNA Damage Theory of Ageing.” *Mutation Research* 728 (1–2): 12–22. https://doi.org/10.1016/j.mrrev.2011.05.001.

Frenk, Stephen, and Jonathan Houseley. 2018. “Gene Expression Hallmarks of Cellular Ageing.” *Biogerontology* 19 (6): 547–66. https://doi.org/10.1007/s10522-018-9750-z.

Freund, Adam, Remi-Martin Laberge, Marco Demaria, and Judith Campisi. 2012. “Lamin B1 Loss Is a Senescence-Associated Biomarker.” *Molecular Biology of the Cell* 23 (11): 2066–75. https://doi.org/10.1091/mbc.E11-10-0884.

Fujita, Kaori, Abdul M. Mondal, Izumi Horikawa, Giang H. Nguyen, Kensuke Kumamoto, Jane J. Sohn, Elise D. Bowman, et al., 2009. “P53 Isoforms, Δ133p53 and P53β, Are Endogenous Regulators of Replicative Cellular Senescence.” *Nature Cell Biology* 11 (9): 1135. https://doi.org/10.1038/ncb1928.

Gallego Romero, Irene, Athma A. Pai, Jenny Tung, and Yoav Gilad. 2014. “RNA-Seq: Impact of RNA Degradation on Transcript Quantification.” *BMC Biology* 12 (1): 42. https://doi.org/10.1186/1741-7007-12-42.

Garagnani, Paolo, Cristina Giuliani, Chiara Pirazzini, Fabiola Olivieri, Maria Giulia Bacalini, Rita Ostan, Daniela Mari, et al., 2013. “Centenarians as Super-Controls to Assess the Biological Relevance of Genetic Risk Factors for Common Age-Related Diseases: A Proof of Principle on Type 2 Diabetes.” Aging. May 31, 2013. https://doi.org/10.18632/aging.100562.

Gems, David, and Linda Partridge. 2013. “Genetics of Longevity in Model Organisms: Debates and Paradigm Shifts.” *Annual Review of Physiology* 75: 621–44. https://doi.org/10.1146/annurev-physiol-030212-183712.

Gerencser, Akos A., Judit Doczi, Beata Töröcsik, Ella Bossy-Wetzel, and Vera Adam-Vizi. 2008. “Mitochondrial Swelling Measurement in Situ by Optimized Spatial Filtering: Astrocyte-Neuron Differences.” *Biophysical Journal* 95 (5): 2583–98. https://doi.org/10.1529/biophysj.107.118620.

Glazar, P.; Papavasileiou, P.; Rajewsky, N. 2014. circBase: A database for circular RNAs. *RNA 20*, 1666–1670

Glessner, Joseph T., Albert Vernon Smith, Saarene Panossian, Cecilia E. Kim, Nagahide Takahashi, Kelly A. Thomas, Fengxiang Wang, et al., 2013. “Copy Number Variations in Alternative Splicing Gene Networks Impact Lifespan.” *PLOS ONE* 8 (1): e53846. https://doi.org/10.1371/journal.pone.0053846.

Glisovic, Tina, Jennifer L. Bachorik, Jeongsik Yong, and Gideon Dreyfuss. 2008. “RNA-Binding Proteins and Post-Transcriptional Gene Regulation.” *FEBS Letters* 582 (14): 1977–86. https://doi.org/10.1016/j.febslet.2008.03.004.

Goldman, Dana P., David Cutler, John W. Rowe, Pierre-Carl Michaud, Jeffrey Sullivan, Desi Peneva, and S. Jay Olshansky. 2013. “Substantial Health and Economic Returns from Delayed Aging May Warrant a New Focus for Medical Research.” *Health Affairs (Project Hope)* 32 (10): 1698–1705. https://doi.org/10.1377/hlthaff.2013.0052.

Gong Binsheng, Xu Joshua and Tong Weida. 2020. “Landscape of CircRNAs Across 11 Organs and 4 Ages in Fischer 344 Rats | Chemical Research in Toxicology.” n.d. Accessed October 1, 2020. https://pubs.acs.org/doi/10.1021/acs.chemrestox.0c00144.

Gonzalez-Suarez, Ignacio, Abena B. Redwood, Stephanie M. Perkins, Bart Vermolen, Daniel Lichtensztejin, David A. Grotsky, Lucia Morgado-Palacin, et al., 2009. “Novel Roles for A-Type Lamins in Telomere Biology and the DNA Damage Response Pathway.” *The EMBO Journal* 28 (16): 2414–27. https://doi.org/10.1038/emboj.2009.196.

Gordin, Daniel, and Per-Henrik Groop. 2016. “Aspects of Hyperglycemia Contribution to Arterial Stiffness and Cardiovascular Complications in Patients With Type 1 Diabetes.” *Journal of Diabetes Science and Technology* 10 (5): 1059–64. https://doi.org/10.1177/1932296816636894.

Green, Douglas R., Lorenzo Galluzzi, and Guido Kroemer. 2011. “Mitochondria and the Autophagy-Inflammation-Cell Death Axis in Organismal Aging.” *Science (New York, N.Y.)* 333 (6046): 1109–12. https://doi.org/10.1126/science.1201940.

Greene, M. A., and R. F. Loeser. 2015. “Aging-Related Inflammation in Osteoarthritis.” *Osteoarthritis and Cartilage* 23 (11): 1966–71. https://doi.org/10.1016/j.joca.2015.01.008.

Greer, Eric L., Philip R. Oskoui, Max R. Banko, Jay M. Maniar, Melanie P. Gygi, Steven P. Gygi, and Anne Brunet. 2007. “The Energy Sensor AMP-Activated Protein Kinase Directly Regulates the Mammalian FOXO3 Transcription Factor.” *Journal of Biological Chemistry* 282 (41): 30107–19. https://doi.org/10.1074/jbc.M705325200.

Gregg, Siobhán Q., Verónica Gutiérrez, Andria Rasile Robinson, Tyler Woodell, Atsunori Nakao, Mark A. Ross, George K. Michalopoulos, et al., 2012. “A Mouse Model of Accelerated Liver Aging Caused by a Defect in DNA Repair.” *Hepatology (Baltimore, Md.)* 55 (2): 609–21. https://doi.org/10.1002/hep.24713.

Gruber, Reinhard, Hannjörg Koch, Bruce A. Doll, Florian Tegtmeier, Thomas A. Einhorn, and Jeffrey O. Hollinger. 2006. “Fracture Healing in the Elderly Patient.” *Experimental Gerontology* 41 (11): 1080–93. https://doi.org/10.1016/j.exger.2006.09.008.

Gruner, Hannah, Mariela Cortés-López, Daphne A. Cooper, Matthew Bauer, and Pedro Miura. 2016. “CircRNA Accumulation in the Aging Mouse Brain.” *Scientific Reports* 6: 38907. https://doi.org/10.1038/srep38907.

Gu, Yonghao, Genjie Ke, Lin Wang, Enliang Zhou, Kai Zhu, and Yingying Wei. 2017. “Altered Expression Profile of Circular RNAs in the Serum of Patients with Diabetic Retinopathy Revealed by Microarray.” *Ophthalmic Research* 58 (3): 176–84. https://doi.org/10.1159/000479156.

Guo, Nini, Erin M. Parry, Luo-Sheng Li, Frant Kembou, Naudia Lauder, Mehboob A. Hussain, Per-Olof Berggren, and Mary Armanios. 2011. “Short Telomeres Compromise β-Cell Signaling and Survival.” *PLoS ONE* 6 (3). https://doi.org/10.1371/journal.pone.0017858.

Gusarov, Ivan, Laurent Gautier, Olga Smolentseva, Ilya Shamovsky, Svetlana Eremina, Alexander Mironov, and Evgeny Nudler. 2013. “Bacterial Nitric Oxide Extends the Lifespan of C. Elegans.” *Cell* 152 (4): 818–30. https://doi.org/10.1016/j.cell.2012.12.043.

Hall, Hana, Patrick Medina, Daphne A. Cooper, Spencer E. Escobedo, Jeremiah Rounds, Kaelan J. Brennan, Christopher Vincent, Pedro Miura, Rebecca Doerge, and Vikki M. Weake. 2017. “Transcriptome Profiling of Aging Drosophila Photoreceptors Reveals Gene Expression Trends That Correlate with Visual Senescence.” *BMC Genomics* 18 (November). https://doi.org/10.1186/s12864-017-4304-3.

Halter, Jeffrey B., Nicolas Musi, Frances McFarland Horne, Jill P. Crandall, Andrew Goldberg, Lawrence Harkless, William R. Hazzard, et al., 2014. “Diabetes and Cardiovascular Disease in Older Adults: Current Status and Future Directions.” *Diabetes* 63 (8): 2578–89. https://doi.org/10.2337/db14-0020.

Ham, Tjakko J. van, Mats A. Holmberg, Annemieke T. van der Goot, Eva Teuling, Moises Garcia-Arencibia, Hyun-eui Kim, Deguo Du, et al., 2010. “Identification of MOAG-4/SERF as a Regulator of Age-Related Proteotoxicity.” *Cell* 142 (4): 601–12. https://doi.org/10.1016/j.cell.2010.07.020.

Ham, Tjakko J. van, James Mapes, David Kokel, and Randall T. Peterson. 2010. “Live Imaging of Apoptotic Cells in Zebrafish.” *The FASEB Journal* 24 (11): 4336–42. https://doi.org/10.1096/fj.10-161018.

Hamatani, Toshio, Geppino Falco, Mark G. Carter, Hidenori Akutsu, Carole A. Stagg, Alexei A. Sharov, Dawood B. Dudekula, Vincent VanBuren, and Minoru S. H. Ko. 2004. “Age-Associated Alteration of Gene Expression Patterns in Mouse Oocytes.” *Human Molecular Genetics* 13 (19): 2263–78. https://doi.org/10.1093/hmg/ddh241.

Han, Shuo, and Anne Brunet. 2012. “Histone Methylation Makes Its Mark on Longevity.” *Trends in Cell Biology* 22 (1): 42–49. https://doi.org/10.1016/j.tcb.2011.11.001.

Hansen, Malene, Stefan Taubert, Douglas Crawford, Nataliya Libina, Seung-Jae Lee, and Cynthia Kenyon. 2007. “Lifespan Extension by Conditions That Inhibit Translation in Caenorhabditis Elegans.” *Aging Cell* 6 (1): 95–110. https://doi.org/10.1111/j.1474-9726.2006.00267.x.

Haque, Shahnaz, and Lorna W. Harries. 2017. “Circular RNAs (CircRNAs) in Health and Disease.” *Genes* 8 (12). https://doi.org/10.3390/genes8120353.

Harries, Lorna W., Dena Hernandez, William Henley, Andrew Wood, Alice C. Holly, Rachel M. Bradley-Smith, Hanieh Yaghootkar, et al., 2011. “Human Aging Is Characterized by Focused Changes in Gene Expression and Deregulation of Alternative Splicing.” *Aging Cell* 10 (5): 868–78. https://doi.org/10.1111/j.1474-9726.2011.00726.x.

Harrison, David E., Randy Strong, Zelton Dave Sharp, James F. Nelson, Clinton M. Astle, Kevin Flurkey, Nancy L. Nadon, et al., 2009. “Rapamycin Fed Late in Life Extends Lifespan in Genetically Heterogeneous Mice.” *Nature* 460 (7253): 392–95. https://doi.org/10.1038/nature08221.

He, Yong-Han, Shao-Yan Pu, Fu-Hui Xiao, Xiao-Qiong Chen, Dong-Jing Yan, Yao-Wen Liu, Rong Lin, et al., 2016. “Improved Lipids, Diastolic Pressure and Kidney Function Are Potential Contributors to Familial Longevity: A Study on 60 Chinese Centenarian Families.” *Scientific Reports* 6 (February). https://doi.org/10.1038/srep21962.

Head, Steven R., H. Kiyomi Komori, Sarah A. LaMere, Thomas Whisenant, Filip Van Nieuwerburgh, Daniel R. Salomon, and Phillip Ordoukhanian. 2014. “Library Construction for Next-Generation Sequencing: Overviews and Challenges.” *BioTechniques* 56 (2): 61-passim. https://doi.org/10.2144/000114133.

Heemst, Diana van. 2010. “Insulin, IGF-1 and Longevity.” *Aging and Disease* 1 (2): 147–57.

Heintz, Caroline, Thomas Koed Doktor, Anne Lanjuin, Caroline Escoubas, Yue Zhang, Heather J. Weir, Sneha Dutta, et al., 2017. “Splicing Factor 1 Modulates Dietary Restriction and TORC1 Pathway Longevity in C. Elegans.” *Nature* 541 (7635): 102–6. https://doi.org/10.1038/nature20789.

Helman, Aharon, Agnes Klochendler, Narmen Azazmeh, Yael Gabai, Elad Horwitz, Shira Anzi, Avital Swisa, et al., 2016. “P16Ink4a-Induced Senescence of Pancreatic Beta Cells Enhances Insulin Secretion.” *Nature Medicine* 22 (4): 412–20. https://doi.org/10.1038/nm.4054.

Hendershott, Melissa C., and Ronald D. Vale. 2014. “Regulation of Microtubule Minus-End Dynamics by CAMSAPs and Patronin.” *Proceedings of the National Academy of Sciences* 111 (16): 5860–65. https://doi.org/10.1073/pnas.1404133111.

Herranz, Nicolás, Suchira Gallage, Massimiliano Mellone, Torsten Wuestefeld, Sabrina Klotz, Christopher J. Hanley, Selina Raguz, et al., 2015. “MTOR Regulates MAPKAPK2 Translation to Control the Senescence-Associated Secretory Phenotype.” *Nature Cell Biology* 17 (9): 1205–17. https://doi.org/10.1038/ncb3225.

Herskind, A. M., M. McGue, N. V. Holm, T. I. Sørensen, B. Harvald, and J. W. Vaupel. 1996. “The Heritability of Human Longevity: A Population-Based Study of 2872 Danish Twin Pairs Born 1870-1900.” *Human Genetics* 97 (3): 319–23. https://doi.org/10.1007/bf02185763.

Hjelmborg, Jacob vB, Ivan Iachine, Axel Skytthe, James W. Vaupel, Matt McGue, Markku Koskenvuo, Jaakko Kaprio, Nancy L. Pedersen, and Kaare Christensen. 2006. “Genetic Influence on Human Lifespan and Longevity.” *Human Genetics* 119 (3): 312–21. https://doi.org/10.1007/s00439-006-0144-y.

Hocine, Sami, Robert H. Singer, and David Grünwald. 2010. “RNA Processing and Export.” *Cold Spring Harbor Perspectives in Biology* 2 (12). https://doi.org/10.1101/cshperspect.a000752.

Hoeijmakers, Jan H. J. 2009. “DNA Damage, Aging, and Cancer.” *The New England Journal of Medicine* 361 (15): 1475–85. https://doi.org/10.1056/NEJMra0804615.

Holly, Alice C., David Melzer, Luke C. Pilling, Alexander C. Fellows, Toshiko Tanaka, Luigi Ferrucci, and Lorna W. Harries. 2013. “Changes in Splicing Factor Expression Are Associated with Advancing Age in Man.” *Mechanisms of Ageing and Development* 134 (9): 356–66. https://doi.org/10.1016/j.mad.2013.05.006.

Holly, Alice C., Luke C. Pilling, Dena Hernandez, Benjamin P. Lee, Andrew Singleton, Luigi Ferrucci, David Melzer, and Lorna W. Harries. 2014. “Splicing Factor 3B1 Hypomethylation Is Associated with Altered SF3B1 Transcript Expression in Older Humans.” *Mechanisms of Ageing and Development* 135 (January): 50–56. https://doi.org/10.1016/j.mad.2014.01.005.

Holzenberger, Martin, Joëlle Dupont, Bertrand Ducos, Patricia Leneuve, Alain Géloën, Patrick C. Even, Pascale Cervera, and Yves Le Bouc. 2003. “IGF-1 Receptor Regulates Lifespan and Resistance to Oxidative Stress in Mice.” *Nature* 421 (6919): 182–87. https://doi.org/10.1038/nature01298.

Horvath, Steve, Chiara Pirazzini, Maria Giulia Bacalini, Davide Gentilini, Anna Maria Di Blasio, Massimo Delledonne, Daniela Mari, et al., 2015. “Decreased Epigenetic Age of PBMCs from Italian Semi-Supercentenarians and Their Offspring.” *Aging (Albany NY)* 7 (12): 1159–70.

Hu, Wei, Qing Han, Lei Zhao, and Li Wang. 2019. “Circular RNA CircRNA_15698 Aggravates the Extracellular Matrix of Diabetic Nephropathy Mesangial Cells via MiR-185/TGF-B1.” *Journal of Cellular Physiology* 234 (2): 1469–76. https://doi.org/10.1002/jcp.26959.

Huang, Hua, Shinsuke Kaku, Chad D. Knights, Byung S. Park, Jane Clifford, and Molly Kulesz-Martin. 2002. “Repression of Transcription and Interference with DNA Binding of TATA-Binding Protein by C-Terminal Alternatively Spliced P53.” *Experimental Cell Research* 279 (2): 248–59. https://doi.org/10.1006/excr.2002.5596.

Hummon, Amanda B., Sharlene R. Lim, Michael J. Difilippantonio, and Thomas Ried. 2007. “Isolation and Solubilization of Proteins after TRIzol Extraction of RNA and DNA from Patient Material Following Prolonged Storage.” *BioTechniques* 42 (4): 467–70, 472. https://doi.org/10.2144/000112401.

Hunt, Steven C, Wei Chen, Jeffrey P Gardner, Masayuki Kimura, Sathanur R Srinivasan, John H Eckfeldt, Gerald S Berenson, and Abraham Aviv. 2008. “Leukocyte Telomeres Are Longer in African Americans than in Whites: The National Heart, Lung, and Blood Institute Family Heart Study and the Bogalusa Heart Study.” *Aging Cell* 7 (4): 451–58. https://doi.org/10.1111/j.1474-9726.2008.00397.x.

Hunter, S. J., and W. T. Garvey. 1998. “Insulin Action and Insulin Resistance: Diseases Involving Defects in Insulin Receptors, Signal Transduction, and the Glucose Transport Effector System.” *The American Journal of Medicine* 105 (4): 331–45. https://doi.org/10.1016/s0002-9343(98)00300-3.

Hurrle, Samantha, and Walter H. Hsu. 2017. “The Etiology of Oxidative Stress in Insulin Resistance.” *Biomedical Journal* 40 (5): 257–62. https://doi.org/10.1016/j.bj.2017.06.007.

Iadevaia, Valentina, Rui Liu, and Christopher G. Proud. 2014. “MTORC1 Signaling Controls Multiple Steps in Ribosome Biogenesis.” *Seminars in Cell &*

Developmental Biology 36 (December): 113–20. https://doi.org/10.1016/j.semcdb.2014.08.004.

Imura, Akihiro, Yoshihito Tsuji, Miyahiko Murata, Ryota Maeda, Koji Kubota, Akiko Iwano, Chikashi Obuse, et al., 2007. “α-Klotho as a Regulator of Calcium Homeostasis.” *Science* 316 (5831): 1615–18. https://doi.org/10.1126/science.1135901.

Inoki, Ken, Tianqing Zhu, and Kun-Liang Guan. 2003. “TSC2 Mediates Cellular Energy Response to Control Cell Growth and Survival.” *Cell* 115 (5): 577–90. https://doi.org/10.1016/S0092-8674(03)00929-2.

“International Diabetes Federation - Home.” n.d. Accessed April 13, 2020. https://www.idf.org/.

Issa, J. P., N. Ahuja, M. Toyota, M. P. Bronner, and T. A. Brentnall. 2001. “Accelerated Age-Related CpG Island Methylation in Ulcerative Colitis.” *Cancer Research* 61 (9): 3573–77.

Issa, J P, P M Vertino, C D Boehm, I F Newsham, and S B Baylin. 1996. “Switch from Monoallelic to Biallelic Human IGF2 Promoter Methylation during Aging and Carcinogenesis.” *Proceedings of the National Academy of Sciences of the United States of America* 93 (21): 11757–62.

Ivanov, Andranik, Sebastian Memczak, Emanuel Wyler, Francesca Torti, Hagit T. Porath, Marta R. Orejuela, Michael Piechotta, et al., 2015. “Analysis of Intron Sequences Reveals Hallmarks of Circular RNA Biogenesis in Animals.” *Cell Reports* 10 (2): 170–77. https://doi.org/10.1016/j.celrep.2014.12.019.

Izuogu, Osagie G., Abd A. Alhasan, Hani M. Alafghani, Mauro Santibanez-Koref, David J. Elliott, David J. Elliot, and Michael S. Jackson. 2016. “PTESFinder: A Computational Method to Identify Post-Transcriptional Exon Shuffling (PTES)

Events.” *BMC Bioinformatics* 17 (January): 31. https://doi.org/10.1186/s12859-016-0881-4.

Jackson, I J. 1991. “A Reappraisal of Non-Consensus MRNA Splice Sites.” *Nucleic Acids Research* 19 (14): 3795–98.

Jacob, S., J. Machann, K. Rett, K. Brechtel, A. Volk, W. Renn, E. Maerker, et al., 1999. “Association of Increased Intramyocellular Lipid Content with Insulin Resistance in Lean Nondiabetic Offspring of Type 2 Diabetic Subjects.” *Diabetes* 48 (5): 1113–19. https://doi.org/10.2337/diabetes.48.5.1113.

Jacobs, Kevin B., Meredith Yeager, Weiyin Zhou, Sholom Wacholder, Zhaoming Wang, Benjamin Rodriguez-Santiago, Amy Hutchinson, et al., 2012. “Detectable Clonal Mosaicism and Its Relationship to Aging and Cancer.” *Nature Genetics* 44 (6): 651–58. https://doi.org/10.1038/ng.2270.

Janzen, Viktor, Randolf Forkert, Heather E. Fleming, Yoriko Saito, Michael T. Waring, David M. Dombkowski, Tao Cheng, Ronald A. DePinho, Norman E. Sharpless, and David T. Scadden. 2006. “Stem-Cell Ageing Modified by the Cyclin-Dependent Kinase Inhibitor P16INK4a.” *Nature* 443 (7110): 421–26. https://doi.org/10.1038/nature05159.

Jeanclos, E., N. J. Schork, K. O. Kyvik, M. Kimura, J. H. Skurnick, and A. Aviv. 2000. “Telomere Length Inversely Correlates with Pulse Pressure and Is Highly Familial.” *Hypertension (Dallas, Tex.: 1979)* 36 (2): 195–200.

Jeck, W.R.; Sharpless, N.E. 2014. Detecting and characterizing circular RNAs. *Nat. Biotechnol. 32*, 453–461.

Jeffery, Nicola, Sarah Richardson, David Chambers, Noel G. Morgan, and Lorna W. Harries. 2019. “Cellular Stressors May Alter Islet Hormone Cell Proportions by

Moderation of Alternative Splicing Patterns." *Human Molecular Genetics* 28 (16): 2763–74. https://doi.org/10.1093/hmg/ddz094.

Jensen, Majken K., Traci M. Bartz, Luc Djoussé, Jorge R. Kizer, Susan J. Zieman, Eric B. Rimm, David S. Siscovick, Bruce M. Psaty, Joachim H. Ix, and Kenneth J. Mukamal. 2013. "Genetically Elevated Fetuin-A Levels, Fasting Glucose Levels, and Risk of Type 2 Diabetes: The Cardiovascular Health Study." *Diabetes Care* 36 (10): 3121–27. https://doi.org/10.2337/dc12-2323.

Jiang, Cizhong, and B. Franklin Pugh. 2009. "Nucleosome Positioning and Gene Regulation: Advances through Genomics." *Nature Reviews. Genetics* 10 (3): 161–72. https://doi.org/10.1038/nrg2522.

Jiang, Guangjian, Yue Ma, Tian An, Yanyun Pan, Fangfang Mo, Dandan Zhao, Yufei Liu, et al., 2017. "Relationships of Circular RNA with Diabetes and Depression." *Scientific Reports* 7 (August). https://doi.org/10.1038/s41598-017-07931-0.

Jin, Chunyu, Jing Li, Christopher D. Green, Xiaoming Yu, Xia Tang, Dali Han, Bo Xian, et al., 2011. "Histone Demethylase UTX-1 Regulates C. Elegans Life Span by Targeting the Insulin/IGF-1 Signaling Pathway." *Cell Metabolism* 14 (2): 161–72. https://doi.org/10.1016/j.cmet.2011.07.001.

Jin, Guoxi, Qiong Wang, Xiaolei Hu, Xiaoli Li, Xiaoyan Pei, Erqin Xu, and Minglong Li. 2019. "Profiling and Functional Analysis of Differentially Expressed Circular RNAs in High Glucose-Induced Human Umbilical Vein Endothelial Cells." *FEBS Open Bio* 9 (9): 1640–51. https://doi.org/10.1002/2211-5463.12709.

Johnson, F. B., D. A. Sinclair, and L. Guarente. 1999. "Molecular Biology of Aging." *Cell* 96 (2): 291–302.

Jones, Christopher M., and Kristien Boelaert. 2015. “The Endocrinology of Ageing: A Mini-Review.” *Gerontology* 61 (4): 291–300. https://doi.org/10.1159/000367692.

Kandoth, Cyriac, Michael D. McLellan, Fabio Vandin, Kai Ye, Beifang Niu, Charles Lu, Mingchao Xie, et al., 2013. “Mutational Landscape and Significance across 12 Major Cancer Types.” *Nature* 502 (7471): 333–39. https://doi.org/10.1038/nature12634.

Kashyap, Sangeeta, Renata Belfort, Amalia Gastaldelli, Thongchai Pratipanawatr, Rachele Berria, Wilailak Pratipanawatr, Mandeep Bajaj, Lawrence Mandarino, Ralph DeFronzo, and Kenneth Cusi. 2003. “A Sustained Increase in Plasma Free Fatty Acids Impairs Insulin Secretion in Nondiabetic Subjects Genetically Predisposed to Develop Type 2 Diabetes.” *Diabetes* 52 (10): 2461–74. https://doi.org/10.2337/diabetes.52.10.2461.

Katajisto, Pekka, Julia Döhla, Christine Chaffer, Nalle Pentinmikko, Nemanja Marjanovic, Sharif Iqbal, Roberto Zoncu, Walter Chen, Robert A. Weinberg, and David M. Sabatini. 2015. “Asymmetric Apportioning of Aged Mitochondria between Daughter Cells Is Required for Stemness.” *Science (New York, N.Y.)* 348 (6232): 340–43. https://doi.org/10.1126/science.1260384.

Kato, Masaomi, Xiaowei Chen, Sachi Inukai, Hongyu Zhao, and Frank J. Slack. 2011. “Age-Associated Changes in Expression of Small, Noncoding RNAs, Including MicroRNAs, in C. Elegans.” *RNA* 17 (10): 1804–20. https://doi.org/10.1261/rna.2714411.

Keane, Kevin Noel, Vinicius Fernandes Cruzat, Rodrigo Carlessi, Paulo Ivo Homem de Bittencourt, and Philip Newsholme. 2015. “Molecular Events Linking Oxidative Stress and Inflammation to Insulin Resistance and β-Cell

Dysfunction." *Oxidative Medicine and Cellular Longevity* 2015: 181643. https://doi.org/10.1155/2015/181643.

Kehler, D. Scott. 2019. "Age-Related Disease Burden as a Measure of Population Ageing." *The Lancet Public Health* 4 (3): e123–24. https://doi.org/10.1016/S2468-2667(19)30026-X.

Kengne, Andre Pascal, Joline W. J. Beulens, Linda M. Peelen, Karel G. M. Moons, Yvonne T. van der Schouw, Matthias B. Schulze, Annemieke M. W. Spijkerman, et al., 2014. "Non-Invasive Risk Scores for Prediction of Type 2 Diabetes (EPIC-InterAct): A Validation of Existing Models." *The Lancet. Diabetes & Endocrinology* 2 (1): 19–29. https://doi.org/10.1016/S2213-8587(13)70103-7.

Kenyon, Cynthia J. 2010a. "The Genetics of Ageing." *Nature* 464 (7288): 504–12. https://doi.org/10.1038/nature08980.

Kirkland, James L. 2016. "Translating the Science of Aging into Therapeutic Interventions." *Cold Spring Harbor Perspectives in Medicine* 6 (3): a025908. https://doi.org/10.1101/cshperspect.a025908.

Kirkwood, T. B. 1977. "Evolution of Ageing." *Nature* 270 (5635): 301–4. https://doi.org/10.1038/270301a0.

Kirkwood, Thomas B. L. 2005. "Understanding the Odd Science of Aging." *Cell* 120 (4): 437–47. https://doi.org/10.1016/j.cell.2005.01.027.

Kitada, Munehiro, Yoshio Ogura, Itaru Monno, and Daisuke Koya. 2019. "Sirtuins and Type 2 Diabetes: Role in Inflammation, Oxidative Stress, and Mitochondrial Function." *Frontiers in Endocrinology* 10 (March). https://doi.org/10.3389/fendo.2019.00187.

Knop, F. K., T. Vilsbøll, S. Madsbad, J. J. Holst, and T. Krarup. 2007. “Inappropriate Suppression of Glucagon during OGTT but Not during Isoglycaemic i.v. Glucose Infusion Contributes to the Reduced Incretin Effect in Type 2 Diabetes Mellitus.” *Diabetologia* 50 (4): 797–805. https://doi.org/10.1007/s00125-006-0566-z.

Koga, Hiroshi, Susmita Kaushik, and Ana Maria Cuervo. 2011. “Protein Homeostasis and Aging: The Importance of Exquisite Quality Control.” *Ageing Research Reviews* 10 (2): 205–15. https://doi.org/10.1016/j.arr.2010.02.001.

Korovila, Ioanna, Martín Hugo, José Pedro Castro, Daniela Weber, Annika Höhn, Tilman Grune, and Tobias Jung. 2017. “Proteostasis, Oxidative Stress and Aging.” *Redox Biology* 13: 550–67. https://doi.org/10.1016/j.redox.2017.07.008.

Kramer, Marianne C., Dongming Liang, Deirdre C. Tatomer, Beth Gold, Zachary M. March, Sara Cherry, and Jeremy E. Wilusz. 2015. “Combinatorial Control of Drosophila Circular RNA Expression by Intronic Repeats, HnRNPs, and SR Proteins.” *Genes & Development* 29 (20): 2168–82. https://doi.org/10.1101/gad.270421.115.

Krssak, M., K. Falk Petersen, A. Dresner, L. DiPietro, S. M. Vogel, D. L. Rothman, M. Roden, and G. I. Shulman. 1999. “Intramyocellular Lipid Concentrations Are Correlated with Insulin Sensitivity in Humans: A 1H NMR Spectroscopy Study.” *Diabetologia* 42 (1): 113–16. https://doi.org/10.1007/s001250051123.

Kuilman, Thomas, Chrysiis Michaloglou, Wolter J. Mooi, and Daniel S. Peeper. 2010. “The Essence of Senescence.” *Genes & Development* 24 (22): 2463–79. https://doi.org/10.1101/gad.1971610.

Laberge, Remi-Martin, Yu Sun, Arturo V. Orjalo, Christopher K. Patil, Adam Freund, Lili Zhou, Samuel C. Curran, et al., 2015. “MTOR Regulates the Pro-Tumorigenic Senescence-Associated Secretory Phenotype by Promoting IL1A Translation.” *Nature Cell Biology* 17 (8): 1049. https://doi.org/10.1038/ncb3195.

Laplante, Mathieu, and David M. Sabatini. 2012. “MTOR Signaling in Growth Control and Disease.” *Cell* 149 (2): 274–93. https://doi.org/10.1016/j.cell.2012.03.017.

Latorre, Eva, Vishal C. Birar, Angela N. Sheerin, J. Charles C. Jeynes, Amy Hooper, Helen R. Dawe, David Melzer, et al., 2017a. “Small Molecule Modulation of Splicing Factor Expression Is Associated with Rescue from Cellular Senescence.” *BMC Cell Biology* 18 (1): 31. https://doi.org/10.1186/s12860-017-0147-7.

Latorre, Eva, and Lorna. W Harries. 2017. “Splicing Regulatory Factors, Ageing and Age-Related Disease.” *Ageing Research Reviews* 36 (July): 165–70. https://doi.org/10.1016/j.arr.2017.04.004.

Latorre, Eva, Elizabeth L. Ostler, Richard G. A. Faragher, and Lorna W. Harries. 2018. “FOXO1 and ETV6 Genes May Represent Novel Regulators of Splicing Factor Expression in Cellular Senescence.” *The FASEB Journal* 33 (1): 1086–97. https://doi.org/10.1096/fj.201801154R.

Latorre, Eva, Luke C. Pilling, Benjamin P. Lee, Stefania Bandinelli, David Melzer, Luigi Ferrucci, and Lorna W. Harries. 2018. “The VEGFA156b Isoform Is Dysregulated in Senescent Endothelial Cells and May Be Associated with Prevalent and Incident Coronary Heart Disease.” *Clinical Science (London, England: 1979)* 132 (3): 313–25. https://doi.org/10.1042/CS20171556.

Latorre, Eva, Roberta Torregrossa, Mark E. Wood, Matthew Whiteman, and Lorna W. Harries. 2018. “Mitochondria-Targeted Hydrogen Sulfide Attenuates

Endothelial Senescence by Selective Induction of Splicing Factors HNRNPD and SRSF2." *Aging* 10 (7): 1666–81. https://doi.org/10.18632/aging.101500.

Laurie, Cathy C., Cecelia A. Laurie, Kenneth Rice, Kimberly F. Doheny, Leila R. Zelnick, Caitlin P. McHugh, Hua Ling, et al., 2012. "Detectable Clonal Mosaicism from Birth to Old Age and Its Relationship to Cancer." *Nature Genetics* 44 (6): 642–50. https://doi.org/10.1038/ng.2271.

Lavasani, Mitra, Andria R. Robinson, Aiping Lu, Minjung Song, Joseph M. Feduska, Bahar Ahani, Jeremy S. Tilstra, et al., 2012. "Muscle-Derived Stem/Progenitor Cell Dysfunction Limits Healthspan and Lifespan in a Murine Progeria Model." *Nature Communications* 3 (January): 608. https://doi.org/10.1038/ncomms1611.

Lawrence, Moyra, Sylvain Daujat, and Robert Schneider. 2016. "Lateral Thinking: How Histone Modifications Regulate Gene Expression." *Trends in Genetics: TIG* 32 (1): 42–56. https://doi.org/10.1016/j.tig.2015.10.007.

Lee, Benjamin, Lorna Mulvey, Gregory Barr, Jemma Garratt, Emily Goodman, Colin Selman, and Lorna W. Harries. 2019. "Dietary Restriction in ILSXISS Mice Is Associated with Widespread Changes in Splicing Regulatory Factor Expression Levels." *Experimental Gerontology* 128: 110736. https://doi.org/10.1016/j.exger.2019.110736.

Lee, Benjamin, Luke Pilling, Florence Emond, Kevin Flurkey, David E. Harrison, Rong Yuan, Luanne L. Peters, et al., 2016. "Changes in the Expression of Splicing Factor Transcripts and Variations in Alternative Splicing Are Associated with Lifespan in Mice and Humans." *Aging Cell* 15 (5): 903–13. https://doi.org/10.1111/acel.12499.

Lee, Jae-Eun, Jee-In Heo, Seong-Hoon Park, Jeong-Hyeon Kim, Yoon-Jung Kho, Hong-Jun Kang, Hae Young Chung, Jong-Lull Yoon, and Jae-Yong Lee. 2011. “Calorie Restriction (CR) Reduces Age-Dependent Decline of Non-Homologous End Joining (NHEJ) Activity in Rat Tissues.” *Experimental Gerontology* 46 (11): 891–96. https://doi.org/10.1016/j.exger.2011.07.009.

Lesnefsky, Edward J., and Charles L. Hoppel. 2006. “Oxidative Phosphorylation and Aging.” *Ageing Research Reviews* 5 (4): 402–33. https://doi.org/10.1016/j.arr.2006.04.001.

Levy, Daniel, Susan L. Neuhausen, Steven C. Hunt, Masayuki Kimura, Shih-Jen Hwang, Wei Chen, Joshua C. Bis, et al., 2010. “Genome-Wide Association Identifies OBFC1 as a Locus Involved in Human Leukocyte Telomere Biology.” *Proceedings of the National Academy of Sciences of the United States of America* 107 (20): 9293–98. https://doi.org/10.1073/pnas.0911494107.

Li, Ning, Francesca Frigerio, and Pierre Maechler. 2008. “The Sensitivity of Pancreatic Beta-Cells to Mitochondrial Injuries Triggered by Lipotoxicity and Oxidative Stress.” *Biochemical Society Transactions* 36 (Pt 5): 930–34. https://doi.org/10.1042/BST0360930.

Liao, Chen-Yu, Brad A. Rikke, Thomas E. Johnson, Vivian Diaz, and James F. Nelson. 2010. “Genetic Variation in the Murine Lifespan Response to Dietary Restriction: From Life Extension to Life Shortening.” *Aging Cell* 9 (1): 92–95. https://doi.org/10.1111/j.1474-9726.2009.00533.x.

Lim Kian Huat, Ferraris Luciana, Filloux Madeleine E., Raphael Benjamin J., and Fairbrother William G . 2011. “Using Positional Distribution to Identify Splicing Elements and Predict Pre-MRNA Processing Defects in Human

Genes.” n.d. Accessed April 17, 2019. https://www.ncbi.nlm.nih.gov/pmc/articles/PMC3131313/.

Ling, Li, Zhen Tan, Changning Zhang, Shuyan Gui, Yanfeng Cui, Yuanyuan Hu, and Libo Chen. 2019. “CircRNAs in Exosomes from High Glucose-Treated Glomerular Endothelial Cells Activate Mesangial Cells.” *American Journal of Translational Research* 11 (8): 4667–82.

Lisowiec, Jolanta, Dorota Magner, Elzbieta Kierzek, Elzbieta Lenartowicz, and Ryszard Kierzek. 2015. “Structural Determinants for Alternative Splicing Regulation of the MAPT Pre-MRNA.” *RNA Biology* 12 (3): 330–42. https://doi.org/10.1080/15476286.2015.1017214.

Liu, Chang, Hui-Min Ge, Bai-Hui Liu, Rui Dong, Kun Shan, Xue Chen, Mu-Di Yao, et al., 2019. “Targeting Pericyte-Endothelial Cell Crosstalk by Circular RNA-CPWWP2A Inhibition Aggravates Diabetes-Induced Microvascular Dysfunction.” *Proceedings of the National Academy of Sciences of the United States of America* 116 (15): 7455–64. https://doi.org/10.1073/pnas.1814874116.

Liu, Geng, John M. Parant, Gene Lang, Patty Chau, Arturo Chavez-Reyes, Adel K. El-Naggar, Asha Multani, Sandy Chang, and Guillermina Lozano. 2004. “Chromosome Stability, in the Absence of Apoptosis, Is Critical for Suppression of Tumorigenesis in Trp53 Mutant Mice.” *Nature Genetics* 36 (1): 63–68. https://doi.org/10.1038/ng1282.

Liu, Huijie, Xueren Wang, Horng-Dar Wang, JinJing Wu, Jing Ren, Lingfeng Meng, Qingfa Wu, et al., 2012. “Escherichia Coli Noncoding RNAs Can Affect Gene Expression and Physiology of Caenorhabditis Elegans.” *Nature Communications* 3 (September): 1073. https://doi.org/10.1038/ncomms2071.

Liu, Ying, Xiaoqing Chen, Jingjing Yao, and Jing Kang. 2019. “Circular RNA ACR Relieves High Glucose-Aroused RSC96 Cell Apoptosis and Autophagy via Declining MicroRNA-145-3p.” *Journal of Cellular Biochemistry*, December. https://doi.org/10.1002/jcb.29568.

Livak, K. J., and T. D. Schmittgen. 2001. “Analysis of Relative Gene Expression Data Using Real-Time Quantitative PCR and the 2(-Delta Delta C(T)) Method.” *Methods (San Diego, Calif.)* 25 (4): 402–8. https://doi.org/10.1006/meth.2001.1262.

Ljubenkov, Peter A., and Michael D. Geschwind. 2016. “Dementia.” *Seminars in Neurology* 36 (4): 397–404. https://doi.org/10.1055/s-0036-1585096.

López-Jiménez, Elena, Ana M. Rojas, and Eduardo Andrés-León. 2018. “RNA Sequencing and Prediction Tools for Circular RNAs Analysis.” In *Circular RNAs: Biogenesis and Functions*, edited by Junjie Xiao, 17–33. Advances in Experimental Medicine and Biology. Singapore: Springer. https://doi.org/10.1007/978-981-13-1426-1_2.

López-Otín, Carlos, Maria A. Blasco, Linda Partridge, Manuel Serrano, and Guido Kroemer. 2013. “The Hallmarks of Aging.” *Cell* 153 (6): 1194–1217. https://doi.org/10.1016/j.cell.2013.05.039.

Luger, K., A. W. Mäder, R. K. Richmond, D. F. Sargent, and T. J. Richmond. 1997. “Crystal Structure of the Nucleosome Core Particle at 2.8 A Resolution.” *Nature* 389 (6648): 251–60. https://doi.org/10.1038/38444.

Luo, Cheng, Yan Li, Hui Wang, Zhihui Feng, Yuan Li, Jiangang Long, and Jiankang Liu. 2013. “Mitochondrial Accumulation under Oxidative Stress Is Due to Defects in Autophagy.” *Journal of Cellular Biochemistry* 114 (1): 212–19. https://doi.org/10.1002/jcb.24356.

Lye, Jed, Latorre, Eva, and Harries, Lorna. 2019. “Astrocyte Senescence May Drive Alterations in GFAP(A), CDKN2A P14ARF and TAU3 Transcript Expression and Contribute to Cognitive Decline. In Press.” *Clinical Science in review*

Ma, Xiaopeng, Ge Zhan, Monica C. Sleumer, Siyu Chen, Weihong Liu, Michael Q. Zhang, and Xiao Liu. 2016. “Analysis of C. Elegans Muscle Transcriptome Using Trans-Splicing-Based RNA Tagging (SRT).” *Nucleic Acids Research* 44 (21): e156. https://doi.org/10.1093/nar/gkw734.

MacIntosh, C., J. E. Morley, and I. M. Chapman. 2000. “The Anorexia of Aging.” *Nutrition (Burbank, Los Angeles County, Calif.)* 16 (10): 983–95. https://doi.org/10.1016/s0899-9007(00)00405-6.

Maedler, Kathrin, Adriano Fontana, Frédéric Ris, Pavel Sergeev, Christian Toso, José Oberholzer, Roger Lehmann, et al., 2002. “FLIP Switches Fas-Mediated Glucose Signaling in Human Pancreatic Beta Cells from Apoptosis to Cell Replication.” *Proceedings of the National Academy of Sciences of the United States of America* 99 (12): 8236–41. https://doi.org/10.1073/pnas.122686299.

Maegawa, Shinji, George Hinkal, Hyun Soo Kim, Lanlan Shen, Li Zhang, Jiexin Zhang, Nianxiang Zhang, Shoudan Liang, Lawrence A. Donehower, and Jean-Pierre J. Issa. 2010. “Widespread and Tissue Specific Age-Related DNA Methylation Changes in Mice.” *Genome Research* 20 (3): 332–40. https://doi.org/10.1101/gr.096826.109.

Magalhães, João Pedro de, João Curado, and George M. Church. 2009. “Meta-Analysis of Age-Related Gene Expression Profiles Identifies Common Signatures of Aging.” *Bioinformatics (Oxford, England)* 25 (7): 875–81. https://doi.org/10.1093/bioinformatics/btp073.

Magalhães, João Pedro de, and João F. Passos. 2018. “Stress, Cell Senescence and Organismal Ageing.” *Mechanisms of Ageing and Development* 170: 2–9. https://doi.org/10.1016/j.mad.2017.07.001.

Mahajan, Anubha, Daniel Taliun, Matthias Thurner, Neil R. Robertson, Jason M. Torres, N. William Rayner, Anthony J. Payne, et al., 2018. “Fine-Mapping Type 2 Diabetes Loci to Single-Variant Resolution Using High-Density Imputation and Islet-Specific Epigenome Maps.” *Nature Genetics* 50 (11): 1505–13. https://doi.org/10.1038/s41588-018-0241-6.

Mahmoudi, E., and M. J. Cairns. 2019. “Circular RNAs Are Temporospatially Regulated throughout Development and Ageing in the Rat.” *Scientific Reports* 9 (February). https://doi.org/10.1038/s41598-019-38860-9.

Mangino, Massimo, Scott Brouilette, Peter Braund, Nighat Tirmizi, Mariuca Vasa-Nicotera, John R. Thompson, and Nilesh J. Samani. 2008. “A Regulatory SNP of the BICD1 Gene Contributes to Telomere Length Variation in Humans.” *Human Molecular Genetics* 17 (16): 2518–23. https://doi.org/10.1093/hmg/ddn152.

Mao Yu-Qin, Liu Jin-Feng, Han Bing and Wang Li-Shun. 2019. “Longevity-Associated Forkhead Box O3 (FOXO3) Single Nucleotide Polymorphisms Are Associated with Type 2 Diabetes Mellitus in Chinese Elderly Women.” n.d. Medical Science Monitor. Accessed September 30, 2020. https://www.medscimonit.com/download/index/idArt/913788.

Marguerat, Samuel, and Jürg Bähler. 2010. “RNA-Seq: From Technology to Biology.” *Cellular and Molecular Life Sciences* 67 (4): 569–79. https://doi.org/10.1007/s00018-009-0180-6.

Matera, A. Gregory, and Zefeng Wang. 2014. “A Day in the Life of the Spliceosome.” *Nature Reviews. Molecular Cell Biology* 15 (2): 108–21. https://doi.org/10.1038/nrm3742.

McGarry, J. Denis. 2002. “Banting Lecture 2001: Dysregulation of Fatty Acid Metabolism in the Etiology of Type 2 Diabetes.” *Diabetes* 51 (1): 7–18. https://doi.org/10.2337/diabetes.51.1.7.

Melzer, David, Joao Correa Delgado, Rachel Winder, Jane Masoli, Suzanne Richards, and Alessandro Ble. n.d. “The Age UK Almanac of Disease Profiles in Later Life,” 67.

Meng, X.; Li, X.; Zhang, P.; Wang, J.; Zhou, Y.; Chen, M. 2017. Circular RNA: An emerging key player in RNA world. *Brief. Bioinform. 18*, 547–557.

Milne, Claire. n.d. “How Much of the NHS Budget Is Spent on People over 85?” Full Fact. Accessed April 2, 2020. https://fullfact.org/health/how-much-nhs-budget-spent-people-over-85/.

Molofsky, Anna V., Shalom G. Slutsky, Nancy M. Joseph, Shenghui He, Ricardo Pardal, Janakiraman Krishnamurthy, Norman E. Sharpless, and Sean J. Morrison. 2006. “Increasing P16INK4a Expression Decreases Forebrain Progenitors and Neurogenesis during Ageing.” *Nature* 443 (7110): 448–52. https://doi.org/10.1038/nature05091.

Moro, Loredana. 2019. “Mitochondrial Dysfunction in Aging and Cancer.” *Journal of Clinical Medicine* 8 (11). https://doi.org/10.3390/jcm8111983.

Morris. B.J, Willcox D.C., Donlon T.A. and Willcox B.J. 2015. “FOXO3: A Major Gene for Human Longevity - A Mini-Review - FullText - Gerontology 2015, Vol. 61, No. 6 - Karger Publishers.” n.d. Accessed September 30, 2020. https://www.karger.com/Article/FullText/375235.

Moskalev, Alexey A., Mikhail V. Shaposhnikov, Ekaterina N. Plyusnina, Alex Zhavoronkov, Arie Budovsky, Hagai Yanai, and Vadim E. Fraifeld. 2013a. “The Role of DNA Damage and Repair in Aging through the Prism of Koch-like Criteria.” *Ageing Research Reviews* 12 (2): 661–84. https://doi.org/10.1016/j.arr.2012.02.001.

Mostoslavsky, Raul, Katrin F. Chua, David B. Lombard, Wendy W. Pang, Miriam R. Fischer, Lionel Gellon, Pingfang Liu, et al., 2006. “Genomic Instability and Aging-like Phenotype in the Absence of Mammalian SIRT6.” *Cell* 124 (2): 315–29. https://doi.org/10.1016/j.cell.2005.11.044.

Moyzis, R K, J M Buckingham, L S Cram, M Dani, L L Deaven, M D Jones, J Meyne, R L Ratliff, and J R Wu. 1988. “A Highly Conserved Repetitive DNA Sequence, (TTAGGG)n, Present at the Telomeres of Human Chromosomes.” *Proceedings of the National Academy of Sciences of the United States of America* 85 (18): 6622–26.

Mutz, Kai-Oliver, Alexandra Heilkenbrinker, Maren Lönne, Johanna-Gabriela Walter, and Frank Stahl. 2013. “Transcriptome Analysis Using Next-Generation Sequencing.” *Current Opinion in Biotechnology* 24 (1): 22–30. https://doi.org/10.1016/j.copbio.2012.09.004.

Nargund, Amrita M., Christopher J. Fiorese, Mark W. Pellegrino, Pan Deng, and Cole M. Haynes. 2015. “Mitochondrial and Nuclear Accumulation of the Transcription Factor ATFS-1 Promotes OXPHOS Recovery during the UPRmt.” *Molecular Cell* 58 (1): 123–33. https://doi.org/10.1016/j.molcel.2015.02.008.

Nargund, Amrita M., Mark W. Pellegrino, Christopher J. Fiorese, Brooke M. Baker, and Cole M. Haynes. 2012. “Mitochondrial Import Efficiency of ATFS-1 Regulates

Mitochondrial UPR Activation." *Science (New York, N.Y.)* 337 (6094): 587–90. https://doi.org/10.1126/science.1223560.

Narita, Masashi, Sabrina Nũnez, Edith Heard, Masako Narita, Athena W. Lin, Stephen A. Hearn, David L. Spector, Gregory J. Hannon, and Scott W. Lowe. 2003. "Rb-Mediated Heterochromatin Formation and Silencing of E2F Target Genes during Cellular Senescence." *Cell* 113 (6): 703–16.

Naughton, Corina, Kathleen Bennett, and John Feely. 2006. "Prevalence of Chronic Disease in the Elderly Based on a National Pharmacy Claims Database." *Age and Ageing* 35 (6): 633–36. https://doi.org/10.1093/ageing/afl106.

Nelson, Glyn, James Wordsworth, Chunfang Wang, Diana Jurk, Conor Lawless, Carmen Martin-Ruiz, and Thomas von Zglinicki. 2012. "A Senescent Cell Bystander Effect: Senescence-Induced Senescence." *Aging Cell* 11 (2): 345–49. https://doi.org/10.1111/j.1474-9726.2012.00795.x.

Newsholme, P., E. Rebelato, F. Abdulkader, M. Krause, A. Carpinelli, and R. Curi. 2012. "Reactive Oxygen and Nitrogen Species Generation, Antioxidant Defenses, and β-Cell Function: A Critical Role for Amino Acids." *The Journal of Endocrinology* 214 (1): 11–20. https://doi.org/10.1530/JOE-12-0072.

Nguyen, M. T. Audrey, Svetlana Favelyukis, Anh-Khoi Nguyen, Donna Reichart, Peter A. Scott, Alan Jenn, Ru Liu-Bryan, Christopher K. Glass, Jaap G. Neels, and Jerrold M. Olefsky. 2007. "A Subpopulation of Macrophages Infiltrates Hypertrophic Adipose Tissue and Is Activated by Free Fatty Acids via Toll-like Receptors 2 and 4 and JNK-Dependent Pathways." *The Journal of Biological Chemistry* 282 (48): 35279–92. https://doi.org/10.1074/jbc.M706762200.

Nicholson, Jeremy K., Elaine Holmes, James Kinross, Remy Burcelin, Glenn Gibson, Wei Jia, and Sven Pettersson. 2012. "Host-Gut Microbiota Metabolic

Interactions.” *Science (New York, N.Y.)* 336 (6086): 1262–67. https://doi.org/10.1126/science.1223813.

Njajou, Omer T., Richard M. Cawthon, Coleen M. Damcott, Shih-Hsuan Wu, Sandy Ott, Michael J. Garant, Elizabeth H. Blackburn, Braxton D. Mitchell, Alan R. Shuldiner, and Wen-Chi Hsueh. 2007. “Telomere Length Is Paternally Inherited and Is Associated with Parental Lifespan.” *Proceedings of the National Academy of Sciences of the United States of America* 104 (29): 12135–39. https://doi.org/10.1073/pnas.0702703104.

Odden, Michelle C., Michael G. Shlipak, Heather E. Whitson, Ronit Katz, Patricia M. Kearney, Chris defilippi, Shani Shastri, et al., 2014. “Risk Factors for Cardiovascular Disease across the Spectrum of Older Age: The Cardiovascular Health Study.” *Atherosclerosis* 237 (1): 336–42. https://doi.org/10.1016/j.atherosclerosis.2014.09.012.

Ortega-Molina, Ana, Alejo Efeyan, Elena Lopez-Guadamillas, Maribel Muñoz-Martin, Gonzalo Gómez-López, Marta Cañamero, Francisca Mulero, et al., 2012. “Pten Positively Regulates Brown Adipose Function, Energy Expenditure, and Longevity.” *Cell Metabolism* 15 (3): 382–94. https://doi.org/10.1016/j.cmet.2012.02.001.

Pan, D. A., S. Lillioja, A. D. Kriketos, M. R. Milner, L. A. Baur, C. Bogardus, A. B. Jenkins, and L. H. Storlien. 1997. “Skeletal Muscle Triglyceride Levels Are Inversely Related to Insulin Action.” *Diabetes* 46 (6): 983–88. https://doi.org/10.2337/diab.46.6.983.

Pan, Qun, Ofer Shai, Leo J. Lee, Brendan J. Frey, and Benjamin J. Blencowe. 2008. “Deep Surveying of Alternative Splicing Complexity in the Human

Transcriptome by High-Throughput Sequencing." *Nature Genetics* 40 (12): 1413–15. https://doi.org/10.1038/ng.259.

Passtoors, Willemijn M., Judith M. Boer, Jelle J. Goeman, Erik B. van den Akker, Joris Deelen, Bas J. Zwaan, Ann Scarborough, et al., 2012. "Transcriptional Profiling of Human Familial Longevity Indicates a Role for ASF1A and IL7R." *PLoS ONE* 7 (1). https://doi.org/10.1371/journal.pone.0027759.

Patel, Abhijit A., and Joan A. Steitz. 2003. "Splicing Double: Insights from the Second Spliceosome." *Nature Reviews. Molecular Cell Biology* 4 (12): 960–70. https://doi.org/10.1038/nrm1259.

Pegoraro, Gianluca, Nard Kubben, Ute Wickert, Heike Göhler, Katrin Hoffmann, and Tom Misteli. 2009. "Ageing-Related Chromatin Defects through Loss of the NURD Complex." *Nature Cell Biology* 11 (10): 1261–67. https://doi.org/10.1038/ncb1971.

Pfaffl, Michael W. 2001. "A New Mathematical Model for Relative Quantification in Real-Time RT–PCR." *Nucleic Acids Research* 29 (9): e45.

Pfister, R., D. Barnes, R. Luben, N. G. Forouhi, M. Bochud, K.-T. Khaw, N. J. Wareham, and C. Langenberg. 2011. "No Evidence for a Causal Link between Uric Acid and Type 2 Diabetes: A Mendelian Randomisation Approach." *Diabetologia* 54 (10): 2561–69. https://doi.org/10.1007/s00125-011-2235-0.

Picca, Anna, Vito Pesce, and Angela Maria Serena Lezza. 2017. "Does Eating Less Make You Live Longer and Better? An Update on Calorie Restriction." *Clinical Interventions in Aging* 12 (November): 1887–1902. https://doi.org/10.2147/CIA.S126458.

Podnar, Jessica, Heather Deiderick, Gabriella Huerta, and Scott Hunicke-Smith. 2014. "Next-Generation Sequencing RNA-Seq Library Construction." *Current*

Protocols in Molecular Biology 106 (April): 4.21.1-19. https://doi.org/10.1002/0471142727.mb0421s106.

Powers, Evan T., Richard I. Morimoto, Andrew Dillin, Jeffery W. Kelly, and William E. Balch. 2009. “Biological and Chemical Approaches to Diseases of Proteostasis Deficiency.” *Annual Review of Biochemistry* 78 (1): 959–91. https://doi.org/10.1146/annurev.biochem.052308.114844.

“Primary Culture - an Overview | ScienceDirect Topics.” n.d. Accessed April 17, 2019. https://www.sciencedirect.com/topics/neuroscience/primary-culture.

Qin, Meilin, Gang Wei, and Xiaomeng Sun. 2018. “Circ-UBR5: An Exonic Circular RNA and Novel Small Nuclear RNA Involved in RNA Splicing.” *Biochemical and Biophysical Research Communications* 503 (2): 1027–34. https://doi.org/10.1016/j.bbrc.2018.06.112.

Ragnauth, Cassandra D., Derek T. Warren, Yiwen Liu, Rosamund McNair, Tamara Tajsic, Nichola Figg, Rukshana Shroff, Jeremy Skepper, and Catherine M. Shanahan. 2010. “Prelamin A Acts to Accelerate Smooth Muscle Cell Senescence and Is a Novel Biomarker of Human Vascular Aging.” *Circulation* 121 (20): 2200–2210. https://doi.org/10.1161/CIRCULATIONAHA.109.902056.

Rahman, Abdul, Amirah, Norwahidah Abdul Karim, Noor Aini Abdul Hamid, Roslan Harun, and Wan Zurinah Wan Ngah. 2013. “Senescence-Related Changes in Gene Expression of Peripheral Blood Mononuclear Cells from Octo/Nonagenarians Compared to Their Offspring.” *Oxidative Medicine and Cellular Longevity* 2013. https://doi.org/10.1155/2013/189129.

Ramanouskaya, Tatsiana V., and Vasily V. Grinev. 2017. “The Determinants of Alternative RNA Splicing in Human Cells.” *Molecular Genetics and Genomics: MGG* 292 (6): 1175–95. https://doi.org/10.1007/s00438-017-1350-0.

Rando, Thomas A., and Howard Y. Chang. 2012. “Aging, Rejuvenation, and Epigenetic Reprogramming: Resetting the Aging Clock.” *Cell* 148 (1–2): 46–57. https://doi.org/10.1016/j.cell.2012.01.003.

Rangaraju, Sunitha, Gregory M Solis, Ryan C Thompson, Rafael L Gomez-Amaro, Leo Kurian, Sandra E Encalada, Alexander B Niculescu, Daniel R Salomon, and Michael Petrascheck. n.d. “Suppression of Transcriptional Drift Extends C. Elegans Lifespan by Postponing the Onset of Mortality.” *ELife* 4. Accessed December 16, 2019. https://doi.org/10.7554/eLife.08833.

Ravassard, Philippe, Yasmine Hazhouz, Séverine Pechberty, Emilie Bricout-Neveu, Mathieu Armanet, Paul Czernichow, and Raphael Scharfmann. 2011. “A Genetically Engineered Human Pancreatic β Cell Line Exhibiting Glucose-Inducible Insulin Secretion.” *The Journal of Clinical Investigation* 121 (9): 3589–97. https://doi.org/10.1172/JCI58447.

Rikke, Brad A., Chen-Yu Liao, Matthew B. McQueen, James F. Nelson, and Thomas E. Johnson. 2010. “Genetic Dissection of Dietary Restriction in Mice Supports the Metabolic Efficiency Model of Life Extension.” *Experimental Gerontology* 45 (9): 691–701. https://doi.org/10.1016/j.exger.2010.04.008.

Rizzacasa, Barbara, Elena Morini, Sabina Pucci, Michela Murdocca, Giuseppe Novelli, and Francesca Amati. 2017. “LOX-1 and Its Splice Variants: A New Challenge for Atherosclerosis and Cancer-Targeted Therapies.” *International Journal of Molecular Sciences* 18 (2). https://doi.org/10.3390/ijms18020290.

Rollins, Jarod A, Dan Shaffer, Santina S Snow, Pankaj Kapahi, and Aric N Rogers. 2019. “Dietary Restriction Induces Posttranscriptional Regulation of Longevity Genes.” *Life Science Alliance* 2 (4). https://doi.org/10.26508/lsa.201800281.

Rossi, Derrick J., David Bryder, Jun Seita, Andre Nussenzweig, Jan Hoeijmakers, and Irving L. Weissman. 2007. “Deficiencies in DNA Damage Repair Limit the Function of Haematopoietic Stem Cells with Age.” *Nature* 447 (7145): 725–29. https://doi.org/10.1038/nature05862.

Rossignol, Rodrigue, Benjamin Faustin, Christophe Rocher, Monique Malgat, Jean-Pierre Mazat, and Thierry Letellier. 2003. “Mitochondrial Threshold Effects.” *The Biochemical Journal* 370 (Pt 3): 751–62. https://doi.org/10.1042/BJ20021594.

Rousakis, Aris, Anna Vlanti, Fivos Borbolis, Fani Roumelioti, Marianna Kapetanou, and Popi Syntichaki. 2014. “Diverse Functions of MRNA Metabolism Factors in Stress Defense and Aging of Caenorhabditis Elegans.” *PLoS ONE* 9 (7). https://doi.org/10.1371/journal.pone.0103365.

Rubinsztein, David C., Guillermo Mariño, and Guido Kroemer. 2011. “Autophagy and Aging.” *Cell* 146 (5): 682–95. https://doi.org/10.1016/j.cell.2011.07.030.

Russell, Steven J., and C. Ronald Kahn. 2007. “Endocrine Regulation of Ageing.” *Nature Reviews. Molecular Cell Biology* 8 (9): 681–91. https://doi.org/10.1038/nrm2234.

Rutledge, R. G. 2004. “Sigmoidal Curve-Fitting Redefines Quantitative Real-Time PCR with the Prospective of Developing Automated High-Throughput Applications.” *Nucleic Acids Research* 32 (22): e178. https://doi.org/10.1093/nar/gnh177.

Ryan, Nicholas A., Kevin A. Zwetsloot, Lenna M. Westerkamp, Robert C. Hickner, Walter E. Pofahl, and Timothy P. Gavin. 2006. “Lower Skeletal Muscle Capillarization and VEGF Expression in Aged vs. Young Men.” *Journal of*

Applied Physiology (Bethesda, Md.: 1985) 100 (1): 178–85. https://doi.org/10.1152/japplphysiol.00827.2005.

Sahin, Ergün, Simona Colla, Marc Liesa, Javid Moslehi, Florian L. Müller, Mira Guo, Marcus Cooper, et al., 2011. “Telomere Dysfunction Induces Metabolic and Mitochondrial Compromise.” *Nature* 470 (7334): 359–65. https://doi.org/10.1038/nature09787.

Sanchis-Gomar, Fabian , Garatachea, Nuria , He, Zi-hong , Pareja-Galeano, Helios , Fuku, Noriyuki , Tian, Ye , Arai, Yasumichi , Abe, Yukiko , Murakami, Haruka , Miyachi, Motohiko , Yvert, Thomas , Santiago, Catalina, Venturini, Letizia, Fiuza-Luces, Carmen, Santos-Lozano, Alejandro, ,Gabriel, Rodríguez-Romo, Ricevuti, Giovanni, Hirose, Nobuyoshi, Emanuele, Enzo, and Lucia, Alejandro. 2014. “FNDC5 (Irisin) Gene and Exceptional Longevity: A Functional Replication Study with Rs16835198 and Rs726344 SNPs.” *Age (Dordr)*n.d. Accessed October 1, 2020. https://www.ncbi.nlm.nih.gov/pmc/articles/PMC4245403/.

Santoro, Aurelia, Rita Ostan, Marco Candela, Elena Biagi, Patrizia Brigidi, Miriam Capri, and Claudio Franceschi. 2018. “Gut Microbiota Changes in the Extreme Decades of Human Life: A Focus on Centenarians.” *Cellular and Molecular Life Sciences: CMLS* 75 (1): 129–48. https://doi.org/10.1007/s00018-017-2674-y.

Sarup, P., P. Sørensen, and V. Loeschcke. 2014. “The Long-Term Effects of a Life-Prolonging Heat Treatment on the Drosophila Melanogaster Transcriptome Suggest That Heat Shock Proteins Extend Lifespan.” *Experimental Gerontology* 50 (February): 34–39. https://doi.org/10.1016/j.exger.2013.11.017.

Saxton, Robert A., and David M. Sabatini. 2017. “MTOR Signaling in Growth, Metabolism, and Disease.” *Cell* 168 (6): 960–76. https://doi.org/10.1016/j.cell.2017.02.004.

Scaffidi, Paola, and Tom Misteli. 2006. “Lamin A-Dependent Nuclear Defects in Human Aging.” *Science (New York, N.Y.)* 312 (5776): 1059–63. https://doi.org/10.1126/science.1127168.

Scarim, Anna L, Marc Arnush, Jeanette R. Hill, Connie A Marshall, Aaron Baldwin, Michael L. McDaniel, and John A Corbett. 1997. “Evidence for the Presence of Type I IL-1 Receptors on β-Cells of Islets of Langerhans.” *Biochimica et Biophysica Acta (BBA) - Molecular Basis of Disease* 1361 (3): 313–20. https://doi.org/10.1016/S0925-4439(97)00039-2.

Schernthaner, Guntram, and Marie Helene Schernthaner-Reiter. 2018. “Diabetes in the Older Patient: Heterogeneity Requires Individualisation of Therapeutic Strategies.” *Diabetologia* 61 (7): 1503–16. https://doi.org/10.1007/s00125-018-4547-9.

Schmittgen, Thomas D., and Kenneth J. Livak. 2008. “Analyzing Real-Time PCR Data by the Comparative C_T Method.” *Nature Protocols* 3 (6): 1101–8. https://doi.org/10.1038/nprot.2008.73.

Schulz, Anna M., and Cole M. Haynes. 2015. “UPRmt-Mediated Cytoprotection and Organismal Aging.” *Biochimica et Biophysica Acta* 1847 (11): 1448–56. https://doi.org/10.1016/j.bbabio.2015.03.008.

Schumacher, Björn, Ingrid van der Pluijm, Michael J. Moorhouse, Theodore Kosteas, Andria Rasile Robinson, Yousin Suh, Timo M. Breit, et al., 2008. “Delayed and Accelerated Aging Share Common Longevity Assurance Mechanisms.” *PLoS Genetics* 4 (8). https://doi.org/10.1371/journal.pgen.1000161.

Schumann, Desiree M., Kathrin Maedler, Isobel Franklin, Daniel Konrad, Joachim Størling, Marianne Böni-Schnetzler, Asllan Gjinovci, et al., 2007. “The Fas Pathway Is Involved in Pancreatic Beta Cell Secretory Function.” *Proceedings of the National Academy of Sciences of the United States of America* 104 (8): 2861–66. https://doi.org/10.1073/pnas.0611487104.

Scuderi, Soraya, Valentina La Cognata, Filippo Drago, Sebastiano Cavallaro, and Velia D’Agata. 2014. “Alternative Splicing Generates Different Parkin Protein Isoforms: Evidences in Human, Rat, and Mouse Brain.” *BioMed Research International* 2014. https://doi.org/10.1155/2014/690796.

Sebastiani, Paola, Monty Montano, Annibale Puca, Nadia Solovieff, Toshio Kojima, Meng C. Wang, Efthymia Melista, et al., 2009. “RNA Editing Genes Associated with Extreme Old Age in Humans and with Lifespan in C. Elegans.” *PLoS ONE* 4 (12). https://doi.org/10.1371/journal.pone.0008210.

Sedelnikova, Olga A., Izumi Horikawa, Christophe Redon, Asako Nakamura, Drazen B. Zimonjic, Nicholas C. Popescu, and William M. Bonner. 2008. “Delayed Kinetics of DNA Double-Strand Break Processing in Normal and Pathological Aging.” *Aging Cell* 7 (1): 89–100. https://doi.org/10.1111/j.1474-9726.2007.00354.x.

Sedelnikova, Olga A., Izumi Horikawa, Drazen B. Zimonjic, Nicholas C. Popescu, William M. Bonner, and J. Carl Barrett. 2004. “Senescing Human Cells and Ageing Mice Accumulate DNA Lesions with Unrepairable Double-Strand Breaks.” *Nature Cell Biology* 6 (2): 168–70. https://doi.org/10.1038/ncb1095.

Seim, Inge, Siming Ma, and Vadim N Gladyshev. 2016. “Gene Expression Signatures of Human Cell and Tissue Longevity.” *NPJ Aging and Mechanisms of Disease* 2 (July): 16014. https://doi.org/10.1038/npjamd.2016.14.

Sekar, Shobana, and Winnie S. Liang. 2019. “Circular RNA Expression and Function in the Brain.” *Non-Coding RNA Research* 4 (1): 23–29. https://doi.org/10.1016/j.ncrna.2019.01.001.

Senn, Joseph J. 2006. “Toll-like Receptor-2 Is Essential for the Development of Palmitate-Induced Insulin Resistance in Myotubes.” *The Journal of Biological Chemistry* 281 (37): 26865–75. https://doi.org/10.1074/jbc.M513304200.

Seo, Arnold Y., Anna-Maria Joseph, Debapriya Dutta, Judy C. Y. Hwang, John P. Aris, and Christiaan Leeuwenburgh. 2010. “New Insights into the Role of Mitochondria in Aging: Mitochondrial Dynamics and More.” *Journal of Cell Science* 123 (Pt 15): 2533–42. https://doi.org/10.1242/jcs.070490.

Shan, Kun, Chang Liu, Bai-Hui Liu, Xue Chen, Rui Dong, Xin Liu, Yang-Yang Zhang, et al., 2017. “Circular Noncoding RNA HIPK3 Mediates Retinal Vascular Dysfunction in Diabetes Mellitus.” *Circulation* 136 (17): 1629–42. https://doi.org/10.1161/CIRCULATIONAHA.117.029004.

Shang, Fei-Fei, Suxin Luo, Xiaoxue Liang, and Yong Xia. 2018. “Alterations of Circular RNAs in Hyperglycemic Human Endothelial Cells.” *Biochemical and Biophysical Research Communications* 499 (3): 551–55. https://doi.org/10.1016/j.bbrc.2018.03.187.

Shaw, Wendy M., Shijing Luo, Jessica Landis, Jasmine Ashraf, and Coleen T. Murphy. 2007. “The C. Elegans TGF-Beta Dauer Pathway Regulates Longevity via Insulin Signaling.” *Current Biology: CB* 17 (19): 1635–45. https://doi.org/10.1016/j.cub.2007.08.058.

Shelton, D. N., E. Chang, P. S. Whittier, D. Choi, and W. D. Funk. 1999. “Microarray Analysis of Replicative Senescence.” *Current Biology: CB* 9 (17): 939–45. https://doi.org/10.1016/s0960-9822(99)80420-5.

Shi, Yu, Zuhua Chen, Juanjuan Gao, Si Wu, Haer Gao, and Guoshuang Feng. 2018. “Transcriptome-Wide Analysis of Alternative MRNA Splicing Signature in the Diagnosis and Prognosis of Stomach Adenocarcinoma.” *Oncology Reports* 40 (4): 2014–22. https://doi.org/10.3892/or.2018.6623.

Shimi, Takeshi, Veronika Butin-Israeli, Stephen A. Adam, Robert B. Hamanaka, Anne E. Goldman, Catherine A. Lucas, Dale K. Shumaker, Steven T. Kosak, Navdeep S. Chandel, and Robert D. Goldman. 2011. “The Role of Nuclear Lamin B1 in Cell Proliferation and Senescence.” *Genes & Development* 25 (24): 2579–93. https://doi.org/10.1101/gad.179515.111.

Shou, Yin, Li Hu, Weibo Zhang, Yuan Gao, Ping Xu, and Bimeng Zhang. 2019. “Determination of Electroacupuncture Effects on CircRNAs in Plasma Exosomes in Diabetic Mice: An RNA-Sequencing Approach.” *Evidence-Based Complementary and Alternative Medicine: ECAM* 2019: 7543049. https://doi.org/10.1155/2019/7543049.

Sibley, Christopher R, Lorea Blazquez, and Jernej Ule. 2016. “Lessons from Non-Canonical Splicing.” *Nature Reviews. Genetics* 17 (7): 407–21. https://doi.org/10.1038/nrg.2016.46.

Sigurgeirsson, Benjamín, Olof Emanuelsson, and Joakim Lundeberg. 2014. “Sequencing Degraded RNA Addressed by 3’ Tag Counting.” *PLOS ONE* 9 (3): e91851. https://doi.org/10.1371/journal.pone.0091851.

Sikora, Ewa, Anna Bielak-Zmijewska, and Grazyna Mosieniak. 2014. “Cellular Senescence in Ageing, Age-Related Disease and Longevity.” *Current Vascular Pharmacology* 12 (5): 698–706. https://doi.org/10.2174/15701611116661312190940 45.

Singh, N. P., C. E. Ogburn, N. S. Wolf, G. van Belle, and G. M. Martin. 2001. “DNA Double-Strand Breaks in Mouse Kidney Cells with Age.” *Biogerontology* 2 (4): 261–70.

Singhal, R. P., L. L. Mays-Hoopes, and G. L. Eichhorn. 1987. “DNA Methylation in Aging of Mice.” *Mechanisms of Ageing and Development* 41 (3): 199–210.

Sizzano Federico, Collino Sebastiano, Cominetti Ornella, Monti Daniela, Garagnani Paolo, Ostan Rita, Pirazzini Chiara, Bacalini Maria Giulia, Mari Daniela, Passarino Giuseppe, Franceschi Claudio, and Palini Alessio. 2018. “Evaluation of Lymphocyte Response to the Induced Oxidative Stress in a Cohort of Ageing Subjects, Including Semisupercentenarians and Their Offspring.” n.d. Accessed October 1, 2020. https://www.hindawi.com/journals/mi/2018/7109312/.

Slagboom, P. E., S. Droog, and D. I. Boomsma. 1994. “Genetic Determination of Telomere Size in Humans: A Twin Study of Three Age Groups.” *American Journal of Human Genetics* 55 (5): 876–82.

Sluss, Hayla K., Heather Armata, Judy Gallant, and Stephen N. Jones. 2004. “Phosphorylation of Serine 18 Regulates Distinct P53 Functions in Mice.” *Molecular and Cellular Biology* 24 (3): 976–84.

Smith, C. W., and J. Valcárcel. 2000. “Alternative Pre-MRNA Splicing: The Logic of Combinatorial Control.” *Trends in Biochemical Sciences* 25 (8): 381–88. https://doi.org/10.1016/s0968-0004(00)01604-2.

So, Kanji, Gen Tamura, Teiichiro Honda, Naoyuki Homma, Takayoshi Waki, Naoyuki Togawa, Satoshi Nishizuka, and Teiichi Motoyama. 2006. “Multiple Tumor Suppressor Genes Are Increasingly Methylated with Age in Non-Neoplastic

Gastric Epithelia." *Cancer Science* 97 (11): 1155–58. https://doi.org/10.1111/j.1349-7006.2006.00302.x.

Sommer, Matthias, Nina Poliak, Sunil Upadhyay, Edward Ratovitski, Barry D. Nelkin, Lawrence A. Donehower, and David Sidransky. 2006. "DeltaNp63alpha Overexpression Induces Downregulation of Sirt1 and an Accelerated Aging Phenotype in the Mouse." *Cell Cycle (Georgetown, Tex.)* 5 (17): 2005–11. https://doi.org/10.4161/cc.5.17.3194.

Song, Xiaofeng, Naibo Zhang, Ping Han, Byoung-San Moon, Rose K. Lai, Kai Wang, and Wange Lu. 2016. "Circular RNA Profile in Gliomas Revealed by Identification Tool UROBORUS." *Nucleic Acids Research* 44 (9): e87. https://doi.org/10.1093/nar/gkw075.

Southworth, Lucinda K., Art B. Owen, and Stuart K. Kim. 2009. "Aging Mice Show a Decreasing Correlation of Gene Expression within Genetic Modules." *PLoS Genetics* 5 (12). https://doi.org/10.1371/journal.pgen.1000776.

Staiger, Harald, Katrin Staiger, Norbert Stefan, Hans Günther Wahl, Fausto Machicao, Monika Kellerer, and Hans-Ulrich Häring. 2004. "Palmitate-Induced Interleukin-6 Expression in Human Coronary Artery Endothelial Cells." *Diabetes* 53 (12): 3209–16. https://doi.org/10.2337/diabetes.53.12.3209.

Stoll, Lisa, Jonathan Sobel, Adriana Rodriguez-Trejo, Claudiane Guay, Kailun Lee, Morten Trillingsgaard Venø, Jørgen Kjems, D. Ross Laybutt, and Romano Regazzi. 2018. "Circular RNAs as Novel Regulators of β-Cell Functions in Normal and Disease Conditions." *Molecular Metabolism* 9 (January): 69–83. https://doi.org/10.1016/j.molmet.2018.01.010.

Storelli, Gilles, Arnaud Defaye, Berra Erkosar, Pascal Hols, Julien Royet, and François Leulier. 2011. "Lactobacillus Plantarum Promotes Drosophila Systemic Growth

by Modulating Hormonal Signals through TOR-Dependent Nutrient Sensing." *Cell Metabolism* 14 (3): 403–14. https://doi.org/10.1016/j.cmet.2011.07.012.

Stuart, J. A., B. Karahalil, B. A. Hogue, N. C. Souza-Pinto, and V. A. Bohr. 2004. "Mitochondrial and Nuclear DNA Base Excision Repair Are Affected Differently by Caloric Restriction." *FASEB Journal: Official Publication of the Federation of American Societies for Experimental Biology* 18 (3): 595–97. https://doi.org/10.1096/fj.03-0890fje.

Suh, Yousin, Gil Atzmon, Mi-Ook Cho, David Hwang, Bingrong Liu, Daniel J. Leahy, Nir Barzilai, and Pinchas Cohen. 2008. "Functionally Significant Insulin-like Growth Factor I Receptor Mutations in Centenarians." *Proceedings of the National Academy of Sciences of the United States of America* 105 (9): 3438–42. https://doi.org/10.1073/pnas.0705467105.

Szoke, Ervin, Muhammad Z. Shrayyef, Susan Messing, Hans J. Woerle, Timon W. van Haeften, Christian Meyer, Asimina Mitrakou, Walkyria Pimenta, and John E. Gerich. 2008. "Effect of Aging on Glucose Homeostasis: Accelerated Deterioration of β-Cell Function in Individuals with Impaired Glucose Tolerance." *Diabetes Care* 31 (3): 539–43. https://doi.org/10.2337/dc07-1443.

Tabrez, Syed Shamsh, Ravi Datta Sharma, Vaibhav Jain, Atif Ahmed Siddiqui, and Arnab Mukhopadhyay. 2017. "Differential Alternative Splicing Coupled to Nonsense-Mediated Decay of MRNA Ensures Dietary Restriction-Induced Longevity." *Nature Communications* 8 (August). https://doi.org/10.1038/s41467-017-00370-5.

Talens, Rudolf P., Kaare Christensen, Hein Putter, Gonneke Willemsen, Lene Christiansen, Dennis Kremer, H. Eka D. Suchiman, P. Eline Slagboom, Dorret I. Boomsma, and Bastiaan T. Heijmans. 2012. "Epigenetic Variation during the

Adult Lifespan: Cross-Sectional and Longitudinal Data on Monozygotic Twin Pairs." *Aging Cell* 11 (4): 694–703. https://doi.org/10.1111/j.1474-9726.2012.00835.x.

Tatar, M., A. Kopelman, D. Epstein, M. P. Tu, C. M. Yin, and R. S. Garofalo. 2001. "A Mutant Drosophila Insulin Receptor Homolog That Extends Life-Span and Impairs Neuroendocrine Function." *Science (New York, N.Y.)* 292 (5514): 107–10. https://doi.org/10.1126/science.1057987.

Temperley, Richard J., Sara H. Seneca, Katarzyna Tonska, Ewa Bartnik, Laurence A. Bindoff, Robert N. Lightowlers, and Zofia M. A. Chrzanowska-Lightowlers. 2003. "Investigation of a Pathogenic MtDNA Microdeletion Reveals a Translation-Dependent Deadenylation Decay Pathway in Human Mitochondria." *Human Molecular Genetics* 12 (18): 2341–48. https://doi.org/10.1093/hmg/ddg238.

Tindale, Lauren C., Stephen Leach, John J. Spinelli, and Angela R. Brooks-Wilson. 2017. "Lipid and Alzheimer's Disease Genes Associated with Healthy Aging and Longevity in Healthy Oldest-Old." *Oncotarget* 8 (13): 20612–21. https://doi.org/10.18632/oncotarget.15296.

Tollervey, James R., Tomaž Curk, Boris Rogelj, Michael Briese, Matteo Cereda, Melis Kayikci, Tibor Hortobágyi, et al., 2011. "Characterising the RNA Targets and Position-Dependent Splicing Regulation by TDP-43; Implications for Neurodegenerative Diseases." *Nature Neuroscience* 14 (4): 452–58. https://doi.org/10.1038/nn.2778.

Tollervey, James R., Zhen Wang, Tibor Hortobágyi, Joshua T. Witten, Kathi Zarnack, Melis Kayikci, Tyson A. Clark, et al., 2011. "Analysis of Alternative Splicing

Associated with Aging and Neurodegeneration in the Human Brain." *Genome Research* 21 (10): 1572–82. https://doi.org/10.1101/gr.122226.111.

Tomaru, Utano, Satomi Takahashi, Akihiro Ishizu, Yukiko Miyatake, Aya Gohda, Sayuri Suzuki, Ayako Ono, et al., 2012. "Decreased Proteasomal Activity Causes Age-Related Phenotypes and Promotes the Development of Metabolic Abnormalities." *The American Journal of Pathology* 180 (3): 963–72. https://doi.org/10.1016/j.ajpath.2011.11.012.

Tominaga, Kaoru. 2015. "The Emerging Role of Senescent Cells in Tissue Homeostasis and Pathophysiology." *Pathobiology of Aging & Age-Related Diseases* 5 (May). https://doi.org/10.3402/pba.v5.27743.

Ungvari, Zoltan, Gabor Kaley, Rafael de Cabo, William E. Sonntag, and Anna Csiszar. 2010. "Mechanisms of Vascular Aging: New Perspectives." *The Journals of Gerontology. Series A, Biological Sciences and Medical Sciences* 65 (10): 1028–41. https://doi.org/10.1093/gerona/glq113.

Urakawa, Itaru, Yuji Yamazaki, Takashi Shimada, Kousuke Iijima, Hisashi Hasegawa, Katsuya Okawa, Toshiro Fujita, Seiji Fukumoto, and Takeyoshi Yamashita. 2006. "Klotho Converts Canonical FGF Receptor into a Specific Receptor for FGF23." *Nature* 444 (7120): 770. https://doi.org/10.1038/nature05315.

Vasa-Nicotera, Mariuca, Scott Brouilette, Massimo Mangino, John R. Thompson, Peter Braund, Jenny-Rebecca Clemitson, Andrea Mason, et al., 2005. "Mapping of a Major Locus That Determines Telomere Length in Humans." *American Journal of Human Genetics* 76 (1): 147–51.

Vellai, Tibor, Krisztina Takacs-Vellai, Yue Zhang, Attila L. Kovacs, László Orosz, and Fritz Müller. 2003. "Genetics: Influence of TOR Kinase on Lifespan in C. Elegans." *Nature* 426 (6967): 620. https://doi.org/10.1038/426620a.

Vijg, Jan, and Judith Campisi. 2008. “Puzzles, Promises and a Cure for Ageing.” *Nature* 454 (7208): 1065–71. https://doi.org/10.1038/nature07216.

Vilchez, David, Isabel Saez, and Andrew Dillin. 2014. “The Role of Protein Clearance Mechanisms in Organismal Ageing and Age-Related Diseases.” *Nature Communications* 5 (December): 5659. https://doi.org/10.1038/ncomms6659.

Vitale, Giovanni, Michael P Brugts, Giulia Ogliari, Davide Castaldi, Letizia M. Fatti, Aimee J. Varewijck, Steven W. Lamberts, et al., 2012. “Low Circulating IGF-I Bioactivity Is Associated with Human Longevity: Findings in Centenarians’ Offspring.” *Aging (Albany NY)* 4 (9): 580–89.

Wagatsuma, A. 2006. “Effect of Aging on Expression of Angiogenesis-Related Factors in Mouse Skeletal Muscle.” *Experimental Gerontology* 41 (1): 49–54. https://doi.org/10.1016/j.exger.2005.10.003.

Waki, Takayoshi, Gen Tamura, Makoto Sato, and Teiichi Motoyama. 2003. “Age-Related Methylation of Tumor Suppressor and Tumor-Related Genes: An Analysis of Autopsy Samples.” *Oncogene* 22 (26): 4128–33. https://doi.org/10.1038/sj.onc.1206651.

Wallace, Douglas C. 2005. “A Mitochondrial Paradigm of Metabolic and Degenerative Diseases, Aging, and Cancer: A Dawn for Evolutionary Medicine.” *Annual Review of Genetics* 39 (1): 359–407. https://doi.org/10.1146/annurev.genet.39.110304.095751.

Walther, Dirk M., Prasad Kasturi, Min Zheng, Stefan Pinkert, Giulia Vecchi, Prajwal Ciryam, Richard I. Morimoto, et al., 2015. “Proteome Imbalance Is Linked with Proteostasis Decline and Aggregation in Aging C. Elegans.” *Cell* 161 (4): 919–32. https://doi.org/10.1016/j.cell.2015.03.032.

Wang, Aoxue, Maria A. Toma, Jingxin Ma, Dongqing Li, Manika Vij, Tongbin Chu, Jing Wang, Xi Li, and Ning Xu Landén. 2020. “Circular RNA Hsa_circ_0084443 Is Upregulated in Diabetic Foot Ulcer and Modulates Keratinocyte Migration and Proliferation.” *Advances in Wound Care* 9 (4): 145–60. https://doi.org/10.1089/wound.2019.0956.

Wang, Huiyan, Guangtong She, Wenbai Zhou, Kezhuo Liu, Jun Miao, and Bin Yu. 2019. “Expression Profile of Circular RNAs in Placentas of Women with Gestational Diabetes Mellitus.” *Endocrine Journal* 66 (5): 431–41. https://doi.org/10.1507/endocrj.EJ18-0291.

Wang, Liang, Tianyou Luo, Zhihua Bao, Yuan Li, and WenJin Bu. 2018. “Intrathecal CircHIPK3 ShRNA Alleviates Neuropathic Pain in Diabetic Rats.” *Biochemical and Biophysical Research Communications* 505 (3): 644–50. https://doi.org/10.1016/j.bbrc.2018.09.158.

Wang, Yang, and Zefeng Wang. 2014. “Systematical Identification of Splicing Regulatory Cis-Elements and Cognate Trans-Factors.” *Methods (San Diego, Calif.)* 65 (3): 350–58. https://doi.org/10.1016/j.ymeth.2013.08.019.

Welle S, Brooks AI, Delehanty JM, Needler N, Bhatt K, Shah B, Thornton CA (2004) Skeletal muscle gene expression profiles in 20-29-year-old and 65-71-year-old women. Exp Gerontol 39:369–377. https://doi.org/10.1016/j.exger.2003.11.011

Wen, Si, Shuangliang Li, Lulu Li, and Qiuling Fan. 2020. “CircACTR2: A Novel Mechanism Regulating High Glucose-Induced Fibrosis in Renal Tubular Cells via Pyroptosis.” *Biological & Pharmaceutical Bulletin* 43 (3): 558–64. https://doi.org/10.1248/bpb.b19-00901.

Wheeler, Heather E., and Stuart K. Kim. 2011. “Genetics and Genomics of Human Ageing.” *Philosophical Transactions of the Royal Society B: Biological Sciences* 366 (1561): 43–50. https://doi.org/10.1098/rstb.2010.0259.

Wilding, John P. H. 2014. “The Role of the Kidneys in Glucose Homeostasis in Type 2 Diabetes: Clinical Implications and Therapeutic Significance through Sodium Glucose Co-Transporter 2 Inhibitors.” *Metabolism: Clinical and Experimental* 63 (10): 1228–37. https://doi.org/10.1016/j.metabol.2014.06.018.

Will, Cindy L., and Reinhard Lührmann. 2011. “Spliceosome Structure and Function.” *Cold Spring Harbor Perspectives in Biology* 3 (7). https://doi.org/10.1101/cshperspect.a003707.

Willcox, Bradley J., Timothy A. Donlon, Qimei He, Randi Chen, John S. Grove, Katsuhiko Yano, Kamal H. Masaki, D. Craig Willcox, Beatriz Rodriguez, and J. David Curb. 2008. “FOXO3A Genotype Is Strongly Associated with Human Longevity.” *Proceedings of the National Academy of Sciences* 105 (37): 13987–92. https://doi.org/10.1073/pnas.0801030105.

Wu, Hangyu, Siyang Wu, Yingchao Zhu, Mei Ye, Jun Shen, Yan Liu, Yisheng Zhang, and Shizhong Bu. 2019. “Hsa_circRNA_0054633 Is Highly Expressed in Gestational Diabetes Mellitus and Closely Related to Glycosylation Index.” *Clinical Epigenetics* 11 (1): 22. https://doi.org/10.1186/s13148-019-0610-8.

Wu, Yu, Hua Huang, Zoe Miner, and Molly Kulesz-Martin. 1997. “Activities and Response to DNA Damage of Latent and Active Sequence-Specific DNA Binding Forms of Mouse P53.” *Proceedings of the National Academy of Sciences of the United States of America* 94 (17): 8982–87.

Xiao, Fu-Hui, Xiao-Qiong Chen, Qin Yu, Yunshuang Ye, Yao-Wen Liu, Dongjing Yan, Li-Qin Yang, et al., 2018. “Transcriptome Evidence Reveals Enhanced

Autophagy-Lysosomal Function in Centenarians." *Genome Research* 28 (11): 1601–10. https://doi.org/10.1101/gr.220780.117.

Xu, Huanyu, Sen Guo, Wei Li, and Ping Yu. 2015. "The Circular RNA Cdr1as, via MiR-7 and Its Targets, Regulates Insulin Transcription and Secretion in Islet Cells." *Scientific Reports* 5 (July). https://doi.org/10.1038/srep12453.

Xu, Kaiyu, Chen, Dong, Wang, Zhengbo , Ma, Jian, Zhou, Jian, Chen, Nanhui, Lv, Longbao, Zheng, Yongtang, Hu, Xintian, Zhang, Yi and Jiali, Li . 2018. "Annotation and Functional Clustering of CircRNA Expression in Rhesus Macaque Brain during Aging | Cell Discovery." n.d. Accessed October 1, 2020. https://www.nature.com/articles/s41421-018-0050-1.

Xu, Ming, Allyson K Palmer, Husheng Ding, Megan M Weivoda, Tamar Pirtskhalava, Thomas A White, Anna Sepe, et al., n.d. "Targeting Senescent Cells Enhances Adipogenesis and Metabolic Function in Old Age." *ELife* 4. Accessed April 16, 2019. https://doi.org/10.7554/eLife.12997.

Xu, Ming, Tamar Pirtskhalava, Joshua N. Farr, Bettina M. Weigand, Allyson K. Palmer, Megan M. Weivoda, Christina L. Inman, et al., 2018. "Senolytics Improve Physical Function and Increase Lifespan in Old Age." *Nature Medicine* 24 (8): 1246–56. https://doi.org/10.1038/s41591-018-0092-9.

Xu, Ming, Tamara Tchkonia, Husheng Ding, Mikolaj Ogrodnik, Ellen R. Lubbers, Tamar Pirtskhalava, Thomas A. White, et al., 2015. "JAK Inhibition Alleviates the Cellular Senescence-Associated Secretory Phenotype and Frailty in Old Age." *Proceedings of the National Academy of Sciences of the United States of America* 112 (46): E6301-6310. https://doi.org/10.1073/pnas.1515386112.

Yach, Derek, Corinna Hawkes, C. Linn Gould, and Karen J. Hofman. 2004. "The Global Burden of Chronic Diseases: Overcoming Impediments to Prevention

and Control." *JAMA* 291 (21): 2616–22. https://doi.org/10.1001/jama.291.21.2616.

Yaghootkar, Hanieh, Claudia Lamina, Robert A. Scott, Zari Dastani, Marie-France Hivert, Liling L. Warren, Alena Stancáková, et al., 2013. "Mendelian Randomization Studies Do Not Support a Causal Role for Reduced Circulating Adiponectin Levels in Insulin Resistance and Type 2 Diabetes." *Diabetes* 62 (10): 3589–98. https://doi.org/10.2337/db13-0128.

Yan, Lin, Dorothy E. Vatner, J. Patrick O'Connor, Andreas Ivessa, Hui Ge, Wei Chen, Shinichi Hirotani, Yoshihiro Ishikawa, Junichi Sadoshima, and Stephen F. Vatner. 2007. "Type 5 Adenylyl Cyclase Disruption Increases Longevity and Protects against Stress." *Cell* 130 (2): 247–58. https://doi.org/10.1016/j.cell.2007.05.038.

Yan, Linping, Jie Feng, Feng Cheng, Xianwei Cui, Lingjuan Gao, Yajun Chen, Fei Wang, Tianying Zhong, Yun Li, and Lan Liu. 2018. "Circular RNA Expression Profiles in Placental Villi from Women with Gestational Diabetes Mellitus." *Biochemical and Biophysical Research Communications* 498 (4): 743–50. https://doi.org/10.1016/j.bbrc.2018.03.051.

Yang, Fan, Anqi Li, Ying Qin, Hui Che, Yueqiu Wang, Jie Lv, Yang Li, et al., 2019. "A Novel Circular RNA Mediates Pyroptosis of Diabetic Cardiomyopathy by Functioning as a Competing Endogenous RNA." *Molecular Therapy. Nucleic Acids* 17 (September): 636–43. https://doi.org/10.1016/j.omtn.2019.06.026.

Yang, Zhen, Andrew Wong, Diana Kuh, Dirk S. Paul, Vardhman K. Rakyan, R. David Leslie, Shijie C. Zheng, Martin Widschwendter, Stephan Beck, and Andrew E. Teschendorff. 2016. "Correlation of an Epigenetic Mitotic Clock with Cancer

Risk.” *Genome Biology* 17 (1): 205. https://doi.org/10.1186/s13059-016-1064-3.

Yavropoulou, Maria P., Christos Poulios, Nickos Michalopoulos, Ariadni Gatzou, Sofia Chrisafi, Stylianos Mantalovas, Theodosis Papavramidis, et al., 2018. “A Role for Circular Non-Coding RNAs in the Pathogenesis of Sporadic Parathyroid Adenomas and the Impact of Gender-Specific Epigenetic Regulation.” *Cells* 8 (1). https://doi.org/10.3390/cells8010015.

Ye, Zheng, Stephen J. Sharp, Stephen Burgess, Robert A. Scott, Fumiaki Imamura, InterAct Consortium, Claudia Langenberg, Nicholas J. Wareham, and Nita G. Forouhi. 2015. “Association between Circulating 25-Hydroxyvitamin D and Incident Type 2 Diabetes: A Mendelian Randomisation Study.” *The Lancet. Diabetes & Endocrinology* 3 (1): 35–42. https://doi.org/10.1016/S2213-8587(14)70184-6.

Yerges-Armstrong, Laura M., Sumbul Chai, Jeffery R. O’Connell, Joanne E. Curran, John Blangero, Braxton D. Mitchell, Alan R. Shuldiner, and Coleen M. Damcott. 2016. “Gene Expression Differences Between Offspring of Long-Lived Individuals and Controls in Candidate Longevity Regions: Evidence for PAPSS2 as a Longevity Gene.” *The Journals of Gerontology Series A: Biological Sciences and Medical Sciences* 71 (10): 1295–99. https://doi.org/10.1093/gerona/glv212.

Yuan, Rong, Shirng-Wern Tsaih, Stefka B. Petkova, Caralina Marin de Evsikova, Shuqin Xing, Michael A. Marion, Molly A. Bogue, et al., 2009. “Aging in Inbred Strains of Mice: Study Design and Interim Report on Median Lifespans and Circulating IGF1 Levels.” *Aging Cell* 8 (3): 277–87. https://doi.org/10.1111/j.1474-9726.2009.00478.x.

Zahn, Jacob M., Rebecca Sonu, Hannes Vogel, Emily Crane, Krystyna Mazan-Mamczarz, Ralph Rabkin, Ronald W. Davis, Kevin G. Becker, Art B. Owen, and Stuart K. Kim. 2006. “Transcriptional Profiling of Aging in Human Muscle Reveals a Common Aging Signature.” *PLoS Genetics* 2 (7): e115. https://doi.org/10.1371/journal.pgen.0020115.eor.

Zhang, Guo, Juxue Li, Sudarshana Purkayastha, Yizhe Tang, Hai Zhang, Ye Yin, Bo Li, Gang Liu, and Dongsheng Cai. 2013. “Hypothalamic Programming of Systemic Aging Involving IKKβ/NF-KB and GnRH.” *Nature* 497 (7448): 211–16. https://doi.org/10.1038/nature12143.

Zhang, Rugang, Maxim V. Poustovoitov, Xiaofen Ye, Hidelita A. Santos, Wei Chen, Sally M. Daganzo, Jan P. Erzberger, et al., 2005. “Formation of MacroH2A-Containing Senescence-Associated Heterochromatin Foci and Senescence Driven by ASF1a and HIRA.” *Developmental Cell* 8 (1): 19–30. https://doi.org/10.1016/j.devcel.2004.10.019.

Zhang, Rui, and Aixin Hou. 2013. “Host-Microbe Interactions in Caenorhabditis Elegans.” *ISRN Microbiology* 2013 (August). https://doi.org/10.1155/2013/356451.

Zhang, Shu-Jie, Xue Chen, Chao-Peng Li, Xiu-Miao Li, Chang Liu, Bai-Hui Liu, Kun Shan, Qin Jiang, Chen Zhao, and Biao Yan. 2017. “Identification and Characterization of Circular RNAs as a New Class of Putative Biomarkers in Diabetes Retinopathy.” *Investigative Ophthalmology & Visual Science* 58 (14): 6500–6509. https://doi.org/10.1167/iovs.17-22698.

Zhu, Ke, Xin Hu, Han Chen, Fang Li, Ning Yin, Ai-Lin Liu, Kun Shan, et al., 2019. “Downregulation of CircRNA DMNT3B Contributes to Diabetic Retinal Vascular

Dysfunction through Targeting MiR-20b-5p and BAMBI." *EBioMedicine* 49 (November): 341–53. https://doi.org/10.1016/j.ebiom.2019.10.004.

Zieman, Susan J., Vojtech Melenovsky, and David A. Kass. 2005. "Mechanisms, Pathophysiology, and Therapy of Arterial Stiffness." *Arteriosclerosis, Thrombosis, and Vascular Biology* 25 (5): 932–43. https://doi.org/10.1161/01.ATV.0000160548.78317.29.

Appendix

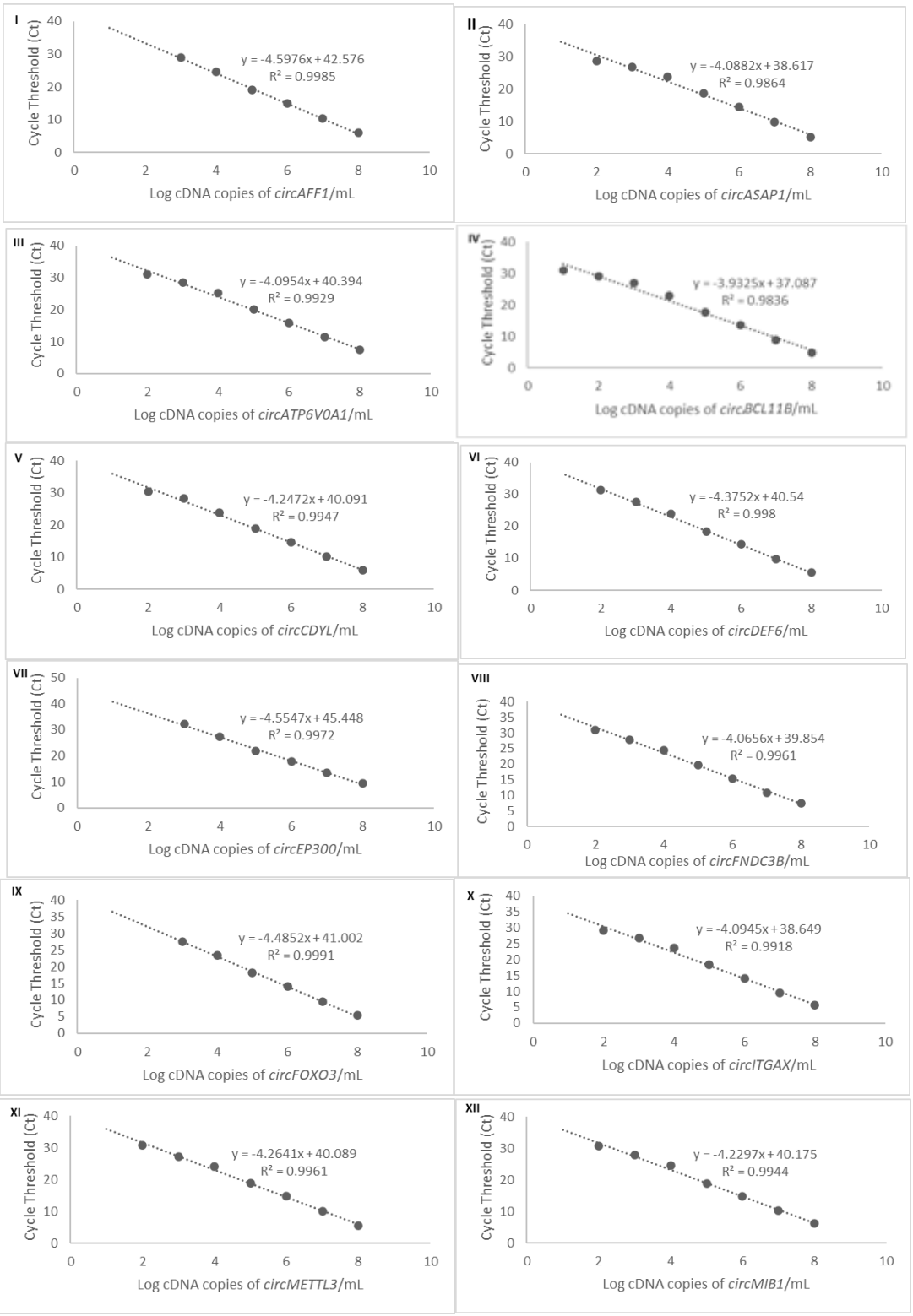
I
Cycle Threshold (Ct)
y = -4.5976x + 42.576
R² = 0.9985
Log cDNA copies of circAFF1/mL
II
y = -4.0882x + 38.617
R² = 0.9864
Log cDNA copies of circASAP1/mL
III
y = -4.0954x + 40.394
R² = 0.9929
Log cDNA copies of circATP6V0A1/mL
IV
y = -3.9325x + 37.087
R² = 0.9836
Log cDNA copies of circBCL11B/mL
V
y = -4.2472x + 40.091
R² = 0.9947
Log cDNA copies of circCDYL/mL
VI
y = -4.3752x + 40.54
R² = 0.998
Log cDNA copies of circDEF6/mL
VII
y = -4.5547x + 45.448
R² = 0.9972
Log cDNA copies of circEP300/mL
VIII
y = -4.0656x + 39.854
R² = 0.9961
Log cDNA copies of circFNDC3B/mL
IX
y = -4.4852x + 41.002
R² = 0.9991
Log cDNA copies of circFOXO3/mL
X
y = -4.0945x + 38.649
R² = 0.9918
Log cDNA copies of circITGAX/mL
XI
y = -4.2641x + 40.089
R² = 0.9961
Log cDNA copies of circMETTL3/mL
XII
y = -4.2297x + 40.175
R² = 0.9944
Log cDNA copies of circMIB1/mL

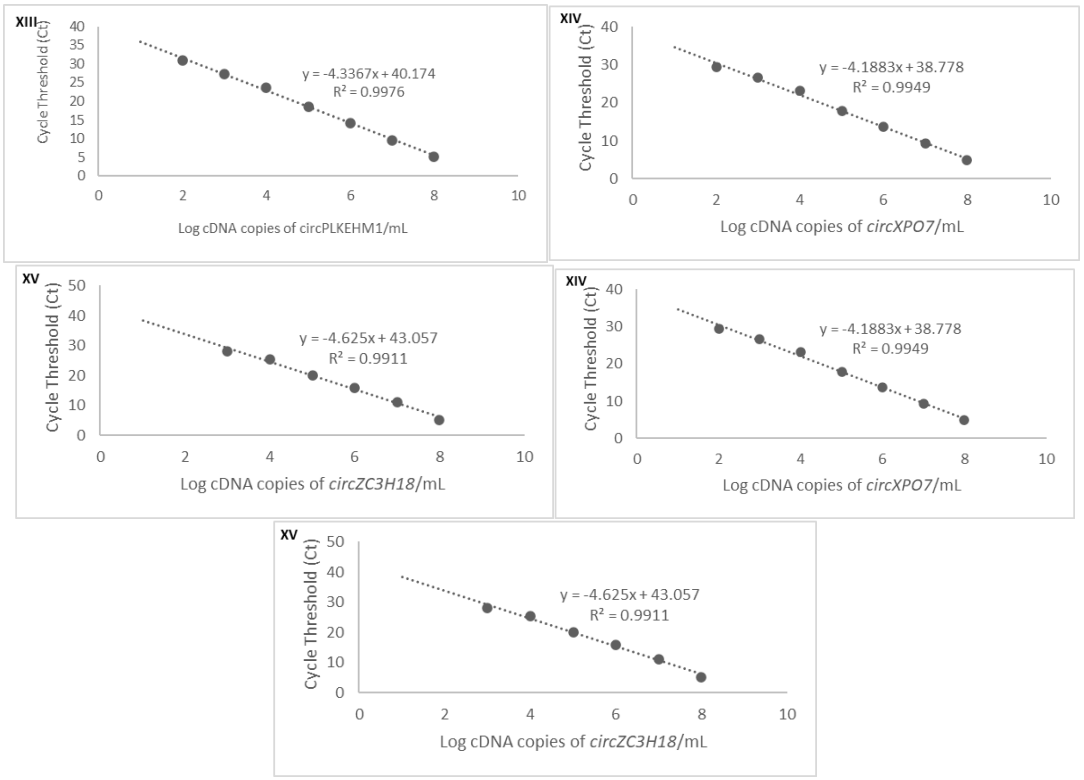

Figure A1 Standard curves for circRNA assays used in ageing study. *Standard curves were generated using standard oligos against the backsplice junction of each circRNA as proxy of cDNA (shown in X-axis). Log dilution of representative cDNA concentration are shown on the X-axis and cycle thershold (Ct) as expected in qPCR shown on the Y-axis. Assays are circAFFA1 (I), circASAP1 (II), circATP6V0A1 (III), circBCL11B (IV), circCDYL (V), circDEF6 (VI), circEP300 (VII), circFNDC3B (VIII), circFOXO3 (IX), circITGAX (X), circMETTL3 (XI), circMIB1 (XII), circPLEKHM1 (XIII), circXPO7 (XIV) and circZC3H18 (XV).*

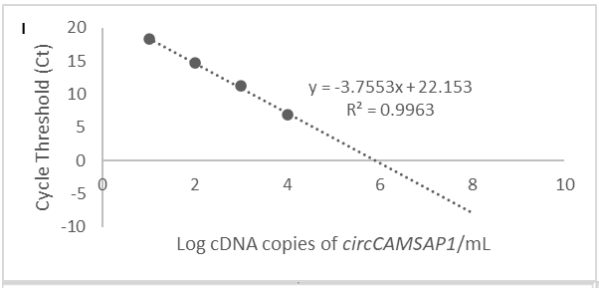
I
Cycle Threshold (Ct)
y = -3.7553x + 22.153
R² = 0.9963
Log cDNA copies of circCAMSAP1/mL

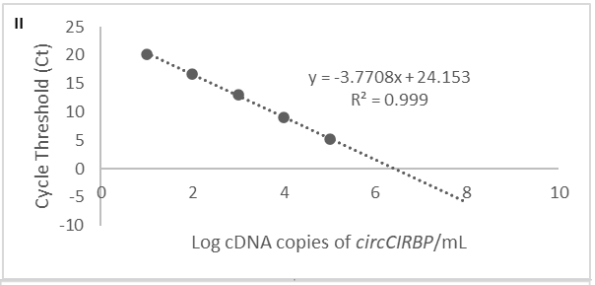
II
Cycle Threshold (Ct)
y = -3.7708x + 24.153
R² = 0.999
Log cDNA copies of circCIRBP/mL

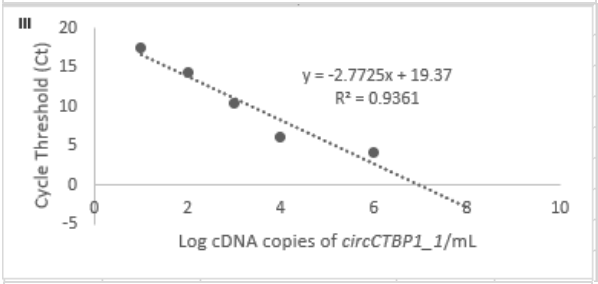
III
Cycle Threshold (Ct)
y = -2.7725x + 19.37
R² = 0.9361
Log cDNA copies of circCTBP1_1/mL

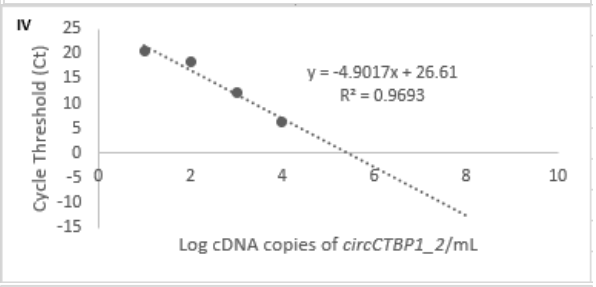
IV
Cycle Threshold (Ct)
y = -4.9017x + 26.61
R² = 0.9693
Log cDNA copies of circCTBP1_2/mL

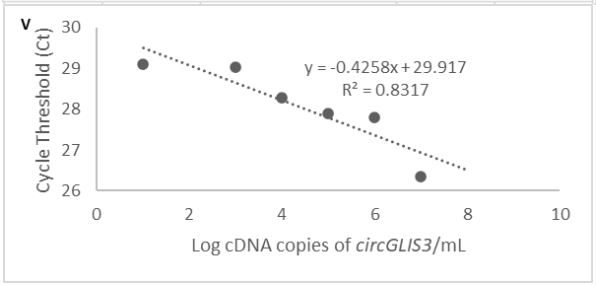
V
Cycle Threshold (Ct)
y = -0.4258x + 29.917
R² = 0.8317
Log cDNA copies of circGLIS3/mL

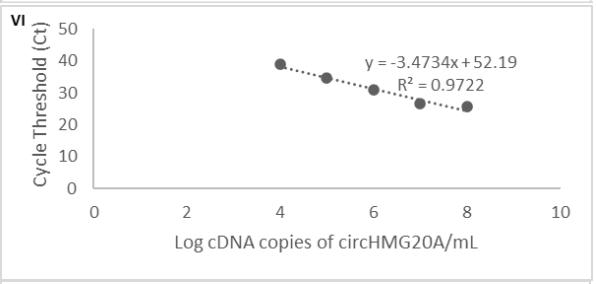
VI
Cycle Threshold (Ct)
y = -3.4734x + 52.19
R² = 0.9722
Log cDNA copies of circHMG20A/mL

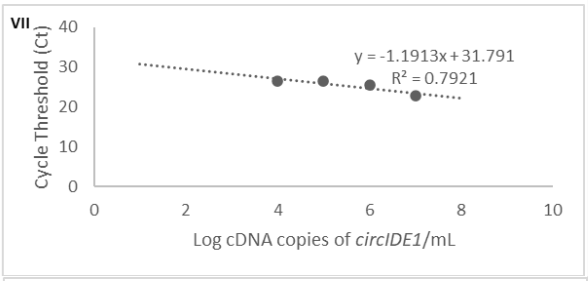
VII
Cycle Threshold (Ct)
y = -1.1913x + 31.791
R² = 0.7921
Log cDNA copies of circIDE1/mL

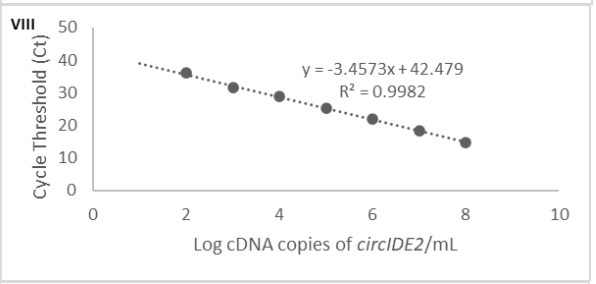
VIII
Cycle Threshold (Ct)
y = -3.4573x + 42.479
R² = 0.9982
Log cDNA copies of circIDE2/mL

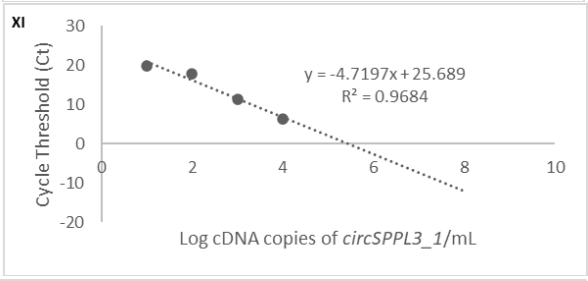
XI
Cycle Threshold (Ct)
y = -4.7197x + 25.689
R² = 0.9684
Log cDNA copies of circSPPL3_1/mL

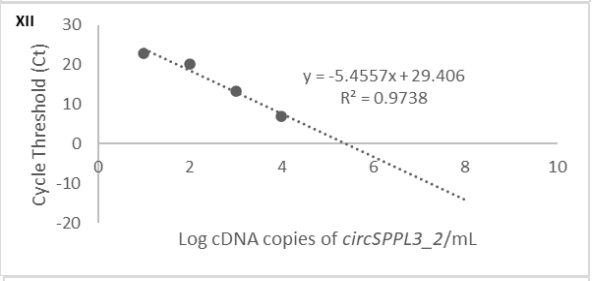
XII
Cycle Threshold (Ct)
y = -5.4557x + 29.406
R² = 0.9738
Log cDNA copies of circSPPL3_2/mL

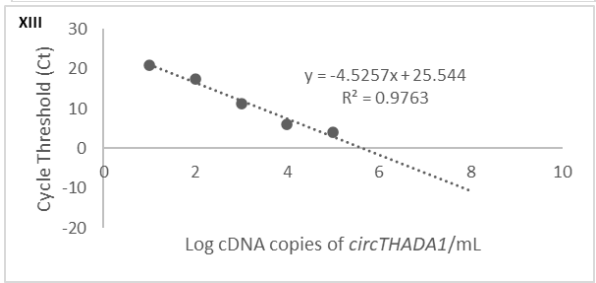
XIII
Cycle Threshold (Ct)
y = -4.5257x + 25.544
R² = 0.9763
Log cDNA copies of circTHADA1/mL

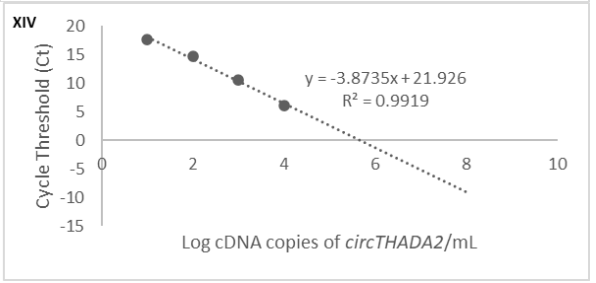
XIV
Cycle Threshold (Ct)
y = -3.8735x + 21.926
R² = 0.9919
Log cDNA copies of circTHADA2/mL

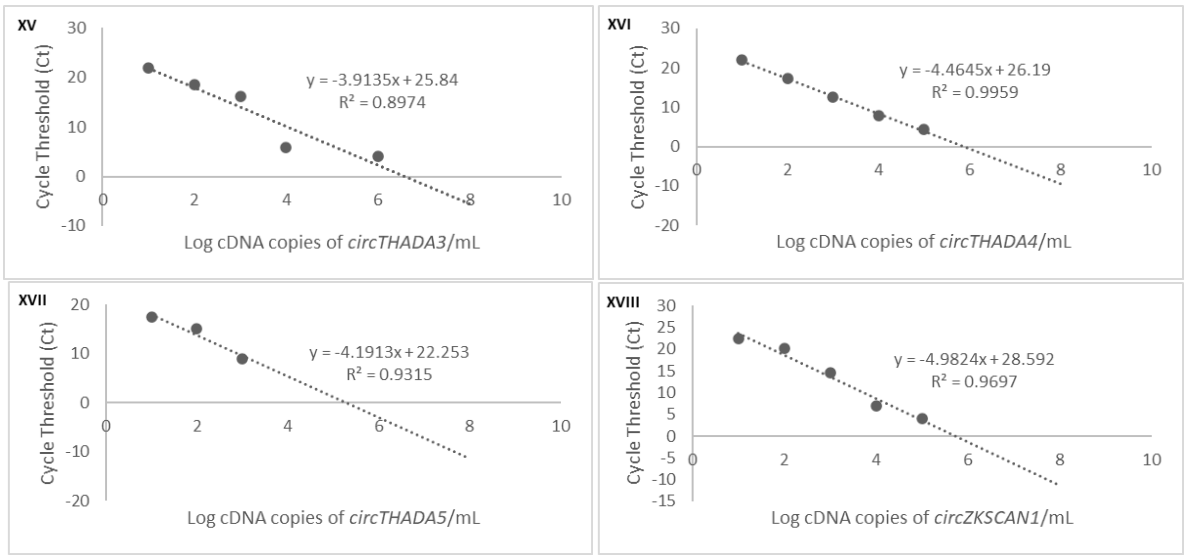

Figure A2 Standard curves for circRNA assays used in diabetes study. *Standard curves were generated using standard oligos against the backsplice junction of each circRNA as proxy of cDNA (shown in X-axis). Log dilution of representative cDNA concentration are shown on the X-axis and cycle thershold (Ct) as expected in qPCR shown on the Y-axis. Assays are circCAMSAP1 (I), circCIRBP (II), circCTBP1_1 (III), circCTBP1_2 (IV), circGLIS3 (V), circHMG20A (VI), circIDE1 (VII), circIDE2 (VIII), circRHOBTB3(IX), circRPH3AL(X), circSPPL3_1(XI), circSPPL3_2(XII), circTHADA1 (XIII), circTHADA2 (XIV), circTHADA3 (XV), circTHADA4(XVI), circTHADA5 (XVII) and circZKSCAN1(XVIII).*

```
import pandas as pd

ptes_islet =
'//isad.isadroot.ex.ac.uk/UOE/User/Desktop/Shahnaz/data/ptes_islet.txt'

cir49 = pd.read_csv(ptes_islet, sep='\t', header=None)
cir49.columns = ['cirID', 'Chr' ,'start' , 'stop']
print(cir49.head())


SNPGWAS = '//isad.isadroot.ex.ac.uk/UOE/User/Desktop/SNPGWAS.txt'

#df = pd.read_csv(SNPGWAS, sep='\t', header=None)
SNPloci = pd.read_csv(SNPGWAS, sep='\s+', header=None)
SNPloci.columns = ['Chr' ,'start' , 'stop']
print(SNPloci.head())

    subset_cir = cir49.loc[cir49['Chr'] == 'chr1']
    print(subset_cir.head())

subset = SNPloci.loc[SNPloci['Chr'] == 'chr1']
print(subset.head())

for index1, row1 in subset_cir.iterrows():
    for index2, row2 in subset.iterrows():
        print('loci-start:{1}\tcir-start:{0}\tcir-stop:{2}\tloci-
stop:{3}'.format(row1['start'], row2['start'],row1['stop'], row2['stop']))
```

Figure A3 Python code used to detect circRNA that co-localised with known T2D GWAS signal. *The co-ordinates of the circRNA were cross-refrenced with the co-ordinates of the windows of established T2D risk GWAS loci. The lead SNP of the GWAS signal within which circRNAs mapped were used as the genotype to examine any association of the genotype with the expression of the concerned circRNAs.*

genes

Review

Circular RNAs (circRNAs) in Health and Disease

Shahnaz Haque and Lorna W. Harries *

RNA-Mediated Mechanisms of Disease Group, Institute of Biomedical and Clinical Sciences, University of Exeter Medical School, Barrack Road, Exeter EX2 5DW, UK; sh683@exeter.ac.uk

* Correspondence: L.W.Harries@exeter.ac.uk; Tel.: +44-1392-406749; Fax: +44-1392-406767

Received: 19 October 2017; Accepted: 22 November 2017; Published: 28 November 2017

Abstract: Splicing events do not always produce a linear transcript. Circular RNAs (circRNAs) are a class of RNA that are emerging as key new members of the gene regulatory milieu, which are produced by back-splicing events within genes. In circRNA formation, rather than being spliced in a linear fashion, exons can be circularised by use of the 3^0 acceptor splice site of an upstream exon, leading to the formation of a circular RNA species. circRNAs have been demonstrated across species and have the potential to present genetic information in new orientations distinct from their parent transcript. The importance of these RNA players in gene regulation and normal cellular homeostasis is now beginning to be recognised. They have several potential modes of action, from serving as sponges for micro RNAs and RNA binding proteins, to acting as transcriptional regulators. In accordance with an important role in the normal biology of the cell, perturbations of circRNA expression are now being reported in association with disease. Furthermore, the inherent stability of circRNAs conferred by their circular structure and exonuclease resistance, and their expression in blood and other peripheral tissues in association with endosomes and microvesicles, renders them excellent candidates as disease biomarkers. In this review, we explore the state of knowledge on this exciting class of transcripts in regulating gene expression and discuss their emerging role in health and disease.

Keywords: Circular RNAs; back-splicing; gene regulation; biomarkers; human disease

1. Introduction

Circular RNAs (circRNAs) are an emerging class of RNA species that are present in species as diverse as archaea, flies, and humans [1–4]. circRNAs in higher organisms are reported to be produced by back-splicing events and can be synthesized from all regions of the genome, deriving mostly from exons but, less commonly, from antisense, intergenic, intragenic, or intronic regions [5]. circRNAs are both spatially and temporally regulated and evidence is emerging that they may have importance in normal development of tissues or organs but also in disease pathogenesis. Most circRNAs have been reported in the brain [2,6–8]. They can be found in most cell sub-compartments, but the majority localize predominantly to the cytoplasm [9]. circRNAs are inherently stable by virtue of their closed covalent structure and exonuclease resistance and are thought to be stable in exosomes [2,5,10–12]. This observation opens up the interesting possibility that circRNAs, like micro RNAs (miRNAs), may have roles in paracrine signalling or have roles in cell-to-cell cross talk.

2. circRNAs Are Formed from Back-Splicing Events of Linear Genes

In conventional linear splicing, the spliceosome joins exons in a 5^0 to 3^0 configuration. In contrast, circRNAs arise when the 3^0 'tail' of a downstream exon of a gene is back-spliced to the 5^0 'head' of an earlier exon (which may include itself) leading to the circularization of exons in between (see Figure 1) [10]. These splicing decisions are, as in linear splicing, regulated by *trans*-acting splicing factors and *cis* sequence elements [13]. Several sequence features influencing circRNA formation have

been described. Firstly, intron length has been reported to play a part; introns flanking back-spliced sites tend to be comparatively longer than those flanking non-circularised exons [4]. This may be because larger introns may form more RNA–RNA interactions, facilitating circularization of embedded exons; the double-stranded RNA-editing enzyme ADAR1, which is capable of melting stem structures within these RNA–RNA interactions, is associated with suppression of circRNA expression in *Caenorhabditis elegans* [14]. Secondly, exon length may also be a factor; exons of single-exon circRNAs are on average 3-fold longer compared with those of non-circularised exons; longer exons may be sterically preferentially favoured for 3^0–5^0 splicing at canonical splice sites [2,15,16]. Thirdly, RNAs that are hyper-edited are enriched for circRNA

sequences [14]. Finally, sequence content may also be important. Repetitive sequences are known to promote back splicing; back-spliced exons that form circRNAs are frequently enriched in paired ALU tandem repeats that have been shown to promote circularization [2]. Miniature introns with as few as 30 to 40-nt inverted repeats are also sufficient to promote circularization [17].

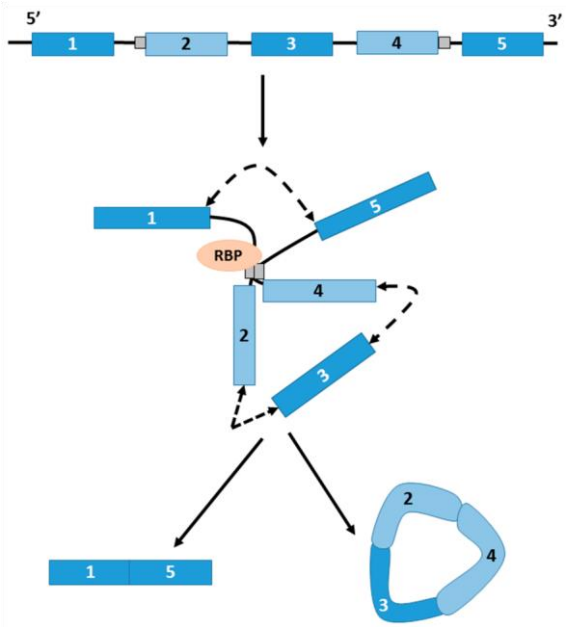

Figure 1. The biogenesis of circular RNA (circRNA). The linear primary transcript contains exons (blue boxes), introns (black lines), and possibly repetitive elements or sequence motifs (grey boxes). Circular exons are generated from back-splicing events between the splice donor site of a downstream exon and the splice acceptor site of an upstream exon. This can be mediated by specific sequence elements (grey boxes) or by interaction with RNA binding proteins (RBPs). Splicing events are indicated by dashed lines with double arrowheads. This may result in the production of a circular RNA and a linear RNA which lacks the circularised exons.

circRNA formation may also be dependent on the specific binding of regulatory proteins. RNA binding proteins such as Quaking (QKI) and Muscleblind (MBL/MBNL1) have been described to bind to introns flanking back-spliced sites and may drive circularization [18,19]. The *MBL* gene itself encodes a circular form which regulates the expression of its linear transcript and modulation of MBL levels strongly affects circMBL expression [18]. circRNA formation has also been shown to depend on the rate of transcription of their parent genes. circRNA producing genes are generally longer and exhibit faster transcription than genes that do not produce circRNAs, and artificially slowing the rate of transcription with mutant RNA polymerases results in lower levels of circRNA biogenesis [20].

Intronic circRNAs (ciRNAs) can also be generated form lariat introns. ciRNAs are devoid of linear fragments spanning the 3^0 end of the intron to the branch point, but are produced by a 2^0,5^0-phosphodiester bond arising from canonical linear splicing [21]. A 7-nt GU-rich element occurring close to a 5^0 splice site and with an 11-nt C-rich motif around the branch point within intronic sequences has been reported to be important for formation of ciRNAs [21].

3. circRNA Online Resources

Over the past few years, at least eleven circRNA detection software systems have been developed. These tools can recognize circRNA sequences from RNA-Seq data based on two different strategies. One approach is the candidate-based approach, also known as the pseudo-reference based approach. KNIFE, NCLScan, and PTESFinder all abide by this approach where putative circRNA sequences need to be provided with information for gene annotation. Although KNIFE can directly retrieve back-spliced junctions prior to gene annotations, the other two software systems generate putative circRNA sequences post-alignment with the genome or transcriptome [22–24].

circRNA_finder, CIRCexplorer, DCC, MapSplice, Segemehl, find-circ, and UROBORUS detect circRNA sequences based on the second approach for identification of circRNA sequences which is the fragmented-base or segmented read approach. In this approach, the software detects back-spliced sites based on reads mapped to alignment of multiple split reads against the genome. While find-circ and UROBORUS detect back-spliced sequences using the first and last 20 bp after mapping the sequences against the genomes, the rest of the detection tools generate splice alignment algorithms to identify back-spliced junctions [22–24]. CIRI is a distinct detection tool in that it extracts information from local alignment with Burrows-Wheeler Aligner-MEM (BWA-MEM) and detects paired chiastic clipping signals from mapped reads (arXiv:1303.3997). Comparisons of the different circRNA detection algorithms have now been made, which add information on the relative strengths and caveats of these different approaches [25]. Searchable repositories for circRNA sequences such as circBase are also now emerging [26], which should prove useful to researchers interested in these RNA species in the future.

4. Molecular Mechanisms of Gene Regulation by circRNAs

circRNAs have been proposed to act through several mechanisms, including miRNA sponges, modifiers of transcription or translation, and as splicing modifiers (Figure 2).

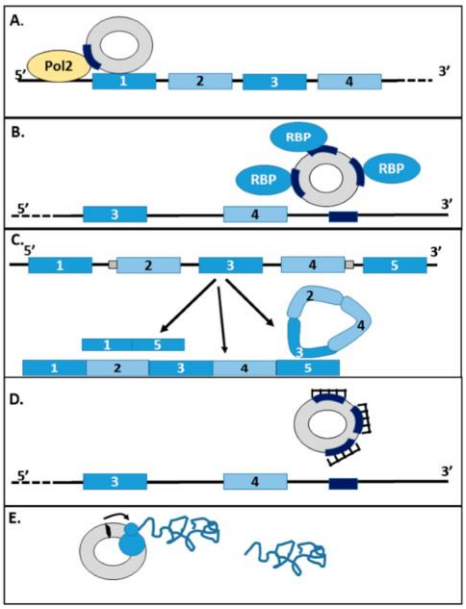

Figure 2. Proposed roles of circRNA in the regulation of transcription and translation. circRNAs may regulate genes at several levels. (**A**) Firstly, nuclear circRNAs can interact with promoter regions of target genes and interact with RNA polymerase II (Pol2) to repress or enhance transcription; (**B**) Secondly, circRNAs can sequester RBPs that regulate mRNA processing and, thus, alter the splicing patterns of the genes in question, or moderate mRNA stability. RBP binding sites are given by dark blue boxes; (**C**) Thirdly, the biogenesis of circular RNAs may results in the production of a linear RNA lacking the circularised exons. The formation of circRNAs can thus reduce the amount of linear transcript produced; (**D**) circRNAs can act as micro RNA (miRNA) sponges, sequestering them away from their binding sites in target genes, which are given by dark blue boxes; (**E**) Circular RNAs can also be translated. The initiation codon is given by a black oval, and the translating ribosome and nascent polypeptide are indicated.

4.1. circRNAs as miRNA Sponges

CircRNA can bind specific miRNAs or groups of miRNAs, sequestering them and suppressing their function [27], in a phenomenon termed the competitive endogenous RNA hypothesis [28]. circRNA *CDR1as* has been documented to contain up to 74 binding sites for the miRNA miR-7, and also binds Argonaute (AGO) proteins of the RNA-induced silencing complex (RISC) that regulate miRNA action [29]. There is also some suggestion that the relationships between circRNAs and miRNAs may be partly autoregulatory; *CDR1as* also binds miR-671, which induces AGO-mediated cleavage of *CDR1as* itself, which could act to release miR-7 [30]. However, circRNAs containing

multiple binding sites for single miRNAs may be the exception rather than the rule since most circRNAs identified to date do not contain enrichment of binding sites for specific miRNAs [31]. Emerging evidence suggests that circRNAs may act by sequestration of modules of coordinately regulated miRNAs; the circRNA *circHIPK3* contains binding sites for nine miRNAs with growth-suppressive properties [32]. The presence of multiple binding sites may not be a prerequisite for efficient miRNA regulation, however, since *circHIPK3* contains only two binding sites for miR-124, yet retains the ability to regulate this miRNA [32]. Most of the research investigating the role of the circRNA–miRNA interaction has been performed through correlation of the levels of miRNA and circRNA expression in vitro. Evidence for circRNAs acting as miRNA sponges can also be seen in data arising from the *CDR1as* knockout mouse. Levels of both miR-7 and miR-671 were seen to be lower in knockout animals, and these changes were also correlated with defects in synaptic transmission [33]. It is likely that a circRNA with multiple binding sites will affect the expression of a larger number of miRNA targets. However, experimental validation of the minimal number of miRNA binding sites for a candidate circRNA to be functional is still required for many circRNAs. An arena to explore is whether a single miRNA binding site would be sufficient for efficient circRNA:miRNA sponging interactions. It would be also interesting to know what levels of circRNA expression is required for the optimal miRNA sequestration ability of these entities. The interaction between circRNAs and miRNAs may also go beyond their role in miRNA sequestration; they may also be important for the storage, sorting, and localization of miRNAs, adding an additional level of regulation to miRNA-controlled regulation of target genes [27,34].

4.2. circRNAs as Transcriptional and Translational Regulators

A specific category of circRNAs, nuclear exon-intron circRNAs (EIciRNAs) can also interact with the transcription machinery. These variant circRNAs, which retain some intronic sequence from their linear gene, can interact with the U1 component of the spliceosomal machinery, recruiting RNA polymerase II to the promoter region of genes and enhancing expression of its target genes [35]. circRNAs can also modulate the expression of the cognate transcript if the circularisation event includes the translation initiation codon of its native gene. This may cause their cognate linear mRNAs arising from the same gene to escape translation, thus regulating protein expression as in the case of *circHIPK3*, *circDMD,* and *circFMN* [2,36–38]. Recently, *circPABPN1* has been

reported to supress binding of *PABPN1* mRNA to HuR. *PABPN1* translation is positively associated with HuR and the interaction of *circPABPN1* interaction with HuR reduces the translational efficiency of *PABPN1* transcripts. Thus, circRNAs like *circPABPN1* can act as competitors with their cognate mRNA for RBPs and can also modulate the rate of translation of target mRNAs [39].

4.3. circRNAs as Competitors of Linear Splicing

All isoforms produced from a given gene arise from a common pre-mRNA. It follows, therefore, that the production of a circRNA may have consequences for the abundance of the remaining transcripts encoded by that gene. An example of this lies in the Muscleblind (*MBL*) gene. *MBL* contains sequences that form a circRNA transcript that contains binding sites for MBL itself. Production of the circMBL therefore forms an autoregulatory loop that regulates the production of the linear transcript in favour of the circular form [18]. In *Arabidopsis*, a circRNA derived from the *SEPALLATA3* gene has been shown to interact with its cognate DNA, forming a R-loop and causing a pause in transcription and also affecting recruitment of splicing factors to the nascent transcript and affecting alternative splicing through exon-skipping [40].

4.4. circRNAs as Sponges (RBPs)

In addition to their role as miRNA sponges, circRNAs can also act as sponges for other entities such as RBPs that can regulate gene expression. RBPs, like miRNAs, bind specific sequences within their target genes and control all stages within the lifecycle of an mRNA from splicing and nuclear export to stability and subcellular localisation [36]. circRNAs interacting with RNA binding protein components of the gene regulatory machinery such as HuR have been reported [39].

5. Translation of circRNAs

Recent in vitro studies have shown that circRNAs have potential to encode proteins. Ribosome footprinting studies in vivo in Drosophila clearly demonstrate that circRNAs are associated with translating polysomes [41]. Accordingly, some circRNA-derived proteins have been identified. For example, circ-FBXW7 has been shown to encode a novel protein in human U251 and U373 cell lines [42]. The inclusion of N6-meythyl adenosine residues is sufficient to promote the initiation of translation of circRNAs in the human cell lines in the presence of initiation factor eIF4G2 and YTHDF3 [43]. Methyltransferase METTL3/14 also accelerates the initiation of translation of this circRNA [43]. Computational analysis of high-throughput sequencing data revealed

that the human transcriptome commonly harbours many circRNAs with coding potential. Smaller circRNAs with relatively fewer exons but longer open reading frames (ORFs) have been reported to be associated with polysomes [43]. For example, circ-ZNF609 has been demonstrated to encode a protein in a splicing-dependent but cap-independent manner in human and murine myoblasts. In vitro analysis of circ-ZNF609 (which contains two start codons) revealed that the circRNA could generate two protein isoforms corresponding to the two ORFs [6].

6. The Roles of circRNAs in Normal Homeostasis

circRNAs are emerging as important regulators of many cellular processes, such as embryonic development, control of cell cycle, cellular senescence, cell signalling, and response to cellular stress.

6.1. circRNAs in Embryonic Development

Approximately 10.4% of human circRNAs and 34.3% of mouse circRNAs are expressed in a tissue specific or age-specific manner, which indicates their potential role in tissue development or differentiation [44]. The difference in abundance of circRNAs between human and mouse is interesting and may represent a real species difference, but may also be a reflection of limited power due to smaller sample numbers of ex vivo human studies because of the inherent difficulties in procuring non-accessible tissues. The albumin (*ALB*) gene generates up to 160 circRNA species, of which 95 are specific to adult liver and only 33 are expressed in developing foetal liver [44]. circRNAs are enriched in the brain and appear to have particular importance in brain development of this organism. *CiRS-7* has been shown to be highly expressed in the cerebellum at embryonic stage E115, but reduced in the cerebral cortex at E60 in embryonic pigs [7]. Embryonic, early postnatal, postnatal, and late postnatal hippocampus from brain samples from embryonic mice also had increased levels of *circDlgap1*, *circMyst4*, *circKlhl2,* and *circAagab*. Expression was localized to the punctate in the dendrites, and abundance fluctuated depending on the stage of synaptogenesis, suggesting that these circRNAs might be involved in synaptic function during developmental stages [45]. *CDR1as* may have important roles in development, since transgenic expression of this circRNA in zebrafish embryos produces fry with smaller midbrain size, which resembles the phenotype of miR-7 knockdown [29]. The *SRY* gene

is located in the sex-determining region of the Y chromosome. Mutations in the coding regions of *SRY* can lead to change in sex [46,47]. Mouse *circSRY* has multiple miR-138 binding sites suggesting a potential role for this circRNA in the regulation of sex determination in mice [29,30].

6.2. circRNAs in Metabolism

High *CDR1as* expression has been shown to have effects on beta-cell function through its regulation of miR-7 in pancreatic beta cells. miR-7 targets include the protein kinase C beta (*PKCB*) gene involved in cellular signalling, the profilin 2 (*PFN2*), and phosphatase and actin regulator 1 (*PHACTR1*) genes involved in cytoskeletal organisation and the gene encoding the transcription factor paired box 6 (*PAX6*). This may have profound implications for beta cell function; up-regulation of murine *Pax6* expression through the sponging action of *CDR1as* on miR-7 has been shown to lead to increased insulin secretion in mouse islets [48]. miR-7 is abundant in adult islets and may prevent β cell proliferation by inactivating the mTOR pathway [49].

6.3. circRNAs in Regulation of Cell Cycle

circRNAs have been found to be involved in the progression of the cell cycle. *circFOXO3* has been shown to engage with p21 and cyclin-dependent kinase 2 (CDK2) proteins to form a ternary structure. The complex formed prevents CDK2 from interacting with cyclin E and p27, which eventually blocks transition from G1 to S phase and cell cycle progression. Similarly, p21, like CDK2, is unavailable for interaction with cyclin A, which leads to cell cycle arrest at G1 phase [50]. Depletion of *circHIPK3* in HEK293T cells has also been shown to supress cell proliferation and is indicative of a role in cellular growth [32].

6.4. circRNAs in Regulation of Cellular Stress

It is vital for living organisms to maintain homeostasis at the cellular level to sustain viability. circRNAs have been reported to be involved with cellular homeostasis both positively and negatively, by regulating aspects of cellular growth, apoptosis, immune-response, and resistance to therapeutics. *CDR1as* has been shown to have potential roles in the regulation p21-activated kinase 1 (PAK1), promoting DNA repair and preventing apoptosis [51]. Mouse embryonic fibroblasts exposed to reactive oxygen species demonstrate upregulation of *circFOXO3*, promoting senescence via reducing nuclear translocation of ID-1, E2F1, and HIF1α and altering the mitochondrial

localization of focal adhesion kinase (FAK), all of which are involved in cellular survival [50]. A circRNA derived from the *DENND4C* gene has also been reported to have roles in adaptation to hypoxic conditions in breast cancer cells [52]. Overexpression of a circRNA produced from the locus encoding the lncRNA *ANRIL* has been shown to induce prolonged nucleolar stress in cultured human cells [53]. circRNAs have also been reported to have roles in macrophage activation and antimicrobial response via positive regulation of the intracellular adhesion molecule 1 (*ICAM1*) gene in the Toll-like receptor 4 (TLR4) pathway [54].

7. circRNAs in Disease

In accordance with a pivotal role in gene regulation, perturbation of circRNA expression is beginning to be reported in association with disease. Altered circRNA expression has been reported in several diseases like cancer, heart disease, neurological disorders, diabetes and atherosclerosis, although the precise mechanisms by which they operate are yet to be disclosed.

7.1. circRNAs in Cancer

In accordance with their known role in modulating cell cycles, proliferation and cellular senescence as demonstrated in vitro studies, circRNAs have been implicated in cancer. circRNA hsa_circ_001569 (circABCC) may play a role in modulating gene expression in colorectal cancer by virtue of its action on miR-145. miR-145 is a negative regulator of target genes such as *E2F5, BAG4,* and *FMNL2* which are known to be involved in the suppression of proliferation [55]. Similarly, *CDR1as* has also been implicated in several cancer subtypes including hepatocellular carcinoma (HCC). *CDR1as* expression is known to be correlated with hepatic microvascular invasion in HCC tissue [56] and hsa_circ_0000520 (circRPPH1), hsa_circ_0005075 (circEIF4G3), hsa_circ_0066444 (circADAMTS9), and hsa_circ_0001649 (circSRPRH) have all been shown to be expressed at different levels in HCC compared to adjacent normal liver tissues [57,58]. hsa_circ_0005075 (circEIF4G3) correlated with tumour size while hsa_circ_0001649 (circSRPRH) was downregulated and also correlated with tumour size in addition to the prevalence of tumour embolus and could be involved in tumorigenesis and metastasis of HCC [57,58]. circRNA *circZKSCAN1* has also been shown to be lower in tumours and correlated with tumour size in HCC [59].

Large-scale dysregulation of circRNA expression has been noted in bladder carcinoma, where microarray analysis revealed that 469 circRNA were differentially expressed, 285 showing increased expression in bladder cancer compared with 184 showing downregulation. Of these, *circTCF25* regulates miRNAs miR-103a-3p/miR-107, with *circTCF25* upregulation being associated with increased levels of 13 targets associated with cell proliferation, migration, and invasion in bladder cancer [60]. Similarly, increased expression of circRNA *circMYLK* in bladder cancer leads to overexpression of *DNMT3B*, *VEGFA,* and *ITGB1* genes, which are involved in promotion of proliferation and are molecular targets of miRNA-29a-3p [61]. circRNA *circHIAT1* has also been reported to respond to signalling through the androgen receptor to promote tumour migration and invasion in clear cell renal cell carcinoma by enhancement of *CDC42* expression through regulation of miR-195-5p/29a-3p and miR-29c-3p target genes [62]. Recently, fusion-circRNAs (f-circRNA) have been shown to accelerate proliferation rate and instigate cellular transformation. Furthermore, f-circRNAs f-circM9 and f-circPR have been shown to confer resistance to therapeutics due to protective effects of drug-induced apoptosis in cancer cells in vitro via a MAPK/AKT dependent signalling pathway [63].

7.2. circRNAs in Neurological Disease

CDR1as has been associated with neurodegenerative conditions such as Alzheimer's disease (AD). In patients with moderate to advanced stages of sporadic AD, *CDR1as* expression has been reported to be reduced, which may lead to elevated miR-7 expression and consequent downregulation of miR-7 dependent mRNAs. One target, ubiquitin protein ligase A, is responsible for the clearance of amyloid peptides in AD and other degenerative disorders [64]. Although most studies with circRNAs have been conducted in vitro, recently, Piwecka et al.,generated a knockout murine model for Cdr1as. The brains of these transgenic mice had upregulated expression of miR-7 genes, such as *c-Fos*. Cdr1as knockout mice demonstrate impaired synaptic transmission and information processing defects [33]. circRNAs also have potential roles in memory; *circPAIP2* has been suggested to upregulate memory-related gene *PAIP2* through the poly A binding protein (PABP)-associated pathway [65]. A role for circRNAs in major depressive disorder is also suggested by the observation that a

significant change of hsa_circRNA_103636 expression was noted in patients after eight weeks on antidepressant therapies [66].

7.3. circRNAs in Osteoarthritis

Osteoarthritis (OA) occurs because of degenerative changes in the joint cartilage. Seventy-one circRNAs were seen to be differentially expressed in the cartilage of patients with OA compared with those of non-OA controls. The circRNA *circ-CER* appears to be of particular importance. *circ-CER* expression was shown to increase with increased expression of pro-inflammatory signalling molecules such as interleukin (IL)-1 and tumour necrosis factor (TNF)α. Suppression of *circ-CER* resulted in reduced matrix metalloproteinase-13 (*MMP13*) expression and remodelling of the extracellular matrix (ECM). The authors suggest that this observation arises from a sponging effect of *circ-CER* on miR-136, which is known to target the *MMP13* gene [67].

7.4. circRNAs in Cardiovascular Disease

The *CDKN2A/CDKN2B* locus expresses an alternatively spliced non-coding transcript, *ANRIL*, which encodes a circular form in addition to its linear form. *circANRIL* has been reported to regulate the pescadillo homologue 1 (*PES1*) gene transcript, which is involved in pre-rRNA processing and ribosome biogenesis. Sequestration of this essential factor and suppression of these key processes in vascular smooth muscle cells and macrophages was shown to cause nucleolar stress and p53 activation, resulting in apoptosis and features of atherosclerosis [68]. Some circRNAs have been shown to be protective in heart function; the circRNA heart-related circRNA *HRCR* has been implicated in protection from cardiac hypertrophy and heart failure, by virtue of its binding of the inflammatory onco-miR miR-223 [69,70]. Some RNA inding Motif Protein 20 (RBM20)-dependent circRNAs have also been reported to be differentially regulated in dilated cardiomyopathy [71]. Similarly, circRNA *MFACR* has been shown to sponge miR-652-3p in the cytoplasm, promoting mitochondrial fission and cardiomyocyte cell death by enhancing translation of *MTP18* in animal models [72]. Similarly, high levels of circRNA_000203 and circRNA_010567 have been reported in cardiomyocytes from diabetic mice treated with angiotensin II. These circRNAs are thought to downregulate miR-26b-5p, miR-141, and miR-141, thereby upregulating the *TGFB1* gene. This leads to suppression of fibrosis-associated protein resection in

collagen 1 (Col I), collagen 3 (Col III), and α-smooth muscle actin (α-SMA), promoting fibrosis in the myocardium [73,74].

7.5. circRNAs in Type 2 Diabetes

In addition to the role of *CDR1as* in regulation of insulin secretion through modulation of PAX6, recent studies have suggested that circRNAs may have utility as biomarkers of diabetes. Four hundred eighty-nine circRNAs were found to be differentially expressed in the peripheral blood of patients with type 2 diabetes, and furthermore, circRNA hsa_circ_0054633 was found to be capable of predicting pre-diabetes with an area under the curve (AUC) of 0.84 ($p \leq 0.001$) [75]. In other studies, several circRNAs have been shown to be differentially expressed in serum of patients with diabetic retinopathy compared to that of both controls and diabetes patients without retinopathy. Of these, hsa_circRNA_100750 is derived from stromal interaction molecule 1 which is upregulated in diabetic patients. hsa_circRNA_104387 is known to sequester miR-29a which prevents the loss of renal function in diabetic patients. hsa_circRNA_103410 is known as a regulator of miR-126, which is known to inhibit *VEGF* and *MMP9* expression. Thus, hsa_circRNA_103410 could promote endothelial injury in the retina, while hsa_circRNA_100192 could, by sequestering miR-146, promote necrosis factor (NF)-κB activation, adenosine deaminase-2 expression, and inflammatory responses as is observed in vitro [76]. These observations raise the exciting possibility that circRNAs expressed in accessible tissues may be useful markers of disease in inaccessible organs such as pancreas. *circHIPK3* has been found to be dysregulated in diabetic retinas, which may contribute to elevated levels of *VEGFC*, *FZD4*, and *WNT2* expression by virtue of its effects on miR-30a-3p [77].

7.6. circRNAs and Pre-Eclampsia

A study has implicated circRNAs in the development of preeclampsia. Qian et al.,identified 143 up-regulated and 158 down-regulated circRNAs in placental tissues from women with pre-eclampsia,

which included upregulated hsa_circRNA_100782 (circHIPK3), hsa_circRNA_102682 (circCRIM1), and hsa_circRNA_104820 (circFAM120A) circRNAs [78]. Altered circ_101222 expression before 20 weeks of pregnancy was seen to correlate with higher levels of endoglin, a component of the transforming growth factor beta (TGFβ)

signalling pathway, which is associated with pre-eclampsia, than women who did not have pre-eclampsia. circRNA circ_101222, in combination with endoglin levels, may therefore have the potential to predict pre-eclampsia very early on in pregnancies [79].

7.7. circRNAs and Infection

Microbial lipopolysaccharide induces the activation of TLR pathways leading to activation of NF-κB and modulation of genes which are key to antimicrobial defences and adaptive immunity. *circRasGEF1B* has been suggested to modulate the expression of ICAM-1 as part of the lipopolysaccharide response. Knock down of this circRNA in vitro leads to 27%–39% reduction in ICAM-1epression in vitro [54]. In mouse macrophage cells, activation of TLR4, TLR9, TLR3, TLR2, and

TLR1 receptors all regulate the expression of *circRasGEF1B* [54]. Genetically modifying *circRasGEF1B* expression was shown to reduce *ICAM1* expression levels, which under normal conditions would promote binding of leukocytes to endothelium cells and their transmigration into target tissues [54]. Thus, deficiency of *circRasGEF1B* may prevent migration of leukocyte cells to inflammatory sites and interfere with the healing process, and in cancer cells may additionally affect the activation of cytotoxic T-lymphocytes needed for driving release of cytolytic granules into tumour cells [54].

A potential role for circRNA in response to viral infection has been reported. HeLa cells transfected with circRNA demonstrated induced expression of 84 innate immunity-related genes, such as *RIGI* and *OASl*, which were upregulated by as much as 500-fold and 200-fold, respectively [80]. Concurrent with these changes was a 10-fold decrease in infection rate against Venezuelan equine encephalitis virus,

which was shared by nearby non-transfected cells, indicating some paracrine action [80]. circRNAs can also act as competitors with viral mitochondrial RNA (mtRNA) for binding to RNA-binding domain containing immune factor NF90 and its isoform NF110. These factors can promote circularization by stabilizing the binding of intronic RNA pairs in the nucleus. Viral infection results in transportation of these factors from the nucleus to the cytoplasm resulting in decreased circRNA expression in infected cells. This acts to render the circRNA available for binding to viral mRNA and prevents viral infection of the host cell [81].

7.8. circRNAs in Ageing and Cellular Senescence

circRNAs are known to accumulate in ageing brains [82].This may be partly due to the

endonuclease-resistant nature of circRNA molecules, but at least two circRNAs have been previously described to have a role in ageing or cellular senescence. circRNA *circPVT1* has been demonstrated to suppress cellular senescence by sequestration of miRNA let-7, which lifts its inhibitory action on its target genes *IGF2BP1*, *KRAS,* and *HMGA2,* which act to promote cell proliferation [83]. Conversely, the *circFOXO3* circRNA was found to promote senescence in the heart muscle of aged mice and humans through its action on the *ID1*, *E2F1*, *FAK,* and *HIF1A* target genes [9]. This circRNA is also known to silence cell proliferation through its regulation of the cell division kinase 2 (*CDK2*) gene and the cyclin dependent kinase inhibitor p21 [9].

8. circRNAs as Diagnostic and Prognostic Markers

Because circRNAs are highly nuclease-resistant, they are more stable than linear transcripts and may be released into the extracellular space via the exosomes [12,84]. Half-lives of circRNAs can vary significantly, but can be as long as 50 h. On average, their half-lives are around 2.5-fold longer than the median half-lives of their linear counterparts [85]. A substantial number of circRNAs are expressed in blood at comparatively higher levels than their linear mRNAs, thus making circRNAs attractive tools for diagnostics to trace the mechanism of coded genes otherwise inaccessible by the canonical RNA pathway-dependent assays [86]. A selection of circRNAs reported as potential biomarkers for different diseases are summarized in Table 1. Over 400 circRNAs have been detected to be present in cell-free saliva and could potentially be used for non-invasive diagnostics approach [87]. circRNAs have been suggested as potential biomarkers for several types of cancer. In murine models, tumour-derived exosomal circRNAs in the serum correlate with tumour mass [88], and thus may be promising biomarkers for cancer detection. circRNA hsa_circ_0001649 (circSHPRH) has shown some utility as a biomarker for hepatocellular carcinoma, is downregulated with tumour status, and is associated with the occurrence of the tumour embolus as well as the size of the tumour [57]. hsa_circ_002059 (circKIAA0907) is downregulated in gastric cancer and is associated with grade and distal metastasis and could, therefore, be used as a prognostic marker [89]. Another circRNA, hsa_circ_0000190 (circDYRK1A), is downregulated in plasma samples of patient with gastric cancer, where its expression levels correlated with tumour diameter, lymphatic metastasis, and distal metastasis [90]. Similarly, hsa_circ_0001895 (circPRRC2B) was also shown to be downregulated in gastric cancer tissues and correlated with cell

differentiation and Borrmann type [91]. In hepatitis B infected hepatocellular carcinoma (HCC) patients, circRNA_100338 (circSNX27) has been shown to regulate levels of miR-141-3p, and its expression correlated with low cumulative survival rate and metastatic progression [92].

Table 1. Examples of circRNA and their potential role in disease.

circRNA	Pathologic Condition	Possible Mode of Function	Potential Application
hsa_circRNA_062557, hsa_circRNA_067130, hsa_circRNA_067209, hsa_circRNA_100914, hsa_circRNA_089761, hsa_circRNA_089763	moyamoya disease	May sequester miRNAs associated with RNF213 and BRCA1/BRCA2-containing complex subunit 3	Potential biomarker expressed in blood [93]
CDR1as	hepatocellular carcinoma	May be a sponge for miR-7	Biomarker with the ability to predict hepatic microvascular invasion; expressed in hepatocellular carcinoma tissues [56]
hsa_circ_0001017, hsa_circ_0061276	gastric cancer		Prognostic, with the ability to predict disease-free survival; expressed in plasma [94]
hsa_circ_0089378, hsa_circ_0083357, hsa_circ_0082824, hsa_circ_0068942, hsa_circ_0057576, hsa_circ_0054537, hsa_circ_0051172, hsa_circ_0032970, hsa_circ_0006323	coronary artery disease	May promote expression of transient receptor potential cation channel subfamily M member 3 by inhibiting hsa-miR-130a-3p	Potential biomarker expressed in plasma [95]
GSDMB circRNA	multiple sclerosis		Potential biomarker expressed in peripheral blood mononuclear cells [96]
hsa_circRNA_105055, hsa_circRNA_086376, hsa_circRNA_102761	colorectal cancer	May act as sponge for miR-7 regulating target genes *PRKCB*, *EPHA3*, *BRCA1,* and *ABCC1*; potential role in lung metastasis	Potential biomarker [97]
hsa_circ_0092285, hsa_circ_0058794, hsa_circ_0088088, hsa_circ_0038644	rheumatoid arthritis	May be involved in response to oxidative stress; endocytic traffic in actin cytoskeleton; could promote lipid breakdown and increase free fatty acid levels; could alter lipopolysacccharide (LPS) immune response	Potential biomarker expressed in peripheral blood mononuclear cells [98]
hsa_circRNA_101308, hsa_circRNA_104423, hsa_circRNA_104916, hsa_circRNA_100269	gastric cancer		May predict the early recurrence of stage III gastric cancer after radical surgery; expressed in tumour tissues [99]
circPVT1	gastric cancer	May act as sponge for miR-125 family; may promote cell proliferation	Potential prognostic marker with the ability to predict overall survival and disease-free survival; expressed in gastric cancer tissues [100]

Table 1. *Cont.*

circRNA	Pathologic Condition	Possible Mode of Function	Potential Application
circRNA_104871, circRNA_003524, circRNA_101873, circRNA_103047	rheumatoid arthritis		Potential biomarker expressed in peripheral blood mononuclear cells [101]
hsa_circ_0058246	gastric cancer		Potential prognostic marker with the ability to predict clinical outcome; expressed in tumour tissues [102]
circ-ITCH	hepatocellular carcinoma	May inhibit Wnt/β-Catenin pathway	Potential prognostic marker with the ability to predict survival; expressed in hepatocellular carcinoma tissues [103]
hsa-circ-0005870	hypertension	May act as sponge for miRNAs, hsa-miR-6807-3p, hsa-miR-5095, hsa-miR-1273g-3p, hsa-miR-5096, and hsa-miR-619-5p, possibly affecting transforming growth factor beta (TGF-beta) pathway important in hypertension	Potential biomarker expressed in plasma [104]
hsa_circ_0124644,	coronary artery disease		Potential diagnostic biomarker; expressed in blood [105]
circR-284	carotid disease and ischemic stroke	May act as an inhibitor of miR-221/miR-222	Potential diagnostic biomarker:expression demonstrated in serum [106]
circ_0005402, circ_0035560	multiple sclerosis		Potential biomarker; expressed in leucocytes [107]
circZKSCAN1	hepatocellular carcinoma	May modulate expression of apoptotic genes *RAC2*, *EFNA3*, and caspase 3 and cell proliferation related genes *TGFB1*, *ITGB4, CXCR4*, *BIRC5,* and *CCND1*; may modulate promoted cell proliferation, migration, and invasion in vitro	Expressed in tumour tissues [59]
circ_101222	pre-eclampsia		Potential biomarker; expressed in blood [79]
hsa_circ_0054633	diabetes		Potential biomarker with the ability to predict pre-diabetes and type 2 diabetic status; expressed in blood [75]

9. Conclusions

circRNAs are a class of non-coding RNAs which appear to regulate the expression of genes by a variety of mechanisms and might also have the potential of encoding proteins, the mechanisms of which are not yet completely understood. Despite this, circRNAs are emerging as potentially important regulators of cellular physiology and as potential biomarkers of disease onset or progression. The state of the current knowledge of circRNA biology is as yet at a very early stage, and further research is urgently required to completely understand their function and potential. Despite this, it is likely that these novel circRNAs will emerge as important players in gene regulation in the future. The origin of circRNAs from throughout the genome raises the possibility

of co-ordinated regulation of modules of genes in a cell, tissue, and developmental stage specific pattern, adding another level of regulation to the already complex field of non-coding RNA (ncRNA) regulation of gene expression. In future years, circRNAs could be exploited as therapeutics. Over-expression of specific circRNA constructs could act to modulate cell behaviour and physiology by sponging oncogenic miRNAs such as miR-21 and miR-221 in cancer cells [108]. Antisense approaches such as morpholino technologies to influence splicing patterns are already in development for diseases such as Duchenne muscular dystrophy [109] and could in theory be developed to target exons that may be circularized to bring about higher expression of beneficial circRNAs once their modes of action have been elucidated.

Acknowledgments: The Harries lab is funded by the Dunhill Medical Trust and Animal Free Research.

Author Contributions: S.H. researched and wrote this review, L.W.H. reviewed and edited this work.

Conflicts of Interest: The authors declare no conflict of interest.

References

1. Danan, M.; Schwartz, S.; Edelheit, S.; Sorek, R. Transcriptome-wide discovery of circular RNAs in Archaea. *Nucleic Acids Res.* **2012**, *40*, 3131–3142. [CrossRef] [PubMed]
2. Jeck, W.R.; Sorrentino, J.A.; Wang, K.; Slevin, M.K.; Burd, C.E.; Liu, J.; Marzluff, W.F.; Sharpless, N.E. Circular RNAs are abundant, conserved, and associated with ALU repeats. *RNA* **2013**, *19*, 141–157. [CrossRef] [PubMed]
3. Nigro, J.M.; Cho, K.R.; Fearon, E.R.; Kern, S.E.; Ruppert, J.M.; Oliner, J.D.; Kinzler, K.W.; Vogelstein, B. Scrambled exons. *Cell* **1991**, *64*, 607–613. [CrossRef]
4. Salzman, J.; Chen, R.E.; Olsen, M.N.; Wang, P.L.; Brown, P.O. Cell-type specific features of circular RNA expression. *PLoS Genet.* **2013**, *9*, e1003777. [CrossRef]
5. Lan, P.H.; Liu, Z.H.; Pei, Y.J.; Wu, Z.G.; Yu, Y.; Yang, Y.F.; Liu, X.; Che, L.; Ma, C.J.; Xie, Y.K.; et al.,Landscape of RNAs in human lumbar disc degeneration. *Oncotarget* **2016**, *7*, 63166–63176. [CrossRef] [PubMed]
6. Legnini, I.; Di Timoteo, G.; Rossi, F.; Morlando, M.; Briganti, F.; Sthandier, O.; Fatica, A.; Santini, T.; Andronache, A.; Wade, M.; et al.,Circ-ZNF609 Is a Circular RNA that Can Be Translated and Functions in Myogenesis. *Mol. Cell* **2017**, *66*, 22. [CrossRef] [PubMed]
7. Veno, M.T.; Hansen, T.B.; Veno, S.T.; Clausen, B.H.; Grebing, M.; Finsen, B.; Holm, I.E.; Kjems, J. Spatio-temporal regulation of circular RNA expression during porcine embryonic brain development. *Genome Biol.* **2015**, *16*, 245. [CrossRef] [PubMed]
8. Barrett, S.P.; Salzman, J. Circular RNAs: Analysis, expression and potential functions. *Development* **2016**, *143*, 1838–1847. [CrossRef] [PubMed]
9. Du, W.W.; Yang, W.; Liu, E.; Yang, Z.; Dhaliwal, P.; Yang, B.B. Foxo3 circular RNA retards cell cycle progression via forming ternary complexes with p21 and CDK2. *Nucleic Acids Res.* **2016**, *44*, 2846–2858. [CrossRef] [PubMed]
10. Cocquerelle, C.; Mascrez, B.; Hetuin, D.; Bailleul, B. Mis-splicing yields circular RNA molecules. *FASEB J.* **1993**, *7*, 155–160. [PubMed]
11. Schwanhausser, B.; Busse, D.; Li, N.; Dittmar, G.; Schuchhardt, J.; Wolf, J.; Chen, W.; Selbach, M. Global quantification of mammalian gene expression control. *Nature* **2011**, *473*, 337–342. [CrossRef] [PubMed]
12. Lasda, E.; Parker, R. Circular RNAs Co-Precipitate with Extracellular Vesicles: A Possible Mechanism for circRNA Clearance. *PLoS ONE* **2016**, *11*, e0148407. [CrossRef] [PubMed]

13. Kramer, M.C.; Liang, D.; Tatomer, D.C.; Gold, B.; March, Z.M.; Cherry, S.; Wilusz, J.E. Combinatorial control of *Drosophila* circular RNA expression by intronic repeats, hnRNPs, and SR proteins. *Genes Dev.* **2015**, *29*, 2168–2182. [CrossRef] [PubMed]
14. Ivanov, A.; Memczak, S.; Wyler, E.; Torti, F.; Porath, H.T.; Orejuela, M.R.; Piechotta, M.; Levanon, E.Y.; Landthaler, M.; Dieterich, C.; et al.,Analysis of Intron Sequences Reveals Hallmarks of Circular RNA Biogenesis in Animals. *Cell Rep.* **2015**, *10*, 170–177. [CrossRef] [PubMed]
15. Salzman, J.; Gawad, C.; Wang, P.L.; Lacayo, N.; Brown, P.O. Circular RNAs are the predominant transcript isoform from hundreds of human genes in diverse cell types. *PLoS ONE* **2012**, *7*, e30733. [CrossRef] [PubMed]
16. Starke, S.; Jost, I.; Rossbach, O.; Schneider, T.; Schreiner, S.; Hung, L.H.; Bindereif, A. Exon Circularization Requires Canonical Splice Signals. *Cell Rep.* **2015**, *10*, 103–111. [CrossRef] [PubMed]
17. Liang, D.M.; Wilusz, J.E. Short intronic repeat sequences facilitate circular RNA production. *Gene Dev.* **2014**, *28*, 2233–2247. [CrossRef] [PubMed]
18. Ashwal-Fluss, R.; Meyer, M.; Pamudurti, N.R.; Ivanov, A.; Bartok, O.; Hanan, M.; Evantal, N.; Memczak, S.; Rajewsky, N.; Kadener, S. circRNA biogenesis competes with pre-mRNA splicing. *Mol. Cell* **2014**, *56*, 55–66. [CrossRef] [PubMed]
19. Conn, S.J.; Pillman, K.A.; Toubia, J.; Conn, V.M.; Salmanidis, M.; Phillips, C.A.; Roslan, S.; Schreiber, A.W.; Gregory, P.A.; Goodall, G.J. The RNA binding protein quaking regulates formation of circRNAs. *Cell* **2015**, *160*, 1125–1134. [CrossRef] [PubMed]
20. Zhang, Y.; Xue, W.; Li, X.; Zhang, J.; Chen, S.; Zhang, J.L.; Yang, L.; Chen, L.L. The Biogenesis of Nascent Circular RNAs. *Cell Rep.* **2016**, *15*, 611–624. [CrossRef] [PubMed]
21. Zhang, Y.; Zhang, X.O.; Chen, T.; Xiang, J.F.; Yin, Q.F.; Xing, Y.H.; Zhu, S.; Yang, L.; Chen, L.L. Circular intronic long noncoding RNAs. *Mol. Cell* **2013**, *51*, 792–806. [CrossRef] [PubMed]
22. Chen, I.; Chen, C.Y.; Chuang, T.J. Biogenesis, identification, and function of exonic circular RNAs. *Wiley Interdiscip. Rev. RNA* **2015**, *6*, 563–579. [CrossRef] [PubMed]
23. Meng, X.; Li, X.; Zhang, P.; Wang, J.; Zhou, Y.; Chen, M. Circular RNA: An emerging key player in RNA world. *Brief. Bioinform.* **2017**, *18*, 547–557. [CrossRef] [PubMed]
24. Jeck, W.R.; Sharpless, N.E. Detecting and characterizing circular RNAs. *Nat. Biotechnol.* **2014**, *32*, 453–461. [CrossRef] [PubMed]
25. Hansen, T.B.; Veno, M.T.; Damgaard, C.K.; Kjems, J. Comparison of circular RNA prediction tools. *Nucleic Acids Res.* **2016**, *44*, e58. [CrossRef] [PubMed]
26. Glazar, P.; Papavasileiou, P.; Rajewsky, N. circBase: A database for circular RNAs. *RNA* **2014**, *20*, 1666–1670. [CrossRef] [PubMed]
27. van Rossum, D.; Verheijen, B.M.; Pasterkamp, R.J. Circular RNAs: Novel Regulators of Neuronal Development. *Front. Mol. Neurosci.* **2016**, *9*, 74. [CrossRef] [PubMed]
28. Tay, Y.; Rinn, J.; Pandolfi, P.P. The multilayered complexity of ceRNA crosstalk and competition. *Nature* **2014**, *505*, 344–352. [CrossRef] [PubMed]
29. Memczak, S.; Jens, M.; Elefsinioti, A.; Torti, F.; Krueger, J.; Rybak, A.; Maier, L.; Mackowiak, S.D.; Gregersen, L.H.; Munschauer, M.; et al.,Circular RNAs are a large class of animal RNAs with regulatory potency. *Nature* **2013**, *495*, 333–338. [CrossRef] [PubMed]
30. Hansen, T.B.; Jensen, T.I.; Clausen, B.H.; Bramsen, J.B.; Finsen, B.; Damgaard, C.K.; Kjems, J. Natural RNA circles function as efficient microRNA sponges. *Nature* **2013**, *495*, 384–388. [CrossRef] [PubMed]
31. Guo, J.U.; Agarwal, V.; Guo, H.L.; Bartel, D.P. Expanded identification and characterization of mammalian circular RNAs. *Genome Biol.* **2014**, *15*. [CrossRef] [PubMed]
32. Zheng, Q.; Bao, C.; Guo, W.; Li, S.; Chen, J.; Chen, B.; Luo, Y.; Lyu, D.; Li, Y.; Shi, G.; et al.,Circular RNA profiling reveals an abundant circHIPK3 that regulates cell growth by sponging multiple miRNAs. *Nat. Commun.* **2016**, *7*. [CrossRef] [PubMed]
33. Piwecka, M.; Glazar, P.; Hernandez-Miranda, L.R.; Memczak, S.; Wolf, S.A.; Rybak-Wolf, A.; Filipchyk, A.; Klironomos, F.; Cerda Jara, C.A.; Fenske, P.; et al.,Loss of a mammalian circular RNA locus causes miRNA deregulation and affects brain function. *Science* **2017**, *357*. [CrossRef] [PubMed]
34. Hansen, T.B.; Wiklund, E.D.; Bramsen, J.B.; Villadsen, S.B.; Statham, A.L.; Clark, S.J.; Kjems, J.

miRNA-dependent gene silencing involving Ago2-mediated cleavage of a circular antisense RNA. *EMBO J.* **2011**, *30*, 4414–4422. [CrossRef] [PubMed]

35. Li, Z.; Huang, C.; Bao, C.; Chen, L.; Lin, M.; Wang, X.; Zhong, G.; Yu, B.; Hu, W.; Dai, L.; et al.,Exon-intron circular RNAs regulate transcription in the nucleus. *Nat. Struct. Mol. Biol.* **2015**, *22*, 256–264. [CrossRef] [PubMed]
36. Grigull, J.; Mnaimneh, S.; Pootoolal, J.; Robinson, M.D.; Hughes, T.R. Genome-wide analysis of mRNA stability using transcription inhibitors and microarrays reveals posttranscriptional control of ribosome biogenesis factors. *Mol. Cell. Biol.* **2004**, *24*, 5534–5547. [CrossRef] [PubMed]
37. Gualandi, F.; Trabanelli, C.; Rimessi, P.; Calzolari, E.; Toffolatti, L.; Patarnello, T.; Kunz, G.; Muntoni, F.; Ferlini, A. Multiple exon skipping and RNA circularisation contribute to the severe phenotypic expression of exon 5 dystrophin deletion. *J. Med. Genet.* **2003**, *40*, e100. [CrossRef] [PubMed]
38. Chao, C.W.; Chan, D.C.; Kuo, A.; Leder, P. The mouse formin (Fmn) gene: Abundant circular RNA transcripts and gene-targeted deletion analysis. *Mol. Med.* **1998**, *4*, 614–628. [PubMed]
39. Abdelmohsen, K.; Panda, A.C.; Munk, R.; Grammatikakis, I.; Dudekula, D.B.; De, S.; Kim, J.; Noh, J.H.; Kim, K.M.; Martindale, J.L.; et al.,Identification of HuR target circular RNAs uncovers suppression of PABPN1 translation by circPABPN1. *RNA Biol.* **2017**, *14*, 361–369. [CrossRef] [PubMed]
40. Conn, V.M.; Hugouvieux, V.; Nayak, A.; Conos, S.A.; Capovilla, G.; Cildir, G.; Jourdain, A.; Tergaonkar, V.; Schmid, M.; Zubieta, C.; et al.,A circRNA from SEPALLATA3 regulates splicing of its cognate mRNA through R-loop formation. *Nat. Plants* **2017**, *3*, 17053. [CrossRef] [PubMed]
41. Pamudurti, N.R.; Bartok, O.; Jens, M.; Ashwal-Fluss, R.; Stottmeister, C.; Ruhe, L.; Hanan, M.; Wyler, E.; Perez-Hernandez, D.; Ramberger, E.; et al.,Translation of circRNAs. *Mol. Cell* **2017**, *66*, 9–21. [CrossRef] [PubMed]
42. Yang, Y.; Gao, X.; Zhang, M.; Yan, S.; Sun, C.; Xiao, F.; Huang, N.; Yang, X.; Zhao, K.; Zhou, H.; et al.,Novel Role of FBXW7 Circular RNA in Repressing Glioma Tumorigenesis. *J. Natl. Cancer Inst.* **2018**, *110*. [CrossRef] [PubMed]
43. Yang, Y.; Fan, X.; Mao, M.; Song, X.; Wu, P.; Zhang, Y.; Jin, Y.; Yang, Y.; Chen, L.L.; Wang, Y.; et al.,Extensive translation of circular RNAs driven by N^6-methyladenosine. *Cell Res.* **2017**, *27*, 626–641. [CrossRef] [PubMed]
44. Xia, S.; Feng, J.; Lei, L.; Hu, J.; Xia, L.; Wang, J.; Xiang, Y.; Liu, L.; Zhong, S.; Han, L.; et al.,Comprehensive characterization of tissue-specific circular RNAs in the human and mouse genomes. *Brief. Bioinform.* **2016**. [CrossRef] [PubMed]
45. You, X.; Vlatkovic, I.; Babic, A.; Will, T.; Epstein, I.; Tushev, G.; Akbalik, G.; Wang, M.; Glock, C.; Quedenau, C.; et al.,Neural circular RNAs are derived from synaptic genes and regulated by development and plasticity. *Nat. Neurosci.* **2015**, *18*, 603–610. [CrossRef] [PubMed]
46. Foster, J.W.; Brennan, F.E.; Hampikian, G.K.; Goodfellow, P.N.; Sinclair, A.H.; Lovell-Badge, R.; Selwood, L.; Renfree, M.B.; Cooper, D.W.; Graves, J.A. Evolution of sex determination and the Y chromosome: SRY-related sequences in marsupials. *Nature* **1992**, *359*, 531–533. [CrossRef] [PubMed]
47. Hawkins, J.R.; Taylor, A.; Berta, P.; Levilliers, J.; Van der Auwera, B.; Goodfellow, P.N. Mutational analysis of SRY: nonsense and missense mutations in XY sex reversal. *Hum. Genet.* **1992**, *88*, 471–474. [CrossRef] [PubMed]
48. Xu, H.; Guo, S.; Li, W.; Yu, P. The circular RNA *Cdr1as*, via miR-7 and its targets, regulates insulin transcription and secretion in islet cells. *Sci. Rep.* **2015**, *5*, 12453. [CrossRef] [PubMed]
49. Wang, Y.; Liu, J.; Liu, C.; Naji, A.; Stoffers, D.A. microRNA-7 regulates the mTOR pathway and proliferation in adult pancreatic beta-cells. *Diabetes* **2013**, *62*, 887–895. [CrossRef] [PubMed]
50. Du, W.W.; Yang, W.; Chen, Y.; Wu, Z.K.; Foster, F.S.; Yang, Z.; Li, X.; Yang, B.B. Foxo3 circular RNA promotes cardiac senescence by modulating multiple factors associated with stress and senescence responses. *Eur. Heart J.* **2016**. [CrossRef] [PubMed]
51. Bachmayr-Heyda, A.; Reiner, A.T.; Auer, K.; Sukhbaatar, N.; Aust, S.; Bachleitner-Hofmann, T.; Mesteri, I.; Grunt, T.W.; Zeillinger, R.; Pils, D. Correlation of circular RNA abundance with proliferation–exemplified with colorectal and ovarian cancer, idiopathic lung fibrosis, and normal human tissues. *Sci. Rep.* **2015**, *5*, 8057. [CrossRef] [PubMed]

52. Liang, G.; Liu, Z.; Tan, L.; Su, A.N.; Jiang, W.G.; Gong, C. HIF1alpha-associated circDENND4C Promotes Proliferation of Breast Cancer Cells in Hypoxic Environment. *Anticancer Res.* **2017**, *37*, 4337–4343. [CrossRef] [PubMed]
53. Burd, C.E.; Jeck, W.R.; Liu, Y.; Sanoff, H.K.; Wang, Z.; Sharpless, N.E. Expression of linear and novel circular forms of an INK4/ARF-associated non-coding RNA correlates with atherosclerosis risk. *PLoS Genet.* **2010**, *6*, e1001233. [CrossRef] [PubMed]
54. Ng, W.L.; Marinov, G.K.; Liau, E.S.; Lam, Y.L.; Lim, Y.Y.; Ea, C.K. Inducible RasGEF1B circular RNA is a positive regulator of ICAM-1 in the TLR4/LPS pathway. *RNA Biol.* **2016**, *13*, 861–871. [CrossRef] [PubMed]
55. Xie, H.; Ren, X.; Xin, S.; Lan, X.; Lu, G.; Lin, Y.; Yang, S.; Zeng, Z.; Liao, W.; Ding, Y.Q.; et al.,Emerging roles of circRNA_001569 targeting miR-145 in the proliferation and invasion of colorectal cancer. *Oncotarget* **2016**, *7*, 26680–26691. [CrossRef] [PubMed]
56. Xu, L.; Zhang, M.; Zheng, X.B.; Yi, P.S.; Lan, C.; Xu, M.Q. The circular RNA ciRS-7 (Cdr1as) acts as a risk factor of hepatic microvascular invasion in hepatocellular carcinoma. *J. Cancer Res. Clin. Oncol.* **2017**, *143*, 17–27. [CrossRef] [PubMed]
57. Qin, M.; Liu, G.; Huo, X.; Tao, X.; Sun, X.; Ge, Z.; Yang, J.; Fan, J.; Liu, L.; Qin, W. hsa_circ_0001649: A circular RNA and potential novel biomarker for hepatocellular carcinoma. *Cancer Biomark. Sect. Dis. Markers* **2016**, *16*, 161–169. [CrossRef] [PubMed]
58. Shang, X.; Li, G.; Liu, H.; Li, T.; Liu, J.; Zhao, Q.; Wang, C. Comprehensive Circular RNA Profiling Reveals That hsa_circ_0005075, a New Circular RNA Biomarker, Is Involved in Hepatocellular Crcinoma Development. *Medicine* **2016**, *95*, e3811. [CrossRef] [PubMed]
59. Yao, Z.; Luo, J.; Hu, K.; Lin, J.; Huang, H.; Wang, Q.; Zhang, P.; Xiong, Z.; He, C.; Huang, Z.; et al.,ZKSCAN1 gene and its related circular RNA (circZKSCAN1) both inhibit hepatocellular carcinoma cell growth, migration, and invasion but through different signaling pathways. *Mol. Oncol.* **2017**, *11*, 422–437. [CrossRef] [PubMed]
60. Zhong, Z.; Lv, M.; Chen, J. Screening differential circular RNA expression profiles reveals the regulatory role of circTCF25-miR-103a-3p/miR-107-CDK6 pathway in bladder carcinoma. *Sci. Rep.* **2016**, *6*, 30919. [CrossRef] [PubMed]
61. Huang, M.; Zhong, Z.; Lv, M.; Shu, J.; Tian, Q.; Chen, J. Comprehensive analysis of differentially expressed profiles of lncRNAs and circRNAs with associated co-expression and ceRNA networks in bladder carcinoma. *Oncotarget* **2016**, *7*, 47186–47200. [CrossRef] [PubMed]
62. Wang, K.; Sun, Y.; Tao, W.; Fei, X.; Chang, C. Androgen receptor (AR) promotes clear cell renal cell carcinoma (ccRCC) migration and invasion via altering the circHIAT1/miR-195-5p/29a-3p/29c-3p/CDC42 signals. *Cancer Lett.* **2017**, *394*, 1–12. [CrossRef] [PubMed]
63. Guarnerio, J.; Bezzi, M.; Jeong, J.C.; Paffenholz, S.V.; Berry, K.; Naldini, M.M.; Lo-Coco, F.; Tay, Y.; Beck, A.H.; Pandolfi, P.P. Oncogenic Role of Fusion-circRNAs Derived from Cancer-Associated Chromosomal Translocations. *Cell* **2016**, *165*, 289–302. [CrossRef] [PubMed]
64. Lukiw, W.J. Circular RNA (circRNA) in Alzheimer's disease (AD). *Front. Genet.* **2013**, *4*, 307. [CrossRef] [PubMed]
65. Khoutorsky, A.; Yanagiya, A.; Gkogkas, C.G.; Fabian, M.R.; Prager-Khoutorsky, M.; Cao, R.; Gamache, K.; Bouthiette, F.; Parsyan, A.; Sorge, R.E.; et al.,Control of synaptic plasticity and memory via suppression of poly(A)-binding protein. *Neuron* **2013**, *78*, 298–311. [CrossRef] [PubMed]
66. Cui, X.; Niu, W.; Kong, L.; He, M.; Jiang, K.; Chen, S.; Zhong, A.; Li, W.; Lu, J.; Zhang, L. hsa_circRNA_103636: Potential novel diagnostic and therapeutic biomarker in major depressive disorder. *Biomark. Med.* **2016**, *10*, 943–952. [CrossRef] [PubMed]
67. Liu, Q.; Zhang, X.; Hu, X.; Dai, L.; Fu, X.; Zhang, J.; Ao, Y. Circular RNA Related to the Chondrocyte ECM Regulates MMP13 Expression by Functioning as a miR-136 'Sponge' in Human Cartilage Degradation. *Sci. Rep.* **2016**, *6*, 22572. [CrossRef] [PubMed]
68. Holdt, L.M.; Stahringer, A.; Sass, K.; Pichler, G.; Kulak, N.A.; Wilfert, W.; Kohlmaier, A.; Herbst, A.; Northoff, B.H.; Nicolaou, A.; et al.,Circular non-coding RNA ANRIL modulates ribosomal RNA maturation and atherosclerosis in humans. *Nat. Commun.* **2016**, *7*, 12429. [CrossRef] [PubMed]
69. Taibi, F.; Metzinger-Le Meuth, V.; Massy, Z.A.; Metzinger, L. miR-223: An inflammatory oncomiR enters the cardiovascular field. *Biochim. Biophys. Acta* **2014**, *1842*, 1001–1009. [CrossRef] [PubMed]

70. Wang, K.; Long, B.; Liu, F.; Wang, J.X.; Liu, C.Y.; Zhao, B.; Zhou, L.Y.; Sun, T.; Wang, M.; Yu, T.; et al.,A circular
RNA protects the heart from pathological hypertrophy and heart failure by targeting miR-223. *Eur. Heart J.* **2016**, *37*, 2602–2611. [CrossRef] [PubMed]
71. Khan, M.A.; Reckman, Y.J.; Aufiero, S.; van den Hoogenhof, M.M.; van der Made, I.; Beqqali, A.; Koolbergen, D.R.; Rasmussen, T.B.; van der Velden, J.; Creemers, E.E.; et al.,RBM20 Regulates Circular RNA
Production From the Titin Gene. *Circ. Res.* **2016**, *119*, 996–1003. [CrossRef] [PubMed]
72. Wang, K.; Gan, T.Y.; Li, N.; Liu, C.Y.; Zhou, L.Y.; Gao, J.N.; Chen, C.; Yan, K.W.; Ponnusamy, M.; Zhang, Y.H.; et al.,Circular RNA mediates cardiomyocyte death via miRNA-dependent upregulation of MTP18 expression. *Cell Death Differ.* **2017**, *24*, 1111–1120. [CrossRef] [PubMed]
73. Tang, C.M.; Zhang, M.; Huang, L.; Hu, Z.Q.; Zhu, J.N.; Xiao, Z.; Zhang, Z.; Lin, Q.X.; Zheng, X.L.; Yang, M.; et al.,circRNA_000203 enhances the expression of fibrosis-associated genes by derepressing targets of miR-26b-5p, Col1a2 and CTGF, in cardiac fibroblasts. *Sci. Rep.* **2017**, *7*, 40342. [CrossRef] [PubMed]
74. Zhou, B.; Yu, J.W. A novel identified circular RNA, circRNA_010567, promotes myocardial fibrosis via suppressing miR-141 by targeting TGF-beta1. *Biochem. Biophys. Res. Commun.* **2017**, *487*, 769–775. [CrossRef] [PubMed]
75. Zhao, Z.; Li, X.; Jian, D.; Hao, P.; Rao, L.; Li, M. hsa_circ_0054633 in peripheral blood can be used as a diagnostic biomarker of pre-diabetes and type 2 diabetes mellitus. *Acta Diabetol.* **2017**, *54*, 237–245. [CrossRef] [PubMed]
76. Gu, Y.; Ke, G.; Wang, L.; Zhou, E.; Zhu, K.; Wei, Y. Altered Expression Profile of Circular RNAs in the Serum of Patients with Diabetic Retinopathy Revealed by Microarray. *Ophthalmic Res.* **2017**, *58*, 176–184. [CrossRef] [PubMed]
77. Shan, K.; Liu, C.; Liu, B.H.; Chen, X.; Dong, R.; Liu, X.; Zhang, Y.Y.; Liu, B.; Zhang, S.J.; Wang, J.J.; et al.,Circular Non-Coding RNA HIPK3 Mediates Retinal Vascular Dysfunction in Diabetes Mellitus. *Circulation* **2017**. [CrossRef] [PubMed]
78. Qian, Y.; Lu, Y.; Rui, C.; Qian, Y.; Cai, M.; Jia, R. Potential Significance of Circular RNA in Human Placental Tissue for Patients with Preeclampsia. *Cell. Phys. Biochem.* **2016**, *39*, 1380–1390. [CrossRef] [PubMed]
79. Zhang, Y.G.; Yang, H.L.; Long, Y.; Li, W.L. Circular RNA in blood corpuscles combined with plasma protein factor for early prediction of pre-eclampsia. *BJOG Int. J. Obstet. Gynaecol.* **2016**, *123*, 2113–2118. [CrossRef] [PubMed]
80. Chen, Y.G.; Kim, M.V.; Chen, X.; Batista, P.J.; Aoyama, S.; Wilusz, J.E.; Iwasaki, A.; Chang, H.Y. Sensing Self and Foreign Circular RNAs by Intron Identity. *Mol. Cell* **2017**, *67*, 228–238. [CrossRef] [PubMed]
81. Li, X.; Liu, C.X.; Xue, W.; Zhang, Y.; Jiang, S.; Yin, Q.F.; Wei, J.; Yao, R.W.; Yang, L.; Chen, L.L. Coordinated circRNA Biogenesis and Function with NF90/NF110 in Viral Infection. *Mol. Cell* **2017**, *67*, 214–227. [CrossRef] [PubMed]
82. Gruner, H.; Cortes-Lopez, M.; Cooper, D.A.; Bauer, M.; Miura, P. circRNA accumulation in the aging mouse brain. *Sci. Rep.* **2016**, *6*, 38907. [CrossRef] [PubMed]
83. Panda, A.C.; Grammatikakis, I.; Kim, K.M.; De, S.; Martindale, J.L.; Munk, R.; Yang, X.; Abdelmohsen, K.; Gorospe, M. Identification of senescence-associated circular RNAs (SAC-RNAs) reveals senescence suppressor circPVT1. *Nucleic Acids Res.* **2017**, *45*, 4021–4035. [CrossRef] [PubMed]
84. Suzuki, H.; Zuo, Y.; Wang, J.; Zhang, M.Q.; Malhotra, A.; Mayeda, A. Characterization of RNase R-digested cellular RNA source that consists of lariat and circular RNAs from pre-mRNA splicing. *Nucleic Acids Res.* **2006**, *34*, e63. [CrossRef] [PubMed]
85. Enuka, Y.; Lauriola, M.; Feldman, M.E.; Sas-Chen, A.; Ulitsky, I.; Yarden, Y. Circular RNAs are long-lived and display only minimal early alterations in response to a growth factor. *Nucleic Acids Res.* **2016**, *44*, 1370–1383. [CrossRef] [PubMed]
86. Memczak, S.; Papavasileiou, P.; Peters, O.; Rajewsky, N. Identification and Characterization of Circular RNAs As a New Class of Putative Biomarkers in Human Blood. *PLoS ONE* **2015**, *10*, e0141214. [CrossRef] [PubMed]
87. Bahn, J.H.; Zhang, Q.; Li, F.; Chan, T.M.; Lin, X.; Kim, Y.; Wong, D.T.; Xiao, X. The landscape of microRNA, Piwi-interacting RNA, and circular RNA in human saliva. *Clin. Chem.* **2015**, *61*, 221–230. [CrossRef] [PubMed]

88. Li, Y.; Zheng, Q.; Bao, C.; Li, S.; Guo, W.; Zhao, J.; Chen, D.; Gu, J.; He, X.; Huang, S. Circular RNA is enriched and stable in exosomes: A promising biomarker for cancer diagnosis. *Cell Res.* **2015**, *25*, 981–984. [CrossRef] [PubMed]
89. Li, P.; Chen, S.; Chen, H.; Mo, X.; Li, T.; Shao, Y.; Xiao, B.; Guo, J. Using circular RNA as a novel type of biomarker in the screening of gastric cancer. *Clin. Chim. Acta* **2015**, *444*, 132–136. [CrossRef] [PubMed]
90. Chen, S.; Li, T.; Zhao, Q.; Xiao, B.; Guo, J. Using circular RNA hsa_circ_0000190 as a new biomarker in the diagnosis of gastric cancer. *Clin. Chim. Acta* **2017**, *466*, 167–171. [CrossRef] [PubMed]
91. Shao, Y.; Chen, L.; Lu, R.; Zhang, X.; Xiao, B.; Ye, G.; Guo, J. Decreased expression of hsa_circ_0001895 in human gastric cancer and its clinical significances. *Tumour Biol.* **2017**, *39*, 1010428317699125. [CrossRef] [PubMed]
92. Huang, X.Y.; Huang, Z.L.; Xu, Y.H.; Zheng, Q.; Chen, Z.; Song, W.; Zhou, J.; Tang, Z.Y.; Huang, X.Y. Comprehensive circular RNA profiling reveals the regulatory role of the circRNA-100338/miR-141-3p pathway in hepatitis B-related hepatocellular carcinoma. *Sci. Rep.* **2017**, *7*, 5428. [CrossRef] [PubMed]
93. Zhao, M.; Gao, F.; Zhang, D.; Wang, S.; Zhang, Y.; Wang, R.; Zhao, J. Altered expression of circular RNAs in Moyamoya disease. *J. Neurol. Sci.* **2017**, *381*, 25–31. [CrossRef] [PubMed]
94. Li, T.; Shao, Y.; Fu, L.; Xie, Y.; Zhu, L.; Sun, W.; Yu, R.; Xiao, B.; Guo, J. Plasma circular RNA profiling of patients with gastric cancer and their droplet digital RT-PCR detection. *J Mol. Med.* **2017**. [CrossRef] [PubMed]
95. Pan, R.Y.; Liu, P.; Zhou, H.T.; Sun, W.X.; Song, J.; Shu, J.; Cui, G.J.; Yang, Z.J.; Jia, E.Z. Circular RNAs promote TRPM3 expression by inhibiting hsa-miR-130a-3p in coronary artery disease patients. *Oncotarget* **2017**, *8*, 60280–60290. [CrossRef] [PubMed]
96. Cardamone, G.; Paraboschi, E.M.; Rimoldi, V.; Duga, S.; Solda, G.; Asselta, R. The Characterization of GSDMB Splicing and Backsplicing Profiles Identifies Novel Isoforms and a Circular RNA That Are Dysregulated in Multiple Sclerosis. *Int. J. Mol. Sci.* **2017**, *18*. [CrossRef] [PubMed]
97. Zeng, Y.; Xu, Y.; Shu, R.; Sun, L.; Tian, Y.; Shi, C.; Zheng, Z.; Wang, K.; Luo, H. Altered expression profiles of circular RNA in colorectal cancer tissues from patients with lung metastasis. *Int. J. Mol. Med.* **2017**, *40*, 1818–1828. [CrossRef] [PubMed]
98. Zheng, F.; Yu, X.; Huang, J.; Dai, Y. Circular RNA expression profiles of peripheral blood mononuclear cells in rheumatoid arthritis patients, based on microarray chip technology. *Mol. Med. Rep.* **2017**, *16*, 8029–8036. [CrossRef] [PubMed]
99. Zhang, Y.; Li, J.; Yu, J.; Liu, H.; Shen, Z.; Ye, G.; Mou, T.; Qi, X.; Li, G. Circular RNAs signature predicts the early recurrence of stage III gastric cancer after radical surgery. *Oncotarget* **2017**, *8*, 22936–22943. [CrossRef] [PubMed]
100. Chen, J.; Li, Y.; Zheng, Q.; Bao, C.; He, J.; Chen, B.; Lyu, D.; Zheng, B.; Xu, Y.; Long, Z.; et al.,Circular RNA profile identifies circPVT1 as a proliferative factor and prognostic marker in gastric cancer. *Cancer Lett.* **2017**, *388*, 208–219. [CrossRef] [PubMed]
101. Ouyang, Q.; Wu, J.; Jiang, Z.; Zhao, J.; Wang, R.; Lou, A.; Zhu, D.; Shi, G.P.; Yang, M. Microarray Expression Profile of Circular RNAs in Peripheral Blood Mononuclear Cells from Rheumatoid Arthritis Patients. *Cell. Physiol. Biochem.* **2017**, *42*, 651–659. [CrossRef] [PubMed]
102. Fang, Y.; Ma, M.; Wang, J.; Liu, X.; Wang, Y. Circular RNAs play an important role in late-stage gastric cancer: Circular RNA expression profiles and bioinformatics analyses. *Tumour Biol.* **2017**, *39*. [CrossRef] [PubMed]
103. Guo, W.; Zhang, J.; Zhang, D.; Cao, S.; Li, G.; Zhang, S.; Wang, Z.; Wen, P.; Yang, H.; Shi, X.; et al.,Polymorphisms and expression pattern of circular RNA circ-ITCH contributes to the carcinogenesis of hepatocellular carcinoma. *Oncotarget* **2017**, *8*, 48169–48177. [CrossRef] [PubMed]
104. Wu, N.; Jin, L.; Cai, J. Profiling and bioinformatics analyses reveal differential circular RNA expression in hypertensive patients. *Clin. Exp. Hypertens.* **2017**, *39*, 454–459. [CrossRef] [PubMed]
105. Zhao, Z.; Li, X.; Gao, C.; Jian, D.; Hao, P.; Rao, L.; Li, M. Peripheral blood circular RNA hsa_circ_0124644 can be used as a diagnostic biomarker of coronary artery disease. *Sci. Rep.* **2017**, *7*, 39918. [CrossRef] [PubMed]
106. Bazan, H.A.; Hatfield, S.A.; Brug, A.; Brooks, A.J.; Lightell, D.J., Jr.; Woods, T.C. Carotid Plaque Rupture Is Accompanied by an Increase in the Ratio of Serum circR-284 to miR-221 Levels. *Circ. Cardiovasc. Genet.* **2017**, *10*. [CrossRef] [PubMed]

107. Iparraguirre, L.; Munoz-Culla, M.; Prada-Luengo, I.; Castillo-Trivino, T.; Olascoaga, J.; Otaegui, D. Circular RNA profiling reveals that circular RNAs from ANXA2 can be used as new biomarkers for multiple sclerosis. *Hum. Mol. Genet.* **2017**, *26*, 3564–3572. [CrossRef] [PubMed]
108. Liu, Y.; Cui, H.; Wang, W.; Li, L.; Wang, Z.; Yang, S.; Zhang, X. Construction of circular miRNA sponges targeting miR-21 or miR-221 and demonstration of their excellent anticancer effects on malignant melanoma cells. *Int. J. Biochem. Cell Biol.* **2013**, *45*, 2643–2650. [CrossRef] [PubMed]
109. Lee, T.; Awano, H.; Yagi, M.; Matsumoto, M.; Watanabe, N.; Goda, R.; Koizumi, M.; Takeshima, Y.; Matsuo, M. 2^{0}-*O*-Methyl RNA/Ethylene-Bridged Nucleic Acid Chimera Antisense Oligonucleotides to Induce Dystrophin Exon 45 Skipping. *Genes* **2017**, *8*. [CrossRef] [PubMed]

Summary of research publications

Circular RNAs (circRNAs) are non-coding RNAs that may have the portential to regulate gene expression . CircRNAs have been shown to accumulate during ageing models. The research publications associated with this thesis assessed wheher circRNAs were dysregulated of in ageing human peripheral blood of a relatively ageing human cohort and in a disease related to ageing ie. T2D. Whether the expression of circRNA were associated with various ageing outcomes in human, mammalian longevity and senescence in human cell types of various lineages, and in blood as well as islet samples from patients was assessed.

Of the 15 candidate circRNAs followed up in the ageing InCHIANTI population study study, four were associated with parental longevity or hand grip strength. Some of tehse circRNA wrere also differentially expressed in one or more human senescent cell types and one nominally correlated with median strain lifespanin rodent models.

As type 2 diabetes is an exemplar chronic disease of ageing, I also aimed to examine the role of circRNA in this disorder. I first defined the circRNA repertoire in human pancreatic islets and assessed their differential expression in conjunction with type 2 diabetes status and genotype at T2D risk loci. Following this, I determined their responsiveness to diabetomimetic stimuli in the human EndoC-βH1 beta cell line, and the potential for use as biomarkers of T2D in human peripheral blood. 4 of the five most abundant circRNAs expressed in human pancreatic islets *circCIRBP*, *circZKSCAN*, *circRPH3AL* and *circCAMSAP1,* were associated with diabetes status in islets. C*ircCIRBP* and *circRPH3AL* were also differentially expressed in β-cells in response to elevated fatty acid. Despite this, no associations with T2D diabetes risk

loci was identified. Cumulatively, the data generated from my work suggest that circRNAs have potential as regulators of gene expression during ageing and age-related disease, raising the possibility that they may have future utility as biomarkers or therapeutic targets for the management of age-related chronic disease outcomes.

https://doi.org/10.1007/s11357-019-00120-z

ORIGINAL ARTICLE

circRNAs expressed in human peripheral blood are associated with human aging phenotypes, cellular senescence and mouse lifespan

Shahnaz Haque & Ryan M. Ames & Karen Moore & Luke C. Pilling & Luanne L. Peters & Stefania Bandinelli & Luigi Ferrucci & Lorna W. Harries

Received: 2 October 2019 /Accepted: 4 October 2019 /Published online: 6 December 2019

Abstract Circular RNAs (circRNAs) are an emerging class of non-coding RNA molecules that are thought to regulate gene expression and human disease. Despite the observation that circRNAs are known to accumulate in older organisms and have been reported in cellular senescence, their role in aging remains relatively unexplored. Here, we have assessed circRNA expression in aging human blood and followed up age-associated circRNA in relation to human aging phenotypes, mammalian longevity as measured by mouse median strain lifespan and cellular senescence in four different primary human cell types. We found that circRNAs circDEF6, circEP300, circFOXO3 and circFNDC3B demonstrate associations with parental longevity or hand grip strength in 306 subjects from the InCHIANTI study of aging, and furthermore, circFOXO3 and circEP300 also demonstrate differential expression in one or more human senescent celltypes.Finally,fourcircRNAs tested showed evidence of conservation in mouse. Expression levels of one of these, circPlekhm1, was nominally associated with lifespan. These data suggest that circRNA may represent a novel class of regulatory RNA involved in the determination of aging phenotypes, which may show future promise as both biomarkers and future therapeutic targets for age-related disease.

Electronic supplementary material The online version of this article (https://doi.org/10.1007/s11357-019-00120-z) contains supplementary material, which is available to authorized users.

S. Haque：L. W. Harries (*)
RNA-Mediated Mechanisms of Disease Group, Institute of Biomedical and Clinical Sciences, University of Exeter Medical
School, University of Exeter, RILD South, Barrack Road, Exeter EX2 5DW, UK
e-mail: L.W.Harries@exeter.ac.uk

R. M. Ames
Biosciences, University of Exeter, Exeter, UK

K. Moore
College of Life and Environmental Sciences, University of Exeter,
Exeter, UK

L. C. Pilling
Epidemiology and Public Health, University of Exeter Medical School, University of Exeter, Exeter, UK

L. L. Peters
The Jackson Laboratory Nathan Shock Centre of Excellence in the Basic Biology of Aging, Bar Harbor, ME, USA

S. Bandinelli
Geriatric Unit, USLToscana Centro, Florence, Italy

L. Ferrucci
National Institute on Aging, Clinical Research Branch, Harbor Hospital, Baltimore, MD 21225, USA

Keywords CircularRNA . Aging phenotypes. Senescence . Medianstrainlifespan

Introduction

Aging is a multifactorial process leading to gradual deterioration of physical and physiological functionality at the cellular, tissue and organ levels. It is the primary risk factor for chronic aging pathologies such as cancer, sarcopenia, diabetes, cardiovascular disorders and neurodegenerative illnesses that account for the bulk of morbidity and mortality in both the developed as well as developing world (Kirkland 2016). Physiological parameters such as loss of muscle mass, frailty, immobility and cognitive impairment increase the risk of developing geriatric syndromes (Fabbri et al., 2016; Narici and Maffulli 2010). The molecular processes that decline with advancing age underpin the phenotypes of aging. At the cellular level, hallmarks of aging include genomic instability, telomere attrition, epigenetic alterations, loss of proteostasis, deregulated nutrient sensing, mitochondrial dysfunction, cellular senescence, stem cell exhaustion and altered intercellular communication (Lopez-Otin et al., 2013).

Changes in gene expression have been reported in many age-related diseases (Yang et al., 2015). In addition to an increase in transcriptional noise and aberrant production and maturation of mRNA transcripts (Bahar et al., 2006; Harries et al., 2011), studies report associations between gene expression and the development of age-associated syndromes of the muscle (Noren Hooten et al., 2010; Welle et al., 2004) as well as neurodegenerative conditions such as Alzheimer's disease and Parkinson's disease (Miller et al., 2017; Shamir et al., 2017). Differential expression of genes involved in inflammatory, mitochondrial and lysosomal degradation in aging tissues has also been reported (de Magalhaes et al., 2009). Gene expression is regulated at many levels. Changes in the regulation and pattern of alternative splicing are associated with age in several human populations and are also evident in senescent cells of different lineages, where they may drive cellular senescence, since restoration of

levels reverses multiple senescence phenotypes (Latorre et al., 2017; Latorre et al., 2018a; Latorre et al., 2018b; Latorre et al., 2018c; Lye et al., 2019). Notably, non-coding RNAs also demonstrate associations with aging or senescence and may be of equal importance (Abdelmohsen et al., 2012; Boulias and Horvitz 2012; Gorospe and Abdelmohsen 2011).

Circular RNAs (circRNAs) are a recently discovered class of non-coding RNA molecules that are thought to have important roles in regulation of gene expression and human disease (Haque and Harries 2017). circRNAs are formed by the back splicing of downstream exons to the 3′ acceptor splice site of upstream exons and result in a covalently closed circular structure containing one or more exons. They have been proposed to be key regulators of gene expression by various mechanisms including sequestration of RNA-binding proteins and miRNAs or by acting as a competitor of linear splicing of their cognate genes (Memczak et al., 2013). The possibility that a single circRNA could sequester several such RNA regulators suggests that this class of non-coding RNAs could modulate many cellular and physiological processes through multiple pathways. circRNAs are known to accumulate in older organisms (Gruner et al., 2016), and some have been reported to be implicated in cellular senescence (Du et al., 2017; Du et al., 2016). Despite these promising findings, their role in aging remains relatively unexplored.

We hypothesized that expression of some circRNAs may be associated with advancing age, aging phenotypes, lifespan or cellular senescence. Changes in circRNA expression over a 5-year period were assessed in relation to age, combined parental longevity score (PLS) and hand grip strength. We then assessed expression levels of 15 circRNAs in early passage and late passage primary human dermal fibroblasts, cardiomyocytes, astrocytes and vascular endothelial cells. Finally, the junction sequences of relevant exons were examined for conservation between mouse and humans and where evidence was present that the back-spliced junction, and thus, the circular RNA were

conserved; we assessed expression in relation to longevity in six strains of mice with differential median strain longevities.

We present here evidence thatalthough effects on age itself did not replicate in the wider sample set, the expression levels of circEP300 (β = −0.065, P = 0.001) and circFOXO3 (β = −0.060, P = 0.002) were negatively associated with parental longevity score. circDEF6 was positively associated with parental longevity score (β = 0.070, P = 0.024) although this did not reach multiple testing thresholds. circFNDC3B was also nominally associated with hand gripstrength(β = 0.004, P = 0.039). circRNAs (7/12 (58%)) expressed in senescent human primary astrocytes, endothelial cells, fibroblasts or cardiomyocytes also demonstrated dysregulated expression in one or more cell types. Comparative sequence analysis suggested that four circRNAs may be conserved in mice. When assessed, circPlekhm1 transcript level in spleen was also demonstrated to be positively associated with mouse median strain lifespan (β = 0.0025; P = 0.017). These results suggest that some age-related circRNAs may play roles in molecular drivers of aging such as cellular senescence, and hence may represent potential contributors to lifespan or other human aging phenotypes.

Methods

InCHIANTI cohort and selection of participants

The InCHIANTI study of Aging is a population study of aging (Ferrucci et al., 2000). Participants undertook detailed assessment of health and lifestyle parameters at baseline, and again at three subsequent follow-ups (FU2 2004–2006, FU3 2007–2010and FU4 2012–2014).The present study used participants from the third and fourth follow-up visits (FU3 and FU4). RNA samples and clinical/phenotypic data were already available for 698 participants at FU3. The collection of the FU4 samples and data comprise part of this study. During the FU4 interviews in 2012/2013, blood and clinical/phenotypic data were collected from 455 study participants. These data were cross-

checked against RNA samples and clinical/phenotypic data already held from FU3, to ensure that sample and phenotypic data was available from both collections. Sample-associated data included measures of potential confounding factors such as BMI, sex, level of education (none, elementary, secondary, high school and university), study site, smoking and white blood counts (neutrophil, lymphocyte, monocyte, eosinophil percentages). Characteristics of the study populationare given inTable 1. Informedconsent was obtained from all participants. Ethical approval was obtained from the Instituto Nazionale Riposo e Cura Anziani institutional review board, Italy.

Generation of circRNA profiles from old and young human peripheral blood

Circular RNA profiles were initially generated in parallel from two sets of pooled peripheral blood total RNA samples using a modified 'CircleSeq' procedure (LopezJimenez et al., 2018). 2 μg RNA (RNA integrity number (RIN) = 6.4) was assessed in two separate pools from 20 'young' samples (median age = 33 years, range 30–36 years, 55% female, 45% male; RIN 5.6) and 20 'old' samples (median age 87 years, range 86–95 years, 90% female 10% male, RIN 7.7). Each pooled sample was divided into two aliquots, one of which was treated with 20 units RNAse R (Epicentre, Madison, USA) at 30 °C for 30 min to remove linear RNA, the other sample being mock-treated using 1 μL RNase-free water in place of the enzyme. Both aliquots were cleaned and concentrated using 2 volumes of RNA clean beads (Beckman Coulter, Indianapolis, USA) to remove the enzyme. The results of the RNase R treatment were confirmed on a highsensitivity RNA screentape (Agilent, Santa Clara, USA). Ribosomal RNA was removed, and indexed sequencing libraries made using the libraries were determined by qPCR and adjusted for size using Tapestation D1000 analysis (Agilent, Santa Clara, USA). Ribosomal RNA was removed, and indexed sequencing libraries made using the Illumina RNASeq protocol. The library concentrations were determined by

qPCR and adjusted for size using the data from the Tapestation D1000 analysis. Libraries were pooled in equimolar quantities, denatured and diluted to 12.0 pM + 1% PhiX for clustering and then underwent 125 paired-end Illumina sequencing in four lanes using TruSeq SBS reagents (V3).

Analysis of circRNA profiles

RNase R and mock-treated sequence data were assembled, and putative circular RNAs were identified using PTESFinder (Izuogu et al., 2016) with the human genome (hg19) reference files provided with the software, a segment size of 65 and a uniqueness score of 7. The remaining parameters were left to default settings. To calculate a comparable measure of circular RNA abundance between samples, we used a measure termed back-spliced reads per million mapped reads (bpm) for each circular RNA defined as

$$bpm^{i} ¼ \frac{\sum^{n}_{a¼1} j_a}{\sum^{n}_{b¼1} C_b} \; 10_6$$

where J_i is the number of reads mapped to the backspliced junction of the circular RNA, c is the number of reads mapped to canonical sites of the gene with the circular RNA and n is the number of circular RNAs identified. This measure is designed to be similar to the commonly used reads per kilobase per million mapped reads (RPKM) metric used regularly to estimate gene expression from RNA-Seq data.

In addition to circular RNA detection using PTESFinder, reads from all samples were also mapped to the human genome reference (hg19) obtained from

Table 1 Participant demographics, population demographics and clinical characteristics of InCHIANTI study participants assessed in this work, (A) demographics and (B) clinical characteristics

A	Number	Percentage
Participants	306	100
Age (years)		
30–39	24	7.84
40–49	37	12.09
50–59	31	10.13
60–69	32	10.46
70–79	116	37.91
80–89	63	20.59

90–100			3		0.98
Gender					
Male			143		46.73
Female			163		53.27
Pack years smoked (lifetime)					
None			164		53.59
< 20			79		25.82
20–39			43		14.05
40+			20		6.54
Study site					
Greve			146		47.71
Bagno			160		52.29
Education level attained					
Nothing			22		7.19
Elementary			124		40.52
Secondary			56		18.30
High school			50		16.34
Professional school			34		11.11
University or equivalent			20		6.54
B	n	Mean	SD	Min	Max
Age (years)	306	66.96	16.06	30.00	94.00
BMI	305	27.15	4.35	15.01	42.99
White blood cell count (n, K/μLs)	305	6.40	1.59	2.10	13.00
Neutrophils (%)	305	56.59	8.35	34.20	81.20
Lymphocytes (%)	304	31.69	7.67	9.80	51.20
Monocytes (%)	304	8.04	2.20	3.90	21.30
Eosinophils (%)	304	3.18	2.17	0.00	21.50
Parental longevity score	206	− 0.02	0.81	− 2.46	1.71
Mean hand-grip strength (kg)					
Follow-up 3	305	29.65	12.49	2.50	70.75
Follow-up 4	291	28.66	12.30	5.00	65.50

iGenomes using Tophat v2.1.0 with the pre-set sensitive alignment parameters in paired-end mode (Trapnell et al., 2009). The number of reads mapping to each exon of each gene was then calculated using FeatureCounts v2.0.0 with parameters for unstranded alignment, paired reads, count multimapping reads and assigning reads to overlapping features (Liao et al., 2013; Liao et al., 2014). Counts were used to calculate RPKM per exon using the standard method to compare the expression of each exon across samples.

Pathway analysis of differentially regulated circRNA host genes

circRNAs showing expression differences between the pooled old and the pooled young samples were ranked by RPKM and fold change. To assess whether circRNAs demonstrating expression differences between young and old pools were enriched in genes derived from specific molecularorbiochemicalfunctiongroups,

wecarriedouta Cytoscape version 2.5.2 plug-in ClueGO analysis. This platform queries over-representation of query genes in specific KEGG, REACTOME and WikiPathways
(Bindea et al., 2009). The linear genes hosting the top 10% most abundantly expressed circRNAs in young and old pools for the circRNA profile were queried against KEGG_20.11.2017,REACTOME_Pathways_20.11.2017 and WikiPathways_20.11.2017. Outputs were selected based on 'enrichment/depletion' through a two-sided hypergeometric test with Bonferronistep down for P value correction with the selected ontology reference set of chosen genes. The GO terms were used to group functional pathways, and the leading functional grouping was based on highest significant kappa score.

Design of qPCR assays for circRNA validation

Levels of individual circRNA in young and old pools were ranked by abundance. circRNAs demonstrating evidence of altered expression with age fell into three classes: those expressed exclusively in old, those expressed exclusively in young, and those expressed in both young and old, but with evidence that levels were different between the pools. WeselectedfivecircRNAsexclusivelyexpressedinyoung (circITGAX, circPLEKHM1, circDEF6, circATP6V0A1 and circASAP1), five exclusively expressed in the old (circFOXO3, circFNDC3B, circAFF1, circCDYL and circXPO7), as well as five expressed in both pools but demonstrating evidence of altered expression (circMIB1, circMETTL3, circBCL11B, circZC3H18 and circEP300), where sequence and assay design constraints allowed for to design specific assays to unique back-spliced junction for qRTPCR follow-up.
circRNA probe design

Custom-designed qRTPCR assays for quantification of relative expression were designed to unique backspliced circRNA junctions (Thermo Fisher, Foster City, USA), the sequences of which are given in Online Resource 1. Each target sequence was checked for the presence

of single nucleotide polymorphisms in potential primer or probe binding regions prior to ordering. Assays were ordered as custom single-tube assays from Thermo Fisher (Foster City, USA). Each circRNA probe was validated using standard curve analysis using 1:10 serial dilutions of synthetic oligonucleotides homologous to the back-spliced junctions.

Assessment of associations between circRNA expression and aging phenotypes in the InCHIANTI cohort

RNA samples and phenotypic data were available from 306 individuals at both follow-up 3 (FU3) and followup 4 (FU4) of the InCHIANTI study of aging. Characteristics of participants are given in Table 1. We assessed the expression of 15 age-associated circRNAs demonstrating the most marked differential expression with age between young and old pools as described above. Aging parameters assessed were age itself, parental longevity score (PLS) and hand grip strength. Participants aged 65 + years were categorised for PLS based on the age at death of their parents. Short, intermediate and long-lived cut-offs were calculated separately for mothers and fathers based on the normal distribution of age at death in the cohort, as described in Dutta et al.,(2013a). Mothers and fathers aged < 49 years or < 52 years at death respectively were classed as premature and excluded. To standardize parental age of death, a Z score was generated for combined maternal and paternal measures of parental longevity. Hand-grip strength was measured in kilograms using a dynamometer, with repeated measurements at both FU3 and FU4.

Reverse transcription and pre-amplification of circRNAs in human peripheral blood RNA

cDNA synthesis was carried out using 100 ng total RNA using the High-Capacity cDNA Reverse Transcription Kit (Thermo Fisher, Foster City, USA) according to manufacturer's instructions (Fisher Scientific, New Hampshire, USA) in a final reaction volume of 10.0 μL per sample. Reactions (samples in 96-well plates) were run at 25 °C for 10 min, 37 °C for 120 min, 85 °C for 5 min followed by an inactivation period for 95 °C for 10

min. Pre-amplification of circRNA expression was carried out using 5 μL TaqMan PreAmp master mix (Thermo Fisher, Foster City, USA), 2.5 μL pooled assay mix and 2.5 μL cDNA in a final reaction volume of 10 μL per sample. Cycling conditions were one cycle of 95 °C for 10 min followed by 14 cycles of 95 °C for 15 s with 60 °C for 4 min followed by 95 °C for 10 min. Pre-amplified samples were then diluted 1:10 and maintained on ice prior to analysis.

Assessment of associations between circRNA expression in peripheral blood RNA and human aging phenotypes

The expression profiles of selected circRNAs were then measured in total peripheral blood mRNA using customdesigned OpenArray plates on the Thermo Fisher 12K Flexplatform(ThermoFisher,FosterCity,USA).Reaction mixes contained 2.5 μL 2× OpenArray Real-Time Master Mix,dilutedpre-amplifiedcDNA(1.2μL)andRNase-free dH_2O (1.3 μL) (Thermo Fisher, Foster City, USA). circRNA expression was measured relative to the geometric mean of the entire set of transcripts, with the expression of each individual circRNA normalised to the global mean ofexpressionofthatcircRNA acrossthesamples.Samples were run in three technical triplicates. Association of circRNAs with age in InCHIANTI was carried out by multivariate linear regression, adjusted for potential confounders BMI, sex, level of education (none, elementary, secondary,highschoolanduniversity),studysite,smoking and white blood counts (neutrophil, lymphocyte, monocyte, eosinophil percentages) while age was additionally adjusted for all other measures of association in the aging human cohort. We assessed association of circRNA with hand grip strength and parental longevity score (PLS) (Dutta et al., 2013b; Dutta et al., 2013c) as a proxy measure of longevity in humans. Statistical analysis was completed using StataSE15 (StataCorp, TX, USA). Figures were generated using GraphPad Prism 8.1.2 (GraphPad Software, San Diego, USA).

Assessment of circRNA expression in human primary senescent cells of different lineages

The expression levels of the 15 candidate circRNAs analysed above were also assessed in relation to cellular senescence, in senescent and early passage primary human primary fibroblasts, endothelial cells, astrocytes and cardiomyocytes using high-throughput qRTPCR on the 12K Flex OpenArray platform (Thermo Fisher, Foster City, USA). Samples were run in three biological replicates and three technical replicates. Senescent cells had been generated and characterised in previous work by our group, and culture conditions and details of assessment of senescence are reported elsewhere (Latorre et al., 2017; Latorre et al., 2018a; Latorre et al., 2018b; Latorre et al., 2018c; Lye et al., 2019). RNA samples from this work were available for use. circRNA levels were assessed in three biological and three technical replicates from early and late passagehumanprimarycells offour differentcell types. Early passage young cells were at population doubling (PD) of 24 for astrocytes, 28 for cardiomyocytes, 24 for endothelial cells and 25 for fibroblasts, whilst late passage senescent cells were at PD = 84 for astrocytes, 75 for cardiomyocytes, 65 for endothelial cells and 63 for fibroblasts. Senescent cell load in these samples was ~ 75% for fibroblasts, ~ 55% for endothelial cells, ~ 38% for cardiomyocytes and ~ 36% for cardiomyocytes (Latorre et al., 2017; Latorre et al., 2018a; Latorre et al., 2018b; Latorre et al., 2018c; Lye et al., 2019). In all cases, growth of the culture had slowed to less than 0.5 PD/week. Differential circRNA expression in senescent cells was then assessed by one-way ANOVA using StataSE15 (StataCorp, TX, USA). Figures were generated using GraphPad Prism 8.1.2 (GraphPad Software, San Diego, USA).

Assessment of circRNA conservation between mouse and human

We assessed whether the 15 circRNAs identified in our human study were likely to be conserved in mouse by aligning the mouse and human exon junction

sequences using the Blat tool in the UCSC genome browser (https://genome.ucsc.edu). Quantitative real-time PCR assays were developed to unique back-spliced junctions of conserved circRNAs. Probe and primer sequences are given in Online Resource 2. circRNA expression was then measured in mouse spleen and muscle tissue and assessed in relation to lifespan by analysis of levels in six strains of male mice (A/J, NOD.B10Sn-H2^{b}/J, PWD/PhJ, 129S1 /SvlmJ, C57BL/6J and WSB/EiJ) selected on the basis of divergent median strain longevity (Yuan et al., 2009). Animal husbandry, handling, animal characteristics and sample preparation protocols have been previously described (Lee et al., 2016). Tissue samples were obtained from cross-sectional study conducted in the same compartment and in the same period of time as described in Yuan et al.,(2009). Spleen and quadricep muscle tissues were excised immediately after sacrifice and shipped from the Jackson Laboratory using RNAlater-ICE Collection protocol (Life Technologies, Carlsbad, CA). In this method, tissues are submerged in RNAlater stabilization solution; an aqueous tissue storage reagent used to rapidly permeate tissues and stabilize RNA from fresh specimens and stored at – 20 °C or below for later use.

RNA extraction and reverse transcription from mouse
tissues

Total RNA was extracted using the TRI Reagent/ chloroform phase separation according to manufacturer's instructions. Briefly, tissues stored in RNA later were drained, and then placed in 1 mL TRI Reagent solution containing 10 mM $MgCl_2$. Samples were homogenized for 15 min (spleen) or 30 min (muscle) using bead mills (Retsch Technology GmbH, Haan, Germany). This was followed by a phase separation using chloroform. Total RNAs in the separated RNAs were precipitated from the aqueous phase through overnight incubation with isopropanol at – 20 °C. The following morning, RNA pellets were washed twice with ethanol and resuspended in RNase-free dH_2O. Complementary DNA (cDNA) was generated from 100 ng RNA using

the Evocript Universal cDNA Master Synthesis kit according to the manufacturer's instructions (Roche, Switzerland).

Assessment of circRNA expression in mouse spleen and muscle

circRNAs selected on the basis of interspecies sequence conservation were validated in mouse spleen and muscle tissue. Expression levels of conserved circRNAs were assessed in relation to median strain lifespan by relative quantification. Quantitative qRTPCR was carried out for circRNAs (circFoxo3, circMib1, circPlekhm1 and circXpo7) in relation to the Pol2ra, Trfc and Ipo8 endogenous control genes, selected on the basis of lack of age association in a previous study (Harries et al., 2011). Reaction mixes contained cDNA (0.5 μL), TaqMan Universal PCR mastermix II (2.5 μL, no AmpErase UNG (Thermo Fisher, Foster City, USA), dH_2O (1.75 μL, Fisher Scientific, USA), and TaqMan gene assay (0.25 μL, Thermo Fisher, Foster City, USA) in a 5 μL final reaction volume. The reaction mixes were centrifuged at 3000 rpm, vortexed and centrifuged again at 3000 rpm and transferred to 384-well qRTPCR plates. qRTPCR was run at 50 °C for 2 min, 95 °C for 10 min and 50 cycles of 15 s at 95 °C for 30 s and 1 min at 60 °C. Each sample assay was conducted in three technical triplicates. Expression levels of circRNAs in young and old mouse tissues were measured relative to the geometric mean of the entire set of transcripts, with the expression of each individual circRNA normalised to the global mean of expression of each circRNA across the samples. Linear regression analysis was carried out to assess the association of expression of circRNA using StataSE15 (StataCorp, TX, USA).

Results

circRNA profile in peripheral blood of aging humans

One hundred sixty-six to 167M reads were obtained from the RNAse R-treated pools and 157–163M reads from the mock-treated pools with a mean Q score of 34.6–35.1 and total error rate of 0.47–0.53%. A total of 2207 circRNAs were expressed in human peripheral blood. Of

these, 184 circRNAs were found in both the young and old samples, 431 were exclusively expressed in the young sample pool and 1592 were exclusively expressed in the old sample pool (Online Resource 3). We selected 15 circRNAs for further analysis: 5 expressed exclusively in the young pool, 5 expressed exclusively in the old pool and 5 expressed in both pools but showing the most discrepant expression for further study. These were circITGAX, circPLEKHM1, circDEF6, circATP6V0A1 and circASAP1 which showed exclusive expression in the young; circFOXO3, circFNDC3B, circAFF1, circCDYL and circXPO7 which showed exclusive expression in the old; and circMIB1, circMETTL3, circEP300, circZC3H18 and circBCL11B that were expressed, but differentially so in both sample pools.

Pathway analysis of circRNA expressed in aging humans

Pathway enrichment for the genes hosting the top 10% most abundant circRNAs in each of young and old pooled peripheral blood samples was performed using ClueGO cytoscape (Bindea et al., 2009). In the young peripheral blood, the top 10% most abundant circRNAs derived from genes associated with negative regulation of ATP metabolic processes and in transmission of synaptic signals. The leading edge genes hosting circRNAs for negative regulation of ATP processes were SNCA, STAT3 and UFSP2, whilst those associated with synaptic vesicle endocytosis were FCH02, PICALM, PIP5K1C and SNCA. Genes hosting circRNAs were primarily localised in pathways involved in phagocytosis, circadian regulation, cancer pathways and golgi-associated vesicle budding in the blood from aged donors (Table 2).

circPLEKHM1, circMETTL and circFNDC3B expression levels are associated with aging phenotypes in humans

The structures of the 15 circRNAs selected for follow-up were predicted based on the sequencing read depth for each exon and are presented in Fig. 1. Exon structures presented as read depth plots are given in Online Resource 4. Although we demonstrated no associations with age itself, we did

identify associations between some circRNAs and human aging phenotypes. circEP300 and circFOXO3 both demonstrated negative associations with combined parental longevity score (β = − 0.065 and − 0.060; P = 0.001 and 0.002 respectively), after adjustment for multiple testing. circDEF6 was positively correlated with parental longevity scores but demonstrated nominal significance only (β = 0.070, P = 0.024) (Table 3, Fig. 2). A positive association was also identified both cross-sectionally (β = 0.004, P = 0.039) and longitudinally (β = 0.004, P = 0.038) between circFNDC3B expression and hand grip strength (Table 4, Fig. 3), although these were nominal only.

Table 2 Pathways enriched in age-associated circRNAs

Pathway	p value	Number Of Genes	Genes
Expressed only in old			
Fc gamma R-mediated phagocytosis	0.005	4	ARPC1B, ASAP1, PIP5K1C, VASP
Exercise-induced Circadian Regulation	0.006	3	CRY2, NCOA4, TAB2
Pathways Affected in Adenoid Cystic Carcinoma	0.018	4	ERBB2, FOXO3, KANSL1, MGA
Endometrial cancer	0.041	3	AXIN1, ERBB2, FOXO3
trans-Golgi Network Vesicle Budding	0.035	3	DNAJC6, IGF2R, PICALM
Clathrin derived vesicle budding	0.049	3	DNAJC6, IGF2R, PICALM
Golgi Associated Vesicle Biogenesis	0.069	3	DNAJC6, IGF2R, PICALM
Cargo recognition for clathrin-mediated endocytosis	0.062	5	FCHO2, IGF2R, PICALM, REPS1, UBQLN1
Clathrin-mediated endocytosis	0.049	8	DNAJC6, FCHO2, GAPVD1, IGF2R, PICALM, PIP5K1C, REPS1, UBQLN1
Expressed only in young			
Negative regulation of ATP metabolic process	0.004	3	SNCA, STAT3, UFSP2
Synaptic vesicle recycling	0.009	4	FCHO2, PICALM, PIP5K1C, SNCA
Presynaptic endocytosis	0.018	4	FCHO2, PICALM, PIP5K1C, SNCA
Synaptic vesicle endocytosis	0.017	4	FCHO2, PICALM, PIP5K1C, SNCA
Expressed in both old and young, but demonst		ating	differential on
Huntington's disease_Homo sapiens_hsa05016	0.014	2	ATP5C1, EP300
Pyruvate metabolism_Homo sapiens_hsa00620	0.037	1	HAGH
Notch signaling pathway_Homo sapiens_hsa04330	0.045	1	EP300

The ClueGo pathway results for pathways potentially targeted by genes generating the top 10% of circRNAs differentially expressed with age are presented here aligned to the hg19 genome alignment. Number of genes = number of differentially expressed genes in each pathway

circRNAs are differentially expressed in early passage and late passage cells

Twelve of 15 circRNAs tested were expressed in astrocytes, endothelial cells, fibroblasts or astrocytes. Seven

(58%) of these demonstrated differential expression between early and late passage cells of one or more cell type (Table 5). circAFF1 and circFOXO3 demonstrated associations in more than one cell type although direction of effect was concordant only for circFOXO3 (in cardiomyocytes and fibroblasts). circCDYL, circEP300, circMIB1, circZC3H18 and circMETTL3 were differentially expressed in only one cell type. circBCL11B, circDEF6 and circITGAX were not expressed in any cell type tested.

Differential expression of circRNAs between mice of different median strain longevities

In silico analyses suggested that four circRNAs (circFoxo3, circMib1, circPlekhm1 and circXpo7) may have conserved back-spliced junction in the mouse. Associations with longevity were then assessed in spleen and muscle tissue from young (6 months) and old (20–22 months) mouse strains of six different median strain longevities. circMib1 and circXpo7 were expressed only in spleen, whereas circFoxo3 and circPlekhm1 were expressed in both tissues (Table 6). The expression of circPlekhm1 demonstrated a nominal positive correlation with median lifespan in young and old ($\beta = 0.0013$, $P = 0.016$) as well as in spleen of young mice ($\beta = 0.0025$, $P = 0.017$),althoughthesewerenotsignificantafteradjustment

for multiple testing (threshold P = 0.013). No associations were seen between muscle circRNA expression levels and median strain longevity.

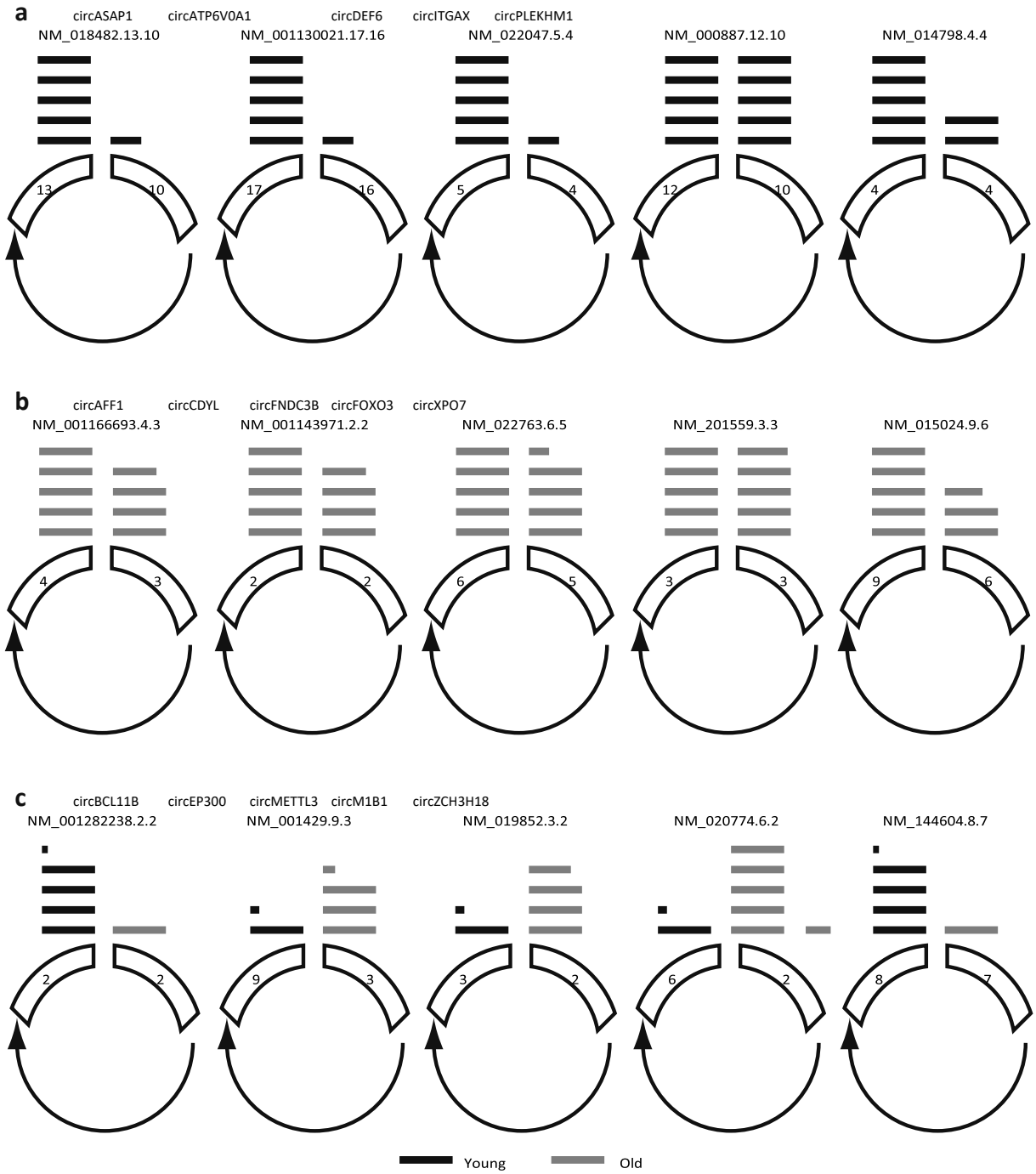

Fig. 1 Circular RNA junction schematics for the top 5 most abundant circular RNAs uniquely found in young (a) and old samples (b). Also shown are junction schematics for the top 2 and 3 most abundant common circular RNAs found in young and old samples respectively (c). Each schematic shows the identified back-spliced exon or exons. The relative read depth at each backspliced junction is shown by the number of bars above each junction and is scaled by linear interpolation, where the backspliced junctions with 1 and 10 bars represent the junctions with the lowest and highest readdepth respectively. Black and greybars show relative read depth at junctions in young and old samples respectively

Discussion

Circular RNAs (circRNAs) are an emerging class of regulatory RNA molecule thought to play a role in human disease (Haque and Harries 2017). These molecules have no free ends, and as such are exonuclease resistant. circRNAs accumulate in aged organisms (Gruner et al., 2016) and have been suggested to play a role in cellular senescence (Du et al., 2017; Du et al., 2016). We hypothesised that the human circRNAome may differ in aged humans compared with younger subjects and that these changes may also be associated with cellular senescence or with longevity in animal models. We identified > 2000 circRNAs in total RNA from human blood, some of which were expressed exclusively in samples from older donors. GSEA pathways enrichment analysis of genes hosting the top 10% most abundant circRNAs in elderly donors suggested that pathways involved in phagocytosis, circadian regulation, cancer pathways and golgi-associated vesicles were the most enriched in these genes. We demonstrated that three circRNAs (circDEF6, circFOXO3 and circEP300) were associated with measures of parental

Table 3 circRNA expression in relation to combined parental longevity score

circRNA	β-Coefficient	p value	95% CI
circAFF1	− 0.012	0.485	− 0.048–0.023
circASAP1	− 0.044	0.064	− 0.090–0.003
circATP6V0A1	0.036	0.223	− 0.022–0.094
circBCL11B	0.042	0.136	− 0.013–0.097
circCDYL	− 0.030	0.109	− 0.067–0.007
circDEF6	0.070	0.024	0.009–0.131
circEP300	− 0.065	0.001	− 0.103–− 0.026
circFNDC3B	0.025	0.239	− 0.016–0.066
circFOXO3	− 0.060	0.002	− 0.098–− 0.021
circITGAX	0.019	0.440	− 0.030–0.068
circMETTL3	0.007	0.730	− 0.034–0.049
circMIB1	− 0.018	0.310	− 0.052–0.017
circPLEKHM1	− 0.009	0.493	− 0.035–0.017
circXPO7	0.038	0.162	− 0.016–0.093
circZC3H18	− 0.036	0.078	− 0.077–0.004

Beta coefficients, p values and 95% confidence intervals (95% CI) are given for associations between circRNAs expression and combined parental longevity (PLS) score. Two hundred ninety-one samples were assessed. Genes demonstrating statistically significant results below the multiple testing limit of 0.003 are indicated initalics, whilst those demonstrating nominal associationsonly are given in bold type

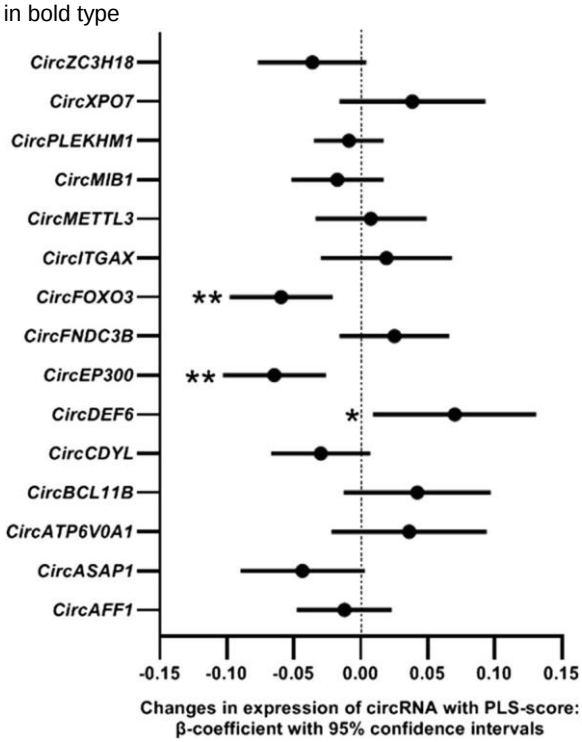

Fig. 2 circRNA expression is associated with combined parental longevity. Forest plot illustrating the association between peripheral blood circRNA expression and combined human parental longevity score (PLS) in participants from the InCHIANTI study of aging. N = 306 individuals. The beta-coefficient of the association is given on the X-axis, and the identity of the gene is given on the Y-axis. Lines attached to each data point represent 95% confidence intervals (95% CI). Statistical significance is indicated by stars, *< 0.05, **< 0.005

longevity, and one (circFNDC3B) was associated with hand grip strength both longitudinally and cross-sectionally. Furthermore, 7 of 12 circRNAs expressed in human senescent cells ofdifferentcell types demonstrated dysregulated expression in one or more cell type and 1 of 4 circRNAs demonstrating conserved expression were associated with median strain longevity in spleen tissue from young mice. These findings are consistent with the hypothesis that some circRNAs have roles in molecular aging and the determination of mammalian aging phenotypes.

circRNAs generated from the FOXO3 and EP300 genes were negatively associated with measures of human parental longevity and also demonstrated dysregulated expression in human senescent cells. circRNAs deriving from the FOXO3 gene have previously been demonstrated to regulate cell cycle when manipulated by gene knockdown in mouse embryonic fibroblasts, cardiac fibroblasts or mammary cancer cell lines (Du

Table 4 circRNA expression in relation to grip strength

circRNA	Grip strength	β-Coefficient	p value	95% CI
circAFF1	Cross-sectional	− 0.001	0.508	− 0.004–0.002
	Longitudinal	− 0.003	0.081	− 0.007–0.000
circASAP1	Cross-sectional	− 0.001	0.713	− 0.005–0.004
	Longitudinal	0.000	0.854	− 0.005–0.004
circATP6V0A1	Cross-sectional	0.000	0.965	− 0.005–0.005
	Longitudinal	− 0.002	0.403	− 0.008–0.003
circBCL11B	Cross-sectional	0.002	0.443	− 0.003–0.007
	Longitudinal	0.000	0.914	− 0.006–0.005
circCDYL	Cross-sectional	− 0.001	0.665	− 0.004–0.003
	Longitudinal	0.000	0.828	− 0.004–0.003
circDEF6	Cross-sectional	0.000	0.903	− 0.005–0.006
	Longitudinal	0.002	0.599	− 0.004–0.008
circEP300	Cross-sectional	− 0.004	0.060	− 0.007–0.000
	Longitudinal	− 0.003	0.112	− 0.007–0.001
circFNDC3B	Cross-sectional	0.004	0.039	0.000–0.008
	Longitudinal	0.004	0.038	0.000–0.008
circFOXO3	Cross-sectional	0.002	0.402	− 0.002–0.005
	Longitudinal	0.000	0.834	− 0.004–0.003
circITGAX	Cross-sectional	0.000	0.997	− 0.004–0.004
	Longitudinal	− 0.001	0.658	− 0.006–0.004
circMETTL3	Cross-sectional	− 0.003	0.139	− 0.007–0.001

given in bold

et al., 2016). Furthermore, FOXO3 circular RNAs also demonstrate elevated expression and association with cellularsenescenceintheheartttissue ofmice andhumans (Du et al., 2017). It is not clear whether the previously reported circular FOXO3 transcripts have the same structure as the one we have identified, since previous studies do not give its exon structure. A circRNA from the FOXO3 gene identical to the one we have identified has also previously been demonstrated to inhibit myoblast differentiation in mouse cells (Li et al., 2019). Genetic variation in the FOXO3 gene itself has previously been associated with extreme longevity (Flachsbart et al., 2017; Fuku et al., 2016) and has also been associated with maintenance of telomere length (Davy et al., 2018).

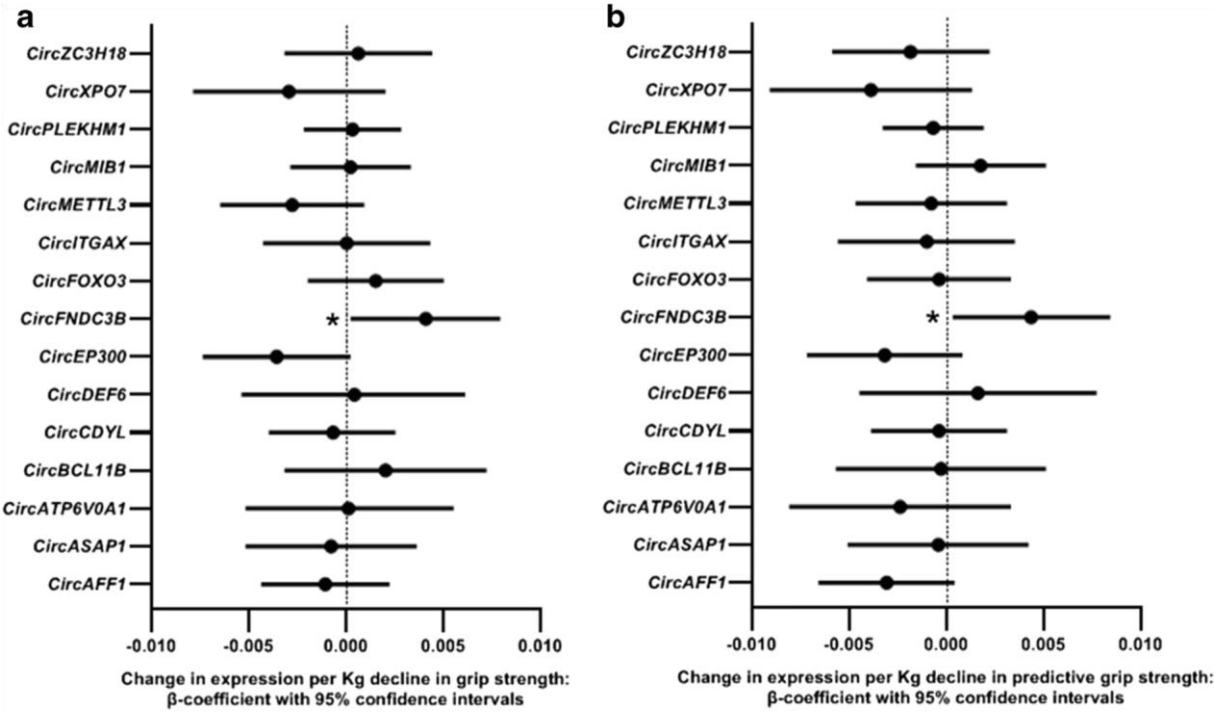

circRNAs deriving from the EP300 gene have not been previously reported. EP300 encodes the repressor histone acetyltransferase protein p300, which also has roles as a transcriptional corepressor protein. EP300 has been implicated in modulation of FOXO3 activity (Mahmud et al., 2019) and in

Fig. 3 Peripheral blood circFNDC3B expression is nominally associated with hand grip strength Forest plot illustrating the association between circRNA expression and hand grip strength in participants from the InCHIANTI study of aging. Associations with grip strength are shown

both a cross-sectionally from followup 3 (FU3) and b longitudinally, from follow-up 4 (FU4). N = 306 individuals. The beta-coefficient of the association is given on the X-axis, and the identity of the gene is given on the Y-axis. Lines attached to each data point represent 95% confidence intervals (95% CI). Statistical significance is indicated by stars, *< 0.05, **< 0.005

antagonism of the FOX03a/SIRT1 signalling axis (Jeung et al., 2016). Inhibition of EP300 has been shown to mimic calorific restriction in human and mouse cells (Pietrocola et al., 2018); calorific restriction is of course a well-known modifier of lifespan in many species (Austad 1989; Hansen et al., 2008; Kapahi et al., 2004; Mitchell et al., 2010). This protein is also a master regulator of autophagy, which is a pivotal factor in stem cell maintenance and evasion of cellular senescence (Vijayakumar and Cho 2019).

circFNDC3B was positively associated with hand grip strength. Although these associations were nominal only, they were present both cross-sectionally and longitudinally. An average person may lose ~ 20–40% of skeletal muscle mass as well as muscle strength from by the time they reach 80 years of age (Carmeli et al., 2002; Doherty 2003) and decline in skeletal muscle strength is predictive of disability and mortality in humans (Giampaoli et al., 1999; Rantanen et al., 1999; Rantanen et al., 2012). Circular RNAs originating from this gene have been reported previously, and suggested to possess tumour suppressor activity (Liu et al., 2018).

The results generated from our mouse data suggest that circPlekhm1, which was associated with median strain longevity, may drive longevity, rather than being consequential to it, since the associations are present in the spleen RNA of young mice alone. The Plekhm1 gene encodes a multivalent adaptor protein that integrates endocytic and autophagic pathways at the lysosome (McEwan and Dikic 2015). Its role in lifespan may therefore stem from moderation of lysosomal trafficking since lysosomes play a critical part in successful aging and longevity (Carmona-Gutierrez et al., 2016; Simonsen et al., 2007).

Our study has both strengths and weaknesses. It represents one of the first circRNA profiles in aging human peripheral blood and provides data not only population-level epidemiological evidence for a role in human aging

phenotypes, or mammalian lifespan, but also in vitro evidence that some circRNA may influence cell senescence phenotypes. Weaknesses

Table 5 circRNA expression in early and late passage primary human cells

circRNA	Median (IQR)		p value
	Early passage	Late passage	
Astrocytes			
circAFF1	0.58 (0.55–0.68)	0.84 (0.79–1.09)	0.040
circASAP1	1.39 (0.97–1.48)	1.22 (1.18–1.36)	0.878
circATP6V0A1	1.60 (1.14–1.87)	1.14 (1.05–1.41)	0.229
circCDYL	0.71 (0.67–0.74)	0.90 (0.90–0.93)	0.001
circEP300	1.01 (0.95–1.04)	1.05 (1.00–1.07)	0.329
circFNDC3B	0.96 (0.85–1.10)	1.38 (1.20–1.48)	0.059
circFOXO3	0.88 (0.80–0.89)	0.89 (0.80–0.98)	0.646
circMETTL3	0.97(0.92–1.08)	0.69 (0.66–1.02)	0.180
circMIB1	0.71(0.69–0.86)	1.03 (0.99–1.04)	0.008
circPLEKHM1	1.05 (1.00–1.09)	0.76 (0.61–1.17)	0.306
circXPO7	1.25 (1.12–1.58)	1.54 (0.81–1.62)	0.987
circZC3H18	1.50 (0.67–2.24)	0.88 (1.00–1.07)	0.346
Cardiomyocytes			
circAFF1	1.15 (1.09–1.26)	1.42 (1.04–1.52)	0.357
circASAP1	0.74 (0.71–1.05)	0.84 (0.83–1.02)	0.643
circATP6V0A1	0.57 (0.44–0.80)	0.41 (0.39–0.54)	0.249
circCDYL	1.47 (1.29–1.48)	1.42 (1.25–1.64)	0.855
circEP300	1.27 (1.02–1.48)	1.10 (0.84–1.45)	0.596
circFNDC3B	1.03 (0.83–1.09)	1.93 (0.96–1.97)	0.139
circFOXO3	1.00(0.99–1.07)	0.82 (0.79–0.92)	0.015
circMETTL3	0.88(0.69–0.99)	0.66 (0.63–0.79)	0.186
circMIB1	0.96 (0.81–1.02)	1.16 (0.97–1.25)	0.129
circPLEKHM1	0.85 (0.84–1.05)	0.82(0.71–1.22)	0.983
circXPO7	0.89 (0.74–0.94)	1.32 (0.75–1.63)	0.227
circZC3H18	0.83 (0.63–1.43)	0.85 (0.77–1.12)	0.862
Endothelial cells			

circAFF1	0.94 (0.91–1.27)	1.07 (0.49–1.11)	0.548
circASAP1	1.03 (0.94–1.28)	1.69 (0.68–1.76)	0.467
circATP6V0A1	0.37 (0.16–0.58)	0.48 (0.48–0.48)	0.821
circCDYL	0.90 (0.76–1.11)	0.89 (0.84–1.02)	0.942
circEP300	0.99 (.75–1.45)	0.58 (0.53–0.80)	0.128
circFNDC3B	1.74 (1.49–3.18)	7.84 (3.18–9.97)	0.080
circFOXO3	0.38 (0.20–1.98)	0.14 (0.04–0.22)	0.275
circMETTL3	1.02 (0.54–1.08)	0.39 (0.39–0.56)	0.072
circMIB1	1.36 (0.98–1.54)	1.11 (1.03–1.43)	0.640
circPLEKHM1	1.02 (0.99–1.42)	1.47(0.83–4.85)	0.380
circXPO7	0.97 (0.72–1.18)	0.87 (0.31–1.22)	0.620
circZC3H18	1.02 (0.98–1.15)	1.51 (1.51–1.51)	0.047
Fibroblasts			
circAFF1	1.06 (0.95–1.16)	0.58 (0.52–0.65)	0.003
circASAP1	0.51 (0.38–1.07)	1.05 (0.85–1.10)	0.196
circATP6V0A1	1.39 (1.00–1.41)	1.10 (0.46–1.35)	0.375

Table 5 (continued)

circRNA	Median (IQR)		p value
	Early passage	Late passage	
circCDYL	1.13 (0.72–1.17)	0.90 (0.81–1.06)	0.640
circEP300	0.96 (0.78–0.98)	0.38 (0.38–0.69)	0.023
circFNDC3B	0.50(0.48–0.94)	0.90 (0.85–0.91)	0.182
circFOXO3	1.91 (1.72–2.01)	1.60 (1.47–1.61)	0.025
circMETTL3	1.23(1.00–1.26)	1.39 (1.58–1.66)	0.030
circMIB1	1.20 (1.14–1.47)	0.85 (0.69–1.11)	0.072
circPLEKHM1	1.00(0.90–1.00)	0.84 (0.79–1.14)	0.716
circXPO7	1.03(0.48–1.08)	0.57 (0.39–1.18)	0.645

circZC3H18	0.93 (0.72–1.21)	0.74 (0.53–0.94)	0.432

Results reaching statistical significance are indicated in bold typeface IQR interquartile range

Table 6 Differential expression of conserved circRNAs in mice of differential median strain longevities

circRNA	Tissue	β-Coefficient	p value	95% CI	
circFoxo3	Muscle	0.00	0.403	− 0.0010	0.0024
	Young (muscle)	0.0001	0.936	− 0.0028	0.0031
	Old (muscle)	0.0008	0.478	− 0.0015	0.0031
	Spleen	− 0.0003	0.815	− 0.0027	0.0021
	Young (spleen)	0.0002	0.922	− 0.0039	0.0043
	Old (spleen)	− 0.0005	0.757	− 0.0037	0.0027
circMib1	Muscle	ND	ND	ND	ND
	Young (muscle)	ND	ND	ND	ND
	Old (muscle)	ND	ND	ND	ND
	Spleen	0.0001	0.924	− 0.0023	0.0026
	Young (spleen)	− 0.0018	0.150	− 0.0044	0.0008
	Old (spleen)	0.0021	0.299	− 0.0020	0.0062
circPlekhm1	Muscle	0.0003	.813	− 0.0022	0.0028
	Young (muscle)	− 0.0022	0.161	− 0.0054	0.0010
	Old (muscle)	0.0016	0.365	− 0.0020	0.0053
	Spleen	0.0013	0.016	0.0002	0.0024
	Young (spleen)	0.0025	0.017	0.0005	0.0046
	Old (spleen)	0.00001	0.967	− 0.0008	0.0009

circXpo7	Muscle	ND	ND	ND	ND
	Young (muscle)	ND	ND	ND	ND
	Old (muscle)	ND	ND	ND	ND
	Spleen	0.0009	0.509	− 0.0019	0.0038
	Young (spleen)	0.0003	0.894	− 0.0040	0.0045
	Old (spleen)	0.0020	0.333	− 0.0023	0.0063

circRNA expression is reported here in relation to median strain longevity. Data are assessed separately for young and old animals of each strain. N = 67 (muscle); 90 (spleen). Results reaching statistical significance are indicated in bold typeface

IQR interquartile range, ND not detected

include a relatively low power to detect effects of in the population study, which might be attributed to the biological variation in circRNA levels and limitations in samples size and power. Nevertheless, we were able to identify some interesting associations, which likely represent the largest effects. Future work could include validation of epidemiological data in larger sample sets and also functional delineation of the molecular effects of the circRNA in question. Our data provide evidence that circRNAs may play an important role in the determination of mammalian aging phenotypes. circRNAs are inherently stable, due to their exonuclease resistance, and are found not only in tissues relevant to human diseases, but also in the circulation, raising the possibility that they may prove useful as biomarkers of disease or targets for molecular therapies in the future.

Acknowledgments We acknowledge the generous support of the Exeter Sequencing Service and Computational core facilities at the University of Exeter, Medical Research Council Clinical Infrastructure award (MR/M008924/1), Wellcome TrustInstitutional Strategic Support Fund (WT097835MF), Wellcome Trust Multi User Equipment Award (WT101650MA) and BBSRC LOLA award (BB/K003240/1). The study was also supported in part by the Intramural Research Program of the NIH, National Institute on Aging (NIA) and The Jackson Laboratory Nathan Shock Center of Excellence in the Basic Biology of Aging (NIA grant AG038070). The authors acknowledge Ben Lee for technical support. We also acknowledge Dr Michael Jackson and Dr Santibanez-Koref for useful discussions regarding circRNA analysis.

Authorcontributions SH carried out the experiments, analysed the data and contributed to the manuscript. SB is the curator of the InCHIANTI study and reviewed the manuscript. LF and SB are responsible for the sample cohort and contributed to the manuscript. LLP provided mouse tissues and edited the manuscript. KM carried out the CircleSeq. RMA analysed CircleSeq data and advised on interpretation of circRNA sequence. LCP reviewed and contributed to the manuscript. LWH designed and managed the study, interpreted the data and reviewed the manuscript.

Funding information The study was supported by the Northcott Devon Medical Trust.

Compliance with ethical standards

Conflict of interest The authors declare that they have no conflict of interest.

References

Abdelmohsen K, Srikantan S, Kang MJ, Gorospe M (2012) Regulation of senescence by microRNA biogenesis factors. Ageing Res Rev 11:491–500. https://doi.org/10.1016/j. arr.2012.01.003

Austad SN (1989) Life extension by dietary restriction in the bowl and doily spider. Frontinella pyramitela. Exp Gerontol 24: 83–92. https://doi.org/10.1016/0531-5565(89)90037-5

Bahar R et al (2006) Increased cell-to-cell variation in gene expression in ageing mouse heart. Nature 441:1011–1014. https://doi.org/10.1038/nature04844

Bindea G et al (2009) ClueGO: a Cytoscape plug-in to decipher functionally grouped gene ontology and pathway annotation networks. Bioinformatics 25:1091–1093. https://doi. org/10.1093/bioinformatics/btp101

Boulias K, Horvitz HR (2012) The C. elegans microRNA mir-71 acts in neurons to promote germline-mediated longevity through regulation of DAF-16/FOXO. Cell Metab 15:439– 450. https://doi.org/10.1016/j.cmet.2012.02.014

Carmeli E, Coleman R, Reznick AZ (2002) The biochemistry of aging muscle. Exp Gerontol 37:477–489. https://doi.org/10.1016/s0531-5565(01)00220-0

Carmona-Gutierrez D, Hughes AL, Madeo F, Ruckenstuhl C (2016) The Crucial impact of lysosomes in aging and longevity. Ageing Res Rev 32:2–12. https://doi.org/10.1016/j. arr.2016.04.009

Davy PMC et al (2018) Minimal shortening of leukocyte telomere length acrossage groupsin a cross-sectional study forcarriers of a longevity-associated FOXO3 allele. J Gerontol A Biol Sci Med Sci 73:1448–1452. https://doi.org/10.1093 /gerona/gly071 de Magalhaes JP, Curado J, Church GM (2009) Meta-analysis of age-related gene expression profiles identifies common signatures of aging. Bioinformatics 25:875–881. https://doi. org/10.1093/bioinformatics/btp073

Doherty TJ (2003) Invited review: aging and sarcopenia. J Appl Physiol1985 95:1717–1727. https://doi.org/10.1152 /japplphysiol.00347.2003

Du WW, Yang W, Liu E, Yang Z, Dhaliwal P, Yang BB (2016) Foxo3 circular RNA retards cell cycle progression via forming ternary complexes with p21 and CDK2. Nucleic Acids Res 44:2846–2858. https://doi.org/10.1093 /nar/gkw027

Du WW et al (2017) Foxo3 circular RNA promotes cardiac senescence by modulating multiple factors associated with stress and senescence responses. Eur Heart J 38:1402–1412. https://doi.org/10.1093/eurheartj/ehw001

Dutta A, Henley W, Robine JM, Langa KM, Wallace RB, Melzer D (2013a) Longer lived parents: protective associations with cancer incidence and overall mortality. J Gerontol A Biol Sci Med Sci 68:1409–1418. https://doi.org/10.1093 /gerona/glt061

Dutta A, Henley W, Robine JM, Langa KM, Wallace RB, Melzer D (2013b) Longer lived parents: protective associations with cancer incidence and overall mortality the journals of gerontology series a. Biol sci med sci 68:1409–1418. https://doi. org/10.1093/gerona/glt061

Dutta A, Henley W, Robine JM, Llewellyn D, LangaKM, Wallace RB, Melzer D (2013c) Aging children of long-lived parents experience slower cognitive decline. Alzheimers Dement 18. https://doi.org/10.1016/j.jalz.2013.07.002

Fabbri E et al (2016) Association between accelerated multimorbidity and age-related cognitive decline in older Baltimore longitudinal study of aging participants without dementia. J Am Geriatr Soc 64:965–972. https://doi.org/10.1111/jgs.14092

Ferrucci L, Bandinelli S, Benvenuti E, Di Iorio A, Macchi C, Harris TB, Guralnik JM (2000) Subsystems contributing to the decline in ability to walk: bridging the gap between epidemiology and geriatric practice in the InCHIANTI study. J Am Geriatr Soc 48:1618–1625

Flachsbart F et al (2017) Identification and characterization of two functional variants in the human longevity gene FOXO3. Nat Commun 8:2063. https://doi.org/10.1038/s41467-01702183-y

Fuku N et al (2016) rs2802292 polymorphism in the FOXO3A gene and exceptional longevity in two ethnically distinct cohorts. Maturitas 92:110–114. https://doi.org/10.1016/j. maturitas.2016.07.016

Giampaoli S et al (1999) Hand-grip strength predicts incident disability in non-disabled older men. Age Ageing 28:283–288. https://doi.org/10.1093/ageing/28.3.283

Gorospe M, Abdelmohsen K (2011) MicroRegulators come of age in senescence. Trends Genet 27:233–241. https://doi.org/10.1016/j.tig.2011.03.005

Gruner H, Cortes-Lopez M, Cooper DA, Bauer M, Miura P (2016) CircRNA accumulation in the aging mouse brain. Sci Rep 6: 38907. https://doi.org/10.1038/srep38907

Hansen M, Chandra A, Mitic LL, Onken B, Driscoll M, Kenyon C (2008) A role for autophagy in the extension of lifespan by dietary restriction in C. elegans. PLoS Genet 4:e24. https://doi.org/10.1371/journal.pgen.0040024

Haque S, Harries LW (2017) Circular RNAs (circRNAs) in health and disease. Genes (Basel) 8. https://doi.org/10.3390 /genes8120353

Harries LWet al (2011) Human aging is characterized by focused changes in gene expression and deregulation of alternative splicing. Aging Cell 10:868–878. https://doi.org/10.1111 /j.1474-9726.2011.00726.x

Izuogu OG, Alhasan AA, Alafghani HM, Santibanez-Koref M, Elliot DJ, Jackson MS (2016) PTESFinder: a computational method to identify post-transcriptional exon shuffling (PTES) events. BMC Bioinformatics 17:31. https://doi.org/10.1186/s12859-016-0881-4

Jeung YJ et al (2016) Shikonin induces apoptosis of lung cancer cells via activation of FOXO3a/EGR1/SIRT1 signaling antagonized by p300 Biochim. Biophys Acta 1863:2584–2593. https://doi.org/10.1016/j.bbamcr.2016.07.005

Kapahi P, Zid BM, Harper T, Koslover D, Sapin V, Benzer S (2004) Regulation of lifespan in Drosophila by modulation of genes in the TOR signaling pathway. Curr Biol 14:885– 890. https://doi.org/10.1016/j.cub.2004.03.059

Kirkland JL (2016) Translating the science of aging into therapeutic interventions. Cold Spring Harb Perspect Med 6:a025908. https://doi.org/10.1101/cshperspect.a025908

Latorre E, Birar VC, Sheerin AN, Jeynes JCC, Hooper A, Dawe HR, Melzer D, Cox LS, Faragher RGA, Ostler EL, Harries LW (2017) Small molecule modulation of splicing factor expression is associatedwithrescuefrom cellularsenescence. BMC Cell Biol 18:31. https://doi.org/10.1186/s12860-0170147-7

Latorre E, Ostler EO, Faragher RGA, Harries LW (2018a) FOXO1 and ETV6 genes may represent novel regulators of splicing factor expression in cellular senescence. FASEB J 33:1086– 1097

Latorre E, Pilling LC, Lee BP, Bandinelli S, Melzer D, Ferrucci L, Harries LW (2018b) The VEGFA156b isoform is dysregulated in senescent endothelial cells and may be associated with prevalent and incident coronary heart disease. Clin Sci (Lond) 132:313–325. https://doi.org/10.1042/CS20171556

Latorre E, Torregrossa R, Wood ME, Whiteman M, Harries LW (2018c) Mitochondria-targeted hydrogen sulfide attenuates endothelial senescence by selective induction of splicing factors HNRNPD and SRSF2. Aging (Albany NY) 10: 1666–1681. https://doi.org/10.18632/aging.101500

Lee BP et al (2016) Changes in the expression of splicing factor transcriptsand variations in alternative splicing are associated with lifespan in mice and humans. Aging Cell 15:903–913. https://doi.org/10.1111/acel.12499

Li X et al (2019) Circular RNA circ-FoxO3 inhibits myoblast cells differentiation. Cells 8. https://doi.org/10.3390/cells8060616

Liao Y, Smyth GK, Shi W (2013) The subread aligner: fast, accurate and scalable read mapping by seed-and-vote. Nucleic Acids Res 41:e108. https://doi.org/10.1093 /nar/gkt214

Liao Y, Smyth GK, Shi W (2014) featureCounts: an efficient general purpose program for assigning sequence reads to genomic features. Bioinformatics 30:923–930. https://doi. org/10.1093/bioinformatics/btt656

Liu H et al (2018) Invasion-related circular RNA circFNDC3B inhibits bladder cancer progression through the miR-11783p/G3BP2/SRC/FAK axis. Mol Cancer 17:161. https://doi. org/10.1186/s12943-018-0908-8

Lopez-Jimenez E, Rojas AM, Andres-Leon E (2018) RNA sequencing and Prediction Tools for Circular RNAs Analysis. AdvExp MedBiol1087:17–33. https://doi.org/10.1007/978981-13-1426-1_2

Lopez-Otin C, Blasco MA, Partridge L, Serrano M, Kroemer G (2013) The hallmarks of aging. Cell 153:1194–1217. https://doi.org/10.1016/j.cell.2013.05.039

Lye J et al.,(2019) Astrocyte senescence may drive alterations in GFAP(A), CDKN2A p14ARF and TAU3 transcript expression and contribute to cognitive decline Clinical Science in review

Mahmud Z et al (2019) EP300 and SIRT1/6 Co-Regulate Lapatinib Sensitivity Via Modulating FOXO3-Acetylation and Activity in Breast Cancer. Cancers (Basel) 11. https://doi.org/10.3390/cancers11081067

McEwan DG, Dikic I (2015) PLEKHM1: Adapting to life at the lysosome. Autophagy 11:720–722. https://doi.org/10.1080 /15548627.2015.1034419

Memczak S et al (2013) Circular RNAs are a large class of animal RNAs with regulatory potency. Nature 495:333–338. https://doi.org/10.1038/nature11928

Miller JA et al (2017) Neuropathological and transcriptomic characteristics of the aged brain. Elife 6. https://doi.org/10.7554 /eLife.31126

Mitchell JR et al (2010) Short-term dietary restriction and fasting precondition against ischemia reperfusion injury in mice. Aging Cell 9:40–53. https://doi.org/10.1111/j.14749726.2009.00532.x

Narici MV, Maffulli N (2010) Sarcopenia: characteristics, mechanisms and functional significance. Br Med Bull 95:139–159. https://doi.org/10.1093/bmb/ldq008

Noren Hooten N, Abdelmohsen K, Gorospe M, Ejiogu N, Zonderman AB, Evans MK (2010) microRNA expression patterns reveal differential expression of target genes with age. PLoS One 5:e10724. https://doi.org/10.1371/journal. pone.0010724

Pietrocola F, Castoldi F, Maiuri MC, Kroemer G (2018) Aspirinanother caloric-restriction mimetic. Autophagy 14:1162–1163. https://doi.org/10.1080/15548627.2018.1454810

Rantanen T, Guralnik JM, Foley D, Masaki K, Leveille S, Curb JD, White L (1999) Midlife hand grip strength as a predictor of old age disability. JAMA 281:558–560. https://doi. org/10.1001/jama.281.6.558

Rantanen T, Masaki K, He Q, Ross GW, Willcox BJ, White L (2012) Midlife muscle strength and human longevity up to age 100 years: a 44-year prospective study among a decedent cohort. Age (Dordr) 34:563–570. https://doi.org/10.1007 /s11357-011-9256-y

Shamir R et al (2017) Analysis of blood-based gene expression in idiopathic Parkinson disease. Neurology 89:1676–1683. https://doi.org/10.1212/WNL.0000000000004516

Simonsen A, Cumming RC, Finley KD (2007) Linking lysosomal trafficking defects with changes in aging and stress response in Drosophila. Autophagy 3:499–501. https://doi. org/10.4161/auto.4604

Trapnell C, Pachter L, Salzberg SL (2009) TopHat: discovering splice junctions with RNA-Seq. Bioinformatics 25:1105–1111. https://doi.org/10.1093/bioinformatics/btp120

Vijayakumar K, Cho GW (2019) Autophagy: An evolutionarily conserved process in the maintenance of stem cells and aging. Cell Biochem Funct 37:452–458. https://doi. org/10.1002/cbf.3427

Welle S, Brooks AI, Delehanty JM, Needler N, Bhatt K, Shah B, Thornton CA (2004) Skeletal muscle gene expression profiles in 20-29 year old and 65-71 year old women. Exp Gerontol 39:369–377. https://doi.org/10.1016/j. exger.2003.11.011

Yang J, Huang T, Petralia F, Long Q, Zhang B, Argmann C, Zhao Y, Mobbs CV, Schadt EE, Zhu J, Tu Z, GTEx Consortium (2015) Synchronized age-related gene expression changes across multiple tissues in human and the link to complex diseases. Sci Rep 5:15145. https://doi.org/10.1038 /srep15145

Yuan R et al (2009) Aging in inbred strains of mice: study design and interim report on median lifespans and circulating IGF1 levels. AgingCell8:277–287. https://doi.org/10.1111/j.14749726.2009.00478.x

Haque *et al. BMC Medical Genomics* (2020) 13:64
https://doi.org/10.1186/s12920-020-0713-2

BMC Medical Genomics

RESEARCH ARTICLE Open Access

Islet-expressed circular RNAs are associated with type 2 diabetes status in human primary islets and in peripheral blood

Shahnaz Haque[1], Ryan M. Ames[2], Karen Moore[3], Benjamin P. Lee[1], Nicola Jeffery[1] and Lorna W. Harries[1*]

Abstract

Background: Circular RNAs are non-coding RNA molecules with gene regulatory potential that have been associated with several human diseases. They are stable and present in the circulation, making them excellent candidates for biomarkers of disease. Despite their promise as biomarkers or future therapeutic targets, information on their expression and functionality in human pancreatic islets is a relatively unexplored subject.

Methods: Here we aimed to produce an enriched circRNAome profile for human pancreatic islets by CircleSeq, and to explore the relationship between circRNA expression, diabetes status, genotype at T2D risk loci and measures of glycaemia (insulin secretory index; SI and HbA1c) in human islet preparations from healthy control donors and donors with type 2 diabetes using ANOVA or linear regression as appropriate. We also assessed the effect of elevated glucose, cytokine and lipid and hypoxia on circRNA expression in the human beta cell line EndoC-βH1.

Results: We identified over 2600 circRNAs present in human islets. Of the five most abundant circRNAs in human islets, four (*circCIRBP*, *circZKSCAN*, *circRPH3AL* and *circCAMSAP1*) demonstrated marked associations with diabetes status. *CircCIRBP* demonstrated an association with insulin secretory index in isolated human islets and *circCIRBP* and *circRPH3AL* displayed altered expression with elevated fatty acid in treated EndoC-βH1 cells. *CircCAMSAP1* was also noted to be associated with T2D status in human peripheral blood. No associations between circRNA expression and genotype at T2D risk loci were identified in our samples.

Conclusions: Our data suggest that circRNAs are abundantly expressed in human islets, and that some are differentially regulated in the islets of donors with type 2 diabetes. Some islet circRNAs are also expressed in peripheral blood and the expression of one, *circCAMSAP1*, correlates with diabetes status. These findings highlight the potential of circRNAs as biomarkers for T2D.

Keywords: circRNA, Diabetes, Human, islet, EndoC-βH1 beta cells

* Correspondence: L.W.Harries@exeter.ac.uk
[1]RNA-Mediated Mechanisms of Disease Group, Institute of Biomedical and Clinical Sciences, University of Exeter Medical School, University of Exeter, RILD South, Barrack Road, Exeter EX2 5DW, UK
Full list of author information is available at the end of the article

Background

One of the key difficulties in dissecting the factors driving progression of multifactorial polygenic chronic diseases such as type 2 diabetes (T2D) is the degree of heterogeneity that it presents. Although the development of diabetes like other common chronic disorders has a large lifestyle contribution, there is a substantial genetic component [1]. 70% of individuals with prediabetes eventually develop diabetes [2, 3], with increasing evidence suggesting that diabetic complications such as peripheral nephropathy and retinopathy may initiate at the pre-diabetic stage [2]. Identifying people at risk of type 2 diabetes, or those likely to progress from impaired glucose tolerance to overt disease is thus an important aim. Understanding the molecular causes of T2D, and identification of sensitive and specific biomarkers to indicate those at risk of pre-diabetes, or of transition from pre-diabetes to overt disease is therefore a key aim for research.

Genome wide association studies (GWAS) for T2D have identified over 143 risk loci associated with susceptibility to T2D [1]. More than 85% of these disease-associated variants reside in non-coding regions of the genome [4]. Over 80% of the human genome is predicted to display some degree of functionality [5], so it is likely that many of the diabetes-associated genetic variants may act via dysregulation of gene expression. Disruption of the activity or function of non-coding RNAs that moderate gene activity, such as microRNA (miRNA) or long non-coding RNA (lncRNA) may have particular relevance [6].

Circular RNAs (circRNAs) are an emerging class of non-coding RNA (ncRNA) generated by the back splicing of downstream exons to the 3′ acceptor splice site of upstream exons and result in a covalently closed circular structure containing one or more exons [7]. Their mode(s) of action remain to be fully elucidated but they have been suggested to manipulate gene expression by moderation of transcription [8], interaction with cellular proteins [9], sequestration of RNA-binding proteins [10] or sponging miRNA [11]. Their covalently closed structure means that they are resistant to exonucleases; accordingly, they have half-lives on average 19–24 h [12], being significantly more stable than linear mRNAs from their cognate genes which have half-lives typically in the region of 4–9 h [13]. Data on circRNA abundance can be extracted from conventional NGS data, but such data may also include aberrant back spliced sequences from linear transcripts as well as genuine circRNAs.

CircRNAs may have potential as biomarkers for the development of diabetes or as future molecular targets for novel diabetes therapeutics [14–16]. An important pre-requisite for this is the characterisation of circRNA sequences in diabetes-relevant tissues such as pancreatic islets and in more accessible tissues such as peripheral blood. Cell-type specific circRNA expression has previously been reported in human pancreatic α, β and δ cells [17], but these profiles were not circRNA-specific, being extracted from published NGS data in the absence of RNase R treatment to remove linear RNA. Other human islet circRNA profiles have been generated using microarray approaches, which will capture only known circRNAs [18].

We present here an enriched whole circRNAome profile from primary human pancreatic islets which we have generated using a modified circleSeq technique [19]. This included an RNase R step to remove linear RNA and enrich for circRNAs. We firstly aimed to determine whether expression of the most abundantly-expressed islet circRNAs were associated with insulin secretory index (SI), donor HbA1c or donor diabetes status in human primary islets. Secondly, we aimed to determine whether circRNAs localising to the genomic regions encompassing the GWAS association signals for type 2 diabetes were differentially-expressed according to donor risk genotype. Thirdly, we aimed to explore whether abundantly-expressed circRNAs were responsive to diabetomimetic stimuli (hypo- or hyperglycaemia, hypoxia, elevated fatty acids or inflammatory cytokines), in the human beta cell line EndoC-βH1. Finally, we aimed to determine whether abundant islet circRNAs were differentially expressed in the peripheral blood of individuals with pre-diabetes or overt disease.

We identified 2619 circRNAs that were expressed in islet donors, 47 of which had not been previously identified in data from human tissues. 4/5 of the most abundant circRNA demonstrated differential expression in the islets of donors with T2D, whilst 2/5 demonstrated dysregulated expression in response to elements of the diabetic microenvironment in the human beta cell line EndoC-βH1 in culture. No circRNA co-localising to the GWAS signals for T2D demonstrated associations with risk genotype. Finally, 3/5 of the most abundant islet circRNAs were also expressed in blood, and the expression of one, *circCAMSAP1*, demonstrated an association with T2D status in the peripheral blood of patients with T2D, but not with impaired glucose tolerance (IGT). To conclude, we have produced the first global circRNA-only profile in human pancreatic islets, provided evidence that some are differentially expressed in the islets of donors with diabetes. One islet circRNA (*circCAMSAP1*) is also differentially expressed in the peripheral blood of subjects with T2D, highlighting a potential use for circRNA species as biomarkers of disease.

Methods

Pancreatic islet preparations

Snap-frozen islet preparations were purchased from ProCell Biotech (Newport Beach, CA, USA) or from the

Table 1 Sample and donor characteristics for human islet samples used in this work

A.

	Control (n = 50)		T2D (n = 20)		p-value
	Mean	**SD**	**Mean**	**SD**	
Age	40.66	14.25	53.55	9.22	< 0.001
BMI	28.30	6.83	33.05	10.31	0.027
SI	2.45	1.26	–	–	–
HbA1c	5.44	0.36	–	–	–
Purity	89.28	6.00	80.38	14.92	< 0.001
Viability	93.53	4.80	89.73	4.54	0.003
Sex	F (40%);	M (60%)	F (45%)	M (55%)	0.706
Ethnicity	white (74%)	other (26%)	white (45%)	other (55%)	0.348

B.

	Major allele homozygotes		Heterozygotes and minor allele homozygotes		p-value
	Mean	**SD**	**Mean**	**SD**	
rs6819243 (*CTBP1*)					
Age	40.19	14.12	42.38	11.78	0.620
BMI	27.85	5.34	27.16	7.03	0.715
Purity	89.26	5.86	90.00	3.54	0.671
Viability	93.33	5.68	94.12	2.38	0.633
Sex	F (53%)	M (47%)	F (38%)	M (62%)	0.595
Ethnicity	white (83%)	other (17%)	white (31%)	other (69%)	0.020
rs10758593 (*GLIS3*)					
Age	41.08	15.04	40.88	12.25	0.966
BMI	26.27	4.14	29.07	5.80	0.130
Purity	89.46	4.96	88.50	6.26	0.633
Viability	94.81	3.09	92.33	5.37	0.133
Sex	F (39%)	M (62%)	F (42%)	M (58%)	0.269
Ethnicity	white (69%)	other (31%)	white (73%)	other (27%)	0.916
rs7177055 (*HMG20A*)					
Age	39.97	13.95	43.69	12.35	0.371
BMI	27.83	5.63	29.87	9.46	0.355
Purity	89.13	5.18	89.13	6.18	0.998
Viability	93.37	4.03	93.34	6.70	0.986
Sex	F (47%)	M (53%)	F (38%)	M (63%)	0.547
Ethnicity	white (72%)	other (28%)	white (75%)	other (25%)	0.697
rs1111875 (*IDE*)					
Age	48.58	9.95	33.43	12.20	< 0.001
BMI	30.05	8.52	26.50	4.80	0.088
Purity	88.61	4.91	90.57	4.73	0.175
Viability	94.57	3.30	93.57	4.20	0.374
Sex	F (58%)	M (42%)	F (30%)	M (70%)	0.056
Ethnicity	white (67%)	other (33%)	white (74%)	other (26%)	0.733
rs12427353 (*SPPL3*)					
Age	39.68	14.15	46.80	9.02	0.137
BMI	29.03	7.32	25.03	4.00	0.104

Table 1 Sample and donor characteristics for human islet samples used in this work *(Continued)*

Purity	89.98	5.22	87.78	5.65	0.267
Viability	93.48	5.28	94.33	3.50	0.645
Sex	F (40%)	M (60%)	F (70%)	M (30%)	0.092
Ethnicity	white (68%)	other (33%)	white (80%)	other (20%)	0.949
rs10203174 (*THADA*)					
Age	42.18	13.62	43.36	13.38	0.802
BMI	29.07	7.54	25.54	5.13	0.155
Purity	89.64	4.50	89.09	6.25	0.754
Viability	93.85	4.25	94.64	2.46	0.565
Sex	F (47%)	M (53%)	F (36%)	M (64%)	0.546
Ethnicity	white (74%)	other (26%)	white (55%)	other (45%)	0.920

A. Characteristics of human islet preparations from donors with ($n = 20$) and without ($n = 50$) T2D. B. Characteristics of human islet preparations from control donors used for GWAS genotype analysis ($n = 53$). SD = standard deviation. Islet sets for parts A and B are only partly overlapping; non-diabetic samples used for assessment of effects of diabetes status were selected from the larger pool to allow for matching of islet donors with and without diabetes. Differences in parameters between islet groups was determined by t-test. B. Characteristics of human peripheral blood donors with ($n = 20$) and without ($n = 50$) T2D

NIA IIDP resource (collected with ethical permission at source). Islet purity and viability was determined by dithizone and fluorescein diacetate/propidium iodide staining. Samples were shipped in RNAlater-ICE (Life Technologies, Carlsbad, CA, USA) to maintain transcript stability, and RNA was extracted using the total RNA extraction protocol of the miRVana miRNA isolation kit, as per the manufacturers' instructions. Sample RNA Integrity Number (RIN) was determined using an Agilent Bioanalyser (Agilent, Santa Clara, USA). Fifty three islet samples were available from healthy donors, and 20 from donors with T2D. Islet donor characteristics are given in Table 1, with expanded information on each donor in Supplementary Table S1.

Generation of human primary islet circRNA profile

For our initial description of the islet circRNome, we generated circular RNA profiles from a pooled sample consisting of 5 individual islet preparations from donors without T2D using a modified 'CircleSeq' procedure [20] as in our previous work [21]. Samples were derived from 3 females and 2 males, with an average age of 50.2 years and an average BMI of 26.4, and were pooled to prevent any bias arising from signals arising from single donors. Islet preparations had, an average viability 94.4% and an average purity of 81%. CircRNA sequencing was carried out as previously published [21]. Sixty-two M reads were obtained from the RNase R-treated sample and 41 M reads from the mock-treated sample. The mean Q score was 38.9–39.1 and the total error rate was 0.24%. CircRNA sequences were then determined and quantified as in our previous work [21].

Pathway analysis of genes hosting differentially-regulated circRNA

To determine whether circRNAs identified were derived from genes clustered into specific gene ontology pathways, we carried out an initial gene set enrichment GSE analysis using the ClueGO Cytoscape version 2.5.2 plug-in (Bindea et al., 2009), as described in our previous work [21].

Selection of circRNA for validation

CircRNA were selected for follow up on two criteria. Firstly, levels of individual circRNA in the islet were ranked by abundance. We selected the 5 circRNAs most abundantly expressed in islets (*circCAMSAP1, circCIRBP, circRHOBTB3, circRPH3AL and circZKSCAN1*) for further analysis. We also assessed the expression of the linear reference transcript for each circRNA in each case. The second class of circRNAs selected for follow up were those mapping to the GWAS loci for T2D.

The circRNA profile in our study was mapped against the T2D susceptibility loci [22]. The co-ordinates of the upstream and downstream exons predicted to constitute each circRNA were then cross-referenced against the T2D GWAS signals using a custom Python 2.7 script to determine whether any circRNAs co-localized within the recombination windows. Thirteen circRNAs fulfilled these criteria and were selected for follow up (*circCTBP1_1, circCTBP1_2, circGLIS3, circHMG20A, circIDE1, circIDE2, circSPPL3_1, circSPPL3_2, circTHADA1, circTHADA2, circTHADA3, circTHADA4 and circTHADA5*). The expression of both circRNA and their host linear transcripts were assessed.

Design of RT-qPCR assays for circRNA validation

We designed and validated custom quantitative RT-qPCR assays specific to the unique back-spliced junctions of each circRNA to be followed up. Assay sequences are given in Supplementary Table S2. Probes and primers were placed to avoid genetic variation. Assay efficiency, linear range and accuracy were

determined by 1:10 serial dilutions of synthetics oligonucleotides corresponding to each back spliced junction (ThermoFisher, Foster City, USA).

Reverse transcription

cDNA synthesis for analysis of circRNA expression in islets, EndoC-βH1 cells and across a panel of tissues was carried out using the Superscript® VILO™ cDNA synthesis kit (ThermoFisher, Foster City, USA) according to manufacturer's instructions. Reactions contained 100 ng/μL RNA in a final reaction volume of 20 μL. Reaction conditions were 25 °C for 10 min, 42 °C for 60 min and 85 °C for 5 min.

Expression of islet circRNAs in other tissues

The expression of the 13 circRNAs co-localizing to T2D-GWAS loci and the 5 most abundant circRNAs expressed in pancreatic islets and their parent linear transcripts were assessed in 39 different tissues by quantitative RT-qPCR. The tissue panel was commercially-sourced panel consisting of pooled samples from different donors (tissue RNA samples were sourced from Ambion (Bath, UK), Biochain (Newark, USA) or BD Biosciences (Swindon, UK). Reaction mixes contained 2.5 μL Taqman® Universal PCR mastermix II, no AmpErase® UNG, (ThermoFisher, Foster City, USA), 1.75 μL dH_2O, 0.5 μL cDNA and 0.25 μL Taqman® gene expression assay (ThermoFisher, Foster City, USA) in a 5 μL final reaction volume. Cycling conditions were 50 °C for 2 min, 95 °C for 10 min and 50 cycles of 15 s at 95 °C for 30 s and 1 min at 60 °C. Reactions were carried out on the 12 K Flex platform (ThermoFisher, Foster City, USA) in 3 technical replicates. Target abundance was assessed using the Comparative Ct method, and was expressed relative to the geometric mean of the target and control set as a whole, since endogenous controls alone did not provide a robust baseline. Data for each target within the tissue panel was then normalised to its median level of expression across the entire panel.

Assessment of associations between the islet expression of abundant circRNAs, insulin secretory index (SI), HbA1c or T2D status

RNA samples and clinical data were available for islet preparation from 50 non-diabetic donors and from 20 donors with T2D. Islet donor characteristics are given in Table 1. We assessed the expression of the 5 most abundant circRNAs expressed in pancreatic islets as well as their host linear transcripts in relation to insulin secretory index, HbA1c or diabetes status in these samples by quantitative RT-qPCR. Reaction mix contained 2.5 μL Taqman® Universal PCR mastermix II, no AmpErase® UNG, (ThermoFisher, Foster City, USA), 1.75 μL ddH_2O, 0.5 μL cDNA and 0.25 μL Taqman® gene expression assay (ThermoFisher, Foster City, USA) in a 5 μL final reaction volume. Cycling conditions were 50 °C for 2 min, 95 °C for 10 min and 50 cycles of 15 s at 95 °C for 30 s and 1 min at 60 °C. Reactions were carried out on the 12 K Flex platform (ThermoFisher, Foster City, USA) in 3 technical replicates. Target abundance was assessed using the Comparative Ct method, and expressed relative to the geometric mean of the assay set. Levels of target expression in the islets of donors with T2D were then normalised to the median level of that transcript in non-diabetic islets controls. For assessment of SI or HbA1c, expression was normalised to the median level of each circRNA in control samples. Differential expression by diabetic status, SI or HbA1C was then assessed by one way ANOVA using StataSE15 (StataCorp, Texas, USA), with adjustment made for potential confounders including age, sex, BMI and ethnicity.

Determination of donor genotype at T2D risk SNPs

RNA samples and phenotypic data were available from 53 non-diabetic islet donors. Characteristics of participants are given in Table 1 and supplementary Table S1. The expression of 13 circRNAs co-localising to the genomic regions containing the GWAS association loci for T2D was assessed in relation to genotype. Genotype at the GWAS association loci for T2D with expression of circRNAs located in those regions was accessed by virtue of the small amounts of genomic DNA which are co-eluted in RNA preparations upon RNA extraction. We used a whole genome amplification (WGA) approach to amplify co-eluted DNA for genotyping using the REPLI-g Mini kit (Qiagen, Paisley, UK). WGA was carried out using 2.5 μL RNA and was performed according to manufacturer's instructions. Genotype was then determined by Sanger Sequencing of PCR amplicons containing the SNP in question. PCR reaction mixes included 2.4 μL primer mix containing a 1:1 ratio of forward: reverse primers (ThermoFisher, Foster City, USA), 4 μL MegaMix-Royal (Microzone , Brighton, UK) and 1.60 μL cDNA in a final reaction volume of 8 μL. Reaction condition for PCR were 95 °C for 12 min, 40 cycles for 95 °C for 30s, annealing for 1 min, 72 °C for 1 min followed by 72 °C for 10 min. In one case, sequence analysis proved inconclusive. In this case, genotype was determined by qPCR with TaqMan® Genotyping assay. Reactions contained 2.5 μL TaqMan® Genotyping Master Mix (ThermoFisher, Waltham, MA, USA), 0.25 μL Taqman® genotyping assay (rs6819243) (ThermoFisher, Waltham, MA, USA), 1.75 μL dH_2O and 0.5 μL whole genome amplified template in a 5 μL final reaction volume. Target abundance was assessed using the Comparative Ct method, and expressed relative to the geometric mean of the target and control set as a whole. The expression of each target was then normalised to median levels of that

target across the collection. Expression levels were then related to genotype of the islet donors by one way ANOVA using StataSE15 (StataCorp, Texas, USA) with adjustment for age, sex, BMI and ethnicity.

Assessment of circRNA expression in EndoC-βH1 under diabetomimetic conditions

The expression levels of the 5 circRNAs chosen on the basis of islet abundance and their linear transcripts were also assessed in the human pancreatic beta cell line EndoC-βH1, following exposure to dysregulated glucose (2.5 mM and 25 mM), hypoxia (1% O_2), dyslipidaemia (0.5 mM palmitic acid) or proinflammatory cytokines (TNFα (1000 U/ mL, INFγ (750 U/ mL) and IL1β (75 U/ mL) as described in our previous work [23]. Analysis was from RNA from different time points selected to exclude effects due to compromised cell viability (up to 48 h for glycemia and lipid treatment, up to 36 h for cytokine treatment and up to 24 h for hypoxia exposure). CircRNA expression was measured using RT-qPCR as described above on the 12 K Flex platform (ThermoFisher, Foster City, USA). Target abundance was assessed using the Comparative Ct method, and expressed relative to the geometric mean of the target and control set as a whole, since endogenous controls alone did not provide a robust baseline. Levels of each target were then normalised to the median level of each circRNA in untreated cells. Samples were run in 3 biological replicates and 3 technical replicates. Differential circRNA expression in treated cells was then assessed by one way ANOVA using StataSE15 (StataCorp, Texas, USA).

RNA extraction from peripheral blood samples from control donors, donors with IGT and those with T2D

We assessed the expression of the 5 most abundant islet circRNAs in relation to diabetes status in RNA extracted from 285 peripheral blood samples from the Exeter 10, 000 study (http://www.peninsulacrf.org/node/155). Our sample set consisted of 133 non-diabetic patients (fasting glucose < 100.8 mg/dL), 46 individuals with impaired glucose tolerance (fasting glucose 100.8 to 122.4 mg/dL) and 106 patients with overt diabetes (fasting glucose > 122.4 mg/dL). Participant characteristics are given in Table 2. This collection is a cross sectional population study consisting of samples collected from volunteer individuals living in the South West of England and recruited since 2010. Whole blood samples were collected in 2011/2012 using the PAXgene system [24] and extracted using the PAXgene Blood RNA kit (Qiagen, Paisley, UK). Written informed consent was obtained for all participants and ethical permission was granted through the National Institute for Health Research (NIHR) Clinical Facility (REC 09/H0106/75).

Table 2 Participant characteristics for circRNA expression in peripheral blood

A.

	p-value	Control		IGT	
		Mean	SD	Mean	SD
Age	0.016	52.45	17.08	59.26	14.31
BMI	< 0.001	26.51	4.13	28.93	3.68
HbA1c	–	5.61	0.34	–	–
Glucose	–	4.85	0.40	–	–
Sex	0.004	F (60%);	M (40%)	F (40%)	M (60%)
Ethnicity	0.611	white (99%)	other (1%)	white (100%)	other (0%)

B.

	p-value	Control		T2D	
		Mean	SD	Mean	SD
Age	< 0.001	52.45	17.08	68.74	10.65
BMI	< 0.001	26.51	4.13	30.61	5.99
HbA1c	–	5.61	0.34	–	–
Glucose	–	4.85	0.40	–	–
Sex	0.001	F (60%);	M (40%)	F (57%)	M (43%)
Ethnicity	0.445	white (99%)	other (1%)	white (99%)	other (1%)

A. Anthropometric characteristics of peripheral blood donors with normal blood glucose ($n = 133$) and those with impaired glucose tolerance (IGT; $n = 46$) B. Anthropometric characteristics of peripheral blood donors with normal blood glucose ($n = 133$) and those with overt T2D ($n = 106$). Differences in parameters between islet groups was determined by t-test

Associations between peripheral blood circRNA expression and fasting glucose, HbA1c or IGT/T2D status

Peripheral blood RNA samples underwent cDNA synthesis using the EvoScript system and Universal cDNA Master kit (Roche Life Science, Burgess Hill, UK). Samples were normalised to 100 ng/ μL RNA prior to reverse transcription. Reactions were executed according to the manufacturer's instructions, with a small amendment to extend the final 65 °C incubation to 30 min. We then assessed the expression of circRNAs that associated with T2D in islets donors by RT-qPCR as described above. Target abundance was assessed using the Comparative Ct method, and expressed relative to the geometric mean of the target and control set as a whole, since endogenous controls alone did not provide a robust baseline. Levels of each circRNA were then normalised to median levels in non-diabetic blood samples. Differential expression by diabetic status (no diabetes or IGT, IGT, overt diabetes) was then assessed by one way ANOVA using StataSE15 (StataCorp, Texas, USA) with adjustment made for potential confounders age, sex, BMI and ethnicity.

Results

CircRNA profiling in islets

Two thousand six hundred nineteen circRNAs were expressed in islet donors in the present study

(Supplementary Table S3). Fourty-seven circRNAs had not been previously identified in data from multiple human tissues (multiple brain regions, muscle, thyroid and liver), and multiple cell types (including stem cells, skin and lung fibroblasts, neurons, lung epithelia, hepatocytes, breast cancer cells, lymphocytes, muscle myoblasts, aortic and vascular endothelial cells) analysed using the circBase and circAtlas databases [25] (http://zhaolab.biols.ac.cn/). These circRNA are given in Supplementary Table S4. The five circRNAs demonstrating the highest expression in human islets derived from the *CAMSAP1, CIRBP, RPH3AL, RHOBTB3* and *ZKSCAN1* loci. Thirteen circRNAs co-localized with the GWAS association signals for T2; these comprised *GLIS3* and *HMG20A* (1 circRNA each), *CTBP1, IDE and SPPL3* (2 circRNAs each) and *THADA* (five circRNAs). We selected these 18 circRNAs for further follow up. circRNA structures were predicted based on the sequencing read depth for each exon and are presented in Fig. 1. Exon structures presented as read depth plots are given in Supplementary Figure S1.

Pathway analyses for genes generating islet-specific or abundant circRNAs

Pathway enrichment analysis was carried out to determine whether the genes hosting the 47 circRNAs not identified in other tissues were enriched in any specific gene ontology (GO) pathways. A similar analysis was also carried out the genes hosting the top 10% most abundant circRNAs. Pathways analysis was performed using ClueGO in Cytoscape (Bindea et al. 2009). The novel circRNAs demonstrated enrichment for genes in the 'pancreatic secretion' pathway ($p = < 0.001$). The 10% most abundantly expressed circRNAs were derived from genes demonstrating enrichment in the lysine degradation ($p = 0.03$), attenuation phase ($p = 0.02$), RUNX3 ($p = 0.02$), carcinoma ($p = 0.01$) and stem cell gene regulation ($p < 0.001$) pathways (Table 3).

CircRNAs are differentially expressed in a tissue-specific pattern

We assessed the expression patterns of the 18 circRNAs selected for further analysis across a panel of human tissues. We demonstrated that the expression patterns of circRNAs did not always correlate with levels of their corresponding linear transcripts. The expression levels of circular and linear forms of the gene were sometimes divergent, indicating that the circRNAs are regulated independently from the mRNAs also deriving from the parental linear gene (Supplementary Figure S2). For instance while *circSPPL3_2* was upregulated in most tissues compared to its linear gene, both *circCAMSAP1* and *circRHOBTB3* roughly followed the pattern of expression of their linear transcript levels across divergent tissues.

The most abundant islet circRNAs are associated with insulin secretory index (SI) or T2D status in human islets

4/5 circRNAs that showed marked expression in the islets demonstrated an association with T2D status (Fig. 2, supplementary Table S5). Three of these circRNAs, *circCAMSAP1*, *circCIRBP* and *circRPH3AL* satisfied the multiple testing threshold ($p < 0.001$). *CircZKSCAN1* showed nominal association with T2D status in islet donors ($p = 0.030$). Of these, the expression of the linear transcripts of three of these circRNAs, *CAMSAP1, CIRBP* and *ZKSCAN1* were also significantly associated with diabetic status ($p < 0.001$). *RHOBTB3* ($p < 0.001$) also demonstrated significant association with T2D status although its circRNA showed no association. The majority of these were positive associations, with the exception of *CIRBP* and *circCIRBP*, which were negatively correlated with T2D status. In addition, *circCIRBP* demonstrated a nominal negative association with insulin secretory index ($p = 0.028$; supplementary Table S5). No associations were identified between islet circRNA expression and donor HbA1c.

CircRNA expression is not driven by genotype

We next assessed the expression of circRNAs located in regions of the genome linked to risk of T2D. Thirteen circRNAs co-localised with the genomic regions encompassing the GWAS association signals for T2D; 2 circRNAs from the *CTBP1* gene (in rs6819243 region), one circRNA from the *GLIS3* gene (rs10758593), one circRNA from the *HMG20A* gene (rs7177055), two circRNAs from the *IDE* gene (rs1111875), two circRNAs from the *SPPL3* gene (rs12427353) and five circRNAs deriving from the *THADA* gene (rs10203174). We identified no associations between any of these circRNAs and genotype at these loci (Table 4).

CircRNAs are differentially expressed upon exposure to stress conditions in EndoC-βH1 cells

Although the 5 most abundant circRNAs expressed in human islets did not show overt responsiveness to altered glucose, hypoxia or pro-inflammatory cytokines when tested in the human beta cell line EndoC-βH1, two (*circCIRBP* and *circRPHAL3*) did demonstrate changes in expression following treatment with 0.5 mM palmitate. *CircCIRBP* expression was increased following treatment ($P = 0.021$) whereas *circRPHAL3* demonstrated reduced expression ($p = 0.022$; Table 5). The expression of the linear transcripts from the *RHOBTB3* and *ZKSCAN1* genes also demonstrated increased expression in EndoC-βH1 cells treated with palmitic acid, in the absence of effects of their respective circRNAs.

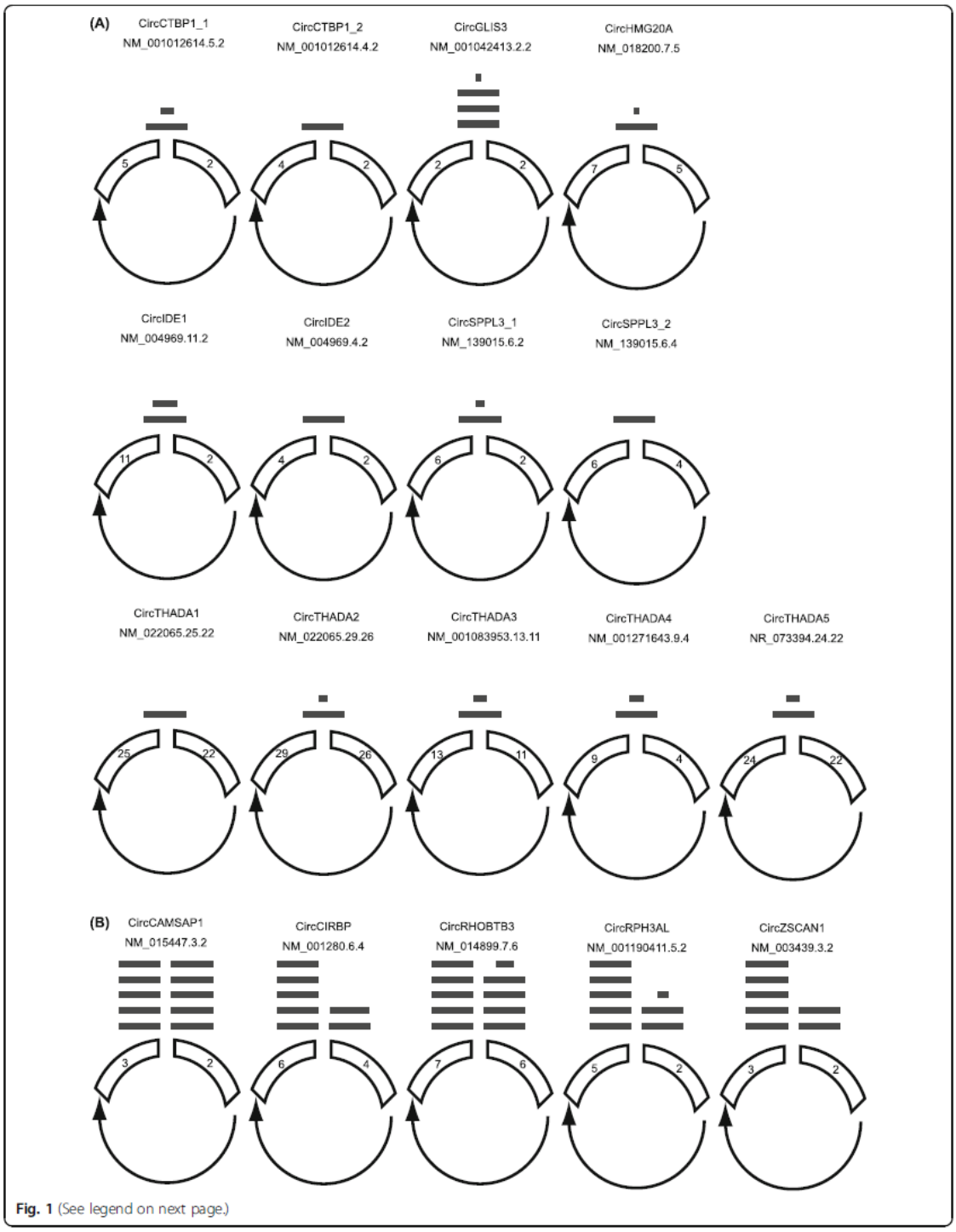

Fig. 1 (See legend on next page.)

(See figure on previous page.)
Fig. 1 Structure of islet circRNAs: CirRNA junction schematics for 13 circular RNAs associated with Type 2 diabetes genome-wide association studies (**a**) and the 5 most abundant circRNAs identified in islets (**b**). Each schematic shows the identified backspliced exon or exons. The relative read depth at each backspliced junction is shown by the number of bars above each junction and is scaled by linear interpolation, where the backspliced junctions with 1 and 10 bars represent the junctions with the lowest and highest read depth respectively

CircCAMSAP1 is differentially expressed in T2D peripheral blood

Of the 4 circRNAs demonstrating evidence of altered expression in the islets of donors with T2D, two (*circIDE1* and *circRPH3AL)* were not expressed in peripheral blood. Of the three remaining circRNAs with expression in peripheral blood (*circCAMSAP1*, *circCIRBP* and *circZKSCAN1*), *circCAMSAP1* demonstrated a nominal negative association with diabetes status in the peripheral blood of patients with T2D (Fig. 3; supplementary Table S6). No difference in expression was detected for any circRNA between control patients and those with IGT, or between those with IGT and those with T2D). No associations were evident between circRNA expression in peripheral blood and either participant fasting glucose or HbA1c.

Discussion

We present here the first enriched circRNA profile from human primary pancreatic islet RNA produced from a modified NGS CircleSeq protocol with enrichment for circRNAs. We have identified 2619 circRNAs expressed in human islets, including 47 circRNAs which were not identified in profiles from multiple other tissues in circBase or circAtlas. Some of these novel circRNA are clustered into pathways representative of pancreatic exocrine function, so it is possible that their expression is pancreatic, rather than islet specific. Of the 18 circRNAs selected for follow up on the basis of abundance or colocalisation to the GWAS association signals for T2D, many also show evidence of regulation independent of their parent gene. Four out of 5 of the most abundant circRNAs in human islets demonstrate strong evidence of dysregulated expression in the islets of human donors with T2D, with one (*circCIRBP*) demonstrating an association with insulin secretory index. Two out of 5 also show dysregulated expression in human EndoC-βH1 beta cells treated with fatty acids although direction of effect was not conserved. Finally, one circRNA (*circCAMSAP1*) also demonstrates an association with diabetes status in the peripheral blood of patients with type 2 diabetes.

To date, there have been two circRNA profiles generated from human pancreatic endocrine cells or intact islets. The first provides a circRNA profile generated from publically-available NGS data from isolated α, β and δ cell transcriptomes [17]. This study reported 10,832 putative circRNAs expressed in total, with 382 shared across cell types. This study reports more islet circRNAs than identified in our dataset, but this profile is derived from conventional NGS data, with no pre-treatment to remove linear sequences. Back splicing events can be generated from tandem DNA duplications within genes, or from trans-splicing events during linear splicing [26], so it is likely that profiles derived from conventional NGS contain sequences that in fact represent aberrantly spliced linear transcripts rather than genuine circRNAs. Differences will also arise in that this previous circRNA profile derives from isolated α, β and δ cell populations, whereas ours is a profile derived from intact islets. Differences in gene expression patterns may thus reflect the effects of cell:cell crosstalk as occurs in vivo. Nevertheless, there was considerable overlap between our profile and the beta cell circRNA profile of Kaur et al. [17]. Of the top 100 most abundant circRNA in the Kaur profile, all but 12 had counterparts from the same genes in our profile. Clustering between the most abundant genes in the Kaur profile and the most abundant genes in the

Table 3 Pathways enriched in genes generating circRNAs expressed predominantly in human pancreatic islets

A.

Pathways enriched in genes hosting circRNAs not seen in other tissues

Pathway	*p*-value	Number of Genes	Genes
Pancreatic secretion	< 0.0001	5	*CELA3A, CFTR, CPA1, KCNQ1, PNLIPRP2*

B.

Pathways enriched in genes generating the top 10% the most abundantly-expressed circRNAs in islets

Pathway	*p*-value	Number of Genes	Genes
Hematopoietic Stem Cell Gene Regulation	< 0.0001	4	*CREBBP, EP300, FOXO3, GABPB1*
Pathways affected in Adenoid Cystic Carcinoma	0.010	6	*CREBBP,EP300, FOXO3, KANSL1, KMT2C, MAML3*
Attenuation phase	0.020	3	*CREBBP, DNAJB1, EP300*
RUNX3 regulates NOTCH signaling	0.020	3	*CREBBP, EP300, MAML3*
Lysine degradation	0.030	5	*ASHIL, EHMT1, KMT2C, PLOD1, SETD3*

GO pathways analysis to identify pathways enriched in the host genes of A. novel RNAs not previously characterised in other tissues or B. the top 10% most abundant circRNAs in human islets are presented here. Number of genes = number of differentially-expressed genes in each pathway

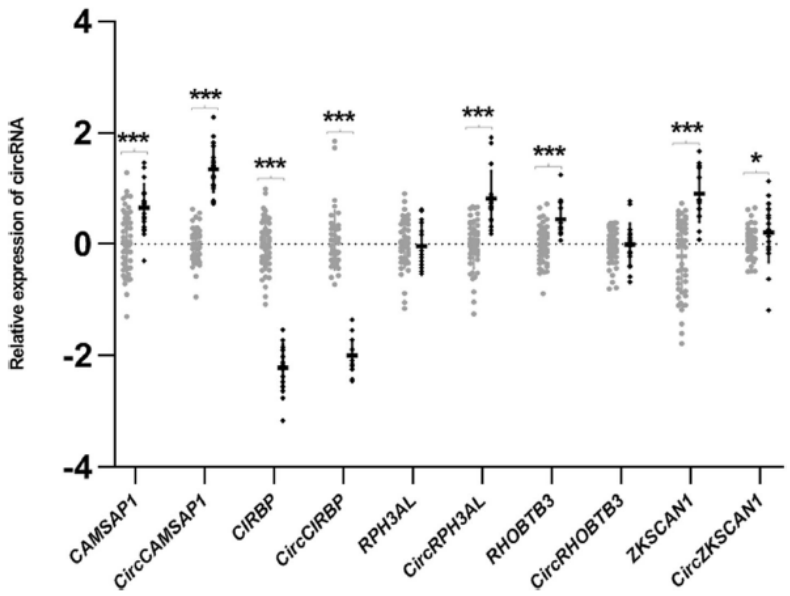

Fig. 2 Differential expression of *circCAMSAP1*, *circCIRBP*, *circRPH3AL* and *circZKSCAN1* in diabetic islets. Expression levels of circular and linear transcripts of the top 5 most abundant circRNAs in human islets are given here in relation to T2D status. Islets from non-diabetic individuals are given in grey ($n = 50$), those from individuals with T2D are given in black ($n = 20$). Relative expression of each linear or circular RNA is given on the Y axis, and was quantified relative to the geometric mean across all samples, since endogenous control genes alone did not provide a stable baseline. Statistical significance in difference of expression between islets from donors with or without T2D is indicated by stars. * = < 0.05, ** = < 0.005, *** = < 0.001

profile reported here was also apparent (supplementary Table S3).

A second islet circRNA profile has also been reported [18]. This profile was based on a microarray approach, identified 3441 islet circRNAs from a study of 3 human islet samples (two female and one male donor). Since this is a microarray-based profile, it will only contain circRNAs that have been already annotated. The most abundant circRNA in this study derived from the *HIPK3* gene. We also identified a circRNA deriving from this gene in the top 75 most abundant circRNA transcripts in our profile. This study differs from ours in that follow up work on circRNA expression in cell lines and in relation to T2D status occurred in animal models and not in human cells and tissues.

Our data, like those reported in previous islet studies [17, 18] suggests that many of the circRNAs we have identified are regulated independently of their linear counterparts (Supplementary Figure S2). In some cases, we have identified associations between cell treatments or T2D status with circRNAs in the absence of apparent effects on their linear transcripts. Comparison of circRNA expression across tissues showed expression patterns of many circRNAs were often higher in brain tissues compared to other tissues, which is in line with existing knowledge that circRNAs accumulate in the brain [27].

Some of our circRNAs are associated with glycaemic traits in human islets. The expression of *circCIRBP* demonstrates a negative association with insulin secretory index (SI) of the donor islets, is elevated in human EndoC-βH1 beta cells treated with palmitic acid and is reduced in islets from donors with T2D. The parent gene *CIRBP* (Cold Inducible RNA Binding Protein) has roles in genotoxic stress response, not only from cold, but also from other cellular stressors such as hypoxia [28]. Elevated levels have been associated with maintenance of glucose metabolism and protection from cold exposure through effects on the AKT pathway [29]. The elevated levels we demonstrate in the human beta cell line EndoC-βH1 treated with palmitate may therefore represent an acute stress response to altered lipid. The lower levels in the islets of individuals with T2D may reflect lower stress tolerance in diabetic islets, and as may the inverse correlation with SI, since we have previously demonstrated that stressed beta cells can transdifferentiate into delta cells in vitro [23].

We also identified elevated levels of both *circCAMSAP1* and its host gene *CAMSAP1* in the islets of donors with T2D. *CAMSAP1* encodes an organisation protein involved in microtubule dynamics and localisation [30]. The dynamics of microtubule assembly and disassembly

Table 4 Association of expression of circRNAs mapping to T2D-GWAS loci and their parental transcripts with genotype in primary non-diabetic islets

Transcript		GG		Gg and gg	
	p-value	Mean	SD	Mean	SD
rs6819243					
CTBP1	0.781	−0.11	0.32	−0.04	0.34
CircCTBP1_1	0.274	−0.03	0.65	0.09	0.37
CircCTBP1_2	0.293	0.00	0.85	0.11	0.85
rs10758593					
GLIS3	0.139	−0.19	0.37	0.02	0.36
CircGLIS3	0.535	0.03	0.37	0.04	0.41
rs7177055					
HMG20A	0.502	−0.03	0.38	0.09	0.37
CircHMG20A	0.952	0.03	0.36	0.03	0.38
rs1111875					
IDE	0.578	−0.66	0.39	−0.46	0.35
CircIDE1	0.953	−0.02	0.40	0.04	0.45
CircIDE2	0.937	−0.02	0.23	0.02	0.36
rs12427353					
SPPL3	0.808	−0.01	0.48	0.05	0.43
CircSPPL3_1	0.677	−0.02	0.45	0.06	0.34
CircSPPL3_2	0.595	0.01	0.48	0.21	0.48
rs10203174					
THADA	0.369	−0.02	0.61	0.22	0.50
CircTHADA1	0.672	0.05	0.40	0.10	0.42
CircTHADA2	0.282	−0.01	0.86	− 0.33	0.96
CircTHADA3	0.133	0.11	0.32	0.16	0.45
CircTHADA4	0.319	0.06	0.39	−0.24	0.46
CircTHADA5	0.651	0.14	0.59	0.27	0.40

The association between circRNA/linear transcript expression and genotype for circRNAs located to GWAS loci for T2D are given. Heterozygous samples and minor allele homozygotes are combined into one category. SD = standard deviation. Genotypes: GG = most common allele observed. Gg = heterozygotes, gg = minor allele heterozygotes

has an impact on the insulin secretion machinery; translocation and movement of insulin granules along microtubules can influence their availability for secretion. Failure to disassemble can impede docking. Microtubule density is higher in the islets of diabetic mice compared with non-diabetic littermates [31]. We also identified an association between *circCAMSAP1* expression and diabetes status in the peripheral blood of individuals with T2D, although this was the inverse of that seen in islets. CAMSAPs are active in multiple tissues, and also have roles in white blood cells, which rely on the tubulin-microtubule system for lymphocyte activation [32]. The effect of T2D status on *circCAMSAP1* expression in blood may therefore reflect potential tissue-specific activities of this circRNA. *ZKSCAN1* and its circular RNA *circZKSCAN1* have been described as inhibitors of cellular proliferation and survival [33]. Both transcripts demonstrate elevated expression in islets from donors with T2D, which may perhaps reflect adverse effects on beta cell survival. *CircRPH3AL* was also upregulated in diabetic islets. Linear transcripts from *RPH3AL* are highly expressed in β-cells and have roles in calcium-dependent exocytosis during granule maturation and insulin secretion [34].

We hypothesised that dysregulation of circRNA expression may underpin some of the GWAS association signals for T2D. Thirteen circRNAs colocalised to the recombination windows surrounding the 6 of the GWAS index loci, but none of these demonstrated differential expression by risk genotype. This suggests that the genetic associations between individual genetic variants and T2D is probably not mediated by dysregulation of islet circRNAs.

Table 5 Expression of most abundantly expressed circRNAs and their parental transcripts in EndoC-βH1 cells treated with diabetes-related stresses *(Continued)*

Transcript	Treatment	*p*-value	Median (IQR)
	25 mM glucose	0.441	0.93 (0.80–1.08)
	Control		1.09 (1.06–1.37)
	1% O_2	0.357	1.55 (1.04–1.56)
	3% O_2	0.205	1.32 (1.28–1.81)
	Control		0.95 (0.87–0.99)
	Palmitic acid	0.102	0.84 (0.70–0.87)
	Control		0.98 (0.02–1.01)
	Cytokines	0.354	1.02 (0.91–1.12)
CircRPH3AL	Control		1.00 (0.45–1.00)
	2.5 mM glucose	0.941	0.85 (0.58–0.97)
	25 mM glucose	0.867	0.76 (0.73–0.86)
	Control		1.09 (1.06–1.37)
	1% O_2	0.357	1.55 (1.04–1.56)
	3% O_2	0.205	1.32 (1.28–1.81)
	Control		1.66 (1.32–1.85)
	Palmitic acid	***0.022***	***0.97 (0.95–1.11)***
	Control		0.68 (0.47–0.77)
	Cytokines	0.295	0.97 (0.55–1.02)
RHOBTB3	Control		1.24 (1.23–1.31)
	2.5 mM glucose	0.188	1.11 (1.00–1.27)
	25 mM glucose	0.117	1.20 (0.72–1.14)
	Control		0.95 (0.69–1.06)
	1% O_2	0.949	0.97 (0.77–0.98)
	3% O_2	0.353	0.67 (0.65–0.93)
	Control		0.80 (0.72–0.90)
	Palmitic acid	**0.003**	**1.18 (1.15–1.21)**
	Control		1.17 (0.29–1.35)
	Cytokines	0.186	1.59 (1.22–1.72)
CircRHOBTB3	Control		0.74 (0.73–1.00)
	2.5 mM glucose	0.836	0.89 (0.65–1.02)
	25 mM glucose	0.351	0.77 (0.57–0.78)
	Control		1.04 (0.72–1.08)
	1% O_2	0.182	0.78 (0.74–0.78)
	3% O_2	0.288	0.79 (0.77–0.86)
	Control		1.16 (0.99–1.27)
	Palmitic acid	0.306	1.03 (0.83–1.13)
	Control		1.01 (0.95–1.08)
	Cytokines	0.628	0.97 (0.89–1.06)
ZKSCAN1	Control		1.24 (1.18–1.33)
	2.5 mM glucose	0.632	1.23 (1.05–1.87)
	25 mM glucose	0.997	1.23 (1.16–1.36)
	Control		0.93 (0.86–1.08)

Table 5 Expression of most abundantly expressed circRNAs and their parental transcripts in EndoC-βH1 cells treated with diabetes-related stresses

Transcript	Treatment	*p*-value	Median (IQR)
CAMSAP1	Control		1.11 (0.95–1.39)
	2.5 mM glucose	0.313	1.03 (0.92–1.05)
	25 mM glucose	0.444	0.96 (0.95–1.17)
	Control		0.92 (0.89–1.06)
	1% O_2	0.694	0.97 (0.73–1.04)
	3% O_2	0.347	0.88 (0.63–0.99)
	Control		1.05 (0.95–1.08)
	Palmitic acid	0.062	0.89 (0.77–0.94)
	Control		0.93 (0.25–1.21)
	Cytokines	0.635	0.95 (0.90–0.99)
CircCAMSAP1	Control		0.84 (0.79–1.11)
	2.5 mM glucose	0.762	1.02 (0.75–1.12)
	25 mM glucose	0.681	0.92 (0.78–1.29)
	Control		0.98 (0.92–1.14)
	1% O_2	0.136	0.89 (0.76–0.93)
	3% O_2	0.292	0.83 (0.63–1.07)
	Control		1.04 (1.02–1.23)
	Palmitic acid	0.090	0.82 (0.65–1.00)
	Control		0.77 (0.27–1.14)
	Cytokines	0.555	0.99 (0.69–1.02)
CIRBP	Control		1.06 (0.83–1.08)
	2.5 mM glucose	0.080	1.38 (1.10–1.53)
	25 mM glucose	0.077	1.30 (1.14–1.56)
	Control		1.01 (0.99–1.09)
	1% O_2	0.146	0.79 (0.39–0.97)
	3% O_2	0.129	0.84 (0.74–1.02)
	Control		0.88 (0.65–1.09)
	Palmitic acid	0.907	0.91 (0.64–1.15)
	Control		0.90 (0.03–1.34)
	Cytokines	0.593	0.95 (0.93–1.06)
CircCIRBP	Control		0.77 (0.61–1.42)
	2.5 mM glucose	0.844	0.86 (0.32–1.37)
	25 mM glucose	0.652	0.77 (0.72–0.94)
	Control		1.10 (1.00–1.23)
	1% O_2	0.955	0.86 (0.56–2.00)
	3% O_2	0.726	0.89 (0.68–1.48)
	Control		0.75 (0.72–1.04)
	Palmitic acid	***0.021***	***1.69 (1.30–1.98)***
	Control		1.17 (1.00–1.33)
	Cytokines	0.180	0.73 (0.69–1.06)
RPH3AL	Control		1.05 (0.93–1.06)
	2.5 mM glucose	0.503	0.99 (0.75–1.07)

Table 5 Expression of most abundantly expressed circRNAs and their parental transcripts in EndoC-βH1 cells treated with diabetes-related stresses *(Continued)*

Transcript	Treatment	*p*-value	Median (IQR)
	1% O_2	0.388	1.06 (0.94–1.12)
	3% O_2	0.218	0.72 (0.66–0.98)
	Control		0.50 (0.39–0.55)
	Palmitic acid	**0.001**	**1.01 (0.94–1.12)**
	Control		1.29 (0.24–1.33)
	Cytokines	0.378	1.30 (1.27–1.35)
CircZKSCAN1	Control		0.86 (0.81–1.17)
	2.5 mM glucose	0.490	0.91 (0.83–1.17)
	25 mM glucose	0.505	0.88 (0.83–1.28)
	Control		1.11 (0.99–1.42)
	1% O_2	0.060	1.65 (1.41–1.79)
	3% O_2	0.631	1.24 (1.02–1.57)
	Control		1.01 (0.81–1.45)
	Palmitic acid	0.252	0.83 (0.75–0.91)
	Control		1.05 (0.10–1.13)
	Cytokines	0.292	1.16 (1.13–1.18)

We assessed the effect of diabetes-related cellular stresses (low/high glucose, elevated fatty acid, hypoxia and exposure to pro-inflammatory cytokines) on the expression of the 5 most abundant islet circRNAs in the Endo-βH1 human beta cell line. IQR = interquartile range. Results meeting the threshold for 4 test conditions are given in bold underlined type, those presenting nominal associations only are indicated in bold italic type

We acknowledge that at present however, our data are largely correlative, and at present do not offer information on causality, definitive mechanistic proof or insight into the regulatory relationships between circRNAs and their host genes. CircRNAs can have effects *in cis* by regulating the transcription, linear splicing or translation of linear transcripts from their host genes [35–40]. In our data, we observe similar responses of linear and circular transcripts in response to challenge (*CAMSAP1/circCAMSAP1*, *CIRBP/circCIRBP*, *ZKSCAN1/circZKSCAN1*). This may be a manifestation of effects on transcription of common pre-RNAs from which both forms can be expressed. Other circRNAs show dysregulated expression for the circRNA alone (*circRPH3AL*). This suggests that the effect of circRNA regulation is post-transcriptional in these cases. CircRNAs can also act *in trans*, by virtue of sponging of other non-coding (nc) RNAs or RNA binding proteins [41–43]. In these cases, it is impossible to deduce from our data what the molecular targets of dysregulated islet circRNAs may be.

Conclusion

In conclusion, we present here an enriched circular RNA profile in human pancreatic islets. Although we find no evidence that the associations between T2D and genetic variation are underpinned by effects on the circRNA milieu, we demonstrate that the majority of the most abundant islet circRNAs display associations between their expression and aspects of glucose homeostasis in human donors, as well as associations with other glycaemic measures. One circRNA, *circCAMSAP1*, also demonstrated altered expression in the peripheral blood of individuals with T2D, and may have future utility as a biomarker.

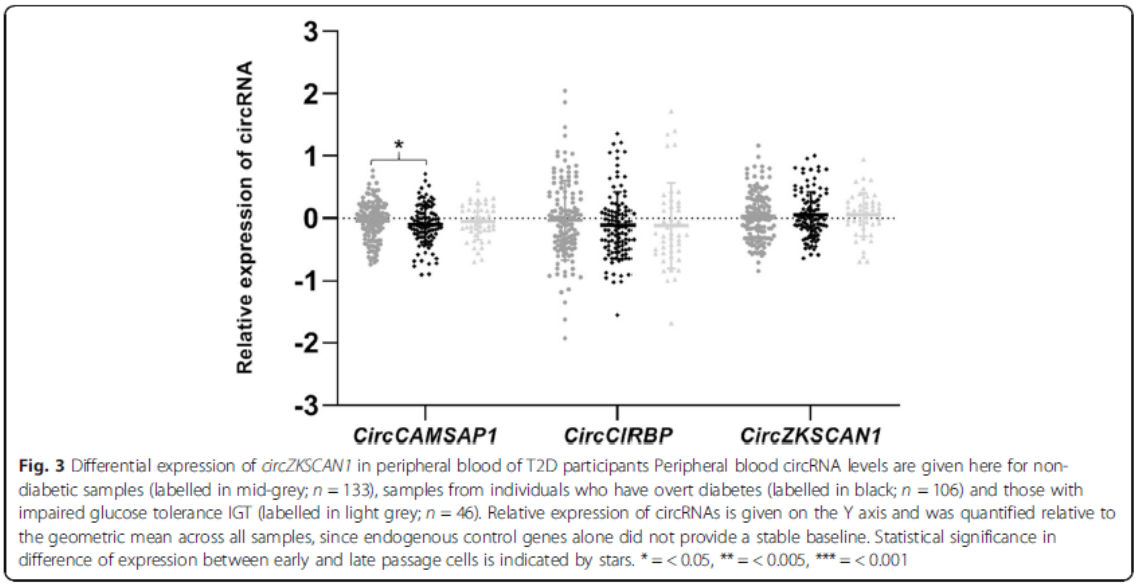

Fig. 3 Differential expression of *circZKSCAN1* in peripheral blood of T2D participants Peripheral blood circRNA levels are given here for non-diabetic samples (labelled in mid-grey; $n = 133$), samples from individuals who have overt diabetes (labelled in black; $n = 106$) and those with impaired glucose tolerance IGT (labelled in light grey; $n = 46$). Relative expression of circRNAs is given on the Y axis and was quantified relative to the geometric mean across all samples, since endogenous control genes alone did not provide a stable baseline. Statistical significance in difference of expression between early and late passage cells is indicated by stars. * = < 0.05, ** = < 0.005, *** = < 0.001

Supplementary information

Supplementary information accompanies this paper at https://doi.org/10.1186/s12920-020-0713-2.

Additional file 1.
Additional file 2.
Additional file 3.
Additional file 4.
Additional file 5.
Additional file 6.
Additional file 7.
Additional file 8.

Abbreviations

T2D: Type 2 diabetes; GWAS: Genome wide association study; ncRNA: Non-coding RNA; miRNA: MicroRNA; NGS: Next generation sequencing; RIN: RNA integrity number; qRT-PCR: Quantitative reverse transcription PCR; WGA: Whole Genome amplification; cDNA: Complementary DNA; TNFa: Tumour necrosis factor alpha; IFNg: Interferon gamma; IL-1b: Interleukin 1 beta; HbA1c: Glycosylated haemoglobin; IGT: Impaired glucose tolerance; SI: Insulin rsecretory index.

Acknowledgements

The authors acknowledge the generous support of the Exeter Sequencing Service and Computational core facilities at the University of Exeter. The work was supported by the National Institute for Health Research (NIHR) Exeter Clinical Research Facility. We also acknowledge Dr. Raphael Scharfmann and INSERM for the provision of the Endo-βH1 cells, Dr. Michael Jackson and Dr. Santibanez-Koref for useful discussions regarding circRNA analysis and Professor Michael Weedon for advice on the GWAS analysis.

Author contributions

SH performed all the experimental work, analysed the data and wrote the first draft on the manuscript. KM designed and carried out the CircleSeq experiments. RMA led on bioinformatics analysis of the CircleSeq data including data analysis and modification of existing analytical pipelines. BPL contributed to circRNA assay design and led on statistical analysis (analysis and interpretation of data). NJ performed the treatment on the EndoC-βH1 cells. LWH managed the study, provided overall leadership and refined the manuscript. All authors have read and approved the manuscript.

Funding

This study was supported by the Medical Research Council (MR/M008924/1), the Wellcome Trust (WT097835MF and WT101650MA) and the BBSRC (BB/K003240/1). The funders had no role in the execution or analysis of this work.

Availability of data and materials

All data generated or analysed during this study are included in this published article and its supplementary information files. Raw reads are deposited in the Sequence Read Archive (SRA) BioProject database using BioProject ID PRJNA607015 (https://www.ncbi.nlm.nih.gov/bioproject/?term=PRJNA607015). The raw reads can be downloaded via their SRR IDs for the mock-treated (SRR11095576) and RNAse R treated samples (SRR11095575). CircRNA data from isolated islet cell subtypes was accessed through the supplementary information given in [17].

Ethics approval and consent to participate

Human islet samples were commercially obtained from ProCell Biotech (Newport Beach, CA, USA) or from the NIA IIDP resource where islets had been collected with ethical permission at source. Human peripheral blood samples were obtained with written informed consent was obtained for all participants and ethical permission was granted through the National Institute for Health Research (NIHR) Clinical Facility (REC 09/H0106/75).

Consent for publication

Human pancreatic islet and peripheral blood samples were obtained with written informed consent. All data are anonymised and no information is traceable to any individual donor.

Competing interests

The authors have no conflicts of interest to declare.

Author details

[1]RNA-Mediated Mechanisms of Disease Group, Institute of Biomedical and Clinical Sciences, University of Exeter Medical School, University of Exeter, RILD South, Barrack Road, Exeter EX2 5DW, UK. [2]Biosciences, University of Exeter, Exeter, UK. [3]College of Life and Environmental Sciences, University of Exeter, Exeter, UK.

Received: 23 November 2019 Accepted: 14 April 2020
Published online: 20 April 2020

References

1. Xue A, Wu Y, Zhu Z, Zhang F, Kemper KE, Zheng Z, Yengo L, Lloyd-Jones LR, Sidorenko J, Wu Y, et al. Genome-wide association analyses identify 143 risk variants and putative regulatory mechanisms for type 2 diabetes. Nat Commun. 2018;9(1):2941.
2. Tabak AG, Herder C, Rathmann W, Brunner EJ, Kivimaki M. Prediabetes: a high-risk state for diabetes development. Lancet. 2012;379(9833):2279–90.
3. Bansal N. Prediabetes diagnosis and treatment: a review. World J Diabetes. 2015;6(2):296–303.
4. Edwards SL, Beesley J, French JD, Dunning AM. Beyond GWASs: illuminating the dark road from association to function. Am J Hum Genet. 2013;93(5):779–97.
5. Qu H, Fang X. A brief review on the human encyclopedia of DNA elements (ENCODE) project. Genomics Proteomic Bioinform. 2013;11(3):135–41.
6. Hrdlickova B, de Almeida RC, Borek Z, Withoff S. Genetic variation in the non-coding genome: involvement of micro-RNAs and long non-coding RNAs in disease. Biochim Biophys Acta. 2014;1842(10):1910–22.
7. Haque S, Harries LW, et al. Genes (Basel). 2017;8(12):353. https://doi.org/10.3390/genes8120353.
8. Bose R, Ain R. Regulation of transcription by circular RNAs. Adv Exp Med Biol. 2018;1087:81–94.
9. Luo J, Liu H, Luan S, Li Z. Guidance of circular RNAs to proteins' behavior as binding partners. Cell Mol Life Sci. 2019;76(21):4233–43. https://doi.org/10.1007/s00018-019-03216-z.
10. Zang J, Lu D, Xu A. The interaction of circRNAs and RNA binding proteins: an important part of circRNA maintenance and function. J Neurosci Res. 2020;98(1):87–97. https://doi.org/10.1002/jnr.24356.
11. Kulcheski FR, Christoff AP, Margis R. Circular RNAs are miRNA sponges and can be used as a new class of biomarker. J Biotechnol. 2016;238:42–51.
12. Enuka Y, Lauriola M, Feldman ME, Sas-Chen A, Ulitsky I, Yarden Y. Circular RNAs are long-lived and display only minimal early alterations in response to a growth factor. Nucleic Acids Res. 2016;44(3):1370–83.
13. Schwanhausser B, Busse D, Li N, Dittmar G, Schuchhardt J, Wolf J, Chen W, Selbach M. Global quantification of mammalian gene expression control. Nature. 2011;473(7347):337–42.
14. Wu H, Wu S, Zhu Y, Ye M, Shen J, Liu Y, Zhang Y, Bu S. Hsa_circRNA_0054633 is highly expressed in gestational diabetes mellitus and closely related to glycosylation index. Clin Epigenetics. 2019;11(1):22.
15. Fang Y, Wang X, Li W, Han J, Jin J, Su F, Zhang J, Huang W, Xiao F, Pan Q, et al. Screening of circular RNAs and validation of circANKRD36 associated with inflammation in patients with type 2 diabetes mellitus. Int J Mol Med. 2018;42(4):1865–74.
16. Zhang SJ, Chen X, Li CP, Li XM, Liu C, Liu BH, Shan K, Jiang Q, Zhao C, Yan B. Identification and characterization of circular RNAs as a new class of putative biomarkers in diabetes retinopathy. Invest Ophthalmol Vis Sci. 2017;58(14):6500–9.
17. Kaur S, Mirza AH, Pociot F. Cell type-selective expression of circular RNAs in human pancreatic islets. Noncoding RNA. 2018;4(4):38. https://doi.org/10.3390/ncrna4040038.
18. Stoll L, Sobel J, Rodriguez-Trejo A, Guay C, Lee K, Veno MT, Kjems J, Laybutt DR, Regazzi R. Circular RNAs as novel regulators of beta-cell functions in normal and disease conditions. Mol Metab. 2018;9:69–83.

19. Lopez-Jimenez E, Rojas AM, Andres-Leon E. RNA sequencing and prediction tools for circular RNAs analysis. Adv Exp Med Biol. 2018;1087:17–33.
20. Jeck WR, Sharpless NE. Detecting and characterizing circular RNAs. Nat Biotechnol. 2014;32(5):453–61.
21. Haque S, Ames RM, Moore K, Pilling LC, Peters LL, Bandinelli S, Ferrucci L, Harries LW. CircRNAs expressed in human peripheral blood are associated with human aging phenotypes, cellular senescence and mouse lifespan. Geroscience. 2020;42(1):183–99.
22. Morris AP, Voight BF, Teslovich TM, Ferreira T, Segre AV, Steinthorsdottir V, Strawbridge RJ, Khan H, Grallert H, Mahajan A, et al. Large-scale association analysis provides insights into the genetic architecture and pathophysiology of type 2 diabetes. Nat Genet. 2012;44(9):981–90.
23. Jeffery N, Richardson S, Chambers D, Morgan NG, Harries LW. Cellular stressors may alter islet hormone cell proportions by moderation of alternative splicing patterns. Hum Mol Genet. 2019.
24. Debey-Pascher S, Eggle D, Schultze JL. RNA stabilization of peripheral blood and profiling by bead chip analysis. Methods Mol Biol. 2009;496:175–210. https://doi.org/10.1007/978-1-59745-553-4_13.
25. Glazar P, Papavasileiou P, Rajewsky N. CircBase: a database for circular RNAs. RNA. 2014;20(11):1666–70.
26. Izuogu OG, Alhasan AA, Alafghani HM, Santibanez-Koref M, Elliot DJ, Jackson MS. PTESFinder: a computational method to identify post-transcriptional exon shuffling (PTES) events. BMC Bioinform. 2016;17(1):31.
27. Gokool A, Anwar F, Voineagu I. The landscape of circular RNA expression in the human brain. Biol Psychiatry. 2020;87(3):294–304. https://doi.org/10.1016/j.biopsych.2019.07.029.
28. Lee HN, Ahn SM, Jang HH. Cold-inducible RNA-binding protein, CIRP, inhibits DNA damage-induced apoptosis by regulating p53. Biochem Biophys Res Commun. 2015;464(3):916–21.
29. Liu P, Yao R, Shi H, Liu Y, Lian S, Yang Y, Yang H, Li S. Effects of cold-inducible RNA-binding protein (CIRP) on liver glycolysis during acute cold exposure in C57BL/6 mice. Int J Mol Sci. 2019;20(6):1470. https://doi.org/10.3390/ijms20061470.
30. Baines AJ, Bignone PA, King MD, Maggs AM, Bennett PM, Pinder JC, Phillips GW. The CKK domain (DUF1781) binds microtubules and defines the CAMSAP/ssp4 family of animal proteins. Mol Biol Evol. 2009;26(9):2005–14.
31. Zhu X, Hu R, Brissova M, Stein RW, Powers AC, Gu G, Kaverina I. Microtubules negatively regulate insulin secretion in pancreatic beta cells. Dev Cell. 2015;34(6):656–68.
32. Sherline P, Mundy GR. Role of the tubulin-microtubule system in lymphocyte activation. J Cell Biol. 1977;74(2):371–6.
33. Yao Z, Luo J, Hu K, Lin J, Huang H, Wang Q, Zhang P, Xiong Z, He C, Huang Z, et al. ZKSCAN1 gene and its related circular RNA (circZKSCAN1) both inhibit hepatocellular carcinoma cell growth, migration, and invasion but through different signaling pathways. Mol Oncol. 2017;11(4):422–37.
34. Matsunaga K, Taoka M, Isobe T, Izumi T. Rab2a and Rab27a cooperatively regulate the transition from granule maturation to exocytosis through the dual effector Noc2. J Cell Sci. 2017;130(3):541–50.
35. Jeck WR, Sorrentino JA, Wang K, Slevin MK, Burd CE, Liu J, Marzluff WF, Sharpless NE. Circular RNAs are abundant, conserved, and associated with ALU repeats. Rna. 2013;19(2):141–57.
36. Grigull J, Mnaimneh S, Pootoolal J, Robinson MD, Hughes TR. Genome-wide analysis of mRNA stability using transcription inhibitors and microarrays reveals posttranscriptional control of ribosome biogenesis factors. Mol Cell Biol. 2004;24(12):5534–47.
37. Gualandi F, Trabanelli C, Rimessi P, Calzolari E, Toffolatti L, Patarnello T, Kunz G, Muntoni F, Ferlini A. Multiple exon skipping and RNA circularisation contribute to the severe phenotypic expression of exon 5 dystrophin deletion. J Med Genet. 2003;40(8):e100.
38. Chao CW, Chan DC, Kuo A, Leder P. The mouse formin (Fmn) gene: abundant circular RNA transcripts and gene-targeted deletion analysis. Mol Med. 1998;4(9):614–28.
39. Abdelmohsen K, Srikantan S, Kuwano Y, Gorospe M. MiR-519 reduces cell proliferation by lowering RNA-binding protein HuR levels. Proc Natl Acad Sci U S A. 2008;105(51):20297–302.
40. Ashwal-Fluss R, Meyer M, Pamudurti NR, Ivanov A, Bartok O, Hanan M, Evantal N, Memczak S, Rajewsky N, Kadener S. CircRNA biogenesis competes with pre-mRNA splicing. Mol Cell. 2014;56(1):55–66.
41. Abdelmohsen K, Panda AC, Munk R, Grammatikakis I, Dudekula DB, De S, Kim J, Noh JH, Kim KM, Martindale JL, et al. Identification of HuR target circular RNAs uncovers suppression of PABPN1 translation by CircPABPN1. RNA Biol. 2017;14(3):361–9.
42. Piwecka M, Glazar P, Hernandez-Miranda LR, Memczak S, Wolf SA, Rybak-Wolf A, Filipchyk A, Klironomos F, Cerda Jara CA, Fenske P, et al. Loss of a mammalian circular RNA locus causes miRNA deregulation and affects brain function. Science. 2017;357(6357):eaam8526. https://doi.org/10.1126/science.aam8526. Epub 2017 Aug 10.
43. Zheng Q, Bao C, Guo W, Li S, Chen J, Chen B, Luo Y, Lyu D, Li Y, Shi G, et al. Circular RNA profiling reveals an abundant circHIPK3 that regulates cell growth by sponging multiple miRNAs. Nat Commun. 2016;7:11215.

Publisher's Note